



HAL
open science

Performance evaluation of optical packet switching technology: access control, resource allocation and QoS management for metropolitan and access networks

Tuan Dung Nguyen

► **To cite this version:**

Tuan Dung Nguyen. Performance evaluation of optical packet switching technology: access control, resource allocation and QoS management for metropolitan and access networks. Other [cs.OH]. Institut National des Télécommunications, 2010. English. NNT : 2010TELE0023 . tel-00688808

HAL Id: tel-00688808

<https://theses.hal.science/tel-00688808v1>

Submitted on 18 Apr 2012

HAL is a multi-disciplinary open access archive for the deposit and dissemination of scientific research documents, whether they are published or not. The documents may come from teaching and research institutions in France or abroad, or from public or private research centers.

L'archive ouverte pluridisciplinaire **HAL**, est destinée au dépôt et à la diffusion de documents scientifiques de niveau recherche, publiés ou non, émanant des établissements d'enseignement et de recherche français ou étrangers, des laboratoires publics ou privés.

Ecole Doctorale EDITE

Thèse présentée pour l'obtention du diplôme de Docteur de Télécom & Management SudParis

Doctorat conjoint Télécom & Management SudParis et Université Pierre et Marie Curie

Spécialité :
Informatique

Par :
Tuan-Dung NGUYEN

Titre :
**Evaluation de performances de la Technologie de Commutation de Paquets
Optiques: Contrôle d'Accès, Allocation des Ressources et Qualité de
Service pour les Réseaux Métropolitains et d'Accès**

Soutenue le 09 Novembre 2010

Sous la direction de :
Professeur Tülin ATMACA

Devant le jury composé de :

Rapporteurs: M. Harry PERROS, Professeur, Université NC State, USA
Mme. Nihal PEKERGIN, Professeur, Université Paris XIII Val de Marne, France
Examineurs: Mme. Tülin ATMACA, Professeur, IT-SudParis, France (Directrice de la thèse)
M. Guy PUJOLLE, Professeur, Université Pierre et Marie Curie Paris VI, France
M. Dominique CHIARONI, Team Leader, Alcatel-Lucent CIT R&I, France
M. Philippe GRAVEY, Professeur, Télécom Bretagne, France
Mme. Catherine LEPERS, Professeur, IT-SudParis, France



**DISSERTATION OF PHILOSOPHY DOCTOR
OF THE UNIVERSITY PIERRE ET MARIE CURIE**

Speciality

Computer Science

Presented by

Tuan Dung NGUYEN

A Dissertation Submitted in Satisfaction of the Requirements for the Degree of
PHILOSOPHY DOCTOR OF THE UNIVERSITY PIERRE ET MARIE CURIE

Thesis Subject:

**Performance Evaluation of Optical Packet Switching Technology:
Access Control, Resource Allocation and QoS Management for
Metropolitan and Access Networks**

November 2010

Under Supervision of
Professor Tülin ATMACA

Committee in Charge:

Reviewers: Mr. Harry PERROS, Professor, University NC State, USA
Mme. Nihal PEKERGIN, Professor, University Paris XII Val de Marne, France
Examiners: Mme. Tülin ATMACA, Professor, IT-Sud Paris, France (Thesis Director)
Mr. Guy PUJOLLE, Professor, University Pierre et Marie Curie Paris VI, France
Mr. Dominique CHIARONI, Team Leader, Alcatel-Lucent CIT R&I, France
Mr. Philippe GRAVEY, Professor, Télécom Bretagne, France
Mme. Catherine LEPERS, Professor, IT-Sud Paris, France

ACKNOWLEDGEMENTS

First of all, I'd like to thank Professor Tülin ATMACA for her willingness to coach me, her promptness, the eye-opening discussions and her valuable comments on the progress of my research. In the same light, I thank Professor Gérard HEBUTERN for his excellent observations, ideas, and creativity that inspired my dissertation. I am grateful to his stimulating feedback.

I would like to thank all the professors in the University of "Pierre & Marie Curie – Paris 6" who were responsible for the PhD courses that I have attended during these years. I have acquired considerable knowledge through their presentations and interactive scientific discussions.

I would like specially to present all my gratitude to Dr. Viet Hung NGUYEN and Dr. Thierry EIDO for their significant collaboration during three years. I also thank my colleagues: özgür can TURNA, Muhammed Ali AYDIN and Van Thiep NGUYEN for their constructive advices and interesting ideas and for creating a pleasant ambiance for me at work.

I would also like to thank all Vietnamese friends of Telecom SudParis for their friendship and support over the past year. To all of them I would like to express my sincere greetings.

Additionally, I would like to thank all people, both at the department and at RST, who have helped with their knowledge and their friendship.

Specially, countless thanks and acknowledgements go to my parents and my family for giving me the best support and the best working conditions. All signs of gratitude go also to my wife and my daughter, for their affection, encouragements and precious help during these years.

ABSTRACT

The rapid growth in client application demands, in terms of bandwidth and Quality of Service (QoS), has motivated the deployment of the optical technology at Metro Access and Metro Core Networks. More diverse and more intelligent optic devices are required for efficiently management of huge capacity in the network. The explosion in demand for network bandwidth is mainly due to the growth in data traffic whose nature is also becoming more and more complex. In general, most of service-based traffics are transported in networks which are now being dominated by the optical switching technology. Nevertheless, such technology has some drawbacks such as inflexible and non-scalable properties. Optical packet switching (OPS), which offers significant benefits in terms of both network efficiency and control scalability, may overcome these limitations. This has motivated the orientation from optical circuit switching to optical packet switching in the future network infrastructure.

In reality, optical packet switching ring (OPSR) networks, which combine the packet switching technology with the well-known advantages of ring topology such as fast service restoration in cases of failure and high gain of statistical traffic multiplexing over the ring, appear to be the technology of choice for the next generation of Metro Area Networks. A new OPSR architecture which is based on the all-optical infrastructure that offers intelligent features with lower cost while maximizing processing time and is now considering being replaced existing opto-electronic architectures such as Resilient Packet Ring, have been presented in the scope of the dissertation. The key element of such network is Packet Optical Add/Drop Multiplexer (POADM) which is implemented inside a ring node, allowing the node to exploit the optical transparency. This dissertation hence focuses on the performance evaluation of the new generation of OPSR network.

In this dissertation, we have investigated the performance analysis (in terms of packet delay and queue-length distribution of access nodes) of an optical synchronous bus-based metropolitan network supporting fixed-size packets. We have modeled each access node by an embedded discrete time Markov chain (EDTMC). The solution of the EDTMC allows us to compute the approximate probability that access nodes on the bus “see” free slots in the transit line. Using a recursive analysis technique, we approximately outline the mean waiting time of client packets coming from the upper layer as well as an approximate queue-length distribution of local buffers at access nodes in two cases: with and without QoS guarantees.

To characterize the performance of an asynchronous OPSR network, we have evaluated the impact of Optical fixed-Size Packet Creation on the network performance without and with different quality of service (QoS) requirements. Performance analysis of such systems has allowed us to identify a reasonable combination of some parameters (timeslot duration, timer expiration values, profile of client traffic and network load) which may be able to improve the bandwidth utilization of the network for a given traffic matrix. The most important point that we have mentioned in the dissertation is the comparison of two architectural approaches: Variable Length – Optical Packet Format (VL-OPF) model supporting empty packets versus Fixed Length – Optical Packet Format (FL-OPF) model. In addition to CoS-Upgrade Mechanism (CUM) which is proposed to improve the filling ratio of the optical container, we have proposed a novel mechanism named Dynamic CoS-Upgrade Mechanism (DCUM) where timers are dynamically changed according to the state of the local buffer of network nodes and the traffic circulating in the network, in order to create containers with a high filling ratio while limiting the time needed for their creation.

As for the access network, we have focused on the shared transmission media between end-users in Ethernet-based passive optical network (EPON). We have proposed an enhanced dynamical bandwidth allocation algorithm to address the idle period problem. The proposed algorithm calculates complementary granted bandwidth according to the arrival rate of electronic packets in a transmission cycle to facilitate the data transmission during the idle time, hence profiting from the whole network bandwidth. Finally, the behaviour of a node which interconnects two different types of the optical metro network has been investigated through a simulation of an end-to-end metropolitan network in which several rings are interconnected.

Résumé

La croissance rapide des applications interactives et ses demandes en termes de bande passante et de qualité de service (QoS), a motivé le déploiement de la technologie optique aux réseaux métropolitains. Beaucoup de dispositifs optiques intelligents sont créés pour gérer efficacement la capacité énorme du réseau. L'explosion du besoin en bande passante est principalement attribuable à la croissance du trafic de données dont la nature devient de plus en plus complexe. Actuellement, la plupart des trafics de données sont transportés dans les réseaux qui sont dominées par la technologie de commutation de circuit optique. Néanmoins, cette technique a quelques inconvénients tels que les propriétés inflexibles. Technologie de commutation de paquets optiques (OPS), qui offre des gains significatifs en termes de capacité de passage à l'échelle et d'efficacité de gestion des ressources du réseau, peut surmonter ces limitations. Cela a motivé l'orientation de la commutation de circuit optique à la commutation de paquet optique dans l'infrastructure future du réseau.

En réalité, un réseau en anneau à commutation de paquet optique (Optical Packet Switching Ring - OPSR), qui combinent la flexibilité et la mise à l'échelle de la technologie de commutation de paquet avec les avantages de la topologie en anneau tels que la restitution rapide du service en cas de panne et un bon gain de multiplexage statistique du trafic, promettaient une bonne solution pour les réseaux MAN du future. Une nouvelle architecture du réseau OPSR qui se base sur l'infrastructure tout optique a proposé par des équipes de recherche chez Alcatel-Lucent. La nouvelle architecture offre des fonctions intelligentes, avec un coût moins élevé en optimisant le temps de traitement. Elle est envisagée de remplacer les architectures optoélectroniques existantes tels que Resilient Packet Ring. L'élément fondamental du réseau est Packet Optical Add/Drop Multiplexer (POADM) qui est implémenté à l'intérieur des nœuds d'accès, permettant aux nœuds d'exploiter la transparence optique. Cette thèse se concentre donc sur l'évaluation des performances de la nouvelle génération des réseaux optiques métropolitains.

Dans cette thèse, nous avons analysé des performances (en termes de délais d'accès et de la distribution du taux de l'occupation au tampon local des nœuds d'accès) d'un bus optique synchrone qui soutient des paquets à taille fixe. Nous avons modélisé chaque nœud d'accès par une chaîne de Markov à temps discret (EDTMC). La solution de l'EDTMC nous permet de calculer la probabilité approximative où les nœuds d'accès dans le bus peuvent "voir" slots libres dans la ligne de transit. En utilisant une technique d'analyse récursive, nous déduisons une formule mesurant le temps moyen d'attente des paquets du client venant de la couche supérieure, ainsi que la distribution du taux de l'occupation au tampon local des nœuds d'accès pour les deux cas: avec et sans garantie de la Qualité de Service (QoS).

Pour caractériser des performances d'un réseau OPSR asynchrone, nous avons évalué l'impact de la création de conteneur optique à taille fixe sur les performances du réseau. L'analyse des performances de ce système nous a permis d'identifier une combinaison raisonnable de certains paramètres (la durée de timeslot, les valeurs d'expiration des temporisateurs, le profil du trafic client, la charge du réseau) qui peuvent améliorer l'utilisation de la bande passante du réseau. Le point le plus important que nous avons mentionné dans la thèse est la comparaison entre deux approches architecturales: le modèle de Variable Length - Optical Packet Format (VL-OPF) versus le modèle de Fixed Length - Optical Packet Format (FL-OPF). En plus de Cos-Upgrade Mécanisme (CUM) qui est proposé d'améliorer le taux de remplissage du conteneur optique, nous avons proposé un nouveau mécanisme appelé Dynamic Upgrade Cos-Mécanisme (DCUM), où les valeurs des temporisateurs sont modifiés dynamiquement en fonction de l'état des tampons locaux aux nœuds d'accès et le trafic circulant dans le réseau, afin de créer des conteneurs optiques avec le taux de remplissage le plus élevé possible en limitant le temps d'attente nécessaire des paquets de client.

Quant au réseau à l'accès, un algorithme d'allocation dynamique de bande passante est proposé pour traiter le problème de période inactive dans le réseau d'Ethernet Passive Optical Network (EPON). L'algorithme proposé calcule la bande passante complémentaire en fonction du taux d'arrivé des paquets électroniques dans un cycle de transmission pour faciliter la transmission de données pendant la période inactif, profitant donc de la bande passante tout entière du réseau. Enfin, le comportement d'un noeud qui relie les deux types de réseau métropolitain optique a été aussi étudié grâce à une simulation d'un réseau métropolitain de bout en bout où des anneaux sont interconnectés.

This thesis has been conducted in the locations
of the Telecoms and Management SudParis,
RST Department (Réseaux et Services des Télécommunications),
9 rue Charles Fourier – 91011 Evry Cedex – France
Tél. +33 (0) 1 60 76 47 24
Fax. +33 (0) 1 60 76 42 91

The contributions and works presented in this dissertation are supported by:
The ECOFRAME / ANR French National Projects and Bilateral INT / Alcatel-Lucent Collaborations

TABLE OF CONTENTS

Chapter 1 - Introduction	1
1.1 Problem Formulation	2
1.2 Dissertation Outline	3
Chapter 2 - Overview and Next Generation of Optical Metropolitan Network	5
2.1 Optical Network Overview	5
2.1.1 Introduction - Concept and Evolution	5
2.1.2 Optical Transport Layer	6
2.1.3 Transmission Techniques	8
2.1.4 Wavelength routing techniques	9
2.2 Emergence of Wavelength-Division Multiplexing	10
2.3 Optical Access Network	10
2.4 Optical Metropolitan Area Network (OMAN)	12
2.4.1 Switching Technique Evolution	13
2.4.2 Well-known OMAN Architectures	15
2.4.3 POADM ring network	16
2.5 Concluding remarks	19
Chapter 3 - Packet Delay Analysis and Queue-length Distribution of Optical Synchronous Bus-based Network	21
3.1 Introduction	21
3.2 Studied Network Architecture	22
3.2.1 Network Architecture Description	22
3.2.2 Considered Model	23
3.3 Embedded Discrete Time Markov Chain (EDTMC) Approach	25
3.3.1 Outline of the “mono-service” model	27
3.3.2 Outline of the “multi-service” model	31
3.4 Performance Evaluation	35
3.5 Concluding remarks and future works	43
3.6 Appendix	45
3.6.1 Solution for Transition Matrix in the “mono-service” case	45
3.6.2 Solution for Transition Matrix in the “multi-service” case	48
3.6.3 Computation of mean waiting times	49
Chapter 4 - Impact of Optical fixed-Size Packet Creation	53
4.1 Synchronous Vs. Asynchronous Networks	53
4.2 MAC in the Synchronous Ring Network	54
4.3 Optical Fixed-Size Packet Creation	54
4.3.1 Basic fix-size packet creation mechanism	54
4.3.2 Timer-based mechanism	55
4.3.3 Simulation Scenarios and Numerical Results	57
4.4 Virtual Synchronization Mechanism	68
4.4.1 Idea of VSC Scheme	68
4.4.2 VSC Algorithm Implementation	70
4.4.3 VSC Performance Evaluation	70
4.5 Concluding remarks	73

Chapter 5 - Medium Access Protocols in Multi-service	75
5.1 Quality of service Overview.....	75
5.1.1 QoS Parameters.....	76
5.1.2 QoS Mapping	77
5.2 Mono-Class Approach	78
5.3 Multi-Class Approach	79
5.3.1 CoS-enabled Timer Mechanism (CTM)	79
5.3.2 CoS-Upgrade Mechanism (CUM)	79
5.3.3 Dynamic CoS-Upgrade Mechanism (DCUM).....	80
5.3.4 Packet Erasing Mechanism (PEM)	83
5.3.5 Extraction and Reemission Mechanism (ERM).....	84
5.4 Performance Evaluation	84
5.4.1 Global parameters	84
5.4.2 Investigation of the Timer duration in CUM	86
5.4.3 Investigation of the erasing threshold in PEM.....	94
5.4.4 Investigation of the Timer duration in ERM.....	100
5.4.5 Mono-class Vs. Multi-class approaches.....	102
5.4.6 Performance evaluation with DCUM.....	105
5.5 Concluding remarks.....	110
Chapter 6 - Access Network's Resource Allocation and Interconnection of Metro Ring Networks.....	113
6.1 Resource Allocation in EPON	113
6.1.1 Passive optical network Overview	113
6.1.2 Dynamic bandwidth allocation (DBA) algorithms	115
6.1.3 Enhanced DBA algorithm	118
6.1.4 Performance Evaluation	121
6.2 Performance Evaluation of Interconnected Metro Ring Networks	124
6.2.1 End-to-End Network Architecture	124
6.2.2 Multi-Ring Network Simulation	125
6.2.3 Access Mechanisms	127
6.2.4 Simulation Parameters	129
6.2.5 Numerical Results	130
6.3 Concluding Remarks and Future Works	132
6.4 Appendix	134
Chapter 7 - General conclusion	135
7.1 General Concluding Remarks	135
7.2 Perspectives for future works.....	137
Bibliography	139

LIST OF FIGURES

Figure 2-1: The mapping sequence of OTN over WDM	7
Figure 2-2: Time-division multiplexing.....	8
Figure 2-3: Wave-division multiplexing uses different wavelengths (frequencies) of light.	8
Figure 2-4: Combination of TDM and WDM multiplexing	9
Figure 2-5: Wavelength routing.....	9
Figure 2-6: Dynamic routing	10
Figure 2-7: The comparison between different access mechanisms [OWN 06].....	11
Figure 2-8: Fiber-to-the-Home deployments [OWN 06].....	12
Figure 2-9: Optical packet switch	13
Figure 2-10: Optical Burst Switching: Reference OBS Switching and Burst transmission	14
Figure 2-11: Resilient Packet Ring.....	15
Figure 2-12: CSMA/CA protocol	15
Figure 2-13: Bidirectional POADM ring network.....	16
Figure 2-14: Synchronous operation.....	17
Figure 2-15: POADM node model supporting fixed-size packets.....	18
Figure 3-1: Network and node architecture	23
Figure 3-2: The considered network with N access nodes (mono-service case).....	24
Figure 3-3: Queuing system inside an access node supporting multi-service (multi-service case).....	24
Figure 3-4: The evolution of process X_k , $k = 1, 2 \dots$	25
Figure 3-5: Example of $p^{(i)}(0^*)$ and $p^{(i)}(0^{**})$	26
Figure 3-6: Embedded Markov chain from state i ($i > 1$).....	27
Figure 3-7: Embedded Markov chain from state (0^{**}).....	28
Figure 3-8: Embedded Markov chain from state (0^*)	28
Figure 3-9: Extended Embedded Markov chain from state i ($i > 1$) for the buffer CoS_j	32
Figure 3-10: Extended Embedded Markov chain from state (0^{**}) for the buffer CoS_j	32
Figure 3-11: Extended Embedded Markov chain from state (0^*) for the buffer CoS_j	32
Figure 3-12: The mean waiting time depending on the offered network load from node 1 to 9	35
Figure 3-13: The mean waiting time depending on the timeslot lengths with the offered load equal to 0.5 from node 1 to 9	36
Figure 3-14: Stationary probabilities at access nodes with the offered network load equal to 0.5.....	37
Figure 3-15: Free probabilities according to the offered load and the timeslot from node 1 to 9	38
Figure 3-16: The mean waiting in varying patterns of offered traffic with the offered load equal to 0.5 from node 1 to 9.	38
Figure 3-17 : Stationary probabilities at access nodes 7, 8 and 9 with uniformly increasing and uniformly decreasing traffic as the offered network load is set to 0.5	39
Figure 3-18: The mean waiting time in three different un-balanced traffic with the offered load equal to 0.5 from node 1 to 9	39
Figure 3-19 : Stationary probabilities at access nodes 7, 8 and 9 in three different un-balanced traffic: case 1, 2 and 3 with the offered network load equal to 0.5.....	40
Figure 3-20: The mean waiting time from node 1..9 for three CoS with the offered network load equal to 0.45.....	40
Figure 3-21: The mean waiting time from node 1..9 for three CoS with the offered network load equal to 0.55.....	41
Figure 3-22: Stationary probabilities at access nodes 1 and 9 with the offered network load equal to 0.45.....	41
Figure 3-23: The ratio of captured free slots to the sample of 200 timeslots.....	42
Figure 3-24: Coefficient Variance measured in the simulation at the network load of 0.50 and 0.60.	43
Figure 4-1: Optical fixed-size packet creation process	55

Figure 4-2: Schema of Timer-based mechanism triggered by an Electronic Packet Arrival.....	56
Figure 4-3: Schema of Timer mechanism: Timer Expiration.....	57
Figure 4-4: IP packet length distribution.....	58
Figure 4-5: Scenario examples of 3 nodes: a) Metro Access and b) Metro Core.....	58
Figure 4-6: The PLR with a timeslot equal to $10\mu s$ and an offered network load set to 0.80.....	59
Figure 4-7: Filling Ratios with the timeslot equal to $10\mu s$ and the network load at 0.80.....	60
Figure 4-8: Mean access delay with a timeslot duration of $10\mu s$ and the offered network load equal to 0.8.....	60
Figure 4-9: Utile and Effective Rates measured at nodes 1 and 9 with the timeslot equal to $10\mu s$ and the workload set to 0.80.....	61
Figure 4-10: Obtained results under unbalanced traffic patterns.....	62
Figure 4-11: Obtained results as the network load varies.....	63
Figure 4-12: Obtained results as the timeslot varies.....	64
Figure 4-13: Measured filling ratios, utile and effective rates as the timeslot varies.....	64
Figure 4-14: Packet loss ratio and mean access delay with the timeslot equal to $10\mu s$ and the offered network load is set to 0.8.....	65
Figure 4-15: Optical Packet's Filling Ratio.....	65
Figure 4-16: Utile and Effective Rates measured at a node with the timeslot equal to $10\mu s$ and the network equal to 0.80.....	66
Figure 4-17: Set of results obtained in varying network load, timeslot and timer size.....	67
Figure 4-18: Utile and Effective Rates measured at a node with timeslot of $10\mu s$ and network equal to 0.40.....	68
Figure 4-19: Example of asynchronous (a) and synchronous networks (b).....	68
Figure 4-20: Example of VSC scheme.....	69
Figure 4-21: Optical Fixed-size packet used in VSC scheme vs. MPB burst.....	69
Figure 4-22: PLR at access nodes with the OU-CSMA/CA protocol and with different VS sizes when the network load is equal to 0.8.....	71
Figure 4-23: Average access delay at access nodes with the OU-CSMA/CA protocol and with different VS sizes when the network load set to 0.8.....	71
Figure 4-24: Average transmission ratio with the OU-CSMA/CA protocol and with different VS sizes as the network load = 0.8.....	72
Figure 4-25: Results obtained at each node with the OU-CSMA/CA protocol and with the VS size of 25 Kbytes.....	72
Figure 4-26: Bandwidth Utilization Ratio (%) under the workload of 0.8.....	73
Figure 5-1: QoS mapping.....	77
Figure 5-2: Mono-class case.....	77
Figure 5-3: Multi-class case (supporting four class of service).....	77
Figure 5-4: Mono-class optical packet creation process.....	78
Figure 5-5: Multi-class optical packet creation process.....	79
Figure 5-6: CoS-Upgrade mechanism function.....	80
Figure 5-7: First procedure of DCUM.....	81
Figure 5-8: Second procedure of DCUM.....	82
Figure 5-9: Optical Packet Creation process.....	83
Figure 5-10: Packet Erasing Mechanism.....	83
Figure 5-11: Filling ratio for values of Timer T: $50\mu s$, $100\mu s$, $150\mu s$, $200\mu s$ and infinite value.....	86
Figure 5-12: The utile / effective rates as the Timer T varies (Scenario Bus).....	87
Figure 5-13: Timer value investigation with CUM.....	89
Figure 5-14: CTM and CUM comparison on the mean access delay.....	89
Figure 5-15: Investigation of the <i>factor k</i>	90
Figure 5-16: FS-OPF model and VS-OPF model without supporting <i>empty packets</i>	91
Figure 5-17: Performance comparison between FS-OPF model and VS-OPF model supporting <i>empty packets</i>	92

Figure 5-18: Filling ratio for values of Timer T: $300\mu s$, $400\mu s$, $500\mu s$, $700\mu s$ and simple aggregation	93
Figure 5-19: PLR and access delay obtained by CUM in 1-N scenario	93
Figure 5-20: The utile rate and the effective rate as the basic Timer T varies (1-N scenario)	94
Figure 5-21: Erasing thresholds investigation in the fixed-size mode (Scenario Bus)	96
Figure 5-22: Timer values and erasing thresholds investigation with the fixed-size mode (Scenario 1-N)	98
Figure 5-23: Erasing thresholds investigation at medium and heavy network loads	99
Figure 5-24: ERM's timer value investigation in Bus scenario	100
Figure 5-25: ERM's timer value investigation in 1-N scenario	101
Figure 5-26: PLR and Access delay under heavy load	101
Figure 5-27: The filling ratio comparison between Mono-class and Multi-class	102
Figure 5-28: PLR and Access delay comparison between Mono-class and Multi-class approaches	102
Figure 5-29: Utile and Effective Rates between Mono-class and Multi-class approaches	103
Figure 5-30: PLR and Access delay between Mono-class and Multi-class under heavy load	103
Figure 5-31: Filling ratios comparison between Mono and Multi class in the core metro	104
Figure 5-32: PLR and access delay of Mono-class and Multi-class for the core metro	104
Figure 5-33: Performance comparison: DCUM vs. CUM with the timer size equal to $100\mu s$	105
Figure 5-34: Filling Ratios (DCUM vs. CUM)	106
Figure 5-35: Utile and Effective Rates with the timeslot equal to $10\mu s$ while the offered ring load set to 70% at node 1	107
Figure 5-36: Performance comparison: DCUM vs. Aggregation case	107
Figure 5-37: Performance comparison: DCUM vs. AM	108
Figure 5-38: Filling ratio comparison between DCUM, CUM and Aggregation Mechanism	109
Figure 5-39: Utile and Effective rates between DCUM, CUM and Aggregation Mechanism	109
Figure 5-40: Performance comparison between DCUM and CUM with the timer size equal to $500\mu s$	109
Figure 6-1 - EPON Architecture	114
Figure 6-2 - MPCP Operation	115
Figure 6-3 - IPACT scheme	116
Figure 6-4 - Dynamic bandwidth allocation with QoS	117
Figure 6-5: enhanced DBA algorithm	119
Figure 6-6: Example of eDBA algorithm	120
Figure 6-7: Mean access delay at the ONU according to the network load	122
Figure 6-8: PLR at the ONU's local buffer according to the network load	123
Figure 6-9: Bandwidth utilization rates (%)	123
Figure 6-10: Access, Core and Backbone Metro Networks [ECO 08]	124
Figure 6-11: End-to-End Metro Network Architecture	125
Figure 6-12: Multi-Ring Network Simulation	126
Figure 6-13: Hub node's traffic	126
Figure 6-14: The synchronization shift between metro rings	127
Figure 6-15: First procedure of COTM	128
Figure 6-16: Last procedure of COTM	128
Figure 6-17: Waiting time of electronic packets elapsed in Hub node	130
Figure 6-18: Filling ratio and Util/Effective Rates obtained with OM and COTM	131
Figure 6-19 - Average accumulated delays and standard of electronic packet jitter at each node for different cases with the access load of 15%	131
Figure 6-20: Waiting time of electronic packets in Hub node in function of Δt	132
Figure 6-21: An example of Synchronization shift	132
Figure 6-22: Average Jitter and Confidence Interval of 95% with 10s simulation	134

LIST OF TABLES

Table 2-1: Fiber optic advantage compared with other media.....	6
Table 2-2: Comparison of different all-optical network technologies.....	14
Table 2-3: Evolution of the optical network architecture.....	17
Table 5-1: CoS identification for metro network.....	76
Table 5-2: Traffic and electronic side hypothesis.....	85
Table 5-3: Optic side hypothesis.....	86
Table 5-4: Recapitulative comparison of FL-OPF vs. VL-OPF models.....	110
Table 6-1: EPON simulation's traffic hypothesis.....	121
Table 6-2: Multi-Rings Simulation Parameters.....	129

ABBREVIATIONS

ADM	Add / Drop Multiplexer
ADSL	Asymmetric Digital Subscriber Line
AFTP	Asynchronous File Transfer
ANSI	American Standard National Institute
AP	Access Point
APON	ATM Passive Optical Network
ATM	Asynchronous Transfer Mode
BE	Best Effort
BLR	Bit (or Burst) Loss Ratio
BPON	Broadband Passive Optical Network
CA	Complementary Allocation
CAC	Call (or Connection) Admission Control
CBR	Constant Bit Rate or Constraint-Based Routing
CCM	Cumulative Credits Mechanism
CENTRAL-SR	CENTRALized Resource ALlocation in a Slotted Ring
CO	Central Office
CoS	Class of Service
CTM	CoS-enabled Timer Mechanism
CUM	CoS-Upgrade Mechanism
CSA	Credit Service Allocation
CSMA	Carrier Sense Multiple Access
CSMA/CA	Carrier Sense Multiple Access with Collision Avoidance
CSMA/CD	Carrier Sense Multiple Access with Collision Detection
CV	Coefficient of Variation
DBA	Dynamic Bandwidth Allocation
DBDQ	Distributed Queue Dual Bus
DBORN	Dual Bus Optical Ring Network
DCUM	Dynamic CoS-Upgrade Mechanism
DDR	Distributed Deflection Routing
DI-MAC	Dynamic Intelligent Medium Access Control
DS	DataStream
DSCU	Distant Subscriber Connection Unit
DSL	Digital Subscriber Loop
DTMC	Discrete Time Markov Chain
DWDM	Dense Wavelength Division Multiplexing

EAPD	end-to-end Accumulated Access Packet Delay
eDBA	enhanced Dynamic Bandwidth Allocation
EDTMC	Embedded Discrete Time Markov Chain
ELAN	Ethernet Local Area Network
EO	Electro-Optical
EON	European Optical Reference Network
EPON	Ethernet Passive Optical Network
EPDU	Ethernet Protocol Data Unit
EPJ	Electronic Packet Jitter
EPLR	end-to-end Packet Loss Ratio
ERM	Extraction and Reemission Mechanism
ESA	Elastic Service Allocation
FCFS	First Come First Serve
FDDI	Fiber Distributed Data Interface
FDL	Fiber Delay Line
FDM	Frequency Division Multiplexing
FIFO	First In First Out
FL-OPF	Fixed-Size Optical Packet Format
FSA	Fixed Service Allocation
FTTB	Fiber to the Building
FTTH	Fiber to the Home
FTTx	Fiber To The x
GE	Gigabit Ethernet
GFP	Generic framing procedure
GMPLS	Generalized MultiProtocol Label Switching
GPFO	Graduated Packet Filling Optimization
GPON	Gigabit Passive Optical Network
HOL	Head Of the Line
IEEE	Institute of Electrical and Electronics Engineers
IETF	Internet Engineering Task Force
IOF	Inter Office
IP	Internet Protocol
IPACT	Interleaved Polling with Adaptive Cycle Time
IPG	Inter-Packet Gap
IPP	Interrupted Poisson Process
ISO	International Standard Organization
ISP	Internet Service Provider
ITU	Internet Telecommunication Union
JET	Just Enough Time
JIT	Just In Time
LAN	Local Area Network
LLC	Logical Link Control
LM	Link Multiplexing
LMP	Link Management Protocol
LSA	Limited Service Allocation
LSC	Lambda Switch Capable
LSP	Label Switched Path
LSR	Label Switched Router

MAC	Medium Access Control
MAN	Metropolitan Area Network
MEF	Metro Ethernet Forum
MMPP	Markov-Modulated Poisson Process
MPB	Modified Packet Bursting
MPCP	Multi-Point Control Protocol
MPLS	Multi-Protocol Label Switching
MTU	Maximum Transmission Unit
MTW	Maximum Transmission Window
NGS	Next-Generation SONET
NNI	Network-Network Interface
NS	Network Simulator
OA&M	Operations, Administrations, and Maintenance
OADM	Optical Add / Drop Multiplexer
OBS	Optical Burst Switching
OC	Optical Channel
OCC	Optical Connection Controller
OCS	Optical Circuit Switching
oDBA	older Dynamic Bandwidth Allocation
OE	Opto-Electronic
OLT	Optical Line Terminal
OMAN	Optical Metropolitan Area Network
ONU	Optical Network Unit
OPS	Optical Packet Switching
OPSR	Optical Packet Switching Ring
OTDM	Optical Time Division Multiplexing
OTN	Optical Transport Network
O-UNI	Optical User Network Interface
OU-CSMA/CA	Optical Unslotted Carrier Sense Multiple Access with Collision Avoidance
OWS	Optical Wavelength Switching
OXC	Optical Cross Connect
P2P	Peer to Peer
PDF	Probability Density Function
PDH	Plesiochronous Digital Hierarchy
PDU	Protocol Data Unit
PEM	Packet Erasing Mechanism
PLR	Packet Loss Ratio
POADM	Packet Optical Add / Drop Multiplexer
PON	Passive Optical Network
POP	Point of Presence
PR2A	Peer to Peer Real Time Resource Allocation
PtMT	Point to Multipoint
PtP	Point to Point
QoS	Quality of Service
R2A	Real time Resource Allocation
RPR	Resilient Packet Ring
RTP	Real-time Transport Protocol
RTT	Round Trip Time

RWA	Routing and Wavelength Assignment
SAR	Segmentation and Reassembly
SDH	Synchronous Digital Hierarchy
SLA	Service Level Agreement
SNMP	Simple Network Management Protocol
SOA	Semiconductor Optical Amplifier
SONET	Synchronous Optical Network
TCARD	Traffic Control Architecture using Remote Descriptor
TCP	User Datagram Protocol
TDM	Time Division Multiplexing
TEAM	Tag-based Enhanced Access Mechanism
UDP	Transmission Control Protocol
UNI	User Network Interface
VL-OPF	Variable Size Optical Packet Format
VLAN	Virtual Local Area Network
VOA	Variable Optical Attenuator
VoIP	Voice Over IP
VPN	Virtual Private Network
VS	Virtual Slot
VSC	Virtual Synchronization sScheme
WADM	Wavelength Add / Drop Multiplexer
WAN	Wide Area Network
WDM	Wavelength Division Multiplexing
WFQ	Weighted Fair Queuing
xDSL	x- Digital Subscriber Line (x might be A- Asymmetric, S- Symmetric, etc.)

Chapter 1

Introduction

Optical network makes use of wavelength-division multiplexing (WDM) technology and optical amplifiers to transmit a large number of wavelength channels over large optic fibers. In current data centric networks, bursty traffic is now becoming dominant and network operators should be able to provide huge bandwidth under a very high speed. Such optical technology is promising as a practical choice for the high speed network.

One of the major drawbacks in the optical technology is the difficulty of processing and storing data in the optical domain due to the lack of suitable components. Therefore, the first types of the optical network implemented circuit switching techniques to overcome this drawback. Although such a circuit-switched network infrastructure can provide a large capacity and robustness, it suffers from poor bandwidth efficiency because of the static or semi-static bandwidth assignment per wavelength.

A dynamic bandwidth utilization and a faster response to traffic variations than in circuit-switched Dense WDM (DWDM) networks can be achieved by employing optical packet switching (OPS) [TEQ 01] or optical burst switching (OBS) [BST 00]. The main advantage of those techniques is an improvement in bandwidth utilization through limiting the wavelength occupation time by a single connection, thereby gaining increased wavelength utilization from statistical multiplexing in the optical layer. However, the enabling technology for ultrahigh-speed switching is not widely commercial due to its complexity.

Next-generation of Metropolitan Area Network (MAN) demands more architectural flexibility, scalability and manageability. As a MAN directly interconnects large enterprises or business corporations, it needs to provide much more types of service to their customers relative to the access or backbone networks. The ring topology is widely adopted in MAN thanks to its fast restoration time and spatial reuse. This is the main reason to explain a number of standards for MAN using ring topology such as Resilient Packet Ring (RPR) [RPR 03] and Dual Bus Optical Ring Network (DBORN) [DBO 02]. Additionally, bandwidth requirement in MAN is different for different interactive applications; hence applications having common features should be captured into a proper class of traffic in order to be efficiently served. Quality of Service management becomes an important role of mechanisms applied in the optical network such as queuing-priority management and resource reservation. Optical packets provide a good way to efficiently integrate the quality of service into

different layers while reducing the network operating cost. OPS based on commercially available components could be a good choice for a dynamic and efficient high-capacity optical MAN.

Research works on OPS in the ring-based metropolitan network have been stimulated by National French ANR research projects such as KEOPS [GRG 98], DAVID [SSO 03], ROM-EO [ROM 02] and particularly by ECOFRAME [ECO 08] which is based on a promising Packet Optical Add/Drop Multiplexer (POADM) architecture. However, lots of work is still to be done in order to provide simple and efficient integration of the packet switching technology on WDM architectures before bringing it from laboratory to commercial deployment.

In the scope of this dissertation, we aim to provide a study of different OPS-based network architectures, organized not only in metropolitan networks but also in the access network. Our main objective in MAN is to identify and address some problems that characterize different choices of network parameters such as the network traffic matrix, the transmission mode (synchronous Vs asynchronous) and the optical packet format (fixed-size Vs variable-size). As for the access network, we focus on Ethernet Passive Optical Network (EPON), which addresses the first mile of the communication infrastructure and is beginning to be used widely in the access network thanks to the decline in the cost of fiber optics and Ethernet-based equipments. This dissertation includes also the Quality of Service (QoS) management that guarantees the respect of Service Level Agreement (SLA) contracted to customers.

1.1 Problem Formulation

Depending on the format of the transport unit, the optical network can be classified according to the transmission mode: synchronous or asynchronous. The packet format represents a key issue in any optical packet oriented network and has an important impact on the QoS delivering to the end user (in terms of end-to-end delay and bandwidth loss). An open question includes a comparative study of two packet length formats defined for the optical network architecture: fixed length (supported by synchronous optical network) and variable length (supported by asynchronous optical network).

In the synchronous network, the creation of the fixed-size optical packet is required in order to accommodate electronic packets with variable sizes into the payload of the optical packet, which size closely fits a timeslot. The transmission of large fixed-size optical packets in the synchronous mode offers significant gain in the network throughput, since it avoids the bandwidth fragmentation [NGA 05] and reduces the number of additional optical headers. However, this circumstance wastes a piece of bandwidth transmission resource when the last electronic packet's size is larger than the remaining space of the optical packet which is being under construction without the segmentation. The more the optical packet size decreases, the more the bandwidth transmission wasted. As far as the optical header is concerned, the remaining space becomes important comparing to the size of the optical payload. This problem needs be considered in order to reduce the amount of the lost bandwidth.

Another factor which has a significant impact on the network performance is the choice of the duration of timer which is used in the fixed-size optical packet procedure. An unsuitable choice of timer values may lead to the wastage of the network bandwidth: small timer values generate optical packets with a very low filling ratio while a very big timer value leads to excessive packet creation delays.

The problem of defining the type and the number of services supported by the optical metro network remains a highly controversial issue. The development trend of an optical MAN is driven by the change and the difference in service requirements. On the one hand, the small number of classes of

service (CoS) could lead to the low consumed resource bandwidth while facilitating the resource management. On the other hand, the high number of CoS could guarantee QoS and increase the flexibility in QoS management. Therefore, the impact of the number of CoS on the network performance should be carefully investigated.

Given the fact that more than 90% of today's data traffic originates from and terminates in Ethernet networks, EPON appears to be a natural candidate for future first-mile solutions. EPON is a point-to-multipoint access network with no active element in the signal's path from source to destination. Resource allocation algorithm, which needs to share the bandwidth resource in a fair and efficient manner, becomes very important in EPON. The resource allocation problem raises-up in both circuit switching and packet switching solutions. There have been a lot of researches carried out on the subject of resource allocation in EPON. It can be either static [ICT 03, EAS 04] or dynamic ways [WAD 98, INF 03, ORW 00]. Dynamic algorithms provide more flexible resource allocation map which is dynamically adapted to explicit client demands. However, no researches are done about the efficiency of these dynamic methods when one or multiple EPON networks are connected to MAN.

1.2 Dissertation Outline

This dissertation is composed of seven chapters. These chapters are organized as follows. Chapter 2 provides an introduction to high capacity network communication and an overview of the MAN infrastructure and its evolution towards all-optical network. The chapter provides benefits by using WDM dimension with load balancing. In addition, a comparison between circuit-switched networks with burst-switched and packet-switched networks is introduced, in terms of performance characteristics. At the end of this chapter, we introduce a promising architecture for the optical MAN in future: the optical packet switching ring (OPSR) architecture using POADM component based on synchronous protocol, which is the main topic of our work.

Chapter 3 investigates performance analysis of a slotted bus-based MAN using fixed length packet format on a single wavelength by an analytical method. The network considered is a unidirectional bus on which many nodes compete to transmit fixed length packets to a centralized Hub node over a single wavelength. This chapter proposes an analytical model for bus nodes in both mono-service and multi-service cases which operates in the synchronous transmission mode. Each node is modeled by an embedded discrete time Markov chain (EDTMC). By using the recurrent analysis technique, an approximate queue-length distribution as well as a formula approximately computing the mean waiting time will be presented.

An important topic of chapter 4, which will be studied, is the fixed-size packet creation process. The first part investigates the impact of the timer duration on the network performance by simulating synchronous networks (metro access and metro core networks) without supporting QoS. The second part of the chapter is dedicated to study a new access scheme, called VSC standing for Virtual SynChronization (VSC) Mechanism. The concept of VSC, which aims at solving the unfairness and bandwidth fragmentation problems related to a bus-based architecture, is described in details. Performance analysis of VSC through simulations is also carefully investigated, including comparison with an existing fairness access scheme (named MPB [NGA 05]).

Chapter 5 starts with an outline of service requirements that an integrated network needs to provide. As a continuous work, chapter 5 provides results obtained by simulating synchronous metro networks (in both metro access and metro core networks) supporting QoS for two cases of Fixed-Size Optical Packet Creation: with and without QoS-Upgrade. This work also includes the comparison between two possible approaches of QoS mapping: Mono-class Vs Multi-class and a comparative study of two

architectural approaches: the Variable Length – Optical Packet Format (VL-OPF) model versus the Fixed Length – Optical Packet Format (FL-OPF) model. At the end of the chapter, we propose a novel mechanism that improves the optical packet’s filling-ratio. The proposed algorithm (so called DCUM for Dynamic CoS-Upgrade Mechanism) is based on the use of dynamic timers, whose values will be changed dynamically, in order to create optical packets with a maximum filling ratio as much as possible while limiting the time needed for the creation.

Chapter 6 focuses on the resource allocation in EPON network. The proposed resource allocation algorithm (that we call eDBA – enhanced Dynamic Bandwidth Allocation) allows to effectively and fairly allocating bandwidth between end-users. The algorithm calculates complementary granted bandwidth according to the arrival rate of electronic packets in a transmission cycle to address the idle period problem. To compare with well-known algorithms, we simulate the EPON-based multi-service network in which proposed algorithm will be implemented. Finally, the performance evaluation of interconnected ring networks will be presented in more details at the end of this chapter.

Chapter 7 concludes the dissertation with a summary of the main topics covered in this thesis, followed by some perspectives for following researches.

Chapter 2

Overview and Next Generation of Optical Metropolitan Network

The advent of the fiber-optic transmission system and the wavelength-division multiplexing (WDM) has led to a dramatic increase in the bandwidth capacity of the single-fiber system. As the network bandwidth requirement increases, the optical communication and networking technologies have been moving from their telecom origin into the enterprise. The reduction of bandwidth cost motivates the adoption and the acceptance of fiber-optic networks. As a result, dominant systems in the optical networking world such as Synchronous Optical Network (SONET)/Synchronous Digital Hierarchy (SDH), the evolution of Dense WDM (DWDM) and the merger of Internet Protocol (IP) become key elements on future enterprise networks. This chapter provides basic concepts of the optical network and requirements for the next-generation metropolitan network (MAN). A novel optical architecture, which is developed to deal with new requirements, and its specifications will be presented.

2.1 Optical Network Overview

2.1.1 Introduction - Concept and Evolution

Optical technology now becomes a practical choice for the high speed network due to its huge capacity, reliable transmission path, and flexibility. An optical network means a communication network in which data is transmitted over fiber optic lines as pulses of light. It is developed in order to transmit data signals at high bit rates over a long distance. The optical communication benefits from numerous advantages of the optical fiber over the copper wire. As we know, the fiber optic is very flexible, lightweight and hair-thin medium leading to a very low propagation loss while the transmission bandwidth is extremely large, enabling a high-speed, broad-bandwidth and long-distance transmission. Main benefits of the fiber optic over other media are shown in Table 2-1[MGH 01].

Lower Errors	Bit Error Rates (BER) approximates 10^{-15} for fiber optic, whereas copper will be in the range of 10^{-3} to 10^{-8} for coaxial cable.
Attractive cost per foot	Cost per foot for fiber is now approximately \$0.20 compared with \$0.13 for copper (category 5+).
Performance	Immune from Radio Frequency Interference (RFI) and Electromagnetic Interference (EMI) without extra cost of shielding on copper.
Ease of installation	Ease of installation due to lower weight and thickness.
Distances	Greater distance with fewer repeaters. Now it can achieve 30 to 200 miles without repeaters. Copper and radio are limited to less than 30 miles.
Bandwidth improvements	Fiber is nearly 1.6 Tbps, copper achieves 100 Mbps, and coax can carry up to 1 Gbps.
Capable of carrying analog and digital	Fiber optic is both digital and frequency multiplexed, increasing its capacity.

Table 2-1: Fiber optic advantage compared with other media.

The optical network have passed through two main generations and begin now its 3rd generation [OPN 02]. The first generation begins in 1980s with the birth of SONET systems in North America as well as SDH systems for the rest of the globe. Standard optical systems were built based on the point-to-multipoint electrical network concept by employing electrical Add/Drop Multiplexer (ADM) and cross-connect functions. Optical technologies such as Time-Division Multiplexing (TDM), Wavelength-Division Multiplexer (WDM) or their combinations may still be categorized into the first-generation of optical networks.

However, if the WDM network includes additional functionality of wavelength-routing, it may be sorted into the second-generation of the optical network. The Optical ADM (OADM) or Wavelength ADM (WADM), which provides wavelength-based ADM functions, is the key of this second-generation. Since the bandwidth demand and the transmission speed required at network nodes increase very rapidly, hence switching and routing processes in the transmission path must become faster. The required processing speed can be accomplished by adopting an optical processing. Indeed, the optical switching and routing treat optical signals at high rate and they do not require O/E/O (*optical to electrical to optical*) conversions. In addition, the optical circuit switching may be further replaced by the optical packet switching. Therefore, the optical network supporting packet switching and routing functions done in the optical domain may be considered as the third-generation of the optical network.

2.1.2 Optical Transport Layer

An optical network consists of nodes that are interconnected in one of topologies such as mesh, ring and point to point networks. For their effectiveness and efficiency, the optical network is described in terms of functionality that is related to payload transport, multiplexing, service and network supervision. To meet network efficiency, the optical transport network at the transmitting side is composed of independent transport layer networks [KNI 08]. The optical transport network (OTN)

was developed for a long-haul transport at data rates from 2.5 to 40 Gbps per optical channel. In addition, OTN can support unidirectional, bidirectional point-to-point connections and unidirectional point-to-multipoint connections.

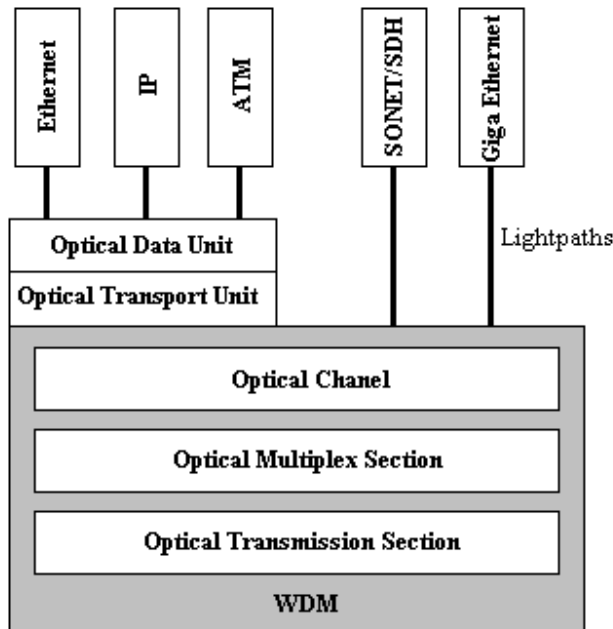


Figure 2-1: The mapping sequence of OTN over WDM

The OTN structure consists of three layers: the optical channel, the optical multiplex section, and the optical transmission section layer networks as described in [KNI 08]:

- The *optical channel layer network* provides end-to-end networking of optical channels to convey transparently client information in different formats, such as SONET/SDH and ATM. This is accomplished by including capabilities such as optical channel connection rearrangement for flexible network routing, optical channel overhead ensuring integrity of the optical channel adapted information, optical channel OA&M functions (operations, administrations, and maintenance) for enabling connection provisioning, quality of service parameter exchange, and network survivability.
- The *optical multiplex section layer network* provides functionality for networking of a multi-wavelength (WDM) optical signal. This is accomplished by including capabilities such as optical multiplex section overhead to ensure integrity of the multi-wavelength optical multiplex section adapted information, optical multiplex section OA&M for enabling section level operations and management functions and multiplex section survivability.
- The *optical transmission section layer network* provides functionality for the transmission of optical signals on optical media of various types. This is accomplished by including capabilities such as optical transmission section overhead processing to ensure integrity of the optical transmission section adapted information, optical transmission section OA&M for enabling section level operations and management functions and transmission section survivability.

The OTN is defined to transport different optical signals over WDM. Using WDM technology, it is possible to transmit over optical channels both SONET/SDH and Gigabit Ethernet frames without encapsulating their frames into an optical transport unit.

2.1.3 Transmission Techniques

This section introduces keys of optical transmission techniques. In order to provide a very high transmission rate, the fiber-optic transmission capacity has been increased by using multiplexing techniques. In fact, there are two main multiplexing techniques: Time-Division Multiplexing (TDM) and Wavelength-Division Multiplexing (WDM). Now, we present these two main concepts that are shortly described in [MGH 01].

Time-division multiplexing (TDM)

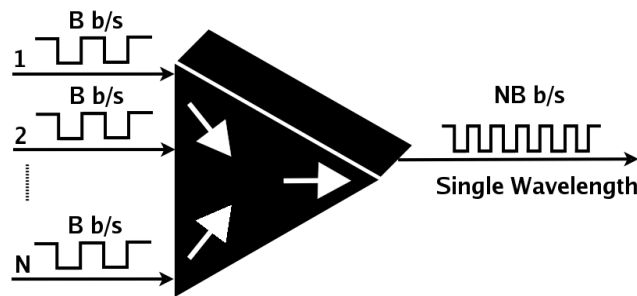


Figure 2-2: Time-division multiplexing

It is a scheme in which numerous signals are combined for transmission on a single communication line or channel. Each signal is broken up into many segments, each having a very short duration. The circuit, that combines signals at the transmitting end of a communication link, is known as a *multiplexer*. It accepts the input from each individual end-user, breaks each signal into segments and assigns segments to the composite signal in a rotating, repeating sequence. The composite signal thus contains data from all end users. At the other end of the long-distance cable, individual signals are separated by means of a circuit called a *demultiplexer* and routed to proper end users. This is shown in Figure 2-2 with a bridge analogy.

Wavelength-division multiplexing (WDM)

WDM is a technology which multiplexes multiple optical carrier signals on a single optical fiber by using different wavelengths (colours) of laser light to carry different signals. A fiber optic device is used to separate signals of different wavelengths carried on one fiber. Several signals can be sent along an optical fiber using lights of different frequencies (colors). At the receiving end, WDM “listens” to different frequencies and separates different signals. This is shown in Figure 2-3.

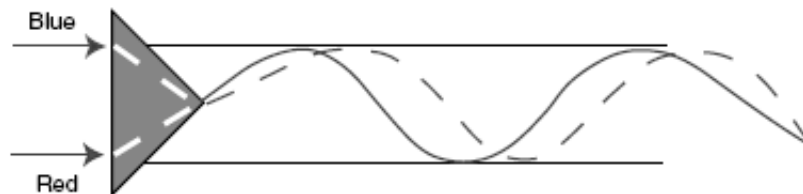


Figure 2-3: Wave-division multiplexing uses different wavelengths (frequencies) of light.

Combination of TDM and WDM multiplexing

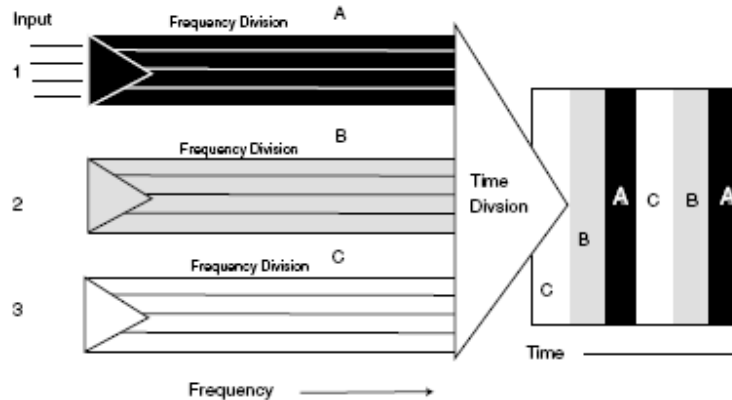


Figure 2-4: Combination of TDM and WDM multiplexing

By using the combination of frequency (different wavelengths) and time (timeslots), the fiber can be used to carry orders of magnitude more than traditional fiber based systems. Figure 2-4 shows the combination of two multiplexing arrangements in a single format.

Dense Wavelength-division multiplexer (DWDM)

Dense WDM was developed to produce even better results on a single fiber pair than original techniques deployed. Expanding capacity with DWDM can produce some significant improvements for today’s technology. Using different light wavelengths, DWDM simultaneously transmits densely packed data streams on a single fiber. Currently, thanks to DWDM, single fibers have been able to transmit data at speeds up to 400 Gbps. DWDM-based network can transmit data in IP, ATM, SONET/SDH and Ethernet at different speeds over an optical channel.

2.1.4 Wavelength routing techniques

Standing beside transmission techniques, the wavelength routing technique is also considered as one of key elements of existing optic technologies. The basic idea of the wavelength routing is to reuse a maximum capacity of same wavelengths. Figure 2-5 illustrates the network enabling the wavelength routing in which the same wavelength is used several times.

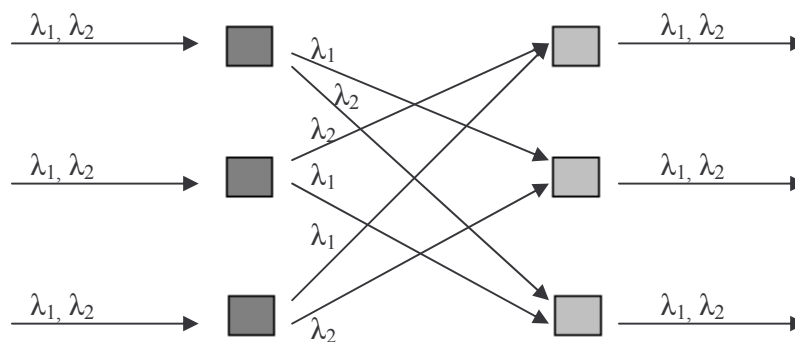


Figure 2-5: Wavelength routing

The above architecture corresponds to a fixed routing based on wavelengths. We can also develop wavelength routing networks with the dynamic routing in the time domain. Therefore, it is necessary to insert optic or opto-electronic switches between input and output gates. An example of this technique is illustrated in Figure 2-6.

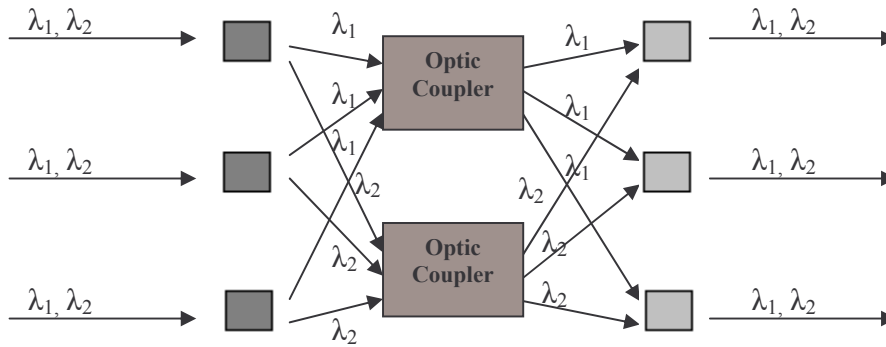


Figure 2-6: Dynamic routing

2.2 Emergence of Wavelength-Division Multiplexing

SONET/SDH was the hottest discussion topic in terms of emerging backbone fiber standards of all future telecommunication networks. Both SONET and SDH were promised for carriers in developing multiplexing standards and techniques to reinforce their networks. Ten years ago, WDM suddenly became a big promise. Researchers and engineers alike saw the benefit that multiple wavelengths could add to the capacity of fiber-based networks. In fact, SONET/SDH standards were originally designed for TDM systems. Using TDM, a data stream at a higher bit rate is directly generated by multiplexing lower-bit-rate channels. The high-capacity TDM system operates at levels up to 10 Gbps. The problem comes with moving to higher bandwidth speeds. The current TDM equipment has trouble operating at these higher speeds. In contrast, WDM (and then DWDM) emerges as a reliable technology, which can carry multiple data bit rates. It enables multiple channels to be carried on a single fiber. [FOM 07] exhibits the benefit of the WDM dimension by adapting rapid traffic growth. This technology also includes the optical switching for recovering from failures as well as the expansion of add/drop multiplexing functions.

2.3 Optical Access Network

Telecommunication networks are normally classified into a three-tier hierarchy: access, metropolitan, and long-haul (backbone). The long-haul (backbone) network extends inter-regional/global distances (1000 km or more) and is optimized for transmission and related costs. At the other end of the hierarchy is the access network, providing the connectivity to end-users. Standing in the middle is the metropolitan (metro) network, averaging regions from 10 to 100 km and interconnecting access and long-haul networks.

The access network, known as the "first-mile" network [OWN 06], connects the service provider central offices (COs) to businesses and residential subscribers. Subscribers demand first-mile access solutions that have a high bandwidth, offer Internet services, and are comparable in price with existing networks. Also, this is a broadband infrastructure in which local-area networks can be connected to the Internet backbone.

Backbone network operators currently provide high-capacity (about 10Gbps) links. However, current-generation access network technologies such as Digital Subscriber Loop (DSL) provide 1.5Mbps of downstream bandwidth and 128kbps of upstream bandwidth at best. Hence, the access network becomes the bottleneck for providing broadband services such as video-on-demand, interactive games, video conference... to end users. Therefore, faster access-network technologies are clearly desired for next-generation broadband applications. The FTTx model - Fiber-to-the-Home (FTTH), Fiber-to-the-Building (FTTB)...- offers the potential for unprecedented access bandwidth to end users. These technologies aim at providing fiber connection directly to the home. FTTx solutions are mainly based on the Passive Optical Network (PON). The comparison between different access mechanisms is presented in Figure 2-7.

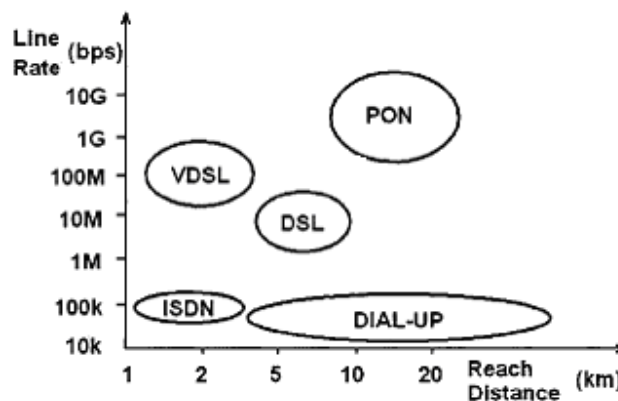


Figure 2-7: The comparison between different access mechanisms [OWN 06]

Optical fiber is capable of providing bandwidth-intensive at distances of 20 kilometers or beyond in the subscriber access network. A logical way to deploy optical fiber in the local access network is to use a point-to-point (PtP) topology, from the CO to each end-user subscriber (Figure 2-8a). This deployment way uses very long fiber length as well as high numbers of connector terminals, leading to excessive cost. For instance, considering N subscribers at an average distance L km from the central office, a PtP design requires $2N$ transceivers and $N \times L$ total fiber length (assuming that a single fiber is used for bi-directional transmission).

To reduce fiber length, it is possible to deploy a curb switch as show in Figure 2-8b but it requires electrical power at the curb switch. Therefore, it is better to replace the curb-side switch by an inexpensive passive splitter. Passive Optical Network (PON) is a technology viewed as an attractive solution to the first-mile problem. PON minimizes the number of optical transceivers, CO terminations, and fiber length. A PON is a point-to-multipoint (PtMP) optical network with no active elements in the signal path from source to destination. An access network based on a single-fiber PON only requires $N+1$ transceivers and L km of fiber (Figure 2-8c).

The most innovative options of PONs are Ethernet PON (EPON), ATM PON (APON), and Gigabit PON (GPON). However, GPON offers some technique advantages over EPON. This is due to GPON's higher splitting ratio, line rate, and bandwidth efficiency. These advantages may result in important reductions in the number of required CO nodes. On the contrary, EPON equipment costs may be significantly lower than the cost of GPON equipments. In addition, EPON presents a well-know infrastructure based on the Ethernet layer. Consequently, the number of researches on the EPON's bandwidth allocation for recent years increases rapidly. Chapter 6 of this dissertation is devoted to investigate different schemes for the bandwidth allocation in EPON.

Furthermore, another PON technology called WDM-PON, is widely believed to be the route towards the next generation of PONs. Recently the interest in WDM-PONs has grown significantly, especially in parts of Asia. The technology challenge for WDM-PON has been to avoid the need for

expensive wavelength components in each end-user. In practice, this means that it is cost prohibitive to use types of lasers currently available for the long haul dense WDM (DWDM) transmission within a WDM-PON. Moreover, it would be impractical for each terminal to be built with a fixed single wavelength laser because managing the inventory of lasers would be complex and costly for the network operator.

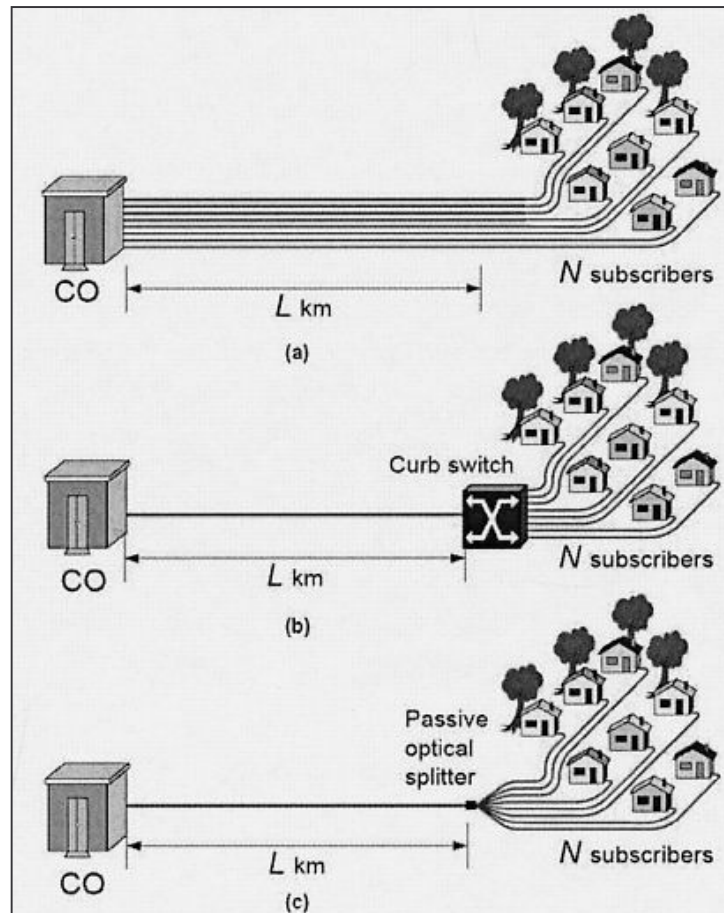


Figure 2-8: Fiber-to-the-Home deployments [OWN 06]

2.4 Optical Metropolitan Area Network (OMAN)

Metro networks today are based on the SONET/SDH optical network ring architecture. It provides a common solid infrastructure over which various services could be delivered. Namely, an inter-office (IOF) ring interconnects central office (CO) locations at higher bit rates, e.g., OC-48/STM-16 (2.5 Gbps).

The topology of a MAN may be ring, mesh, bus... Among them, the ring topology is widely used in MAN. For instance, there are many standards for MAN having the ring topology such as Fiber Distributed Data Interface (FDDI) [FDI 86] token ring, Distributed Queue Dual Bus (DBDQ) [DQB 91]. This is due to the fact that the ring topology facilitates the switching decision as well as routing algorithms. Indeed, to address data to a destination, a ring node transmits data on the existing direction in which the node can receive it. On the other hand, if a problem occurs such as link cut or

node failure, data may be redirected to the other direction of the ring during only a negligible time thanks to simple routing algorithms.

2.4.1 Switching Technique Evolution

As mentioned above, MAN is constructed over SONET/SDH based on the circuit switching technology. SONET/SDH standards were originally designed for TDM but current TDM equipments have trouble operating at high speed. The most important limitation of SONET/SDH is the lack of flexibility and scalability to deal with new services such as distributed applications, center data storage... One of other important disadvantages of the circuit switching is the long-term established connection. This means that a SONET/SDH connection is usually established and dimensioned for some months or years, and then traffic transported into this connection must be unchanged. If such connection type is terminated or MAN opens a new connection, SONET/SDH needs a very long time to reserve a new circuit. Therefore, the circuit switching may not be able to accommodate the bursty nature of Internet traffic in an effective manner [SRT 05].

As optical switching technology improves, the emergence of a photonic packet-switched network in which packets are switched and routed independently through the network entirely in the optical domain without conversion back to electronics at each node is predictable. Such optical packet-switched (OPS) network allows a greater degree of statistical multiplexing on optical fiber links and is better suited for handling bursty traffic than the optical circuit-switched network.

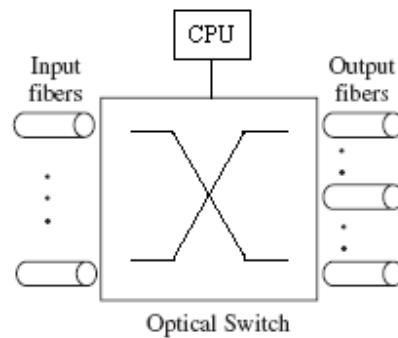
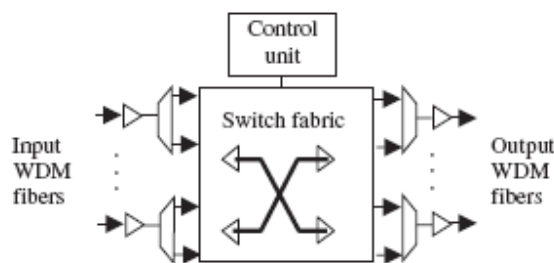


Figure 2-9: Optical packet switch

Nevertheless, the statistical multiplexing property introduces packet contentions at the output node entry. Contention occurs whenever two or more packets try to leave the photonic switch at the same output port on the same wavelength. In an optical packet switch, since the electronic memory is not used, thus a contention problem may be resolved by one of following methods: deflection routing, feedback, spectral resolution or temporal resolution.



a. Reference OBS Switching

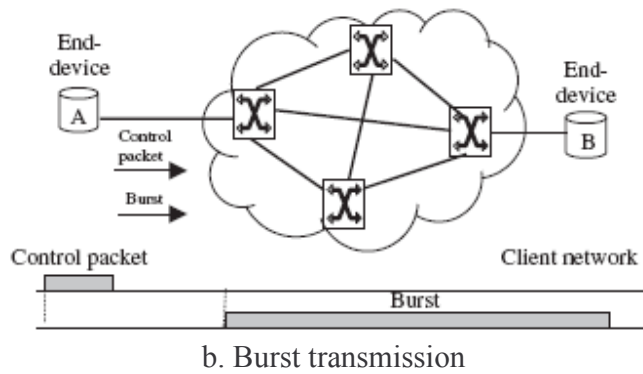


Figure 2-10: Optical Burst Switching: Reference OBS Switching and Burst transmission

Another challenge in the OPS is the synchronization. In a synchronous OPS network, time is slotted, and the switch fabric at each individual node can only be reconfigured at the beginning of a slot. All packets in a synchronous network have the same size, and the duration of slot is equal to the sum of the packet size and the optical header length. The synchronization of packets at switch input ports is often desired in order to minimize the contention.

An optical burst switching (OBS) is designed to achieve a balance between the optical circuit switching and the optical packet switching. In an OBS scheme, the user data is collected at the edge of the network, sorted by destination address and transmitted across the network in variable size bursts. Prior to the transmission of each data burst, a control packet is sent into the network in order to establish a memory-less connection all along the way to the destination. The offset time (Figure 2-10) allows the control packet to be processed and the switch to be set up before the burst arrives at the intermediate node; thus, no electronic or optical buffering is necessary at intermediate nodes while the control packet is being processed.

By reserving resources only for a specified period of time rather than reserving resources for an indefinite period of time, resources can be allocated in a more efficient manner and a higher degree of statistical multiplexing. Thus, the OBS is able to overcome some of limitations of the static bandwidth allocation incurred by the optical circuit switching. Furthermore, since data is transmitted in large bursts, the optical burst switching reduces the technical requirement of fast optical switch.

Optical Switching Techniques	Bandwidth Utilization	Setup Latency	Switching Req.	Speed	Proc. Overhead	Traffic Adaptively
Optical Circuit Switching	Low	High		Slow	Low	Low
Optical Packet Switching	High	Low		Fast	High	High
Optical Burst Switching	High	Low		Medium	Low	High

Table 2-2: Comparison of different all-optical network technologies

Table 2-2 summarizes the three different all-optical transport paradigms [SRT 05]. The table shows that the optical burst switching has the advantages over both optical circuit switching (and wavelength routed networks) and optical packet switching. Although the optical burst switching seems to offer advantages over the optical circuit switching and the optical packet switching; several issues, including burst assembly, signaling schemes, contention resolution, burst scheduling and quality of service, need to be considered before the optical burst switching can be deployed in the metropolitan network.

2.4.2 Well-known OMAN Architectures

Resilient Packet Ring (RPR) standing for Packet Add/Drop Multiplexer (ADM) solution has attracted much focus in the recent years. RPR defines a modified Ethernet *media access control* (MAC) protocol running over dual “ringlets” comprising multiple “Packet ADM” nodes. Each ring node contains electronic-buffers in a transit line, and forward transparently transit packets. RPR uses various methods to increase bandwidth “re-use” across a ring, i.e., *bandwidth multiplication* [RPR 03]. As a result, the total ring throughput of a spatial reuse packet ring can be significantly higher than the capacity of a single link. So, both ringlets can simultaneously carry working traffic and only need to activate the protection capacity during failure events. Additionally, RPR is cost-effective for the packet transport. Packet ADM nodes are deployed to deliver a large converged service, e.g., data (Internet, LAN extension, storage extension), voice-over-IP, video-conferencing, virtual leased line.

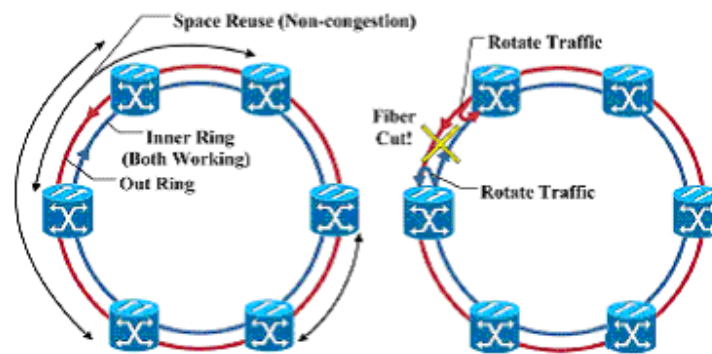


Figure 2-11: Resilient Packet Ring

Another famous architecture for metro network is Dual Bus Optical Ring Network (DBORN [DBO 04]) which functions in the asynchronous mode. This considered network logically consists of two unidirectional buses: upstream and downstream. In the upstream bus, access nodes share a common transmission medium for carrying their traffic to a centralized node (called Hub node) while the downstream bus carries traffic from Hub node to all access nodes. For the cost-effective solution, each ring node possesses passive components, leading to the fact that they can not drop any transit packets in upstream line. Another different point of DBORN with regard to RPR is the replacement of inline-buffers by Fiber Delay Line (FDL). Thanks to FDL, instead of containing transit packets in the electronic buffer, DBORN’s access nodes delay each optical transit packet in several time units (a Maximum Transmission Unit). In this context, the access node does not require O/E/O conversion as compared to RPR, in the upstream transit line. DBORN employs optical unslotted CSMA/CA protocol for detecting voids between two consecutive optical transit packets, which are usually occurred in the asynchronous mode. Since all transit packets pass across the FDL, CSMA/CA protocol can measure the size of voids and notify the node of inserting a local packet in the detected void.

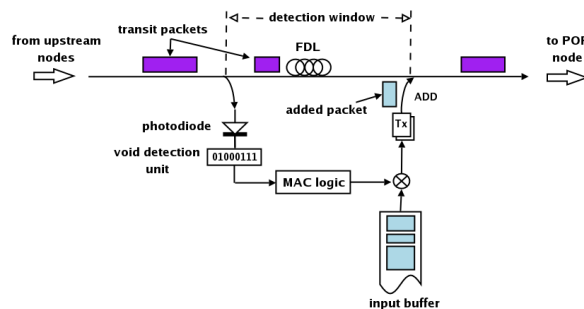


Figure 2-12: CSMA/CA protocol

A well known optical architecture, SONET/SDH ring network, can be also applied for OMAN architecture. SONET/SDH ring networks provide multiplexing efficiency, reliability and timely transport of client signals but they require a high infrastructure cost and the protocol complexity for client signals. The most common implementation today is GFP (generic framing procedure) over a SONET/SDH physical layer to supports all existing protocols at client layers. GFP protocol approved by ITU-T (International Telecommunication Union) provides a framing format capable of supporting a diverse array of higher-layer protocols over any transport network. GFP supports two protocol mapping modes: frame mode and transparent mode. These two mapping modes are able to map all existing and emerging protocols. The frame mode is capable of adapting packet (ou PDU) oriented protocols while the transparent mode is defined for adapting time-sensitive protocols that require very low transmission latency. The high cost of deploying high-speed data services over SONET/SDH network has retarded many service operators to update their existing network.

2.4.3 POADM ring network

Through this section, a new Optical Packet Switching Ring (OPSR) network architecture, which is promising for the next generation of MAN, is presented. This architecture is based on an all-optical infrastructure that offers equivalent features with lower cost while maximizing processing time as compared to other well-known architectures such as RPR or DBORN.

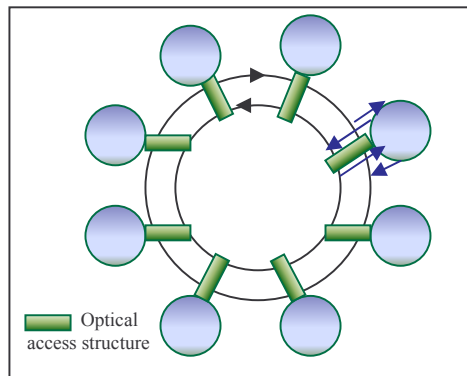


Figure 2-13: Bidirectional POADM ring network

The key element of such network is Packet Optical Add/Drop Multiplexer (POADM) (as shown in Table 2-3 [ECO 08]), so-called POADM ring network. POADM is necessary to deal with the WDM dimension in the optical domain while significantly reducing packet processing time as compared to the opto-electronic model (RPR). POADM module allows the node to exploit the optical transparency in the transit line. The advantage of POADM over the opto-electronic technology has shown in Table 2-3.

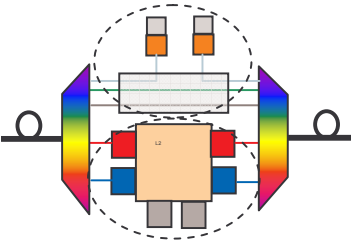
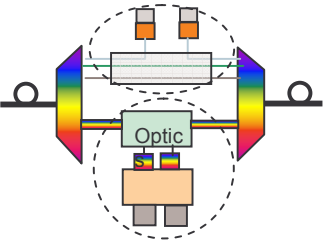
Today (opto-electronic)	Tomorrow (POADM)
	
<ul style="list-style-type: none"> • All the traffic is demodulated • Full capacity required • Correlation between the ring 	<ul style="list-style-type: none"> • Only the dropped traffic is demodulated • Partial capacity required • No correlation between the ring

Table 2-3: Evolution of the optical network architecture

POADM ring network specifications are presented as follows. Basically, POADM nodes are connected by a bidirectional ring (2 fibers), allowing the implementation of security and resilience policies (as mentioned above). The operation on each direction is unidirectional. Thanks to active components, each node can receive, transmit or delete packets in the transit line of the node.

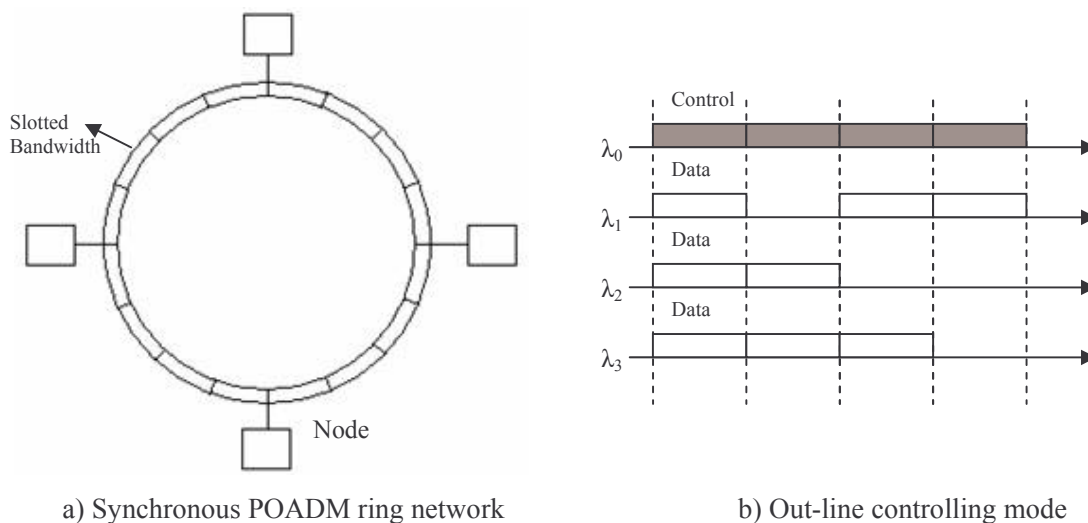


Figure 2-14: Synchronous operation

POADM ring network functions in the synchronous mode with fixed-size packets. This solution avoids the bandwidth fragmentation problem [NGA 05] since the ring path is divided into slots of equal durations (Figure 2-14a). Voids on the ring will be multiple of the slot duration. As shown in Figure 2-14b, the network link consists of several wavelengths: one for synchronization and control procedures, others for data transmission. Each out-line control packet, circulating on the control wavelength, provides information about the corresponding data carried on the same time interval on data channels. The control packet allows the node to detect whether corresponding data slots are occupied by an optical payload which is sent from an upstream node or not. Figure 2-15 shows the

architecture of a POADM node with fixed-size packets. The logical structure of nodes mainly consists of accordable optical transmitters and burst mode receivers.

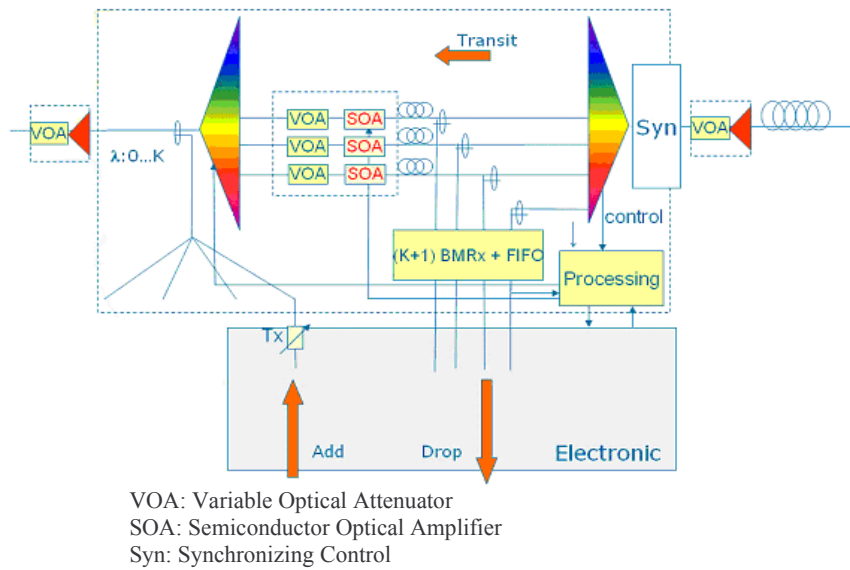


Figure 2-15: POADM node model supporting fixed-size packets

POADM architecture has some advantages as follows:

- It relies on shared optical wavelengths, which contributes to reduce the number of transponders required in the network.
- Transmitters and Receivers are out of the transit line, making it easier for the node to be upgraded, while limiting the service interruption and reducing the protection cost.

The scheme of the POADM model with fixed-size packets in a node is mainly enumerated as follows. Transit packets pass through a synchronization stage before being controlled by the current node. Packet headers are sent in the control plane according to an in-band mode [FOM 06], [FOM 07]. To have sufficient time for the processing of the control packet, each optical transit payload is delayed in a Fibre Delay Line (FDL). In the studied architecture, the traffic coming from client networks consists of small electronic packets of variable-size. These electronic packets are collected and put together into large fixed-size optical payloads (also called optical containers¹). In the following chapters, we refer to this procedure as the *fixed-size packet (container) creation mechanism*. The resulted optical payloads are stored in the Add electronic buffer (also called optical buffer) waiting for transmission on the optical wavelength. At the same time, the node reads control packets (sent by upstream nodes) on the control channel, seeking for free data slots on data wavelengths. The main specification of the node's design is the synchronization. So, if an Add optical payload arrives during a free data slot, it must wait till the end of the slot to be inserted on the next free data slot. The node can insert an Add optical payload while updating the content of the corresponding control packet. The transmission time of each optical payload is equal to timeslot duration. Due to the synchronization, bandwidth is not segmented in the ring. For this reason, POADM ring can be used not only for the metro access but also for the metro core network.

¹ Fixed-size payloads are converted to the optical domain right before being transmitted on the ring. However, we refer to them as optical containers in order to distinguish them from incoming client packets.

2.5 Concluding remarks

Metro and access network infrastructures occupy a strategic position in the network hierarchy. Although SONET/SDH has traditionally dominated this space, progressive bandwidth demand have given a rise to serious service provisioning. New technologies, which provide multi-service and the high flexibility with cost-effectiveness, are required in the metropolitan area. To meet urgent requirements, WDM transport is fast rising as the technology of choice.

Given the continuous evolution of end-user demands, it is important to also consider further switching evolutions. Many researchers are studying the optical packet switching to overcome the inherent inefficiencies of circuit-switched optical networks. The key objective of the optical packet switching is to perform as much of the packet routing operation (switching, buffering...) in the optical domain as possible. Although this technology is currently in its infancy, continuous advances are showing much promise.

At the end of this chapter, a promising architecture (called POADM ring network) has been introduced. Its main characteristics are the followings: firstly, its nodes own active optical components; secondly, it supports synchronous protocol for controlling access to medium. Since this type of network is still at its experimental stage, hence there are a lot of problems that must be solved before it becomes commercialized. Two of the most important questions are: the performance of the POADM ring network and whether the network is able to deliver QoS to end-users. The remainder of this dissertation is dedicated to answer these questions.

Chapter 3

Packet Delay Analysis and Queue-length Distribution of Optical Synchronous Bus-based Network

In this chapter, we investigate the performance analysis (in terms of packet delay and queue-length distribution of access nodes) of an optical synchronous bus-based metropolitan network supporting fixed-size packets. The network may be considered as a particular case of the synchronous POADM ring network. The considered network is a unidirectional bus on which many nodes compete to transmit fixed-size packets to a centralized Hub node on a single wavelength. In such network, access nodes are equipped with passive components, leading to the fact that last nodes on the bus can not interrupt the coming traffic from first nodes. For performance analysis purpose, we model each access node by an embedded discrete time Markov chain (EDTMC). The solution of the EDTMC allows us to compute the approximate probability that access nodes on the bus “see” the free slot in the transit line. Using a recursive analysis technique, we approximately outline the mean waiting time of client packets coming from the upper layer as well as an approximate queue-length distribution of the local buffer at access nodes in two cases: with and without Quality of Service (QoS) guarantee.

3.1 Introduction

The asynchronous OPSR supporting CSMA/CA protocol uses ring topology, in which a master (Hub) node communicates with access nodes in a point-to-multipoint mode, and access nodes communicate with the master node in a multipoint-to-point mode. A major problem in such architecture is how to efficiently control the access to transmission resources for the upstream communication, where many access nodes compete for sending packets to the Hub node. It may exhibit the unfairness property when upstream nodes (the nodes that are closest to the beginning of the shared transmission medium) monopolize all bandwidth and prevents other downstream nodes from transmitting. Additionally, the asynchronous network suffers from the bandwidth fragmentation problem because it supports the variable packet format. Small voids created at upstream nodes increase the unfairness transmission at downstream nodes.

We consider in this work a synchronous bus-based MAN, and specially focus on the upstream multipoint-to-point communication. The upstream bus is a unidirectional bus connecting a number of access nodes to the Hub. The bus consists of two wavelengths: one for the data transmission, the other

for the synchronizing and controlling purpose. The time is slotted into fixed length slots and an access node can insert a fixed-size packet of the same length at the beginning of each time slot. In order to reduce the network cost, access nodes use optical passive components (coupler) on the data plane. Therefore optical packets sent by an upstream access node transparently pass through downstream access nodes to the Hub. And downstream access nodes can only insert optical packets into empty slots left by upstream access nodes.

In such a typical bus-based network, it is well known that the performance of an access node strongly depends on its position on the bus due to the transmitting correlation with other upstream nodes. The mutual correlation among bus nodes makes the performance analysis of such types of network difficult. For the asynchronous bus-based network, there have been a number of works (e.g. [TNH 06]) that approximately computed the queue length distribution (and hence the mean queue length) of each access node on the bus. To our knowledge, there have been also some works that specifically investigated the analytical model of the synchronous bus-based network with passive optical components such as [CCH 05], [HGJ 05], [TTE 08]. Regarding M/G/1 priority queuing systems, [CCH 05], [HGJ 05] following Jaiswal [JAI 66] and Takagi [TAK 91] are commonly derived the mean waiting time at each ring node while [TTE 08] uses numerical methods to obtain the stationary probability of the free slot in the transit line before computing the mean waiting time but obviously no works approximately computed the queue length distribution in the synchronous network.

To estimate the queue length distribution, we model the steady-state queue-length of each class of service in the access node by an EDTMC thanks to the probability that the access node “sees” the free slot in the transit line (so-called free probability). Hence, we use a level-by-level (node-by-node) analysis technique from the upstream node to the downstream node. In this context, a downstream node “sees” only the state of a slot when upstream nodes completely finished their “decision” over this slot. “Decision” means that the node can use or release the slot. To be able to solve EDTMCs, we need to know these free probabilities that are usually unknown parameters. Fortunately, for node 1, the probability that it “sees” the free slot is always equal to 1. Thus, from the solution of node 1, we are able to compute the probability that the next downstream node “sees” free slots, and so on.

The detail of this chapter is organized as follows. We first describe our analytical model based on EDTMCs. Next, we present the node-by-node analysis technique, and then outline an approximate formula computing the mean waiting time as well as an approximate queue-length distribution of the local buffer at access nodes thanks to free probabilities, in two cases: without and with QoS guarantee. Numerical results are then provided, and compared with simulation results. Finally, we give some conclusions and discussions of future works.

3.2 Studied Network Architecture

3.2.1 Network Architecture Description

The upstream bus of the optical slotted bus-based network considered in this work consists of two wavelengths (Figure 3-1). The data wavelength is shared by access nodes for data transmission. The control wavelength is used by access nodes for sending control packets containing the information about respective optical payloads and slots circulating on the data wavelength. In order to reduce the network cost, a network node uses passive optical components in the data plane, in the sense that the incoming transit optical payloads pass transparently without being converted to electronic signals or dropped by intermediate nodes. There is no direct communication between access nodes in this architecture. Any communication between two nodes is done through the Hub node (the so-called “hub and spoke” architecture). We recall that the downstream communication is out of the topic treated in this work.

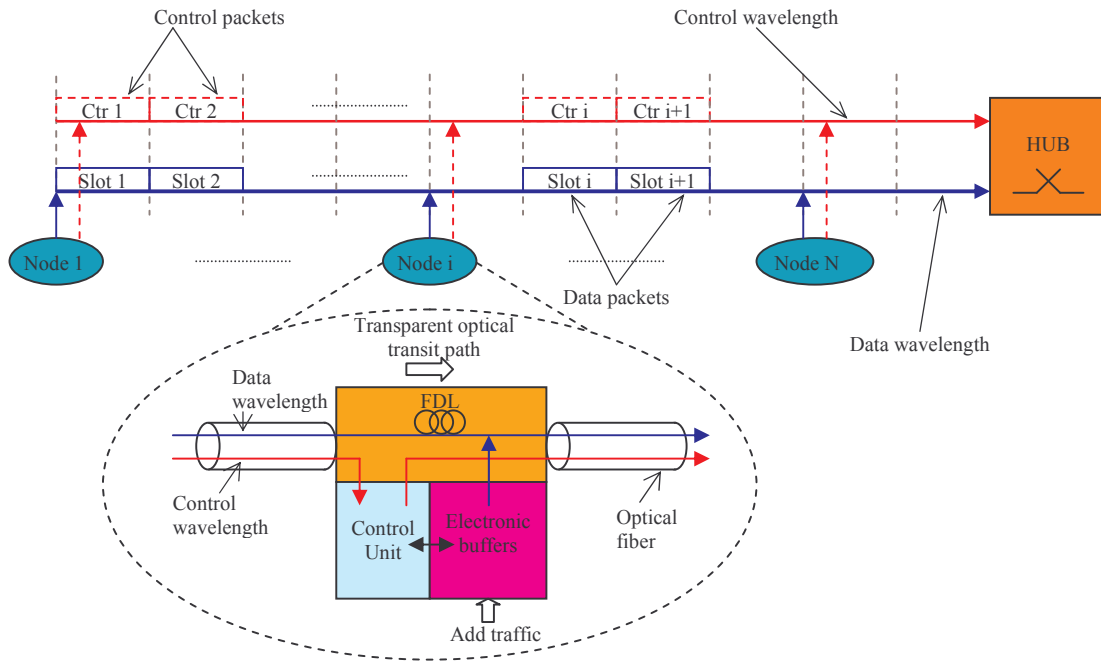


Figure 3-1: Network and node architecture

As shown in Figure 3-1, the time is slotted into fixed length slots. Each control packet circulating on the control wavelength allows the node to detect whether the corresponding data slot is *free* or *busy* (i.e., occupied by an optical payload sent by an upstream node). To have sufficient time for the processing of control packets, each optical transit payload in considered network is delayed in the Fibre Delay Line (FDL) of the node. Here we consider the FDL length equal to one time slot.

3.2.2 Considered Model

In the first time, we try to model the network without Quality of Service (QoS) guarantee. From the modelling perspective, we describe the operation of the optical slotted bus-based network as follows. An access node transmits its local packet as soon as it detects a free slot in the transit line. On the other hand, the transmission will be blocked when the transit slot is occupied by an upstream node. Thus the local packet must wait in the local buffer until the next free slot. At the detection of the next free slot, the node starts again transmitting the packet. The process repeats until the packet is successfully transmitted. For modelling purposes, a successful transmission of a packet in the synchronous network may be viewed as the number of occupied slots followed by one successful transmission.

We assume that the network with N access nodes sharing one wavelength operating at R Gbps (Figure 3-2). Starting with the most upstream node (highest priority), we number nodes from 1 to N , so that an upstream node i has priority over a downstream node j : $1 \geq i > j \geq N$. We assume that each node has an infinite local buffer (so-called the Add buffer), and client packets stored in the Add buffer are served in the First-Come-First-Serve (FCFS) order. We also assume that client packets arrive at node i according to the Poisson process with a rate λ_i without the optical fixed-size packet creation, and that their service time is deterministic. In other words, Poisson sources directly generate client packets having the fixed-size equal to a timeslot duration (the packet size is measured in time

units). The assumption of Poisson process simplifies the modelling since the Poisson’s packet arrival distribution is exponential.

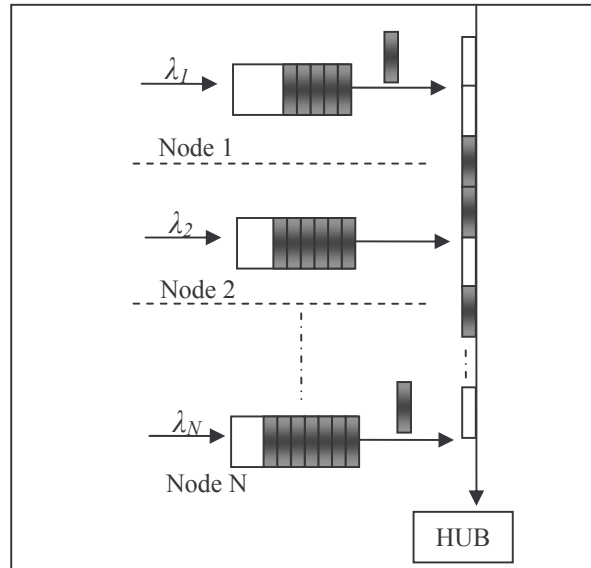


Figure 3-2: The considered network with N access nodes (mono-service case)

In the second time, we will model the network supporting multi-service. In this case, each node encloses M electronic buffers in order to accommodate a number of M Classes of Service (CoS). These buffers have unlimited capacity. Figure 3-3 shows the queuing system inside a ring node. We suppose that packets CoS_q (which size equal a timeslot duration T) arrive to node i following the Poisson process with a rate $\lambda_{i,q}$.

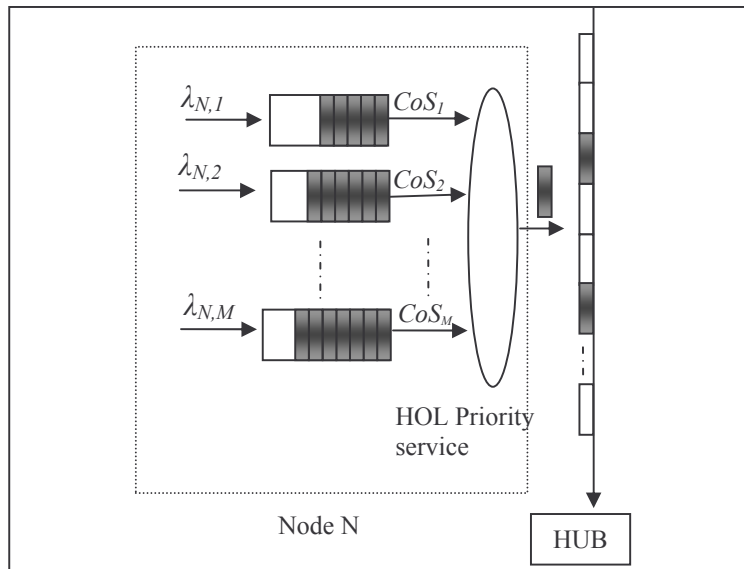


Figure 3-3: Queuing system inside an access node supporting multi-service (multi-service case)

Hereafter, we consider a ring node i in which, local queues are served in the HOL (Head-Of-the-Line) priority scheduling discipline. In such priority queuing system, the priority order is described as: $CoS_1 > CoS_2 > .. > CoS_M$. In this context, transit slots are firstly “served” by buffer CoS_1 and then by buffer CoS_2 ... so on. Thus, the steady state of a slot is “viewed” by node $(i+1)$ when buffer CoS_M at node i finished its “decision” over the slot.

3.3 Embedded Discrete Time Markov Chain (EDTMC) Approach

To obtain a tractable model for considered network, we are interested in particular moments in the evolution of states of the system. Instead of analyzing the state of the system at continuous time, we analyze the state of the system at discrete moments t_k [BBH 00] that are the beginning of each data slot $k, k = 1, 2, 3, \dots$, with $t_{k+1} = t_k + T$ where T is the slot length. This consideration brings the system to a simple description of state for studying. At the beginning of each timeslot, we have:

- A new optical packet is transmitted if the data slot is free.
- If the data slot is busy, all optical packets must wait in the local buffer until detection of next free data slot.

Therefore, at these moments, the queue-state is completely defined by a number of packets in the Add buffer and the free-busy state of slots.

Let $X_k, k = 1, 2, 3, \dots$, be the number of client packets in the Add buffer at t_k . Let $p_k, k = 1, 2, 3, \dots$, be the state of data slot k at t_k which take values 0 if the slot is busy and 1 otherwise. The couple (X_k, p_k) is enough to predict the later evolution of the system. However, this description has not the Markov property because between two instants (t_k, t_{k+1}) , the evolution of X_k depends on the Poisson arrival of optical packets while the probability p_k depends on an unknown arrival process of the transit traffic coming from upstream nodes.

We may now observe node 1, which is the most upstream node beginning the transmission on the shared wavelength. The probability p_k “observed” at node 1 always equal to 1 at any instant t_k . So, node 1 would be completely characterized by Markov process $\{X_k\}$. With nodes $i > 1$, since we do not know the evolution of the process $\{p_k\}$, so we are only interested in the mean value $p^{(i)}$ of the process:

$$p^{(i)} = \lim_{n \rightarrow \infty} \left(\sum_{k=1}^n p_k \right) / n \text{ (the formula computing } p^{(i)} \text{ will be given in next section). Therefore, to}$$

obtain a well-known model, we suppose that slot k is free with probability $p^{(i)}$ and busy with probability $(1-p^{(i)})$ at any instant t_k . In other words, the mean value $p^{(i)}$ corresponds to the probability that node i “sees” the free slot in the transit line. Replacing $\{p_k\}$ by its mean $p^{(i)}$ in the description of the system, we obtain the process $\{X_k, p^{(i)}\}$. Because $p^{(i)}$ is constant, process $\{X_k, p^{(i)}\}$ thus can be described as $\{X_k\}$ for simplification. It is clear that $\{X_k\}$ is a Markov stochastic process. Figure 3-4 presents the process $\{X_k\}$. We call the probability of having n clients in the Add buffer at t_k as $p_{ts}(n)^{(k)}$. As the definition, we have the equation: $p_{ts}(n)^{(k)} = P[X_k = n]$. For performance analysis purpose, we need to know the stationary probability $\lim_{k \rightarrow \infty} \{p_{ts}(n)^{(k)}\}$.

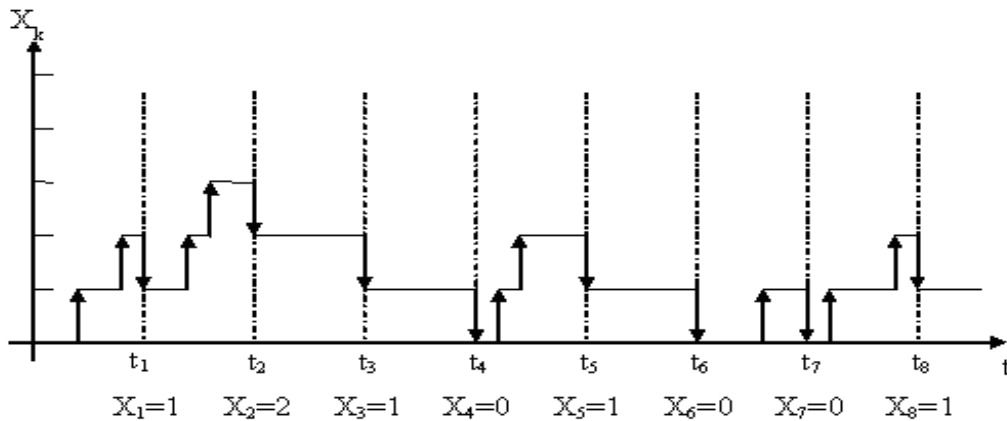


Figure 3-4: The evolution of process $X_k, k = 1, 2, \dots$

We may now consider an access node i ($i \geq 1$), which “sees” the free slot in the transit line with probability $p^{(i)}$. As stated earlier, probability $p^{(i)}$ is constant at any time. By using Poisson process with an arrival rate λ , we have α_c , which denotes the probability so that c packets arrive during a timeslot T , like following:

$$\alpha_c = \frac{(\lambda_i T)^c}{c!} e^{-\lambda T} \quad (3.1)$$

For the multi-class system, the probability so that c packets of CoS_j arrive during a timeslot T as

$\alpha_{(c,j)} = \frac{(\lambda_{(i,j)} T)^c}{c!} e^{-\lambda T}$. Let denote $p^{(i)}(n)$ the probability of having n optical packets in the local buffer: $\lim_{k \rightarrow \infty} \{p^{(i)}_{ts}(n)^{(k)}\}$. So we have the probability corresponding to the empty Add buffer as:

$$p^{(i)}(0) = \lim_{k \rightarrow \infty} \{p^{(i)}_{ts}(0)^{(k)}\} = \lim_{k \rightarrow \infty} \{X(t_k) = 0\} \quad (3.2)$$

We decompose, in particular, the empty state of the local buffer (state 0) into two states: state 0^* and state 0^{**} as follows:

- i. State 0^* that there is no departure at the beginning of the data slot;
- ii. State 0^{**} that there is a packet just sent at the beginning of the data slot;
- iii. From our assumptions, we have: $p^{(i)}(0) = p^{(i)}(0^*) + p^{(i)}(0^{**}) \quad (3.3)$

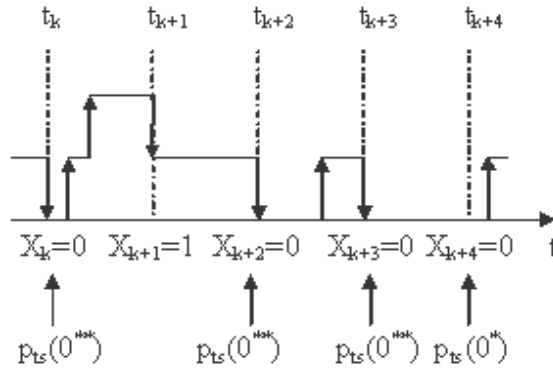


Figure 3-5: Example of $p^{(i)}(0^*)$ and $p^{(i)}(0^{**})$

Figure 3-5 shows two sub-probabilities that we have proposed. Regarding node i , if Add buffer is in state (0^*) , the node releases the current free slot for access node $(i+1)$. So, we have the following equation:

$$p^{(i)}(0^*) = p^{(i+1)} \quad (3.4)$$

For node 1, the probability to find a free slot is always equal to 1, therefore we have $p^{(1)} = 1$. So, using the EDTMC solution, we can approximately compute probability $p^{(1)}(0^*)$ and derive probability $p^{(2)}$ for node 2 to find free slots. The work is recursively realized till the last downstream node.

3.3.1 Outline of the “mono-service” model

In this section, we mainly introduce our model solution in an access node without QoS guarantee. We derive some formulas to approximately compute the mean waiting time of client packets as well as the queue-length distribution.

A. Transition matrix

We may now consider the queue-state of the local (Add) buffer inside node i ($i \geq 1$) just after data slot $(k-1)$. At this instant, we suppose that there are i packets in Add buffer, i.e. $X(t_k) = i$ ($i > 0$). In order to determine possible transitions starting from state i , we are interested in the next evolution: the beginning of slot $(k+1)$. At instant t_{k+1} , we have $(i-1)$ packets in Add buffer if, during a timeslot T , no more packets arrive and slot $(k+1)$ is not occupied by upstream nodes (i.e. the first packet in the Add buffer will be sent). On the other hand, there are $(i-1+c)$ packets in the buffer if, during a timeslot T , c packets arrive and the following slot is free or if $(c-1)$ packets arrive but the following slot is occupied. Thus, we have the probability, that state i returns state $(i-1)$, as $\alpha_0 p^{(i)}$; the probability, that state i returns itself, as $\alpha_0(1 - p^{(i)}) + \alpha_1 p^{(i)}$; and the probability, that state i comes to state $(i+c)$, as $\alpha_c(1 - p^{(i)}) + \alpha_{c+1} p^{(i)}$.

As a result, we have the EDTMC from state i like following:

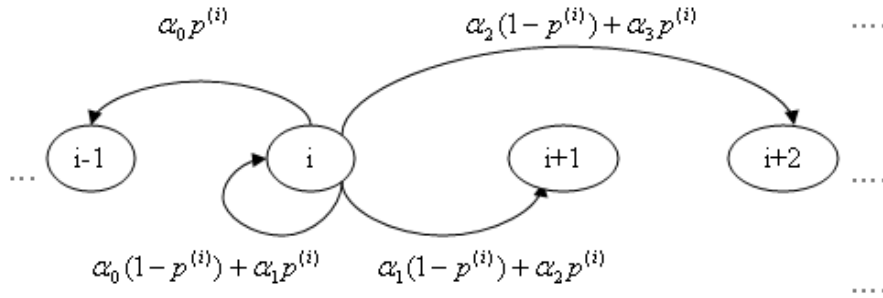


Figure 3-6: Embedded Markov chain from state i ($i > 1$)

Let us consider the case $X(t_k)=0$ in which a packet is sent, leaving Add buffer in the empty state (i.e. the state (0^{**})). As explained above, the probability that state (0^{**}) returns state (0^*) , is equal to $\alpha_0 p^{(i)}$. If no more packets arrive in the current slot and the following slot is occupied by upstream nodes, the system still remains in state (0^{**}) . Additionally, if only a client packet arrives in the current slot and then, this packet is sent in the following slot (if the following slot is free), the system returns state (0^{**}) . On the other hand, the system comes to state c ($c > 0$) if, during a timeslot T , $(c+1)$ packets arrive and the following slot is free; or if c packets arrive but the following slot is occupied. Finally, we have the probability that state (0^{**}) returns itself as $\alpha_0(1 - p^{(i)}) + \alpha_1 p^{(i)}$ and the probability that state (0^{**}) comes to state c like $\alpha_c(1 - p^{(i)}) + \alpha_{c+1} p^{(i)}$. The EDTMC from state (0^{**}) is described as follows:

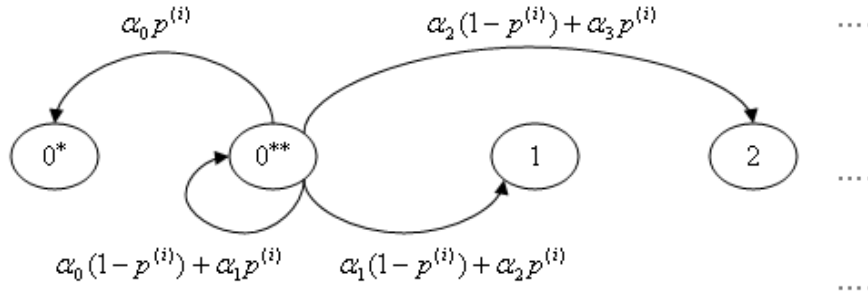


Figure 3-7: Embedded Markov chain from state (0^{**})

Let us consider now the case $X(t_k)=0$ in which no packet is sent (i.e. the state (0^*)). It is not difficult to deduce the embedded Markov chain from state (0^*) thanks to the explanation as mentioned above like following:

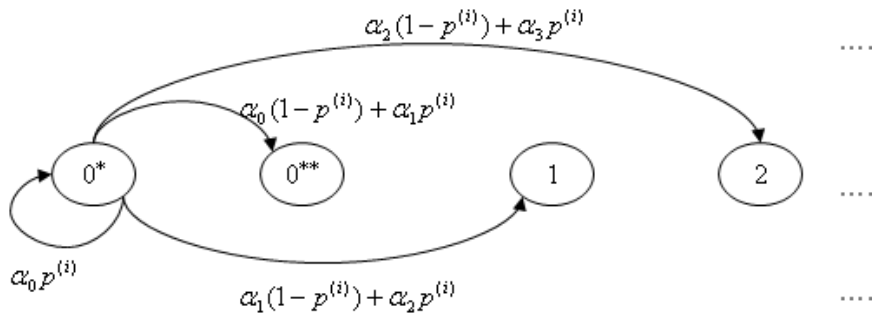


Figure 3-8: Embedded Markov chain from state (0^*)

From EDTMCs that we obtained, we construct the transition matrix of the queue-state for the Add buffer at node i as follows:

$$P = \begin{bmatrix} \alpha_0 p^{(i)} & (\alpha_0(1-p^{(i)}) + \alpha_1 p^{(i)}) & (\alpha_1(1-p^{(i)}) + \alpha_2 p^{(i)}) & \cdots \\ \alpha_0 p^{(i)} & (\alpha_0(1-p^{(i)}) + \alpha_1 p^{(i)}) & (\alpha_1(1-p^{(i)}) + \alpha_2 p^{(i)}) & \cdots \\ 0 & \alpha_0 p^{(i)} & (\alpha_0(1-p^{(i)}) + \alpha_1 p^{(i)}) & \cdots \\ 0 & 0 & \alpha_0 p^{(i)} & \cdots \\ \vdots & \vdots & \vdots & \ddots \end{bmatrix}$$

For simple, we call α'_0 and $\alpha'_k, k \geq 1$ as:

$$\alpha'_0 = \alpha_0 p^{(i)} \quad (3.5)$$

$$\alpha'_k = \alpha_{k-1}(1-p^{(i)}) + \alpha_k p^{(i)}, k \geq 1 \quad (3.6)$$

So the transition matrix P becomes:

$$P = \begin{bmatrix} \alpha'_0 & \alpha'_1 & \alpha'_2 & \alpha'_3 & \alpha'_4 & \cdots \\ \alpha'_0 & \alpha'_1 & \alpha'_2 & \alpha'_3 & \alpha'_4 & \cdots \\ 0 & \alpha'_0 & \alpha'_1 & \alpha'_2 & \alpha'_3 & \cdots \\ 0 & 0 & \alpha'_0 & \alpha'_1 & \alpha'_2 & \cdots \\ 0 & 0 & 0 & \alpha'_0 & \alpha'_1 & \cdots \\ 0 & 0 & 0 & 0 & \alpha'_0 & \cdots \\ \vdots & \vdots & \vdots & \vdots & \vdots & \ddots \end{bmatrix}$$

Notice that obtained chains are irreducible and aperiodic [BBH 00]. All its states are thus recurrent not-null (because of $\alpha'_0 \geq \alpha'_1 + \alpha'_2 + \alpha'_3 + \dots$), this property then allows affirming that stationary probabilities $p^{(i)}(0^*)$, $p^{(i)}(0^{**})$, $p^{(i)}(1)$, ... exist.

Therefore, matrix P can be written in form:

$$\begin{cases} p^{(i)}(0^*) = p^{(i)}(0^*)\alpha'_0 + p^{(i)}(0^{**})\alpha'_0 \\ p^{(i)}(0^{**}) = p^{(i)}(0^*)\alpha'_1 + p^{(i)}(0^{**})\alpha'_1 + p^{(i)}(1)\alpha'_0 \\ \vdots \\ p^{(i)}(k) = p^{(i)}(0^*)\alpha'_k + p^{(i)}(0^{**})\alpha'_k + \sum_{j=1}^k p^{(i)}(j)\alpha'_{k-j} \\ \vdots \end{cases} \quad (3.7)$$

Solving these equations, we obtain $p^{(i)}(0^*) = p^{(i)} - \rho^{(i)}$ (3.8), where $\rho^{(i)}$ is the offered load at node i (the offered load is defined as the ratio of the sum of traffic volume offered to node i to the network transmission capacity). We give in the Appendix additional details of our solution solving the (3.7). Using the first equation of (3.7), we have:

$$p^{(i)}(0) = p^{(i)}(0^*) + p^{(i)}(0^{**}) = p^{(i)}(0^*) / \alpha'_0 = (p^{(i)} - \rho^{(i)}) / \alpha'_0 \quad (3.9)$$

From $p^{(i)}(0)$, we can easily deduce stationary probabilities $p^{(i)}(1)$, $p^{(i)}(2)$, $p^{(i)}(3)$,... Finally, we resume our works in (3.5-9) as follows:

$$\begin{cases} p^{(1)} = 1 \\ p^{(i)}(0^*) = p^{(i+1)} = p^{(i)} - \rho^{(i)} = p^{(i)}(0)\alpha'_0, i \geq 1 \end{cases} \quad \text{with } \alpha'_0 = \alpha_0 p^{(i)}$$

Thanks to stationary probabilities, we may approximately compute the mean waiting time in the next section.

B. Mean waiting time computation

The mean waiting time at a node is defined as the expected time elapsed from the moment when a client packet arrives at Add buffer of the node until its transmission begins. If we consider K timeslots, $K \rightarrow \infty$, observed at node i , then the number of occupied slots equals to the number of client packets transmitted by all upstream nodes $j = 1, \dots, i-1$ during K timeslots. Thus, the probability that a slot is busy seen by node i , is easily computed as follows:

$$1 - p^{(i)} = \frac{1}{K} \sum_{j=1}^{i-1} \lambda^{(j)} * K * T = \sum_{j=1}^{i-1} \rho^{(j)} \quad (3.10)$$

where $\rho^{(j)} = \lambda^{(j)} * T$ is the mean offered load of node j . We have the following equations for $p^{(i)}$:

$$p^{(1)} = 1 \text{ and } p^{(i)} = 1 - \sum_{j=1}^{i-1} \rho^{(j)}, \quad i=2, \dots, N \quad (3.11)$$

It is worth mentioning that (3.11) exactly matches (3.8) which we have demonstrated by using ETDMCs. We may now compute the mean waiting time in Add buffer of node i . Let \overline{W} be the mean waiting time of a client packet, \overline{W}_0 be the mean waiting time of a client packet arriving in an empty buffer, and \overline{W}_n be the mean waiting time of a client packet arriving in a non-empty buffer containing n client packets, we have:

$$\overline{W} = \overline{W}_0 + \overline{W}_n \quad (3.12)$$

Since a client packet can be inserted only at the beginning of a slot, if it arrives during a slot, it must first synchronize to the beginning of the next slot, then looking for a free slot for transmission. We can compute \overline{W}_0 as follows:

$$\overline{W}_0 = p^{(i)}(0) * (\overline{t}_s + \overline{W}_R) \quad (3.13)$$

where \overline{t}_s is the mean synchronization time, and \overline{W}_R is the mean searching time a packet takes to find a free slot and begins its transmission. During a timeslot T , a client packet has the same probability to arrive just after the beginning, or at the middle, or at the end of the timeslot. Thus \overline{t}_s is the mean value of a uniform distribution in interval T :

$$\overline{t}_s = T/2 \quad (3.14)$$

Concerning \overline{W}_R , it is computed as follows:

$$\overline{W}_R = p^{(i)} * 0 + (1 - p^{(i)})[T + \overline{W}_R] \Rightarrow \overline{W}_R = \frac{1 - p^{(i)}}{p^{(i)}} T \quad (3.15)$$

Now we may come to compute \overline{W}_n . A client packet, arriving in the non-empty buffer containing n client packets, must wait for the following services before being transmitted:

- A residual service time \overline{t}_R of the packet being transmitted; since the service has constant length of T , we have:

$$\overline{t}_R = T/2 \quad (3.16)$$

- The service completion time \overline{t}_C of all n preceding client packets; each service completion time is composed of a research time \overline{W}_R for free slot followed by a constant service of length T :

$$\overline{t}_C = \overline{W}_R + T \quad (3.17)$$

- \overline{W}_R that the packet itself must wait to find a free slot for transmission.

Therefore we obtain the following equation for \overline{W}_n :

$$\overline{W}_n = \sum_{n=1}^{\infty} [p^{(i)}(n) * (\overline{t}_R + \overline{W}_R + n * \overline{t}_C)] \quad (3.18)$$

Using the normalization condition $p^{(i)}(0) = 1 - \sum_{n=1}^{\infty} p^{(i)}(n)$ and the Little formula for computing mean waiting time $\overline{W} = \frac{1}{\lambda_i} \sum_{n=1}^{\infty} n p^{(i)}(n)$, combined with equations (3.12) – (3.18), we are able to compute the final formula of \overline{W} :

$$\overline{W} = \frac{\frac{T}{2} + \frac{T(1-p^{(i)})}{p^{(i)}}}{1 - \frac{\rho^{(i)}}{p^{(i)}}} \quad (3.19)$$

The more details of the computation of (3.19) are presented in the Appendix. Notice that the formula computing the mean waiting time depends on the workload and the timeslot as expected. We refer (3.19) as method 1.

Thanks to stationary probabilities that we have, we can directly deduce waiting time as follows (so-called method 2):

$$\overline{W} = \frac{\sum_{n=0}^{\infty} p^{(i)}(n)}{\rho^{(i)}} + \overline{t}_R = \frac{\sum_{n=0}^{\infty} p^{(i)}(n)}{\rho^{(i)}} + \frac{T}{2} \quad (3.20)$$

We have applied two methods (3.19) and (3.20) to compute the mean waiting time of coming client packets in our simulation. As expected they give us the same results of the waiting time.

3.3.2 Outline of the “multi-service” model

We may now apply the method used in the preceding section to the case with QoS guarantee in which each access node supports M classes of service. Theoretically, we can divide one state of EDTMC into 2^M states of the new EDTMC according to the number of classes of service but the number of transition states becomes very large, leading to a very complex chain. So, we propose, in the next sub-section, an approximate solution to simplify the multi-service system.

A. Transition matrix

We now focus the queue-state of the local buffer CoS_j ($0 < j < M$) at node i ($i \geq 1$). It is worth mentioning that the queue-state of the buffer CoS_j depends on the queue-state of the buffer $CoS_{(j-1)}$. Let us denote $p^{(i,j)}$ the probability by which the buffer CoS_j at node i “sees” the free slot in the transit line. Since the traffic coming from upstream nodes is “viewed” by all CoS , hence we have: $p^{(i,j)} = p^{(i)}$ for any class. So, to simplify the transition matrix of the multi-service system, we assume that the buffer CoS_j “sees” a free slot when the buffer $CoS_{(j-1)}$ completely finished its decision over the slot. This means that the buffer CoS_j “sees” only a free slot when the buffer $CoS_{(j-1)}$ is in state (0^*) . Just after data slot $(k-1)$, we suppose that there are i packets in the buffer CoS_j , i.e. $X(t_k) = i$ ($i > 0$). At instant t_{k+1} , we consider two following cases: the buffer $CoS_{(j-1)}$ is in or out of state (0^*) . Thus, we have $(i-1)$ packets (of CoS_j) in the buffer if, during a timeslot T , no more packets arrive and slot $(k+1)$ is not occupied by upstream nodes (i.e. the first packet in the buffer will be sent) while the buffer $CoS_{(j-1)}$ is still in state (0^*) at the same time. On the other hand, there are $(i-1+c)$ packets in the

buffer if, during a timeslot T , c packets arrive and the following slot is free or if $(c-1)$ packets arrive but the following slot is occupied while the buffer $CoS_{(j-1)}$ always remains in state (0^*) . Also, the buffer $CoS_{(j)}$ returns $(i-1+c)$ state if no more packets arrive while at the same time the buffer $CoS_{(j-1)}$ is out of state (0^*) . Figure 3-9 presents the extended EDTMC from state i for the buffer $CoS_{(j)}$.

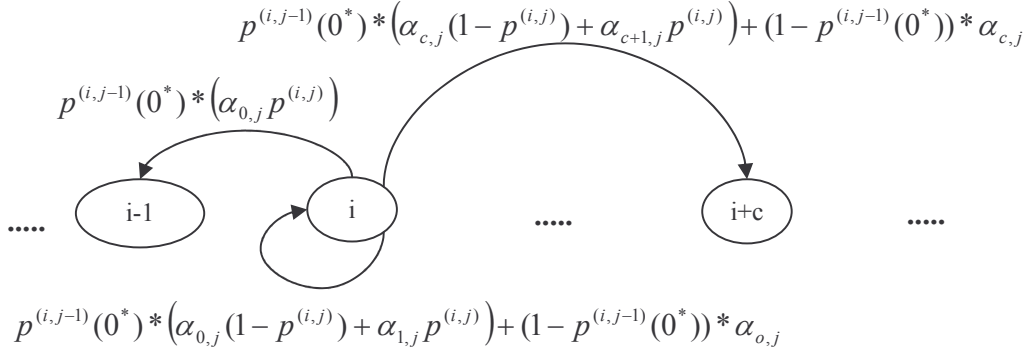


Figure 3-9: Extended Embedded Markov chain from state i ($i > 1$) for the buffer CoS_j

The extended embedded Markov chain from state (0^{**}) and (0^*) is presented like following figures:

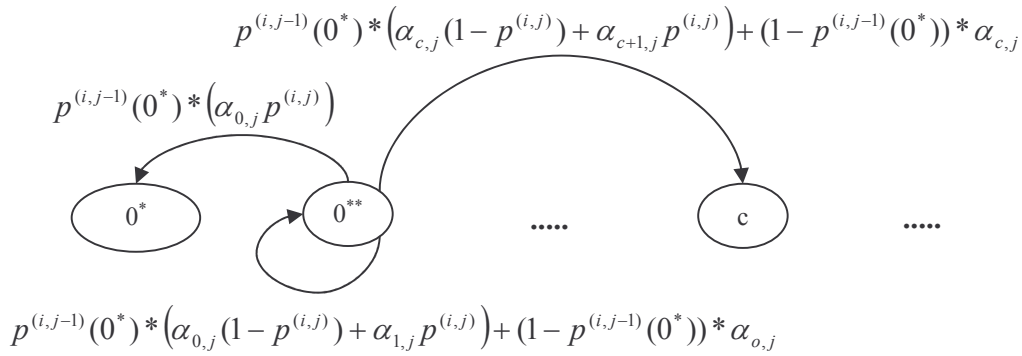


Figure 3-10: Extended Embedded Markov chain from state (0^{**}) for the buffer CoS_j

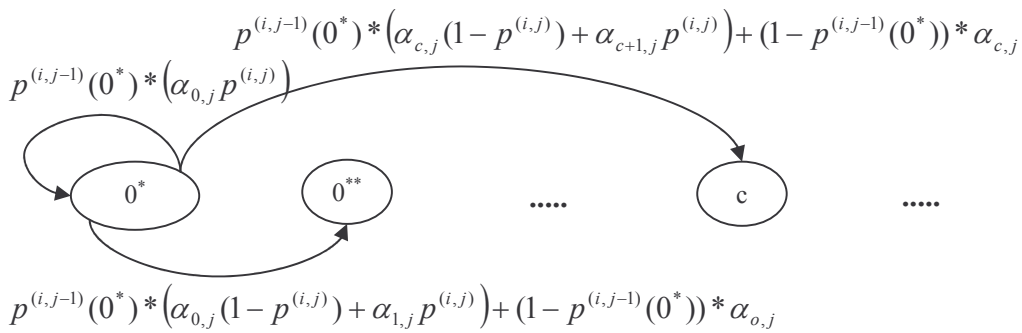


Figure 3-11: Extended Embedded Markov chain from state (0^*) for the buffer CoS_j

For simple, we call α''_0 and α''_k , $k \geq 1$ as:

$$\alpha''_0 = p^{(i,j-1)}(0^*) * (\alpha_{0,j}p^{(i,j)}) \quad (3.21)$$

$$\alpha''_k = p^{(i,j-1)}(0^*) * (\alpha_{k-1,j}(1-p^{(i,j)}) + \alpha_{k,j}p^{(i,j)}) + (1-p^{(i,j-1)}(0^*)) * \alpha_{k-1,j}, k \geq 1 \quad (3.22)$$

From extended EDTMCs that we have, we construct the transition matrix of the queue-state for CoS_j buffer at node i as follows:

$$P' = \begin{bmatrix} \alpha''_0 & \alpha''_1 & \alpha''_2 & \alpha''_3 & \alpha''_4 & \cdots \\ \alpha''_0 & \alpha''_1 & \alpha''_2 & \alpha''_3 & \alpha''_4 & \cdots \\ 0 & \alpha''_0 & \alpha''_1 & \alpha''_2 & \alpha''_3 & \cdots \\ 0 & 0 & \alpha''_0 & \alpha''_1 & \alpha''_2 & \cdots \\ 0 & 0 & 0 & \alpha''_0 & \alpha''_1 & \cdots \\ 0 & 0 & 0 & 0 & \alpha''_0 & \cdots \\ \vdots & \vdots & \vdots & \vdots & \vdots & \ddots \end{bmatrix}$$

Therefore, matrix P' can be written in form:

$$\begin{cases} p^{(i,j)}(0^*) = p^{(i,j)}(0^*)\alpha''_0 + p^{(i,j)}(0^{**})\alpha''_0 \\ p^{(i,j)}(0^{**}) = p^{(i,j)}(0^*)\alpha''_1 + p^{(i,j)}(0^{**})\alpha''_1 + p^{(i,j)}(1)\alpha''_1 \\ \vdots \\ p^{(i,j)}(k) = p^{(i,j)}(0^*)\alpha''_k + p^{(i,j)}(0^{**})\alpha''_k + \sum_{l=1}^k p^{(i,j)}(l)\alpha''_{k-l} \\ \vdots \end{cases} \quad (3.23)$$

Note that matrix P' have the same form as P . Solving these equations, we obtain $p^{(i,j)}(0^*) = p^{(i,j)} p^{(i,j-1)}(0^*) - \rho^{(i,j)}$ (3.24), where $\rho^{(i,j)}$ is the offered load of CoS_j at node i (see the Appendix for more details). Using the first equation of (3.23), we have:

$$p^{(i,j)}(0) = (p^{(i,j)} p^{(i,j-1)}(0^*) - \rho^{(i,j)}) / \alpha''_0 \quad (3.25)$$

Regarding in (3.25), if $p^{(i,j-1)}(0^*) = 1$, it becomes the well-known formula (3.9) corresponding to the case of the mono-class. From $p^{(i,j)}(0)$, we can deduce stationary probabilities $p^{(i,j)}(1)$, $p^{(i,j)}(2)$, $p^{(i,j)}(3)$,... Finally, we resume our works in (3.21-25) as follows:

$$\begin{cases} p^{(i,j)} = p^{(i)} \\ p^{(i,j)}(0) = p^{(i,j)} p^{(i,j-1)}(0^*) - \rho^{(i,j)} / \alpha''_0 \quad i, j \geq 1 \end{cases}$$

Because $p^{(i,j-1)}(0^*)$ can be deduced from $CoS_{(j-1)}$, therefore $p^{(i,j-1)}(0)$ can be easily computed thanks to above equations. In the next section, we try to derive a formula that approximately computes the mean waiting time of client packets resided on the buffer CoS_j at node i , certainly based on $p^{(i,j-1)}(0^*)$ of $CoS_{(j-1)}$.

B. Mean waiting time computation

We may now compute the mean waiting time of client packets in the buffer CoS_j at node i . Let $\overline{W}^{(j)}$ be the mean waiting time of client packets CoS_j , $\overline{W}_0^{(j)}$ be the mean waiting time of client packets arriving in the empty buffer CoS_j , and $\overline{W}_n^{(j)}$ be the mean waiting time of client packets arriving in the non-empty buffer CoS_j containing n client packets, we have the following equation (as the “mono-service” case):

$$\overline{W}^{(j)} = \overline{W}_0^{(j)} + \overline{W}_n^{(j)} \quad (3.26)$$

where:

$$\overline{W}_0^{(j)} = p^{(i,j)}(0) * (\overline{t}_s + \overline{W}_R^{(j)}) \quad (3.27)$$

with \overline{t}_s is the mean synchronization time, while $\overline{W}_R^{(j)}$ is the mean searching time that a packet CoS_j takes to find a free slot and begins its transmission.

Concerning $\overline{W}_R^{(j)}$, it is computed like following:

$$\overline{W}_R^{(j)} = p^{(i,j-1)}(0^*) \overline{W}_R + (1 - p^{(i,j-1)}(0^*)) (\overline{W}^{(j-1)} + \overline{W}_R) \quad (3.28)$$

where $\overline{W}_R = \frac{1 - p^{(i)}}{p^{(i)}} T$ and $\overline{W}^{(j-1)}$ is the mean waiting time of client packets in the buffer $CoS_{(j-1)}$.

(3.28) is explained as follows. When an packet CoS_j arrives, it may be find the buffer $CoS_{(j-1)}$ in the empty state, hence it wait only a time \overline{W}_R in order to be inserted into the medium transit. On the contrary, it must wait a time equal to $(\overline{W}^{(j-1)} + \overline{W}_R)$ before its transmission.

By the same explanation as the “mono-service” case in regarding (3.28), we have the formula to compute $\overline{W}_n^{(j)}$ from following descriptions:

- A residual service time $\overline{t}_R = T/2$ of the packet being transmitted.
- The service completion time $\overline{t}_C^{(j)}$ of all n preceding client packets. Each service completion time is composed of a research time $\overline{W}_R^{(j)}$ for free slot followed by a constant service of length T :

$$\overline{t}_C^{(j)} = \overline{W}_R^{(j)} + T \quad (3.29)$$

- $\overline{W}_R^{(j)}$ that the packet itself must wait to find a free slot for transmission.

We obtain thus the following equation for $\overline{W}_n^{(j)}$ as: (see the Appendix for more details)

$$\overline{W}_n^{(j)} = \sum_{n=1}^{\infty} [p^{(i,j)}(n) * (\overline{t}_R + \overline{W}_R^{(j)} + n * \overline{t}_C^{(j)})] \quad (3.30)$$

Using the normalization condition $p^{(i,j)}(0) = 1 - \sum_{n=1}^{\infty} p^{(i,j)}(n)$ and the Little formula for computing the mean waiting time $\overline{W}^{(j)} = \frac{1}{\lambda_{i,j}} \sum_{n=1}^{\infty} np^{(i,j)}(n)$, combined with equations (3.26) – (3.30), we are able to compute the final formula of $\overline{W}^{(j)}$ as follows:

$$\overline{W}^{(j)} = \frac{T/2 + \overline{W}_R^{(j)}}{1 - \rho^{(i,j)} \left[1 + \frac{p^{(i,j-1)}(0^*)(1 - p^{(i)})}{p^{(i)}} + (1 - p^{(i,j-1)}(0^*)) \left(\frac{\overline{W}^{(j-1)}}{T} + \frac{1 - p^{(i)}}{p^{(i)}} \right) \right]} \quad (3.31)$$

Note that the formula computing the mean waiting time depends on network load, timeslot and $p^{(i,j-1)}(0^*)$ as expected. It is worth mentioning that (3.31) tightly matches (3.19) if $p^{(i,j-1)}(0^*) = 1$.

3.4 Performance Evaluation

We may now attempt to analyze the accuracy of our model in evaluating the performance of the slotted bus-based OPSR network discussed earlier. We use the discrete-event network simulation tool [NWS 05] to simulate the network with 10 ring nodes transmitting on one wavelength at 10Gbs. All mean values in our simulation results are computed with an accuracy of no more than a few percents at 95% confidence level using Batch Means method [MCD 87] (each mean waiting time is computed by collecting at least 7 batches of 200.000 successful packet transmissions). In the Markov model, we have assumed that each optical packet is always 100% filled. By contrast, in the simulation optical packets can not be created with the filling ratio equal to 100%. Thus, we directly generate the optical fixed-size packet from Poisson source; this means that Optical Packet Creation Mechanism (detailed in the next chapter) is disabled in the simulation.

In the first set of results, illustrated in Figure 3-12, we assume that all nodes share the same rate of packet arrivals (the offered network load distribution is uniform between access nodes on the bus). The offered network load is defined as the ratio of the sum of traffic volume offered to all nodes to the network transmission capacity. This figure shows the mean waiting time of the system at each access node for the timeslot equal to $1\mu s$ as the offered network load increases. For this experiment, we first observe that both simulation and analytic models capture the expected behavior of the mean waiting time in slotted bus-based OPSR network: the mean waiting time is likely to increase rapidly as the node priority decreases. For instance, simulation results show that the mean waiting time at node 1 is about $0.526\mu s$ but some $1.51\mu s$ at node 9 as the offered network load equals 0.45.

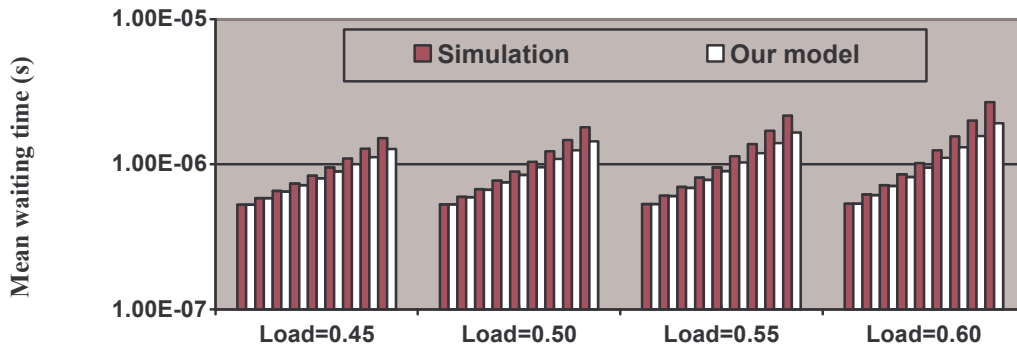


Figure 3-12: The mean waiting time depending on the offered network load from node 1 to 9

Moreover, the mean waiting time also increases rapidly as the offered network load increases. With the offered network load equal to 0.45, simulation results show that the mean waiting time at node 9 is about $1.51\mu s$, but it increases to $2.67\mu s$ as the offered network load rises to 0.6. The interpretation for these results is explained as follows. A successful transmission at low priority nodes takes on average a longer time than at higher priority nodes. The number of occupied slots becomes more and more important as the offered network load increases, leading to the excessive waiting time at the lowest priority nodes.

In addition, we observe in this experiment that at high priority nodes, results obtained by the analytical model are very close to those obtained by the simulation. For instance, the difference between analytical and simulation results at high priority nodes for all offered network loads is negligible, but it becomes more significant at the lower priority nodes (for example, we have relative difference of 23.9% for the mean waiting time at node 9 when the offered network node equals 0.55 but it increases to 28.7% at node 9 when the offered network load equals 0.60).

We may now study the impact of the timeslot length on the network performance. To access the behaviour of our model, we focus on the analysis of the mean waiting time obtained with the same offered network load but for different timeslot lengths. Figure 3-13 illustrates the mean waiting time from node 1 to 9 as the offered network load is set to 0.5, according to different timeslot lengths.

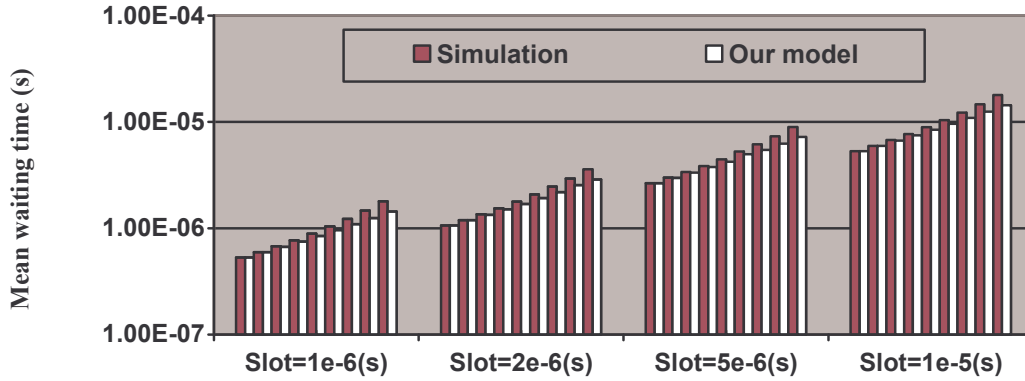


Figure 3-13: The mean waiting time depending on the timeslot lengths with the offered load equal to 0.5 from node 1 to 9

In this experiment, the timeslot varies from $1\mu s$ to $10\mu s$. We observe that the mean waiting time also increases as the timeslot length increases. This increase of the mean waiting time has the same ratio as compared to the timeslot. For example, with the timeslot equal to $1\mu s$, simulation results show that the mean waiting time at node 9 is about $1.8\mu s$, and it increases to $18\mu s$ as the timeslot comes to $10\mu s$. This phenomenon is more clearly described by analytical results in the formula (3.19), in which the mean waiting time is directly calculated from timeslot T . The effect of the timeslot duration on the mean waiting time is readily explained by the synchronizing time and the constant service time that are both equal to timeslot T .

Now, we consider the stationary probability at each node in the case where the offered workload equals 0.5 and the timeslot equals $1\mu s$. The set of results in Figure 3-14 presents these probabilities. We first describe how we obtain these probabilities from the simulation. As the probability definition above, we observe the state of Add buffer at the beginning of each slot, and we count the number of the timeslot in which the Add buffer containing n client packets. The probability $p^{(i)}(n)$ is hence measured as the ratio of the counted timeslot to total timeslots elapsed in the simulation. For more details, the stationary probability $p^{(i)}(n)$ is calculated at node i from the simulation as follows:

$$p^{(i)}(n) = \frac{\text{number of timeslot}(\text{buffer length} = n)}{\text{total timeslot}} \quad (3.32)$$

In fact, the duration of our simulation is about $10s$. If the timeslot duration is equal to $1\mu s$, we thus have *total timeslot* is about 10^7 . This value is big enough to exactly measure the stationary probability from (3.32). Measured probabilities are then compared to analytical probabilities in (3.9). Since Markov models are stables (corresponding to $\alpha'_0 > \alpha'_1 > \alpha'_2 > \alpha'_3 \dots$), so we have theoretically: $p^{(i)}(0) > p^{(i)}(1) > p^{(i)}(2) > p^{(i)}(3) > \dots > p^{(i)}(n) > \dots, n \geq 0$. As a result, the probability $p^{(i)}(n)$ reaches “zero” as n tends to infinity.

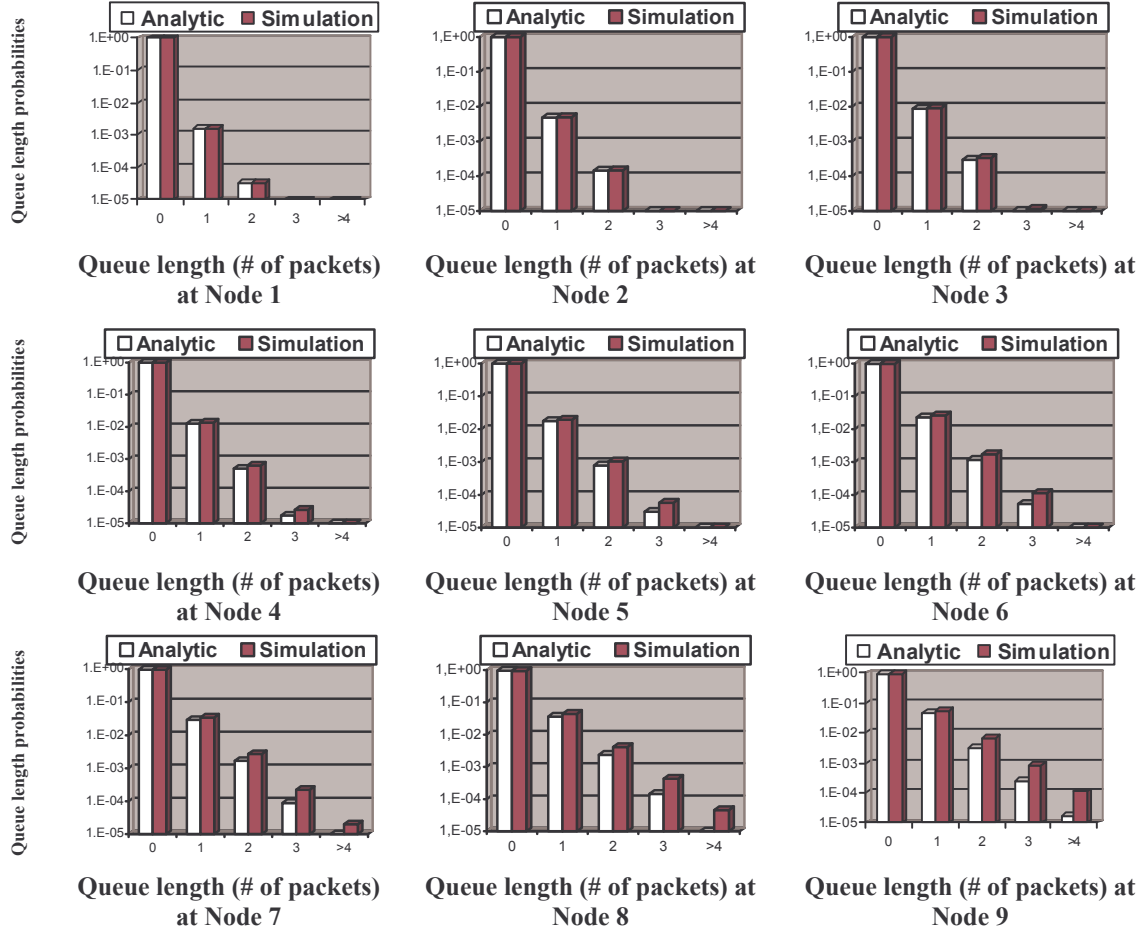


Figure 3-14: Stationary probabilities at access nodes with the offered network load equal to 0.5

For this experiment, we have seen that both simulation and analytic models capture the expected behaviour of the stationary probability. The difference between analytical and simulation results increases as the priority of access nodes in the upstream path decreases. Additionally, we observe that when n increases, this difference increases also. For instance, we focus at node 9 that presents the largest difference between analytical and simulation results. At node 9, with probability $p^{(9)}(0)$, the relative difference is about 1.57% but it increases to a very high value (60%) when $n = 3$ ($p^{(9)}(3)$).

In results shown in Figure 3-15, we consider analytical and simulation results of the free probability in the transit line “seen” by each access node for two values of network load: 0.55 and 0.6 when the timeslot is respectively equal to $1\mu s$ and $10\mu s$. As the explication above, this probability calculated as the ratio of “viewed” free slots to total slots elapsed in the simulation. Thus, we have:

$$p = \frac{\text{number of free slots}}{\text{total slot}} \quad (3.33)$$

Note that the free probability decreases as the node priority decreases. So, both simulation and analytical models capture the expected behaviour: the free probability decreases when we go down on the bus. Additionally, it is clearly to say that the difference between analytical and simulation results is very small (about 0.01% at node 9 when the simulation time is about 20 seconds). On the other hand, the free probability depends only on the offered load as presented in the left figure (i.e. at node 9, the free probability is equal to 0.5112 when network load is set to 0.55, as compared to 0.467 with the network load at 0.6) but it does not depend on the timeslot duration as presented in the right figure. In this figure, the free probability has the same value as that obtained in the left one when regarding a bus node.

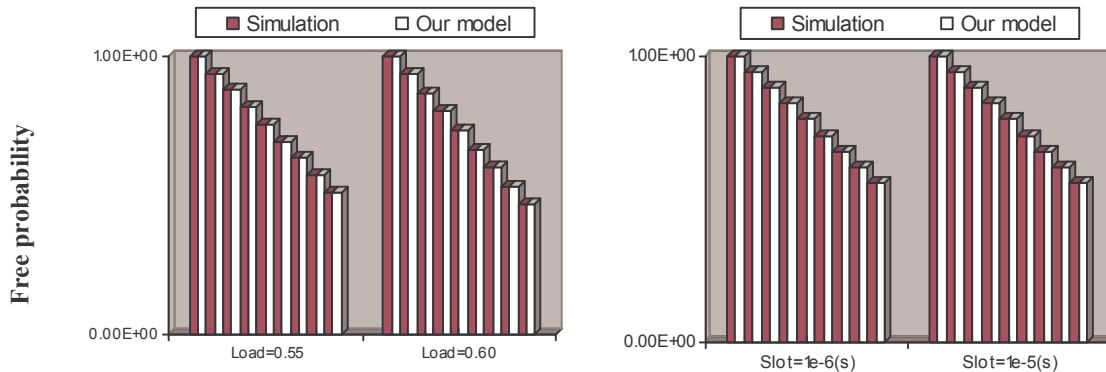


Figure 3-15: Free probabilities according to the offered load and the timeslot from node 1 to 9

In numerical results shown in Figure 3-16, we study the effect of varying patterns of the offered traffic on the bus performance. Note that we use the timeslot equal to $1\mu s$. In addition to the uniform traffic considered before, we include the case where the traffic increases uniformly as we move downstream on the bus, as well as the case where the traffic decreases uniformly as the node priority decreases. We observe that uniformly decreasing traffic appears most penalizing in terms of mean waiting time at lowest priority nodes, compared to two other cases. Besides, the case with the uniformly increasing traffic seems to have a better performance than the uniform case. Indeed, at node 9, we have the relative difference ratio between two models equal to 17% for the uniformly increasing traffic as compared to 20% of the uniform traffic.

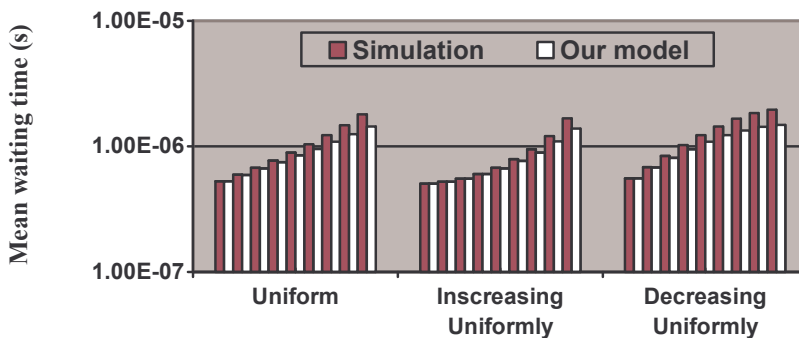


Figure 3-16: The mean waiting in varying patterns of offered traffic with the offered load equal to 0.5 from node 1 to 9.

In Figure 3-17, we compare the distribution of the number of packets in Add buffer at four lowest priority nodes for three pattern traffic considered in Figure 3-16. We observe that our model results are very close to those obtained from the network simulation, notably with first probabilities.

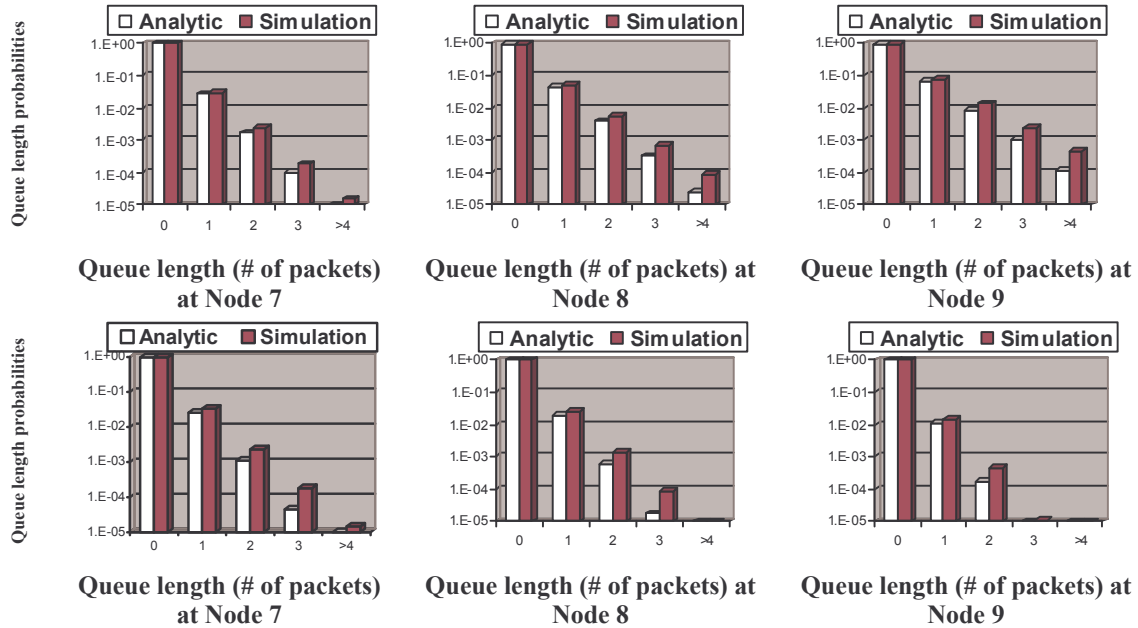


Figure 3-17 : Stationary probabilities at access nodes 7, 8 and 9 with uniformly increasing and uniformly decreasing traffic as the offered network load is set to 0.5

For more various experiments, we consider also unbalanced traffic but with more interesting cases shown in Figure 3-18: the highest priority node carried almost 70% of the traffic while remaining nodes sharing uniformly the remaining 30% of the load. We show here obtained results from three different cases: node 1, node 5 and node 9 respectively carry 70% volume traffic, so-called case 1, 2 and 3. We observe that case 1 appears most penalizing in terms of mean waiting time at the lowest priority nodes, as compared to case 2 and 3.

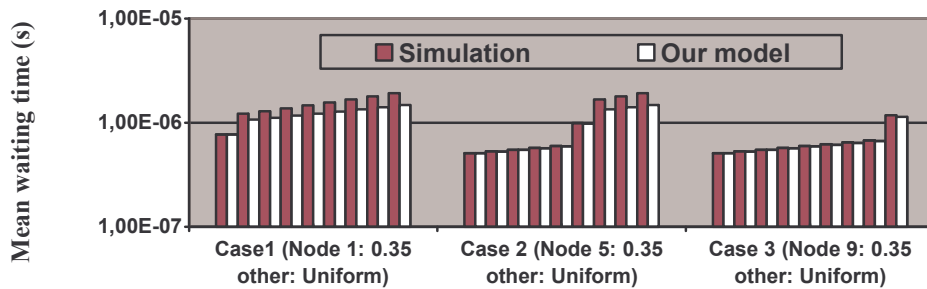


Figure 3-18: The mean waiting time in three different un-balanced traffic with the offered load equal to 0.5 from node 1 to 9

Interestingly, the difference between analytical and simulation models in case 3 seems to be the smallest. This is due to the fact that as node 9 carries most traffic, other upstream nodes suffered small load, leading to the small free probability. As a result, the waiting time obtained at first nodes is very close to the one of the simulation.

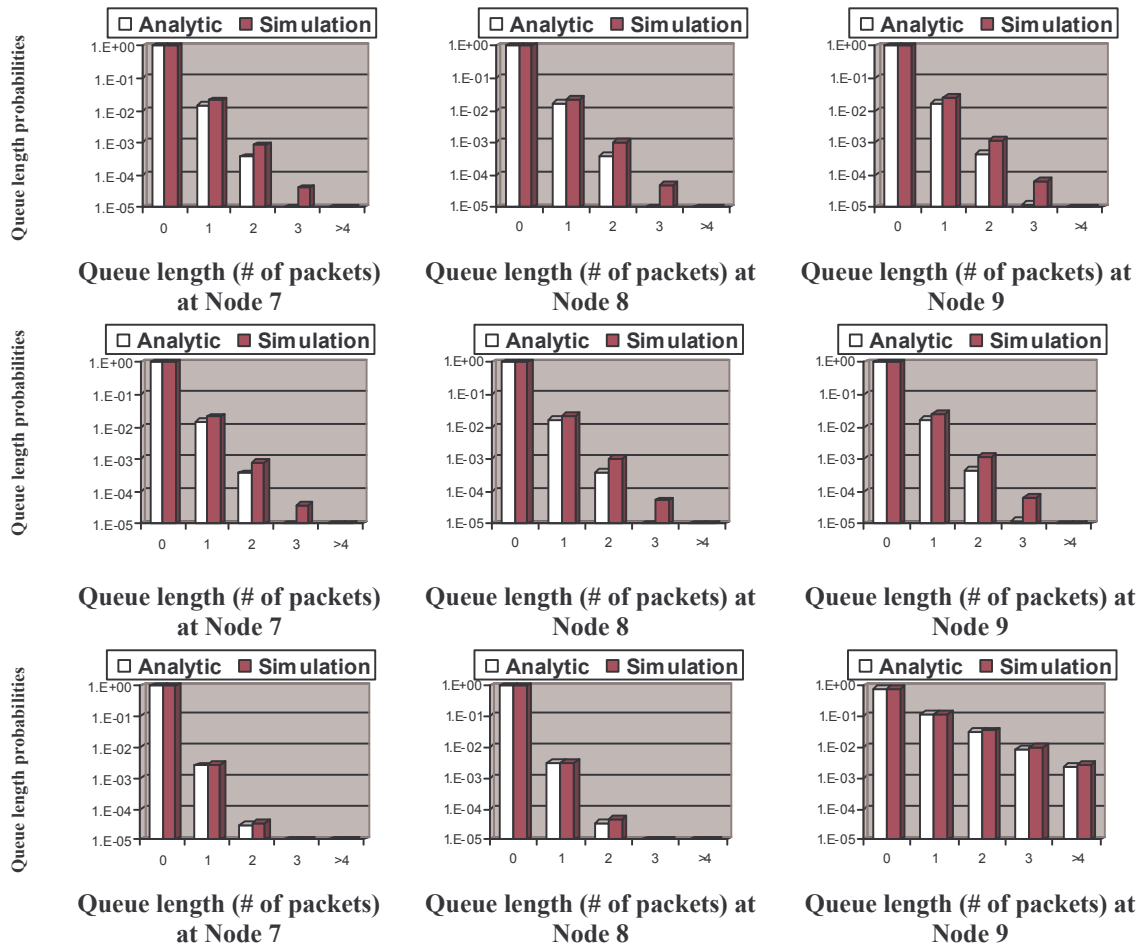


Figure 3-19 : Stationary probabilities at access nodes 7, 8 and 9 in three different un-balanced traffic: case 1, 2 and 3 with the offered network load equal to 0.5

We may now attempt to analyze the accuracy of our “multi-service” model. Figure 3-20 and Figure 3-21 show the mean waiting time of the system at each ring node for three CoS as the offered network load respectively equals 0.45 and 0.55.

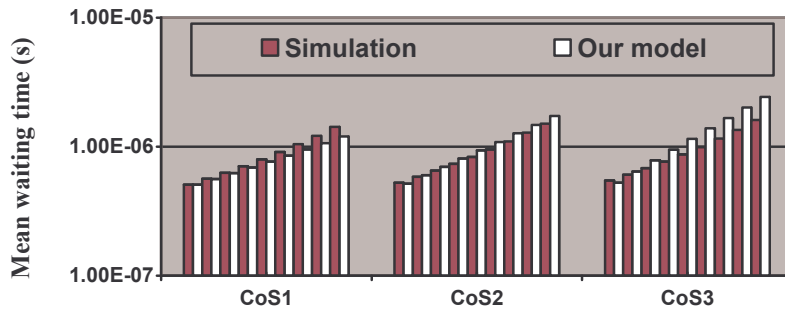


Figure 3-20: The mean waiting time from node 1..9 for three CoS with the offered network load equal to 0.45

For the experiment shown in Figure 3-20, we first observe that both simulation and analytical models capture the expected behaviour of the mean waiting time in the OPSR network with QoS guarantee: the mean waiting time increases when the node priority decreases and the mean waiting

time of higher priority classes is smaller than that of lower priority classes. Indeed, due to the HOL scheduling discipline in which packets CoS_2 must be waited till all packets CoS_1 are transmitted while packets CoS_3 must be waited till all packets of both CoS_1 and CoS_2 are transmitted, leading to the highest waiting time for CoS_3 . Additionally, the difference between analytical and simulation models becomes more important as the node priority decreases. Indeed, at node 9 we observe that the difference between two models is only about 14% for CoS_1 but this value rapidly increases to more 30% for CoS_3 . Regarding CoS_2 , analytical values are interestingly very close to those obtained from simulation (some %).

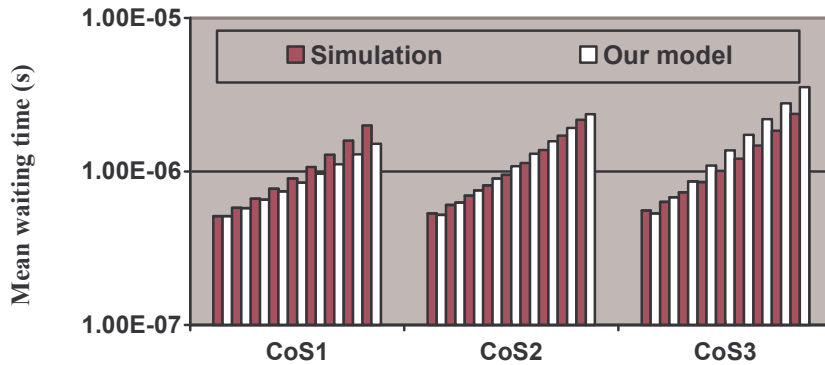


Figure 3-21: The mean waiting time from node 1...9 for three CoS with the offered network load equal to 0.55

Beside, as we enlarge the offered network load (55% shown in Figure 3-21), the mean waiting times are hence increased. As we forecast, the difference between two models also becomes more important. At node 9 we observe the difference between two models increases to 15% for CoS_1 while it reaches more 35% for CoS_3 .

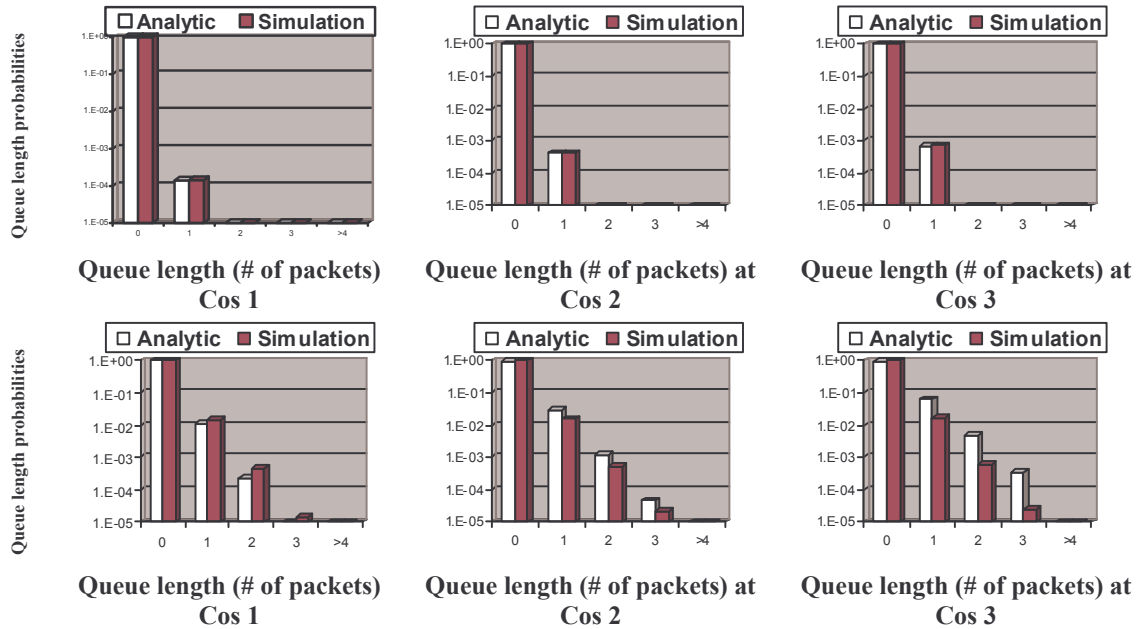


Figure 3-22: Stationary probabilities at access nodes 1 and 9 with the offered network load equal to 0.45

Figure 3-22 presents stationary probabilities measured at node 1 and node 9 for three CoS. Similar to the mean waiting time, the difference of the stationary probability between two models is small for CoS_1 but it becomes more important for CoS_3 , particularly at node 9.

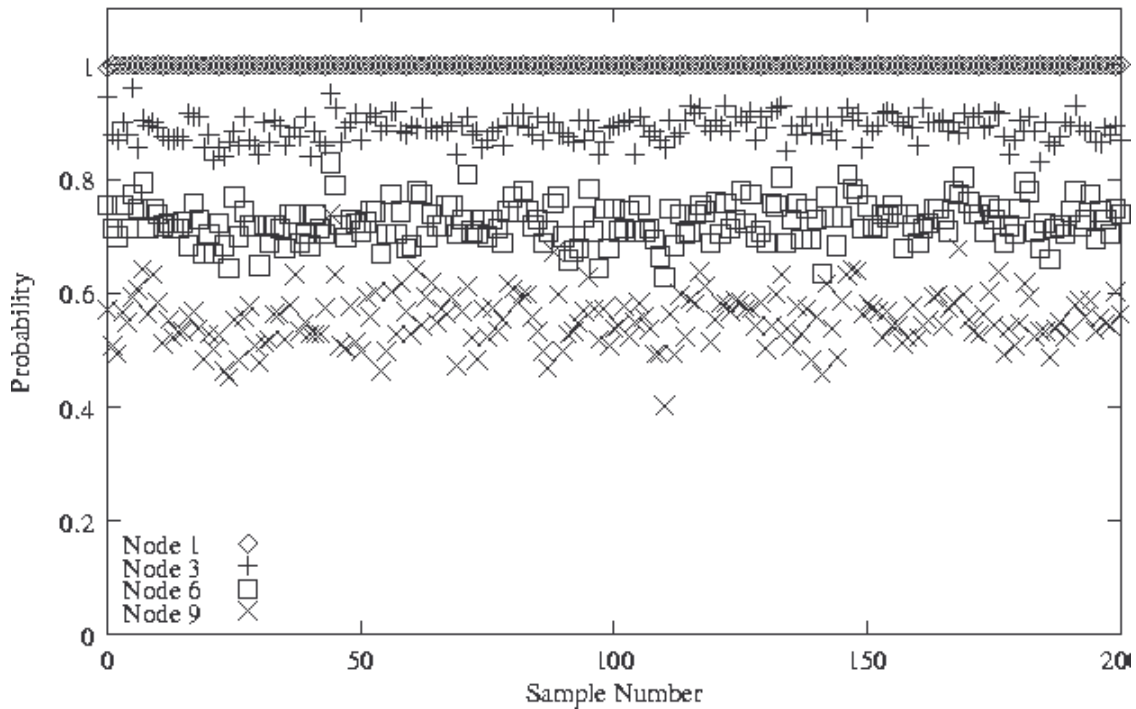


Figure 3-23: The ratio of captured free slots to the sample of 200 timeslots.

Now, we are going to explain why there is a high difference between analytical and simulation results for the mean waiting time at last nodes. The response for this question is illustrated in Figure 3-23 and in Figure 3-24. In Figure 3-23, we presents the free probability $p(i)$ (i from 1 to 9) captured in only a sample of 200 timeslots instead of capturing during all simulation time when the offered load is set to 0.5. We note that with the sample of 200 slots, the “instant” free probability is very variable from the stationary probability, especially for last nodes. It is more clearly shown in the Figure 3-24 that we measure the free slot distribution “viewed” by each bus node thanks to a particular parameter: the distance between two consecutive free slots. This measurement allows us to observe the statistical dispersion of the free slot distribution in the transit line of an access node. To represent the statistical dispersion in the simulation, we used a discrete random variable as follows. If the node “sees” two successive free slots (one after another), a sample, which value equal to 1, is added to the discrete variable. Otherwise the value equal to $1/(X + 1)$ where X is occupied slots between two free slots. We are able to obtain a set of stochastic values and compute the mean (the curve named “simulation mean” as shown in the figure) and variance (the curve named “simulation Var” as shown in the figure) of “real” free slots in the simulation. The discrete variable obtained from the simulation represents the “instant” probability that the node “sees” free slots in the transit line. In the figure, “Analytical mean” and “Simulation mean” are referred to respectively the analytical and simulation stationary probability. Moreover, in order to have a significant comparison, we replace the expected mean of free slots in the simulation by the analytical mean and then compute the variance and the coefficient from the discrete variable over this value, so-called A-S variance and A-S CV.

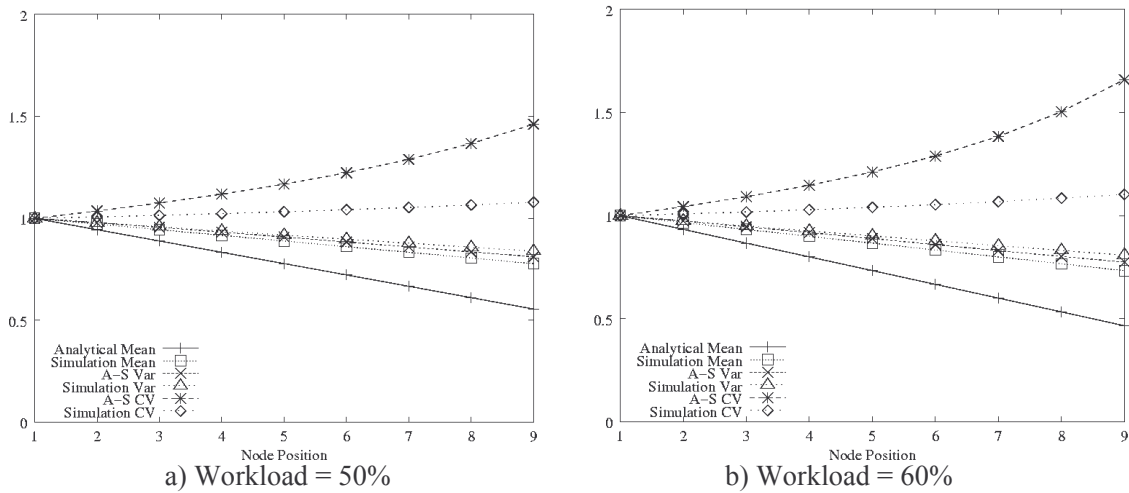


Figure 3-24: Coefficient Variance measured in the simulation at the network load of 0.50 and 0.60.

Firstly, we observe that the mean value obtained from the simulation is higher than the analytical mean value; this means that in the analytical model last nodes “observe” more free slots than those of the simulation. This leads to the mean waiting time obtained from the simulation higher than that of the analytical model, notably at last nodes on the bus. Moreover, the simulation variance is very close to the simulation mean, leading to the simulation coefficient variance unchanged (1.0079 at node 9 compared to 1 at node 1 as the network load equals 0.5). On the other hand, when we use the analytical mean instead of the expected mean in the simulation, the measured variance (A-S Var) is larger than the analytical mean value; leading to the increase of A-S coefficient variance. Therefore, A-S coefficient variance reaches 1.4 at node 9, causing a high difference of the mean waiting time between two models. As we increase the network load to 0.60, A-S coefficient variance increases more rapidly. For concluding remarks, since we use the free slot probability $p^{(i)}$ in the analytical model’s EDTMC, it corresponds to the uniform distribution of the free slot but in reality (as well in the simulation), the distribution of the free slot “viewed” by an access node is not uniform.

3.5 Concluding remarks and future works

We have presented an approximate approach to the performance analysis (in terms of mean waiting delay and queue-state distribution) of a slotted bus-based network supporting fixed-size packets. For the modelling purpose, we have used EDTMC system to model the steady-state of Add buffer at each access node. By resolving these EDTMCs, we have obtained the stationary probability of the steady-state of Add buffer for each bus node and the free probability that the node “sees” the free slot in the transit line. As a result, we are able to approximately compute the mean waiting time at each node thanks some proposed formulas. Theoretically, we have presented that the mean waiting time increases rapidly as the offered network load increases as well as the timeslot length increases.

Secondly, we have applied our model to study the system to support multi-service. We have extended existing EDTMCs to accommodate several *CoS* and proposed some new formulas computing approximately the mean waiting time of client packets in Add buffer for each type of classes of service. As expected, we have seen that the mean waiting time of high priority packets is smaller than that of low priority packets. However, as the “mono-service” case, the difference between analytical and simulation models still exists. It becomes more important as the node-priority decreases.

For the Markov chain solution, we have used the “constant” free probability that corresponds to the uniform distribution of the free slot in the transit line but in reality, the distribution of the free slot

“viewed” by a bus node is not uniform. This leads to a significant difference between simulation and analytical models. Therefore, future works will include an improved matching of the free slot distribution. Additionally, we have also assumed that arriving packets come from Poisson sources with fixed-size while each node has an unlimited buffer size. Thus, a possible extension of our approach will be considered in order to accommodate different packet arrival patterns and with finite buffer sizes.

3.6 Appendix

3.6.1 Solution for Transition Matrix in the “mono-service” case

From EDTMC that we obtained, we construct the transition matrix of the queue-state of the Add buffer in the node i as follows:

$$P = \begin{bmatrix} \alpha_0 p^{(i)} & (\alpha_0(1-p^{(i)}) + \alpha_1 p^{(i)}) & (\alpha_1(1-p^{(i)}) + \alpha_2 p^{(i)}) & \cdots \\ \alpha_0 p^{(i)} & (\alpha_0(1-p^{(i)}) + \alpha_1 p^{(i)}) & (\alpha_1(1-p^{(i)}) + \alpha_2 p^{(i)}) & \cdots \\ 0 & \alpha_0 p^{(i)} & (\alpha_0(1-p^{(i)}) + \alpha_1 p^{(i)}) & \cdots \\ 0 & 0 & \alpha_0 p^{(i)} & \cdots \\ \vdots & \vdots & \vdots & \ddots \end{bmatrix}$$

For simple, we call α'_0 and α'_k , $k \geq 1$ as follows:

$$\begin{aligned} \alpha'_0 &= \alpha_0 p^{(i)} \\ \alpha'_k &= \alpha_{k-1}(1-p^{(i)}) + \alpha_k p^{(i)}, k \geq 1 \end{aligned}$$

So the transition matrix P becomes:

$$P = \begin{bmatrix} \alpha'_0 & \alpha'_1 & \alpha'_2 & \alpha'_3 & \alpha'_4 & \cdots \\ \alpha'_0 & \alpha'_1 & \alpha'_2 & \alpha'_3 & \alpha'_4 & \cdots \\ 0 & \alpha'_0 & \alpha'_1 & \alpha'_2 & \alpha'_3 & \cdots \\ 0 & 0 & \alpha'_0 & \alpha'_1 & \alpha'_2 & \cdots \\ 0 & 0 & 0 & \alpha'_0 & \alpha'_1 & \cdots \\ 0 & 0 & 0 & 0 & \alpha'_0 & \cdots \\ \vdots & \vdots & \vdots & \vdots & \vdots & \ddots \end{bmatrix}$$

Notice that obtained Markov chains are irreducible and aperiodic [BBH 00]. All its states are thus recurrent not-null (because of $\alpha_0 \geq \alpha_1 + \alpha_2 + \alpha_3 + \dots$, this leads to $\alpha'_0 \geq \alpha'_1 + \alpha'_2 + \alpha'_3 + \dots$), this property then enables us to affirm that stationary probabilities $p^{(i)}(0^*)$, $p^{(i)}(0^{**})$, $p^{(i)}(1)$, ... exist. The system can be written as (3.7):

$$\begin{cases} p^{(i)}(0^*) = p^{(i)}(0^*)\alpha'_0 + p^{(i)}(0^{**})\alpha'_0 \\ p^{(i)}(0^{**}) = p^{(i)}(0^*)\alpha'_1 + p^{(i)}(0^{**})\alpha'_1 + p^{(i)}(1)\alpha'_0 \\ \vdots \\ p^{(i)}(k) = p^{(i)}(0^*)\alpha'_k + p^{(i)}(0^{**})\alpha'_k + \sum_{j=1}^k p^{(i)}(j)\alpha'_{k-j} \\ \vdots \end{cases}$$

With $\sum_{n=0}^{\infty} p^{(i)}(n) = 1$ and $p^{(i)}(0) = p^{(i)}(0^*) + p^{(i)}(0^{**})$.

It is not difficult to note that when we refer $p_{ref}^{(i)}(0) = p^{(i)}(0^*)$, $p_{ref}^{(i)}(1) = p^{(i)}(0^{**})$, $p_{ref}^{(i)}(2) = p^{(i)}(1)$, ... $p_{ref}^{(i)}(k+1) = p^{(i)}(k)$, ... with $k \geq 1$, sequence $p_{ref}^{(i)}(k)$, $k = 1 \dots$ does not lose its general property. Hence, (3.7) becomes:

$$\begin{cases} p_{ref}^{(i)}(0) = p^{(i)}_{ref}(0)\alpha'_0 + p^{(i)}_{ref}(0)\alpha'_0 \\ p_{ref}^{(i)}(1) = p^{(i)}_{ref}(0)\alpha'_1 + p^{(i)}_{ref}(1)\alpha'_1 + p^{(i)}_{ref}(2)\alpha'_0 \\ \vdots \\ p_{ref}^{(i)}(k) = p^{(i)}_{ref}(0)\alpha'_k + \sum_{j=1}^{k+1} p^{(i)}_{ref}(j)\alpha'_{k-j+1} \\ \vdots \end{cases} \quad (*)$$

To resolve the system (*), we will use z-transform. We denote respectively $P^{(i)}(z)$ and $V(z)$ as z-transform of the stationary priority $p_{ref}^{(i)}(k)$ and α'_k so that :

$$P^{(i)}(z) = \sum_{k=0}^{\infty} p_{ref}^{(i)}(k)z^k \quad (3.34)$$

$$V(z) = \sum_{k=0}^{\infty} \alpha'_k z^k \quad (3.35)$$

As shown in [BBH 00] that $P^{(i)}(z)$, which is z-transform of stationary probabilities $p_{ref}^{(i)}(n)$, can be expressed as function of $V(z)$, z-transform of probabilities α'_k , like following:

$$P^{(i)}(z) = \frac{(p^{(i)} - \rho^{(i)})V(z)(1-z)}{V(z) - z} \quad (3.36)$$

The demonstration of (3.36) is shown like following. By adding all equations of (*), each multiplied by the corresponding z^k , we get:

$$\sum_{k=0}^{\infty} p_{ref}^{(i)}(k)z^k = \sum_{k=0}^{\infty} p_{ref}^{(i)}(0)\alpha'_k z^k + \sum_{k=0}^{\infty} \left(\sum_{j=1}^{k+1} p_{ref}^{(i)}(j)\alpha'_{k-j+1} \right) z^k \quad (3.37)$$

$$\Leftrightarrow P^{(i)}(z) = p^{(i)}(0)V(z) + \sum_{k=0}^{\infty} \left(\sum_{j=1}^{k+1} p_{ref}^{(i)}(j)\alpha'_{k-j+1} \right) z^k \quad (3.38)$$

We call $N = \sum_{k=0}^{\infty} \left(\sum_{j=1}^{k+1} p_{ref}^{(i)}(j)\alpha'_{k-j+1} \right) z^k$, N is thus transformed as follows:

$$N = \sum_{k=0}^{\infty} \left(\sum_{j=1}^{k+1} p_{ref}^{(i)}(j)\alpha'_{k-j+1} \right) z^k = \frac{1}{z} \sum_{k=0}^{\infty} \left(\sum_{j=1}^{k+1} p_{ref}^{(i)}(j)\alpha'_{k-j+1} \right) z^{k+1}$$

We continue:

$$N = \frac{1}{z} \sum_{k=0}^{\infty} \left(\sum_{j=1}^{k+1} p_{ref}^{(i)}(j)\alpha'_{k-j+1} \right) z^{k+1} = \frac{1}{z} \sum_{k=1}^{\infty} \left(\sum_{j=1}^k p_{ref}^{(i)}(j)\alpha'_{k-j} \right) z^k$$

$$N = \frac{1}{z} \left[\sum_{k=1}^{\infty} \left(\sum_{j=0}^k p_{ref}^{(i)}(j) \alpha'_{k-j} \right) z^k - \sum_{k=1}^{\infty} p_{ref}^{(i)}(0) \alpha'_k z^k \right]$$

$$N = \frac{1}{z} \left[\sum_{k=0}^{\infty} \left(\sum_{j=0}^k p_{ref}^{(i)}(j) \alpha'_{k-j} \right) z^k - p_{ref}^{(i)}(0) \alpha'_0 z^k - \sum_{k=0}^{\infty} p_{ref}^{(i)}(0) \alpha'_k z^k + p_{ref}^{(i)}(0) \alpha'_0 z^k \right]$$

$$\rightarrow N = \frac{1}{z} \left[P^{(i)}(z) V(z) - p_{ref}^{(i)}(0) V(z) \right] \quad (3.39)$$

From (3.36) and (3.39), we deduce:

$$P^{(i)}(z) = \frac{p_{ref}^{(i)}(0) V(z) (1-z)}{V(z) - z} \quad (3.40)$$

It remains now to express $p_{ref}^{(i)}(0)$. For it, we apply the "Hospital's rule" for $P^{(i)}(z) = \frac{C(z)}{D(z)}$ with $C(z) = p_{ref}^{(i)}(0) V(z) (1-z)$ and $D(z) = V(z) - z$. So, we have:

$$\lim_{z \rightarrow 1} \frac{C(z) - C(1)}{D(z) - D(1)} = \lim_{z \rightarrow 1} \frac{C'(z)}{D'(z)}$$

Because $C(1) = D(1) = 0$, hence (3.40) becomes:

$$1 = P^{(i)}(1) = \lim_{z \rightarrow 1} P^{(i)}(z) = \frac{C'(1)}{D'(1)} = - \frac{p_{ref}^{(i)}(0) V'(1)}{V'(1) - 1} \quad (3.41)$$

Note that $V(1) = \sum_{k=0}^{\infty} \alpha'_k = \alpha_0 p^{(i)} + \sum_{k=1}^{\infty} (\alpha_{k-1} (1-p^{(i)}) + \alpha_k p^{(i)}) = \sum_{k=0}^{\infty} \alpha_k = 1$. (3.41) remains only

$V'(1)$ to be solved. We have: $V'(z) = \sum_{k=1}^{\infty} k \alpha'_k z^{k-1}$

Then:

$$\begin{aligned} V'(1) &= \sum_{k=1}^{\infty} k \alpha'_k = \sum_{k=1}^{\infty} k \left[\alpha_{k-1} (1-p^{(i)}) + \alpha_k p^{(i)} \right] \\ \rightarrow V'(1) &= \sum_{k=1}^{\infty} k \alpha_{k-1} (1-p^{(i)}) + \sum_{k=1}^{\infty} k p^{(i)} \alpha_k = (1-p^{(i)}) \sum_{k=0}^{\infty} (k+1) \alpha_k + p^{(i)} \sum_{k=1}^{\infty} k \alpha_k \\ \rightarrow V'(1) &= \sum_{k=0}^{\infty} (k+1) \alpha_k - p^{(i)} \sum_{k=0}^{\infty} (k+1) \alpha_k + p^{(i)} \sum_{k=1}^{\infty} k \alpha_k \\ \rightarrow V'(1) &= \sum_{k=0}^{\infty} k \alpha_k + \sum_{k=0}^{\infty} \alpha_k - p^{(i)} \sum_{k=0}^{\infty} \alpha_k - p^{(i)} \sum_{k=0}^{\infty} k \alpha_k + p^{(i)} \sum_{k=1}^{\infty} k \alpha_k \\ &= \sum_{k=1}^{\infty} k \alpha_k + 1 - p^{(i)} \quad (3.42) \end{aligned}$$

Let us consider M as: $M = \sum_{k=1}^{\infty} k\alpha_k$. Thanks to the definition of Poisson process α_k , we have:

$$\begin{aligned} M &= \sum_{k=1}^{\infty} k\alpha_k = \sum_{k=1}^{\infty} k \int_0^{\infty} \frac{(\lambda_{(i)}x)^k}{k!} e^{-\lambda_{(i)}x} f_X(x) dx \\ \rightarrow M &= \int_0^{\infty} \lambda_{(i)}x \left(\sum_{k=1}^{\infty} \frac{(\lambda_{(i)}x)^{k-1}}{(k-1)!} \right) e^{-\lambda_{(i)}x} f_X(x) dx = \lambda_{(i)} \int_0^{\infty} x f_X(x) dx \end{aligned}$$

We have $\lambda_{(i)} \int_0^{\infty} x f_X(x) dx = \lambda_{(i)} m = \rho^{(i)}$ where m is the mean service time and constant service m equals 1 in the case of the synchronous network. So, M becomes: $M = \rho^{(i)}$ (3.43).

By results obtained in (3.42) and (3.43), we deduce: $V'(1) = \rho^{(i)} + 1 - p^{(i)}$ (3.44)

Replacing $V(1)$, $V'(1)$ in (3.41), we obtain:

$$p'_{ref}(0) = p^{(i)} - \rho^{(i)} \quad (3.45)$$

From (3.45) and the assumption of $p'_{ref}(0)$, so we have finally (3.9) that we want to demonstrate:

$$p^{(i)}(0^*) = p^{(i)} - \rho^{(i)}$$

3.6.2 Solution for Transition Matrix in the “multi-service” case

The matrix P' obtained for the “multi-service” case can be written in form:

$$\begin{cases} p^{(i,j)}(0^*) = p^{(i,j)}(0^*)\alpha_0'' + p^{(i,j)}(0^{**})\alpha_0'' \\ p^{(i,j)}(0^{**}) = p^{(i,j)}(0^*)\alpha_1'' + p^{(i,j)}(0^{**})\alpha_1'' + p^{(i,j)}(1)\alpha_0'' \\ \vdots \\ p^{(i,j)}(k) = p^{(i,j)}(0^*)\alpha_k'' + p^{(i,j)}(0^{**})\alpha_k'' + \sum_{l=1}^k p^{(i,j)}(l)\alpha_{k-l}'' \\ \vdots \end{cases} \quad (3.23)$$

These equations (3.23) have same form as (3.7). By using the same method to solve, it is not difficult to deduce:

$$1 = -\frac{p'_{ref}(0)Q(1)}{Q'(1)-1} \quad (3.46) \text{ where } Q(z) = \sum_{k=0}^{\infty} \alpha_k'' z^k \quad (3.47)$$

Note that:

$$\begin{aligned} Q(1) &= \sum_{k=0}^{\infty} \alpha_k'' \\ &= p^{(i,j-1)}(0^*) * (\alpha_{0,j} p^{(i,j)}) + \sum_{k=1}^{\infty} (p^{(i,j-1)}(0^*) * (\alpha_{k-1,j} (1 - p^{(i,j)}) + \alpha_{k,j} p^{(i,j)}) + (1 - p^{(i,j-1)}(0^*)) * \alpha_{k-1,j}) \\ &= \sum_{k=0}^{\infty} \alpha_k'' = 1 \end{aligned}$$

Hence, (3.46) remains only $Q'(l)$ to be solved. We have: $Q'(z) = \sum_{k=1}^{\infty} \alpha_k'' k z^{k-1}$

Then:

$$\begin{aligned}
 Q'(1) &= \sum_{k=1}^{\infty} k \alpha_k'' = \sum_{k=1}^{\infty} k \left[p^{(i,j-1)}(0^*) * (\alpha_{k-1,j} (1 - p^{(i,j)}) + \alpha_{k,j} p^{(i,j)}) + (1 - p^{(i,j-1)}(0^*)) * \alpha_{k-1,j} \right] \\
 Q'(1) &= \sum_{k=1}^{\infty} k \left[p^{(i,j-1)}(0^*) * \alpha_{k-1,j} (1 - p^{(i,j)}) + p^{(i,j-1)}(0^*) * \alpha_{k,j} p^{(i,j)} + \alpha_{k-1,j} - p^{(i,j-1)}(0^*) * \alpha_{k-1,j} \right] \\
 Q'(1) &= p^{(i,j-1)}(0^*) (1 - p^{(i,j)}) \sum_{k=1}^{\infty} k \alpha_{k-1,j} + p^{(i,j-1)}(0^*) p^{(i,j)} \sum_{k=1}^{\infty} k \alpha_{k,j} + \sum_{k=1}^{\infty} k \alpha_{k-1,j} - p^{(i,j-1)}(0^*) \sum_{k=1}^{\infty} k \alpha_{k-1,j} \\
 Q'(1) &= (-p^{(i,j-1)}(0^*) p^{(i,j)}) \sum_{k=1}^{\infty} k \alpha_{k-1,j} + p^{(i,j-1)}(0^*) p^{(i,j)} \sum_{k=1}^{\infty} k \alpha_{k,j} + \sum_{k=1}^{\infty} k \alpha_{k-1,j} \\
 Q'(1) &= p^{(i,j-1)}(0^*) p^{(i,j)} \sum_{k=1}^{\infty} k \alpha_{k,j} - p^{(i,j-1)}(0^*) p^{(i,j)} \sum_{k=0}^{\infty} (k+1) \alpha_{k,j} + \sum_{k=0}^{\infty} (k+1) \alpha_{k,j} \\
 Q'(1) &= p^{(i,j-1)}(0^*) p^{(i,j)} \sum_{k=1}^{\infty} k \alpha_{k,j} - p^{(i,j-1)}(0^*) p^{(i,j)} \sum_{k=0}^{\infty} k \alpha_{k,j} - p^{(i,j-1)}(0^*) p^{(i,j)} \sum_{k=0}^{\infty} \alpha_{k,j} + \sum_{k=0}^{\infty} (k+1) \alpha_{k,j} \\
 Q'(1) &= \sum_{k=1}^{\infty} k \alpha_{k,j} + \sum_{k=0}^{\infty} \alpha_{k,j} - p^{(i,j-1)}(0^*) p^{(i,j)} \sum_{k=0}^{\infty} \alpha_{k,j}
 \end{aligned}$$

Since $\sum_{k=0}^{\infty} \alpha_{k,j} = 1$ and $\sum_{k=1}^{\infty} k \alpha_{k,j} = \rho^{(i,j)}$, we have:

$$Q'(1) = \rho^{(i,j)} + 1 - p^{(i,j-1)}(0^*) p^{(i,j)} \quad (3.48)$$

From (3.46) and (3.48), we derive finally (3.24):

$$p^{(i,j)}(0^*) = p'_{ref}(0) = p^{(i,j)} p^{(i,j-1)}(0^*) - \rho^{(i,j)}$$

3.6.3 Computation of mean waiting times

The “mono-service” case:

When a client packet arrives to the system, it may see:

- 0 client and its waiting time in the local buffer is null
- n clients and its waiting time in the local buffer is equal to: its residual time in the service + the average time in the service of n other clients before it in the buffer.

We have the following equation for \overline{W} as:

$$\overline{W} = \overline{W}_0 + \overline{W}_n = p^{(i)}(0) * (\overline{t}_s + \overline{W}_R) + \sum_{n=1}^{\infty} [p^{(i)}(n) * (\overline{t}_R + \overline{W}_R + n * \overline{t}_C)] \quad (3.12)$$

Using the normalization condition $p^{(i)}(0) = 1 - \sum_{n=1}^{\infty} p^{(i)}(n)$ and the Little formula for computing the

mean waiting time $\bar{W} = \frac{1}{\lambda_i} \sum_{n=1}^{\infty} n p^{(i)}(n)$, combined with equations (3.12) – (3.18), we obtain:

$$\begin{aligned} \bar{W} &= p^{(i)}(0) * (\bar{t}_s + \bar{W}_R) + (1 - p^{(i)}(0)) * (\bar{t}_R + \bar{W}_R) + \sum_{n=1}^{\infty} [p^{(i)}(n) * n * \bar{t}_C] \\ \bar{W} &= p^{(i)}(0) * (\bar{t}_s + \bar{W}_R) + (1 - p^{(i)}(0)) * (\bar{t}_R + \bar{W}_R) + \bar{W} * \lambda_i * (\bar{W}_R + T) \\ \Rightarrow \bar{W} &= \left(\frac{T}{2} + \bar{W}_R \right) + \bar{W} * \lambda_i * (\bar{W}_R + T) \\ \Rightarrow \bar{W} &= \frac{\frac{T}{2} + \bar{W}_R}{1 - \lambda_i * (\bar{W}_R + T)} = \frac{\frac{T}{2} + \frac{(1 - p^{(i)})T}{p^{(i)}}}{1 - \lambda_i * T \left(\frac{1 - p^{(i)}}{p^{(i)}} + 1 \right)} \\ \Rightarrow \bar{W} &= \frac{\frac{T}{2} + \frac{(1 - p^{(i)})T}{p^{(i)}}}{1 - \left(\frac{\rho_i}{p^{(i)}} \right)} \quad (3.19) \end{aligned}$$

The “multi-service” case:

As the same explanation, we have:

$$\bar{W}^{(j)} = \bar{W}_0^{(j)} + \bar{W}_n^{(j)} = p^{(i,j)}(0) * (\bar{t}_s + \bar{W}_R^{(j)}) + \sum_{n=1}^{\infty} [p^{(i,j)}(n) * (\bar{t}_R + \bar{W}_R^{(j)} + n * \bar{t}_C^{(j)})] \quad (3.26)$$

Using the normalization condition $p^{(i,j)}(0) = 1 - \sum_{n=1}^{\infty} p^{(i,j)}(n)$ and the Little formula for computing the

mean waiting time $\bar{W}^{(j)} = \frac{1}{\lambda_{i,j}} \sum_{n=1}^{\infty} n p^{(i,j)}(n)$, combined with equations (3.26) – (3.30), we obtain:

$$\begin{aligned} \bar{W}^{(j)} &= p^{(i,j)}(0) * (\bar{t}_s + \bar{W}_R^{(j)}) + (1 - p^{(i,j)}(0)) * (\bar{t}_R + \bar{W}_R^{(j)}) + \sum_{n=1}^{\infty} [p^{(i,j)}(n) * n * \bar{t}_C^{(j)}] \\ \bar{W}^{(j)} &= p^{(i,j)}(0) * (\bar{t}_s + \bar{W}_R^{(j)}) + (1 - p^{(i,j)}(0)) * (\bar{t}_R + \bar{W}_R^{(j)}) + \bar{W}^{(j)} * \lambda_{(i,j)} * (\bar{W}_R^{(j)} + T) \\ \Rightarrow \bar{W}^{(j)} &= \left(\frac{T}{2} + \bar{W}_R^{(j)} \right) + \bar{W}^{(j)} * \lambda_{(i,j)} * (\bar{W}_R^{(j)} + T) \\ \Rightarrow \bar{W}^{(j)} &= \left(\frac{T}{2} + \bar{W}_R^{(j)} \right) + \bar{W}^{(j)} * \lambda_{(i,j)} * (\bar{W}_R^{(j)} + T) \\ \Rightarrow \bar{W}^{(j)} &= \frac{\frac{T}{2} + \bar{W}_R^{(j)}}{1 - \rho^{(i,j)} \left[1 + \bar{W}_R^{(j)} \right]} \quad (3.31) \end{aligned}$$

or

$$\Rightarrow \overline{W}^{(j)} = \frac{\frac{T}{2} + p^{(i,j-1)}(0^*) \frac{(1-p^{(i)})T}{p^{(i)}} + (1-p^{(i,j-1)}(0^*))(\overline{W}^{(j-1)} + \frac{(1-p^{(i)})T}{p^{(i)}})}{1 - \rho^{(i,j)} \left[1 + \frac{p^{(i,j-1)}(0^*)(1-p^{(i)})}{p^{(i)}} + (1-p^{(i,j-1)}(0^*)) \left(\frac{\overline{W}^{(j-1)}}{T} + \frac{1-p^{(i)}}{p^{(i)}} \right) \right]}$$

Chapter 4

Impact of Optical fixed-Size Packet Creation on synchronous and asynchronous OPSR networks

In many strategies of the optical fixed-size packet creation in the synchronous OPSR network, the timer-based mechanism is considered as one of the simplest mechanisms. It is based on limiting the waiting time of variable-length client packets, which come from the upper layer by a timer. This chapter is composed of two separated parts. The first part describes the timer-based mechanism in details and introduces two simulation scenarios (metro access and metro core networks) with the aim of evaluating the impact of optical fixed-size packet creation on the network performance. The second part is dedicated to the analysis of a Virtual SynChronization (VSC) mechanism which is proposed in order to enhance the transmission efficiency of a bus-based network using OU-CSMA/CA protocol [TNH 06]. After giving some problems of CSMA/CA protocol, we explain our VSC scheme followed by numerical results.

4.1 Synchronous Vs. Asynchronous Networks

The transmission efficiency [TNH 06] is always one of the most important factors in a network. In order to increase the transmission efficiency of a network, it is necessary to reduce the volume of packet overheads (i.e. information needed for routing, signaling and header processing...). In the synchronous network, where the bandwidth is divided into some constant time-units, the low transmission efficiency occurs when a grand optical container is filled by client packets. It may arise when the last client packet arrives but its length is larger than the remaining space of the container. The circumstance leads to the rejection of the last client packet, thus the remaining of the container is wasted. As a result, this might degrade the transmission efficiency of the network.

It is worth noting that if an electronic packet length is larger than the remaining space, a segmentation process might be used at the node border before creating a complete optical packet. Also, a reassembly process is used at the destination node to rebuild original segmented electronic packets. Since segmentation/reassembly processes are complex, they are hence out of this dissertation scope. In this chapter we focus on the performance enhancement of the optical packet creation process which strongly depends on the following set of parameters: the timeslot duration, the timer expiration value, the profile of electronic traffic and the network load. The impact of the traffic profile on the optical packet creation is investigated in [FHT 05], thus only the timeslot duration, the timer value and the network load are considered in our work. A too long optical packet length may lead to a low transmission efficiency and a low bandwidth utilization of the network because the optical packet

(we suppose that the optical packet size is equal to a timeslot duration) is often not fulfilled due to the ‘peaky’ rate of the offered electronic traffic. This problem can be fixed by increasing the expiration value of used timers but it leads to an excessive waiting time of electronic packets. So, a reasonable combination between these parameters may be able to improve the bandwidth utilization.

4.2 MAC in the Synchronous Ring Network

Optical fixed-Size Packet Creation is one of the most important processes in the synchronous access node [ECO 08]. In recent years, the optical packet creation has been investigated in ROME-O project [ROM 02] and in some studies such as [TDP 05], [FHT 05] and [CCH 05]. [TDP 05] analyzed the performance in the core of an optical network in the presence of fixed and variable packet formats when the aggregation mechanism is enabled. With the fixed packet format, [TDP 05] used a SAR (Segmentation and Reassembly) strategy when the optical packet size is short and then evaluated the efficiency of the aggregation process for three various IP distributions and different wavelength bit rates. As for [FHT 05], authors observed the impact of the optical packet creation on the traffic profile, and changed the traffic burstiness in order to obtain the histogram of the packet creation time and the filling ratio of the optical packet. Unlike these two studies, which are based on simulation results, [CCH 05] is based on the discrete time Markov chain, develops a mathematical model for the performance evaluation of timer and aggregation mechanisms inside a single node without taking into account a “real” network.

In mentioned studies, we remark that none of studies estimated the optical packet creation and evaluated the network performance regarding the timer value and the timeslot duration. The performance evaluation issue of synchronous POADM ring network, in which access nodes implement the timer-based mechanism, remains to be investigated. Regarding fairness results acquired from the timer-based mechanism that could enhance the network performance, we hence propose a new mechanism named “Virtual Synchronization” which comes from the timer-based mechanism idea in order to improve the transmission efficiency in the asynchronous network. The rest of this chapter is devoted to these works.

4.3 Optical Fixed-Size Packet Creation

The key element in the concept of synchronous node design consists in the access interface. Arriving electronic packets should be prepared to be transmitted on the optical layer. This preparation requires developing many supporting processes, such as: the reception of client traffic, the identification of the final destination for each incoming packet, the creation of optical packets and finally their transmission on the optical layer. In the optical model with the fixed-size packet, nodes should implement an optical packet creation mechanism in order to support variable-size electronic packets. At the exit of the optical domain, when optical packets reach their destination node in the optical domain, they are converted again to the initial electronic packet format. In this context, the creation process of optical packets has a major importance since it directly influences the transport efficiency.

4.3.1 Basic fix-size packet creation mechanism

Figure 4-1 illustrates different stages of the optical fix-size packet creation implemented in the synchronous model.

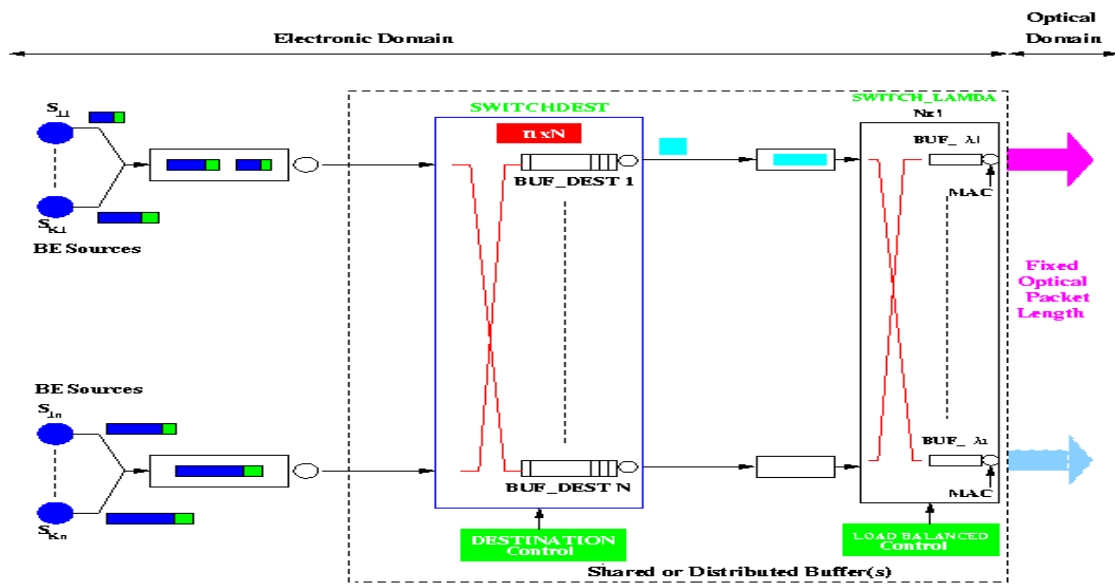


Figure 4-1: Optical fixed-size packet creation process

The optical packet creation mechanism is composed of different stages, which are:

- Traffic aggregation: In this stage, electronic packets are received by aggregation / concentration access points, which are situated at the entrance of each optical node.
- Traffic classification: This step prepares the traffic for the optical packet creation. Packets are directed, according to their destination, into different destination buffers (also called filling buffers and creation buffers). Each creation buffer assembles packets of the same destination in order to create the optical packet. In other terms, each optical packet will include electronic packets of the same destination. A mapping table is used in order to make the association between electronic and optical destinations.
- Optical packet creation: Optical classification buffers are finite-size memories. When the arrival of an electronic packet creates an overflow or a saturation of its target filling buffer, all electronic packets inside this buffer are moved and encapsulated into an optical packet. This packet constitutes a payload, to which an optical header will be added in order to create the optical fix-size packet (note that the optical header is equal to 32 bytes at 10Gbps).

After being created, optical packets go to a stage of load balancing and insertion scheduling mechanisms (these mechanisms are considered in the [TTE 08] and are out of the work).

4.3.2 Timer-based mechanism

During the optical packet creation, incoming electronic packets of the same destination are buffered inside a filling buffer. These packets remain memorized until the moment when sufficient information (bits) is collected for the optical packet creation. Even when the following slot is available, electronic packets must wait until the arrival of an electronic packet which triggers the optical packet creation.

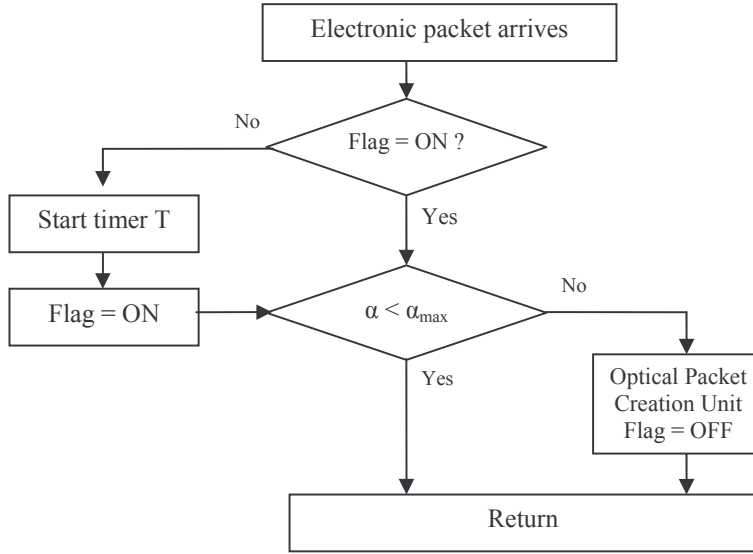


Figure 4-2: Schema of Timer-based mechanism triggered by an Electronic Packet Arrival

When client application services require the limited waiting time, this situation becomes unacceptable. Therefore, the optical packet creation delay should be limited by using a timer. The timer is reset each time the optical packet is created. At the timer expiration moment, the optical packet may be sent partially or fully filled. The optical partially-filled packet causes a waste of resources.

The timer-based mechanism can be defined as follows:

- Reset the Timer
- If the filling buffer exceeds the optical packet size ($\alpha \geq \alpha_{\max}$) then we send the optical packet and go to step 1
- If the timer expires while the filling buffer is not empty, then we send the not-fulfilled optical packet and go to step 1

The flag notifies that the timer has been already activated or not yet. When the size of the last packet coming into the filling buffer exceeds the remaining free space to be filled in the optical packet, there is thus an empty space left in the tail of this one. This empty space is limited by the biggest MTU (Maximum Transmission Unit) of client networks. We refer to this filling phenomenon as “the last packet problem”. Depending on the ratio of the optical packet size to the MTU value and the electronic packet size distribution, the bandwidth loss due to this phenomenon varies.

Thus, we choose the ratio α_{\max} as follows:

$$\alpha_{\max} = \left(1 - \frac{MTU}{\text{container size}}\right) \quad (4.1)$$

By having an optical packet size is bigger than MTU, we can keep this inherent bandwidth lost in safe levels.

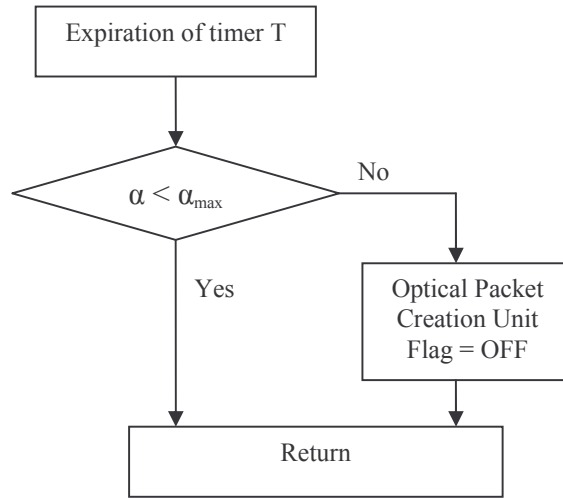


Figure 4-3: Schema of Timer mechanism: Timer Expiration

4.3.3 Simulation Scenarios and Numerical Results

We use the discrete-event network simulator tool [NWS 05] to simulate a synchronous ring network with 10 ring nodes sharing one wavelength operation at rate $R = 10Gbps$. The size of electronic and optical buffers at each node is set to 250 Kbytes to study the network performance under heavy loads. The incoming traffic is modeled as the best-effort traffic generated from many Interrupted Poisson Process (IPP) sources. These sources are configured with the burstiness of 10 and the mean burst length of 5 packets. The length distribution of generated packets is close to ‘real traffic’ Internet captured as shown in [CAD 99]. Figure 4-4 presents the distribution of IP packet sizes based on the traffic measurement from the Internet.

Measurement shows that most packets are ‘short’ and are concentrated around 64 bytes, while other size are of 576 and 1518 bytes. The most important size corresponds to the maximum value of an Ethernet frame. To close the ‘real BE traffic’, we use three types of packets: the short length packet of 50 bytes (10% total traffic volume), the medium length packet of 500 bytes (40% total traffic volume) and the long length packet of 1500 bytes (50% total traffic volume). We suppose that all ring nodes have the identical configuration and share the same arrival rate of electronic packets.

Note that in this chapter we are only interested in the performance evaluation of the network transporting of best-effort data traffic. The case with QoS guarantees will be approached in Chapter 5.

Before analyzing simulation results, we note that all mean values in our simulation results are computed with an accuracy of no more than a few percents at 95% confidence level using Batch Means method [TNH 06]. To follow the impact of the timer on the network performance, we propose two scenarios: bus (bus-topology) and 1-N (symmetric topology) corresponding respectively to access metro and core metro networks. Two scenarios are defined in the next section.

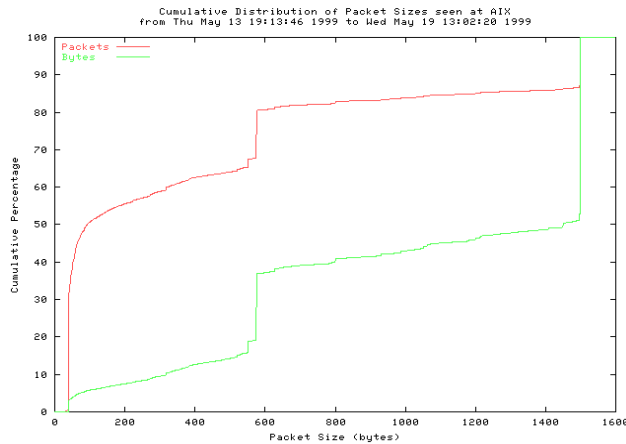


Figure 4-4: IP packet length distribution

In this work, we are not interested in the connected mode or packet sequencing of the network traffic. These studies are great works; so they are listed and investigated in ECOFRAME project [ECO 08] by other teams.

A. Description of Simulation Scenarios

As described above, the synchronous ring network can be used in metro access and metro core networks. To obtain various results, we propose two scenarios representing each type of the metro network: Bus and 1-N scenarios.

- *Bus scenario*: this is typically the case of a bus-based network. We consider in our simulation 10 nodes. One is centralized node while 9 others are access nodes. Access nodes send their traffic on the bus (one wavelength at 10Gbps) to the centralized node. In this scenario, we number access nodes from 1 to 9 starting with node 1 as the most upstream node. The offered ring load is defined as the ratio of the total traffic volume offered by IPP sources to the total ring bandwidth. If the offered workload distribution is uniform on the bus, the offered load at node i is calculated as follows:

$$\rho_i = \frac{\text{offered network load}}{\text{number of nodes}} = \frac{\text{offered network load}}{9} \quad (4.2)$$

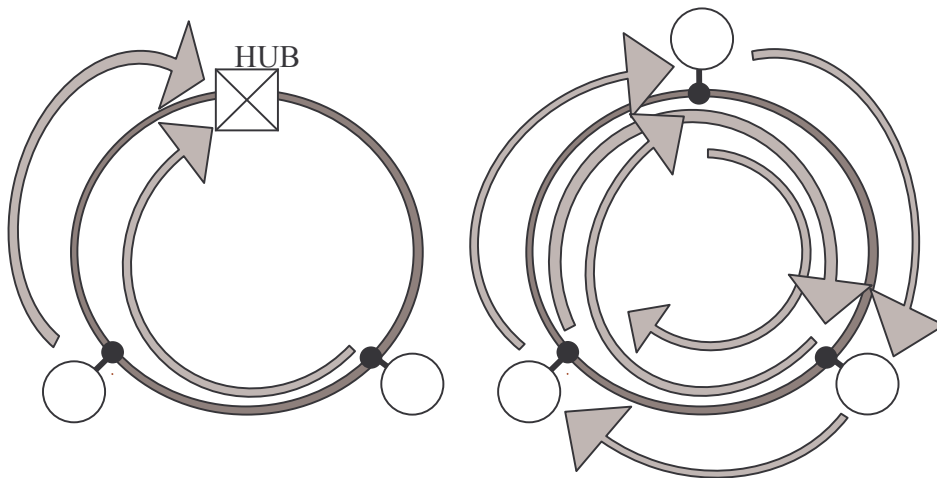


Figure 4-5: Scenario examples of 3 nodes: a) Metro Access and b) Metro Core

The offered load at each node is equal to the total traffic that the node wants to send towards the HUB.

- *1-N scenario*: this is the case representing the OPSR network with active nodes (i.e POADM nodes). In such type of network, a node communicates with all nodes in the ring. Here, the centralized node is not required. We thus consider 10 nodes symmetrically communicate through the ring using one wavelength operating at 10Gbps. The traffic is a full-meshed matrix. Each node generates 10% of the total traffic offered to the network if the network traffic distribution between ring nodes is uniform. Therefore, the offered load at node i is calculated as follows:

$$\rho_i = \frac{2 * offered\ network\ load}{number\ of\ nodes} = \frac{2 * offered\ network\ load}{10} \quad (4.3)$$

The offered load at each node is equal to the total traffic that the node sends to 9 other nodes. Figure 4-5 illustrates examples of two studied scenarios with only 3 nodes. We note that the following simulation is performed over only a unidirectional ring for simplification.

B. Performance Evaluation

Bus scenario

We now analyze the network performance at a given offered network load with different timer values. Figure 4-6 shows packet loss ratios obtained at each access node when the Timer mechanism is enabled with following parameters: the timeslot duration is equal to 10μs and the offered network load is set to 0.80. The packet loss ratio (PLR) is defined as the ratio of the number of electronic packets lost, due to the buffer overflow, to the number of electronic packets generated by sources during the simulation time. We first observe that with small timer values, the PLR tends to increase rapidly as we move down on the transmission bus, notably at last downstream nodes. For instance, with the timer value equal to 100μs, the PLR at nodes 1 to 8 is negligible (less than 0.001%) but it increases rapidly to 7% at node 9 (the last node on the transmission bus). This evolution of the PLR at access nodes is readily explained by the positional property [TNH 06] of the bus-based network. That is, under a heavy load, upstream nodes may monopolize all bandwidth and cause the head-of-the-line (HOL) blocking problem at downstream nodes.

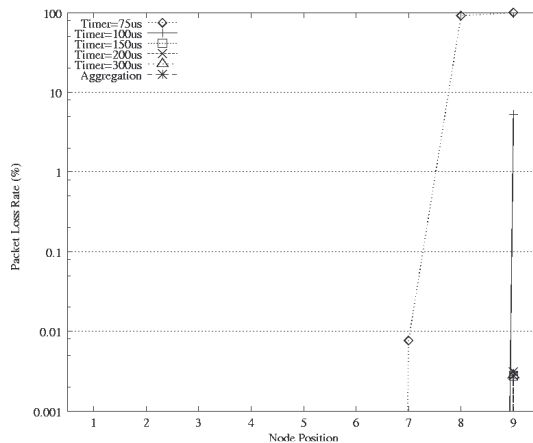


Figure 4-6: The PLR with a timeslot equal to 10μs and an offered network load set to 0.80

Additionally, the PLR strongly decreases at downstream nodes as the timer value increases. Indeed, the packet loss occurs very high at node 7, 8 and 9 with small timer values (e.g. some 98% at node 9 with the timer value equal to 75μs). The bigger the timer value, the smaller the PLR.

To explain the reduction of the PLR, we investigate the filling ratio of optical packets. Figure 4-7 shows the average filling ratio measured at an access node with the timeslot equal to $10\mu s$ while the offered ring load is set to 80%.

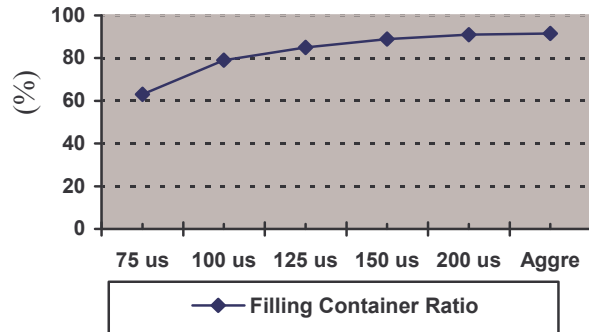


Figure 4-7: Filling Ratios with the timeslot equal to $10\mu s$ and the network load at 0.80

The filling ratio is observed at one node in the network. We observe that under a high workload, the optical packet is well-filled as the timer value increases. Thus, the transmission efficiency at each node increases sharply with the growth of the timer length. Particularly, the infinite duration of the Timer (aggregation case) allows the optical packet to be well filled. As expected, the average filling ratio approximately is equal to α_{max} (more than 90%), so-called “saturated circumstance”. Hence, we observe the smallest packet loss, about 0.002% as compared to other timer values. This is the case in which the network bandwidth is well exploited due to the fact that slots which are released by the current node become available for other downstream nodes on the bus.

Figure 4-8 plots the mean access delay of electronic packets at access nodes. The mean access delay of electronic packets is defined as the expected time elapsed from the moment when an electronic packet arrives at the electronic local buffer until it is successfully transmitted on the optical ring. This corresponds to the waiting time of electronic packets in the Add buffer and optical buffer. As shown in the figure, the mean access delay increases as we move downstream on the bus, due to the unfairness property of the node position on the bus (particularly with small timer values).

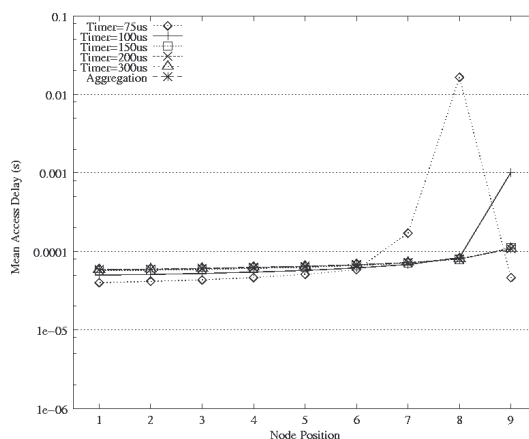


Figure 4-8: Mean access delay with a timeslot duration of $10\mu s$ and the offered network load equal to 0.8

Moreover, larger timer values can balance the access delay as compared to small timer values at last node. For instance, with the timer equal to $100\mu s$, the mean access delay attains some ms at node 9 while this value remains only about $0.0001s$ with the aggregation case. With assumed parameters,

the aggregation case may exhibit the most balanced delays from upstream nodes to downstream nodes on the bus.

Note that the smallest access delay shown for the timer value equal to $75\mu s$ at node 9 is meaningless. It is caused by some successful insertions during the transmitting phase of the simulation while most packets in the stationary phase are rejected. Therefore, the actual mean access delay for this timer value at node 9 is infinite.

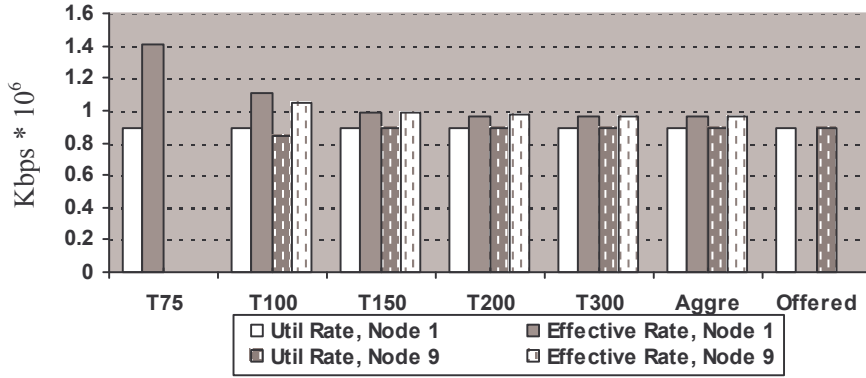


Figure 4-9: Utile and Effective Rates measured at nodes 1 and 9 with the timeslot equal to $10\mu s$ and the workload set to 0.80

Let's call "effective rate" be the rate of the amount of optical packets being transported on the optical ring, and let "utile rate" be the rate of the amount of electronic packets which are traveling inside the optical packet (being encapsulated in the optical packet). In Figure 4-9, we measure utile and effective rates, as the timer value varies, for node 1 (node with the best performance) and node 9 (node with the worst performance) on the bus. Note that "Effective" and "Utile" rates are both measured in *Gbps*. We observe that the utile rate increases and tends to the offered rate as the timer length increases, particularly at node 9. Under a very high arrival rate of electronic packet, optical packets are filled more rapidly, leading to more efficient transmission. In contrast to the utile rate, the effective rate with small timer values is very high as compared to it is obtained with bigger timer values (e.g. the effective rate obtained with a timer value of $100\mu s$ compared with the one measured in the simple aggregation). This is due to the fact that the number of optical packets generated with small timer values is always higher than the one generated with bigger timer values. Using small timer values leads to a very high volume of optical headers added to the optical packets, causing an excessive effective rate. So as the timer value goes up, the utile rate increases while the effective rate decreases. Particularly, with the timer value equal to $75\mu s$, effective and utile rates are seemingly null in node 9 since few packets have been sent at this last node while other packets have been blocked by packets which are sent by upstream nodes.

Now we investigate the performance of the timer-based mechanism under unbalanced traffic partitions. Our aim is to analyze the robustness of the timer-based mechanism under different network traffic. Figure 4-10 respectively shows the cases where the traffic increases and decreases uniformly when we move to downstream nodes on the bus. Note that the timer-based mechanism in increasing and decreasing traffic partitions does not perform good performance as compared with the uniform traffic pattern. The timer-based mechanism in the uniform traffic pattern performs more balanced access delays and less packet loss than that used in unbalanced traffic patterns.

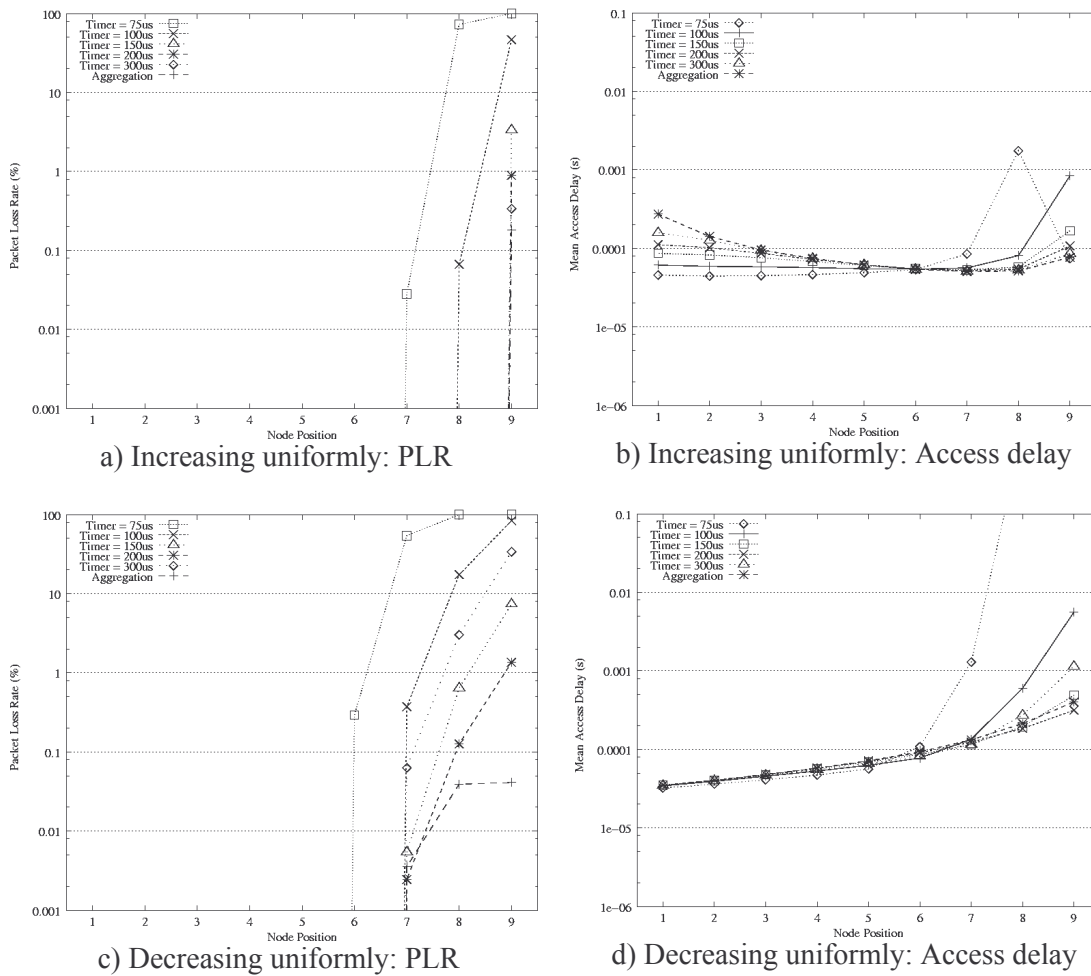


Figure 4-10: Obtained results under unbalanced traffic patterns

As for the increasing traffic, the amount of the traffic offered to first nodes on the bus is smaller than the one at last nodes. Therefore, the filling ratio at first nodes is smaller than the value at last nodes, leading to more wasted bandwidth at first nodes while last nodes, which have many well-filled optical packets, can not find enough space on the bus to transmit their local packets. On the other hand, for the decreasing traffic, well-filled optical packets in first nodes prevent “not well-filled packets” at last nodes from transmitting; it leads to the case in which the mean waiting time is small at first nodes (about $30\mu s$) but very high at last nodes (notably for small timer values).

For all traffic distributions, the simple aggregation always performs the best performance regardless of traffic distribution. It is considered to be the best choice of the timer value. Even with the decreasing traffic partition, it shows a small packet loss ratio (0.05%) while the mean access delay remains about $0.3ms$.

We may now consider the performance evaluation of the timer-based mechanism (Figure 4-11) in the case where the network load varies from 0.40 to 0.90 under the uniform distribution. We consider the timeslot equal to $10\mu s$ while the timer value is respectively $150\mu s$ and infinite (the aggregation mechanism). As explained above, results given by the simple aggregation are always better than those of limited timer values even when the network load is set to 0.90. However, when the network load is very high (about 0.90) the node performance can not be guaranteed by the timer-based mechanism (e.g. the packet loss ratio is nearly 10% even in the aggregation case). Through these experiments, we see that the timer-based mechanism works well when the network load is smaller than 0.8.

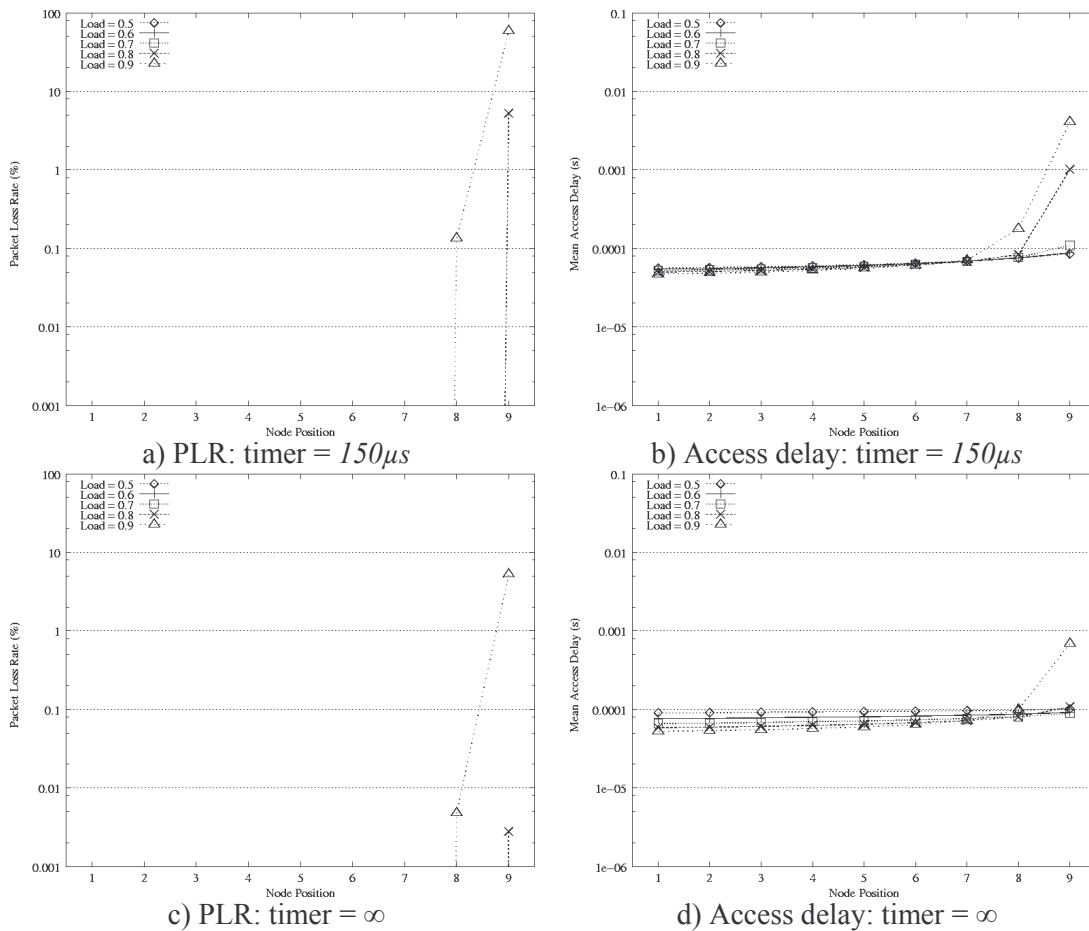


Figure 4-11: Obtained results as the network load varies

We may now analyze the timer-based mechanism when the timeslot varies from $2\mu\text{s}$ to $20\mu\text{s}$ as the network load is set at 0.75. Figure 4-12 plots the mean access delay and the PLR at each access node when the aggregation case is enabled. The mean access delay is shown on the right figure and the PLR is shown on the left one. We observe that access delays with three timeslot values ($10\mu\text{s}$, $15\mu\text{s}$, and $20\mu\text{s}$) are more balanced than the ones with timeslot values of $2\mu\text{s}$ and $5\mu\text{s}$. This is due to the fact that with a very small timeslot, we observe a very low filling ratio of the optical packet since it is limited by α_{max} (which is computed in (4.1)). Indeed, when the timeslot is equal to $2\mu\text{s}$, α_{max} is measured about 60% ($=1500/2500$), corresponding to 40% of remaining space that is usually not filled. This leads to 40% of wasted bandwidth.

In our simulation, the timeslot whose size is bigger than $10\mu\text{s}$ can limit the packet loss at node 9. On the other hand, the timeslot, which length equals $10\mu\text{s}$, is the most reasonable choice because it does not cause the packet loss while having the most balanced delays as compared to other timeslot values ($2\mu\text{s}$, $5\mu\text{s}$, $15\mu\text{s}$, $20\mu\text{s}$). For this reason, we have chosen the timeslot equal to $10\mu\text{s}$ for the first experiment in this chapter.

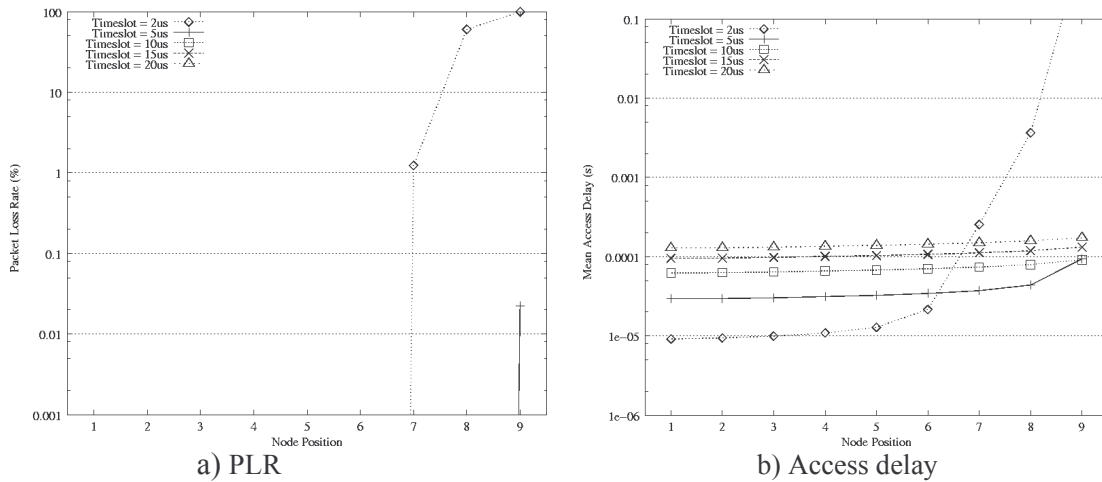


Figure 4-12: Obtained results as the timeslot varies

Figure 4-13 shows the average filling ratio and utile/effective rates with different timeslots. The behavior of measured filling ratios as well as utile and effective rates can be explained as varying the timer duration. Since the aggregation mechanism is used, the optical packet is well filled with the maximum slot duration ($20\mu s$). This is due to the small proportion of the remaining space to the total optical packet size.

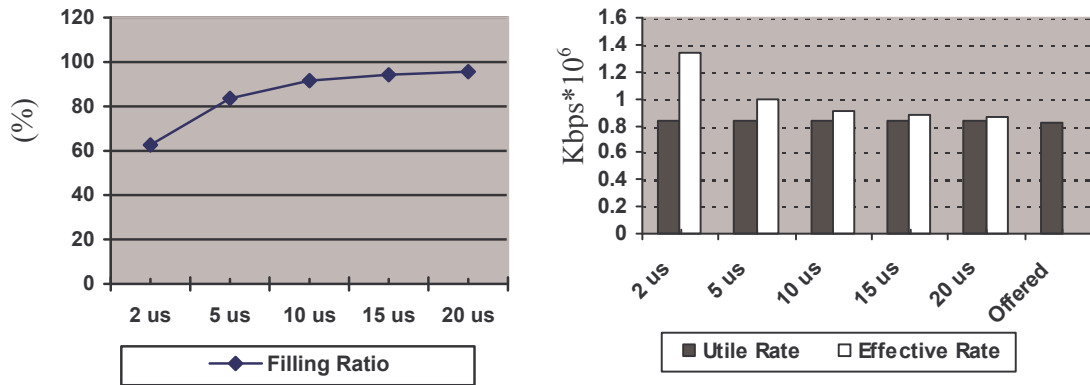


Figure 4-13: Measured filling ratios, utile and effective rates as the timeslot varies

1-N scenario

Now, we analyze the network performance at a given offered network load with different timer values in the 1-N scenario. As mentioned earlier, the arrival rate of electronic packets at ring nodes in this scenario is smaller than the Bus-based scenario, because the offered traffic arriving to the node is divided into several sub-traffic flows going to different destinations. We focus on Figure 4-14 which shows the packet loss ratio and the mean access delay obtained at each ring node. We enable the timer-based mechanism with the timeslot equal to $10\mu s$ and we set the offered network load to 0.8.

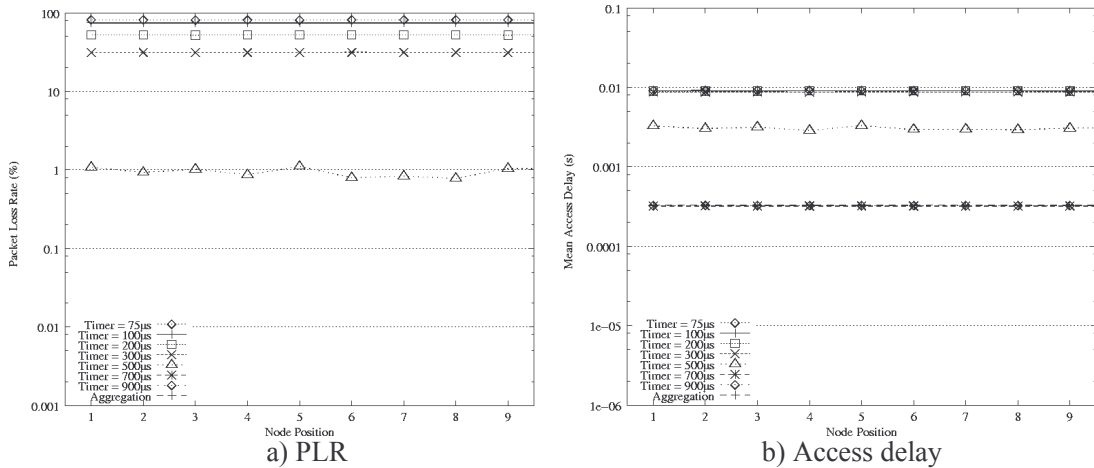


Figure 4-14: Packet loss ratio and mean access delay with the timeslot equal to $10\mu s$ and the offered network load is set to 0.8

Firstly, we observe that results obtained (both PLR and mean access delay) from ring nodes are nearly the same. This is due to the full-meshed traffic matrix. Secondly, the good choice of timer values observed is from $T=700\mu s$ to infinity. For instance, the left figure does not show the packet loss from the timer value of $700\mu s$ while in the right figure, mean access delays obtained from $T=700\mu s$ to infinity are small as compared to other timer values. However, the simple aggregation always offers the best filling ratio as shown in the following figure in which the network load is equal to 0.8.

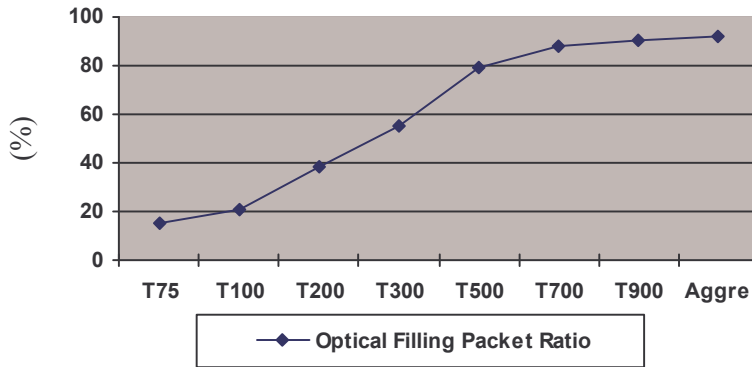


Figure 4-15: Optical Packet's Filling Ratio

As shown in Figure 4-15, the filling ratio increases as the timer value increases. However, the increasing rate of the filling ratio in the 1-N scenario is more rapid than that in the Bus-based scenario, notably as the timer size varies from $100\mu s$ to $700\mu s$. The filling ratio is close to a maximum value when the timer value tends to infinity. Therefore, the transmission efficiency increases clearly with the increase of the timer duration when the workload equal to 0.8.

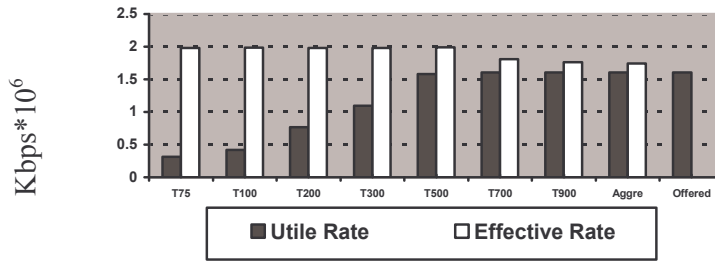
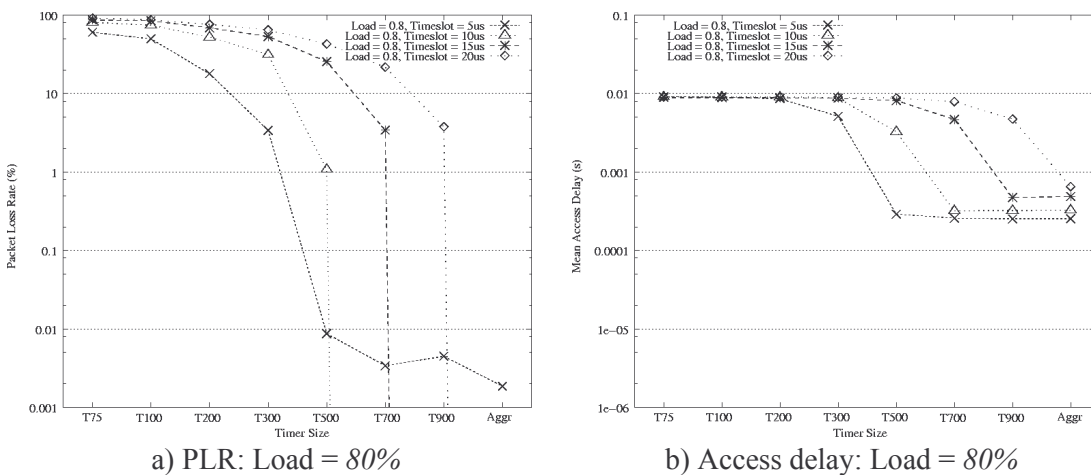


Figure 4-16: Utile and Effective Rates measured at a node with the timeslot equal to $10\mu s$ and the network equal to 0.80

The utile and effective rates in function of the timer value are shown in Figure 4-16. With a high arrival rate of the electronic traffic, the optical packet will not be well-filled when using small timer values. We see that, the optical overhead volume (the difference between effective and utile rates) occupies from 6% (with infinite timer size) to about 700% (with the timer equals $75\mu s$) of the offered traffic. As a result, the effective rate at small timer values becomes very high. So, to transport 100% utile traffic, small timer values need 700% (e.g. the timer equals $75\mu s$) added overhead as compared to 6% added overhead with bigger timer values (e.g. the timer equal to $700\mu s$).

For the 1-N scenario, we continue to consider Figure 4-17 where we vary the network load from 80% down to 60% and 40% respectively as the timer size varies from $75\mu s$ to infinity with four timeslot values: $5\mu s$, $10\mu s$, $15\mu s$ and $20\mu s$. Note that these results are observed only at a ring node. Firstly, we concentrate on Figure 4-17a and Figure 4-17b. Figure 4-17a presents the mean access delay while Figure 4-17b presents the PLR with the workload equal to 80%. We can note that when the timeslot equals $5\mu s$, the packet loss exists at all timer values. The packet loss ratio decreases as the timer value increases and it is reduced to about 0.002% with the maximum timer value. On the other hand, as the timeslot size is bigger than $5\mu s$, only small timer values (e.g. timer values are less than $700\mu s$ with the timeslot equal to $15\mu s$) cause the packet loss. The access delay behavior when the network load equal to 0.8 in the right figure seems to be “acceptable” as referred to the BE packet, notably with big timer values.



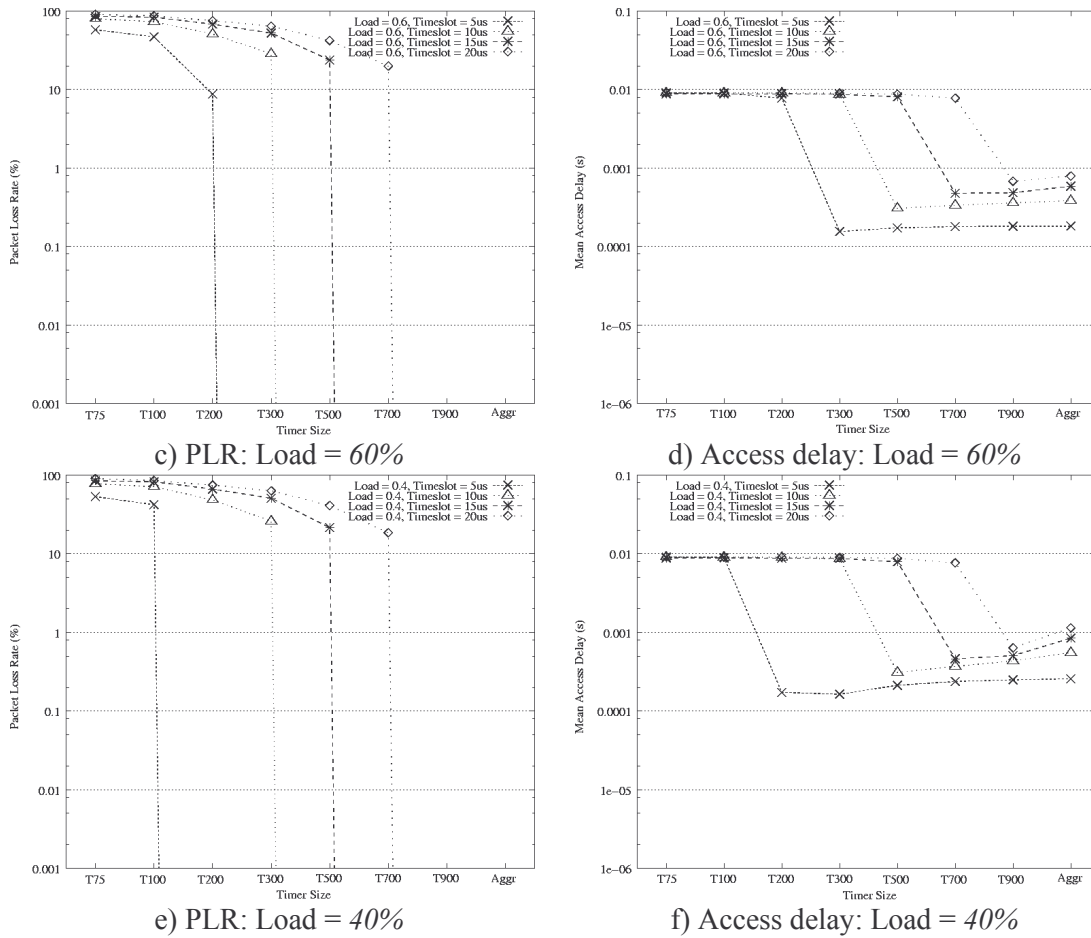


Figure 4-17: Set of results obtained in varying network load, timeslot and timer size

We may now focus on the medium workload. The workload is set to 0.6 presented in Figure 4-17c and Figure 4-17d. Observing the results, there is no loss from big timer sizes. In addition, big timer sizes have the smallest access delay as compared to small timer sizes for any timeslot values. Interestingly, a special behavior with small offered loads is observed in Figure 4-17e and Figure 4-17f where the workload is equal to 0.4. In this case, the aggregation mechanism does not offer the best performance (in terms of access delay and PLR). Regarding the timeslot which is equal to $10\mu\text{s}$, the access delay obtained by the aggregation mechanism is higher than that obtained by other timeslots ($500\mu\text{s}$, $700\mu\text{s}$, and $900\mu\text{s}$). This is mainly due to the fact that under a small network load, electronic packets arrive with a very low rate leading to a circumstance where first electronic packets in the aggregation buffer must wait very long until “the last packet problem” occurs.

On the other hand, regarding Figure 4-18 (the timeslot equal to $10\mu\text{s}$ and the network load equal to 0.4), we observe that the “effective rate” obtained with the aggregation mechanism is always smaller than other cases, thanks to the small optical packet number. And, the “utile rate” measured with the aggregation mechanism is the biggest as compared to other timer values (e.g. with the timer length equal to $500\mu\text{s}$) thanks to the highest filling ratio. So, the simple aggregation always offers the best network performance in terms of “utile and effective rates”.

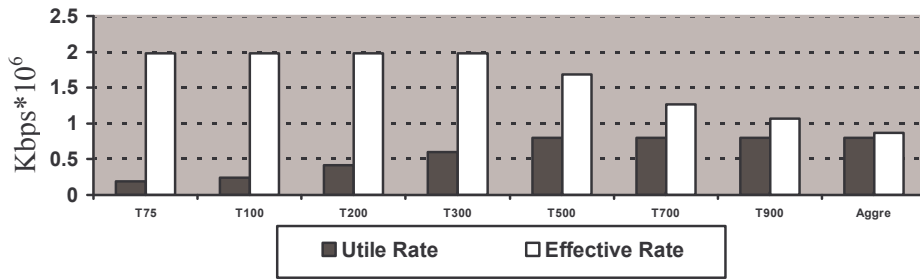


Figure 4-18: Utilite and Effective Rates measured at a node with timeslot of $10\mu s$ and network equal to 0.40

We think that these experiments help us to observe the impact of the timer-based mechanism on the network performance; hence we may choose a reasonable timer value for a given traffic matrix in order to obtain the best performance. This should be very useful because it reduces implementation and maintaining cost of a network which supports optical fixed-size packet while optimizing the resource utilization.

4.4 Virtual Synchronization Mechanism

This section describes an access scheme, which is proposed to improve the performance of the CSMA/CA protocol in the asynchronous OPSR network. Based on the idea of the optical fixed-size packet creation that performs a very good performance in the synchronous network, we now focus on a novel concept called “Virtual SynChronization” (VSC) scheme. The proposed scheme is to improve the bandwidth utilization rate. This section is devoted to the VSC scheme followed by its details. The numerical results illustrating the efficiency of VSC in enhancing the network performance as compared to the original CSMA/CA protocol then will be presented.

In the literature, there are some studies on the fairness improvement for the asynchronous bus-based network using CSMA/CA protocol such as TCARD [BDC 04], GLUE [DPA 05], MPB [NGA 05] and DI-MAC [NGA 06]. Among them, MPB and DI-MAC rise as good solutions but it is not easy to implement them due to the algorithm complexity. For this reason, we propose the VSC scheme.

4.4.1 Idea of VSC Scheme

The problem of the bandwidth fragmentation is well-known in an asynchronous bus-based network using the OU-CSMA/CA protocol where the bandwidth is wastefully used by access nodes. In such network, each access node begins its transmission whenever it detects enough voids without “touching” any transiting packets due to passive components. This leads to the unwanted fragmentation of the bandwidth. Additionally, another major problem is the unfairness property which is known as “position priority” [NGA 06].

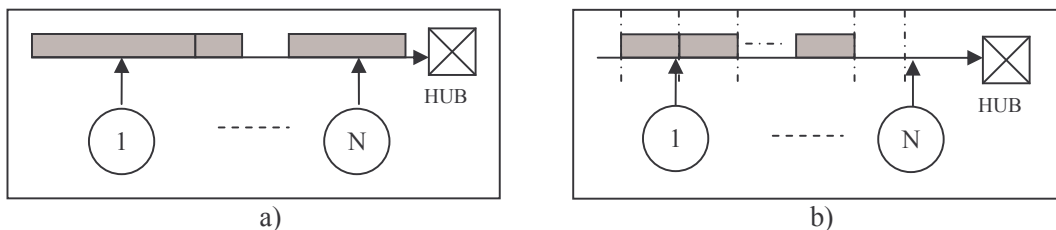


Figure 4-19: Example of asynchronous (a) and synchronous networks (b)

On the contrary, a node in the synchronous network is synchronized with other nodes by a distributed clock while the network bandwidth is slotted in equal time units. The node detects available voids which are equal to one or several slots, and then transmits an electronic packet so that the packet size tightly matches the slot duration.

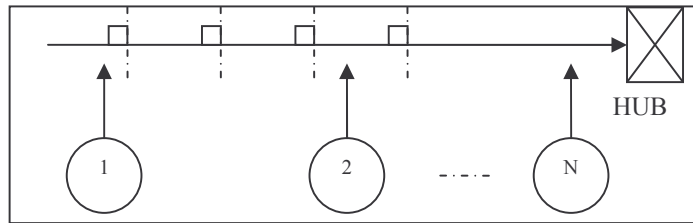


Figure 4-20: Example of VSC scheme

It is worth mentioning that node 1 (the most upstream node) plays a very important role in such network. Indeed, node 1 begins the bus, and at the same time, it begins the fragmentation of the shared bandwidth. The idea of the VSC scheme is very similar to the MPB algorithm except that the first node functions as a “virtual clock” which stands for the bandwidth synchronization. In fact, MPB burst length may be extended as long as the node has electronic payloads to transmit and the bandwidth is still available. The burst ends only when the node has no more data packets or when there is no more available bandwidth. In VSC scheme, an optical packet has fixed size that exactly matches a slotted void “created” by synchronizing packets (see Figure 4-20 and Figure 4-21).

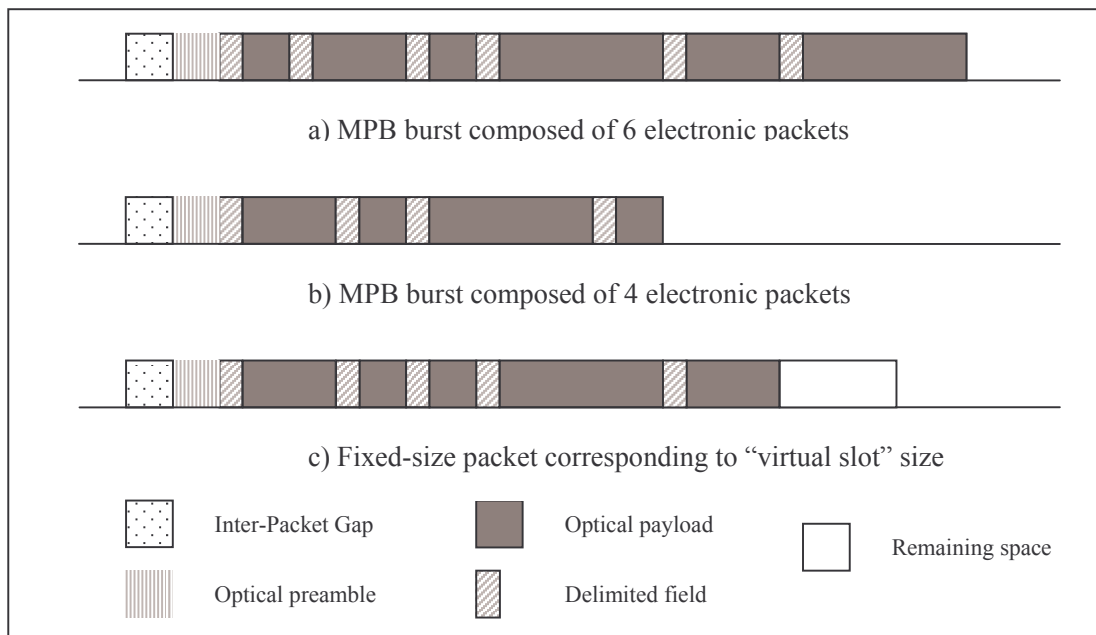


Figure 4-21: Optical Fixed-size packet used in VSC scheme vs. MPB burst

To synchronize the network, node 1 (the most upstream node) always transmits “synchronizing packets” in several time units to the Hub. Small synchronizing packets are sent at regular time intervals of equal duration. Other nodes on the ring observe slotted transmission bandwidth in the transit line and transmit their data only in the so-created Virtual Slots (VS). A synchronizing packet is

defined as an optical packet in which the payload zone is null. At each node, electronic packets of variable size are aggregated and accommodated into large optical fixed-size packets. The transmission time of each optical packet is equal to the duration of one virtual slot (VS). During the process of the optical packet creation, electronic packets from upper layer are stored until enough data (bytes) is collected, even when the network transmission resources are available. Electronic packets must wait until the optical packet creation signal is triggered by the arrival of the “last electronic packet”. Before running in the VSC mode, an access node should run in “initial phase” mode.

“Initial phase” rises at the beginning of the VSC scheme. In fact, downstream nodes must wait until they detect synchronizing packets coming from the first access node before synchronizing its transmission. As a result, access node functions without VSC scheme till it receives synchronizing signals. Therefore the network bandwidth is still fragmented during the “initial phase”. The time that the access node suffers from the “initial phase” depends on the distance between it and the first node (node 1). So, last downstream node suffers the longest time of “initial phase”. Bus nodes synchronize their transmission at the detection of synchronizing packets. The more the distance between access nodes increases, the more the synchronizing time in the initial phase becomes longer.

A drawback of such algorithm comes from the loss probability of synchronizing packets. Indeed, in the case where some synchronizing packets are lost or delayed (because of link failure, etc.), downstream nodes can not detect Virtual Slots. Hence, these nodes must work in the asynchronous mode until they detect a synchronizing packet.

Since all optical fixed-size packets have the same destination (Hub node) and they are commonly not well-filled by electronic packets at source nodes, so a not full-filled packet coming from upstream nodes might be continuously filled at downstream nodes. At the moment whenever an optical packet is delayed in FDL, an intermediate node can add its electronic packets (if its buffer is not empty) until the packet is full-filled. So, we consider two different sub-mechanisms: VSC algorithm with and without “full-filling in transit line”. In our simulation results, we show only results obtained by VSC algorithm with “full-filling in transit line” (so-called shortly VSC algorithm).

4.4.2 VSC Algorithm Implementation

The implementation of the VSC mechanism is described as follows. The procedure executed at the first node on the downstream bus has a little different from the one executed at other nodes. Since the first node is responsible for the generation of synchronizing packets, so access node transmits only optical fixed-size packets after each successful transmission of a synchronizing packet. On the other hand, other nodes on the bus must wait until they detect the first synchronizing packet before enabling the timer.

4.4.3 VSC Performance Evaluation

We may now attempt to analyze the efficiency of our VSC mechanism in enhancing the OPSR network performance supporting the OU-CSMA/CA protocol. As stated above, we are only interested in the performance analysis of an OPSR network transporting best-effort data traffic. We use the discrete-event network simulator tool to simulate the OPSR network with 9 access point nodes and 1 Hub node, sharing one wavelength operating at rate $10Gps$. The size of electronic buffers at each node is equal to 250 Kbytes. We assume also that the incoming best-effort traffic is modeled as an aggregation of many IPP processes configured with the burstiness of 10 and the mean burst length of 5 packets. All access nodes share the same packet arrival rate and the same timer value.

In the simulation, we use synchronizing packets which size equals 70 bytes. This corresponds to a standard Ethernet Protocol Data Unit (EPDU of which we remove the payload field). The virtual slot can accommodate the packet size equal to 12Kbytes. Hence, the optical packet size is about $[12Kbytes - 70 bytes] = 11930$ bytes.

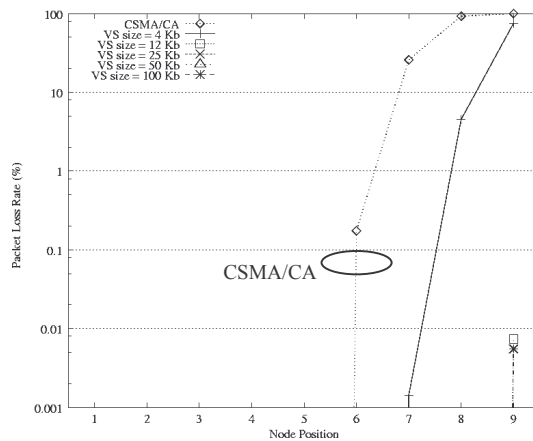


Figure 4-22: PLR at access nodes with the OU-CSMA/CA protocol and with different VS sizes when the network load is equal to 0.8.

Figure 4-22 shows the packet loss ratio at each access node obtained with the OU-CSMA/CA protocol and with VSC mechanism using different values of the “virtual slot” (VS) when we fix the network load equal to 0.8. We first observe that with OU-CSMA/CA protocol, the PLR is likely to increase rapidly as we move downstream on the transmission bus. As shown in the figure, the PLR at node 6 is about 0.3%, but it quickly increases to nearly 95% at node 8 and 100% at node 9. This is due to the nature problem of the positional priority and the bandwidth fragmentation in the bus-based network that we have mentioned. On the other hand, with VSC scheme, PLR results are much smaller, even at the last node when using a reasonable “virtual slot” (VS) size. For example, the packet loss occurs only for small values (4 Kbytes) or for extremely big values of VS (100 Kbytes). This behavior is very similar to results obtained with the timer-based mechanism in the case where we vary the timeslot duration. The VS size of 4 Kbytes corresponds to the case where we enable the timer mechanism with the slot duration equal to $2\mu s$. An extremely big value of VS size corresponds to a very big value of the timer slot. Therefore, the node has to wait extremely long before transmitting, and this may cause the packet loss again.

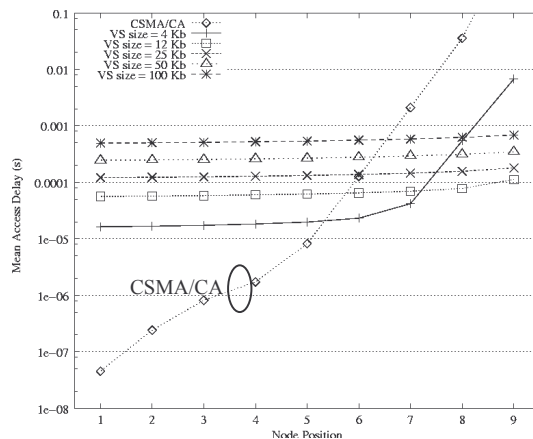


Figure 4-23: Average access delay at access nodes with the OU-CSMA/CA protocol and with different VS sizes when the network load set to 0.8.

Figure 4-23 plots the mean access delay at each node, comparing the case of OU-CSMA protocol to the case of VS scheme with different VS sizes. With OU-CSMA/CA protocol, the mean access delay

increases rapidly as the node priority decreases. Moreover, it particularly “explodes” at the most downstream node (e.g. node 8 and node 9) as shown in the figure. For example, with the VS size of 25 Kbytes, the mean access delay at all nodes is of some *ms*, while the CSMA/CA protocol’s delay becomes more *0.1s*. Regarding the CSMA/CA curve, access delays measured at last nodes are very high. These values are unacceptable in terms of quality of service (QoS) of best-effort traffic.

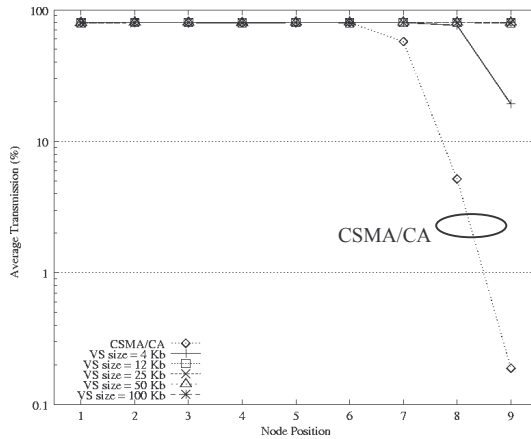


Figure 4-24: Average transmission ratio with the OU-CSMA/CA protocol and with different VS sizes as the network load = 0.8.

We now investigate the average transmission ratio. The average transmission ratio is the utile rate measured at the output node to the offered rate. These values have been plotted in Figure 4-24. Note that under the uniform workload, all nodes in the bus have similar average transmission if they do not show the packet loss (from nodes 1 to 5). The average transmission decrease occurs only at last nodes in which the packet loss occurs. In fact, at last nodes, CSMA/CA protocol shows the smallest average transmission ratio (0.2% at node 9) followed by VSC scheme with the VS size of 4 Kbytes (more 20% at node 9).

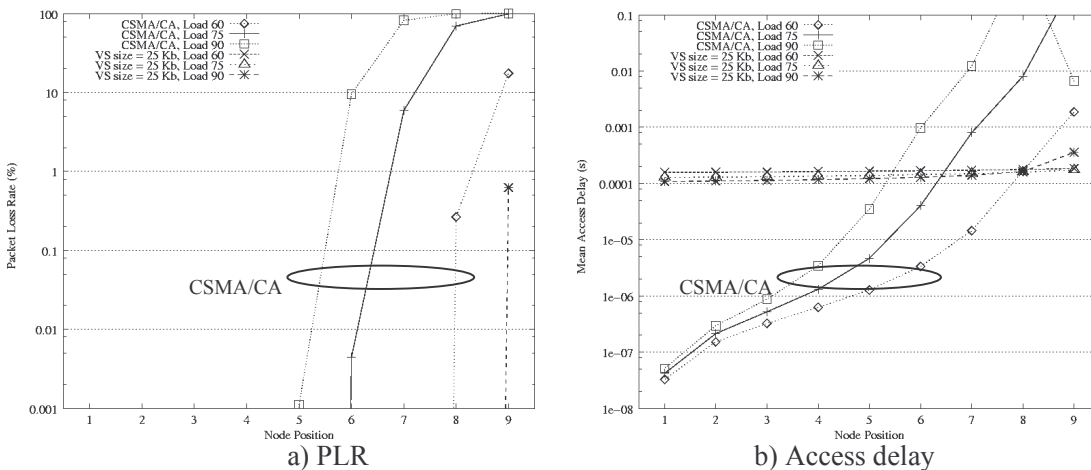


Figure 4-25: Results obtained at each node with the OU-CSMA/CA protocol and with the VS size of 25 Kbytes.

The last set of our simulation (Figure 4-25) is devoted to the analysis of the behavior of VSC scheme towards different access nodes. In this experiment, we fix the VS size equal to 25 Kbytes. Firstly, the network performance (in terms of access delay and PLR) strongly decreases with the

increase of the offered workload in the case using OU-CSMA/CA protocol. By contrast, with VSC scheme, the PLR is not observed except the workload equal to 0.9 (lower than 1%).

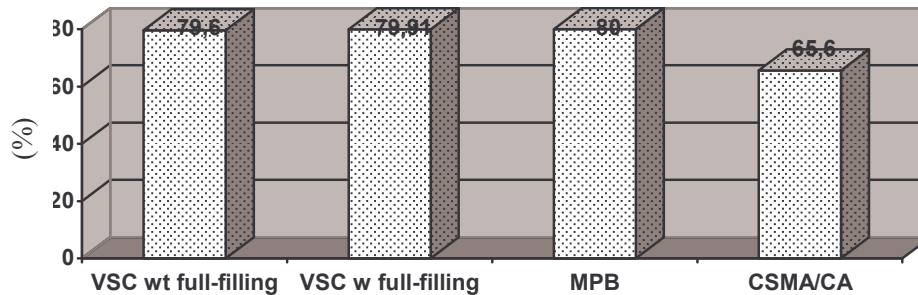


Figure 4-26: Bandwidth Utilization Ratio (%) under the workload of 0.8

Referring to [NGA 05], we observe that the MPB can exploit 80% bandwidth while VSC scheme can exploit 79.91% bandwidth – obviously with “full-filling” (shown in Figure 4-26). This is due to the fact that a small amount of bandwidth in VSC scheme is used to transmit “synchronizing packets”. Another different point between MPB and VSC is that MPB detects free voids while VSC simply checks the free slot. So, MPB spends more resource for this work than VSC.

4.5 Concluding remarks

This chapter firstly describes the impact of the timer-based mechanism on the performance of the synchronous network supporting optical fixed-size packet in two cases: metro access and metro core networks that are respectively represented by Bus and 1-N scenarios. The impact of the timer-based mechanism on network performance depends on traffic matrix as well as on the timeslot duration. We observed that the simple aggregation always offers good performance in both scenarios, notably under the medium ($> 50\%$) and heavy workloads ($> 90\%$). In the bus scenario, the simple aggregation performs the best performance for all experimented cases while this mechanism is one of good choices in 1-N scenario. From these experiments, the reasonable timeslot duration that we should choose is $10\mu s$ regardless of traffic matrix of the network. In addition, these studies become very important when we investigate advanced mechanisms to create optical CoS-enabled fixed-size packet in the next chapter.

In the second section, we have proposed the Virtual Synchronization scheme with the aim of improving the bandwidth utilization in an asynchronous bus-based network that supports variable size electronic packets. Idea of this scheme comes from the optical fixed-size packet creation in the synchronous network. The use of synchronizing packets in VSC mechanism reduces the amount of bandwidth accessible for transmission. However, compared to other mechanisms such as OU-CSMA/CA or TCARD, VSC mechanism clearly improves the network performance in terms of transmission ratio and bandwidth utilization. So, we think that VSC scheme is one of good choices among other mechanisms such as MPB and DI-MAC.

Chapter 5

Medium Access Protocols in Multi-service Metropolitan Optical Synchronous Ring Network

The chapter addresses timer-based and advanced access mechanisms such as Packet Erasing Mechanism (PEM), Extraction/Reemission Mechanism (ERM) [FOM 06], [FOM 07] in the synchronous OPSR network with different quality of service (QoS) requirements. The problem of defining the type and the number of services supported by the optical metro network will be taken into account. Regarding the optical fixed-size packet creation, two possible mapping (electronic-optic) solutions for the optical packet creation: Mono-class and Multi-class are considered. The network performance comparison between mono-class and multi-class becomes hence our focus.

Firstly, we begin the chapter with the description of quality of service supported by the optical metro network and the mapping solutions used in the optical fixed-size packet creation. Then, we introduce PEM, ERM as well as a novel mechanism called Dynamic CoS-Upgrade Mechanism which is proposed with the aim of adapting to the variation of the arrival rate of electronic packets. Finally, we close the chapter with some concluding remarks.

5.1 Quality of service Overview

In recent years, the rapid increase of network traffic leads to the demand of more network capacity. Web traffic, voice and video over IP, and other multimedia applications have significantly contributed to this increase. Moreover, some applications, such as interactive multimedia applications, not only require large amounts of bandwidth, but also require particular services from a network in order to respect to the latency and the loss. The network should guarantee services required by interactive multimedia applications without degrading the performance of other applications in the network.

Quality of service (QoS) is usually specified by four characteristics of the data transmission: bandwidth, data loss ratio, end-to-end delay, and jitter. *Bandwidth* is the maximum amount of data sent on the network per time unit (in seconds for example). The amount of data, which is sent on the network, consists of local data and protocol overheads such as packet headers. Hence, the bandwidth 'seen' by the network node is lower than available network bandwidth. *Data loss ratio* is the total amount of data that can be lost at local node or on the transmission path over total amount of generated data. *End-to-end delay* or *latency* is the maximum amount of time that data will take to

travel from a source to a destination. *Jitter* is the maximum variance in the delay between successively received data amounts. Limiting the jitter is useful for real-time multimedia applications such as voice and video conference.

5.1.1 QoS Parameters

Service Class	Service characteristics	Service performance		
		Packet Loss Rate	Delay	Jitter
Premium	Real time telephony or video Applications	Loss < 0.001%	Delay < 5ms	Jitter < 1 ms
Silver	Bursty mission critical data applications requiring low loss and delay (e.g. Storage)	Loss < 0.01%	Delay < 5ms	Jitter = N/S
Bronze	Bursty data applications requiring bandwidth assurances	Loss < 0.1%	Delay < 15ms	Jitter = N/S
Standard	Best effort service	Loss < 0.5%	Delay < 30ms	Jitter = N/S

Table 5-1: CoS identification for metro network

A typical metropolitan network interconnects enterprises, organizations and academic campus with the variety of applications. Metropolitan network operators are actively seeking the ability to support different levels of QoS for different types of applications, particularly in the enterprise. The necessity of QoS identification is driven by:

- (i) The different QoS requirements of different types of applications (low end-end delay for interactive applications, high throughput for file transfer applications ...);
- (ii) The different relative importance of different applications to the enterprise (Oracle database transactions may be considered critical and therefore high priority, while traffic associated with browsing external web sites is generally less important);
- (iii) The desire to optimize the usage of their existing network infrastructures under finite capacity and cost constraints, while ensuring a good performance for important applications.

We consider four types of the application traffic (Premium, Silver, Bronze and Best Effort) that are supported in the metro network as shown in table 5.1. The table refers to the Metro Ethernet Service Level Agreement (SLA) [MEF 03]. We assume that four CoS's identifications including traffic characteristics, service performance and traffic priority will be referred as expected performance requirements for our study in the rest of this chapter.

5.1.2 QoS Mapping

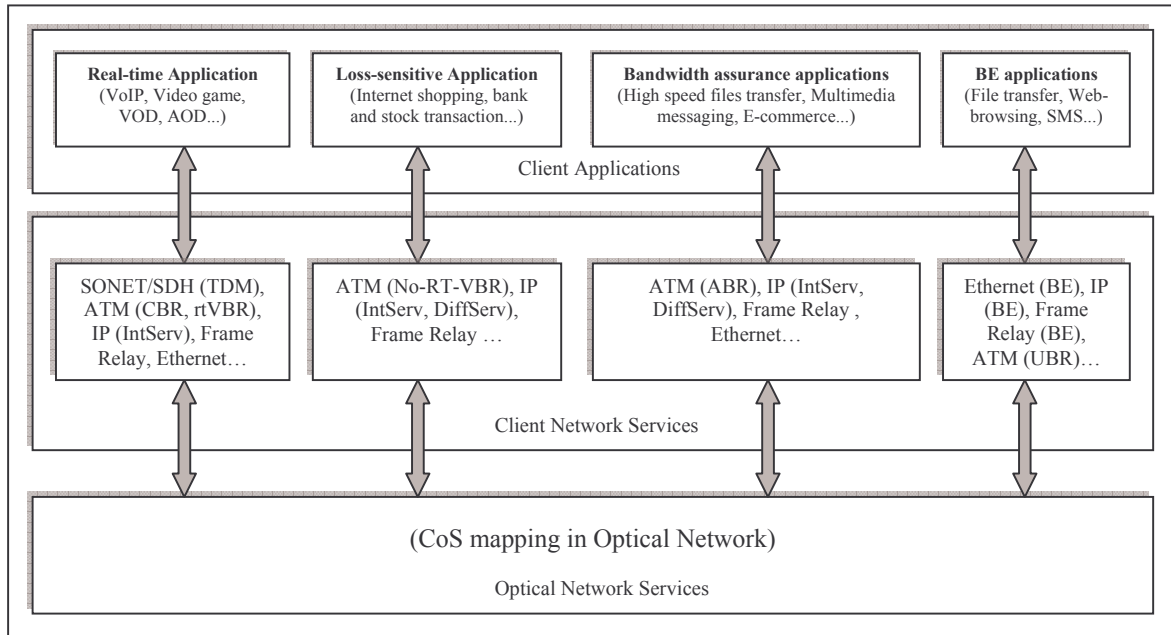


Figure 5-1: QoS mapping

Many types of client network such as SONET/SDH, ATM, Frame Relay, Ethernet... might be interconnected with a metropolitan network. Each client network offers specific service, to satisfy all demands of QoS of metropolitan users. Based on above QoS parameters, we approach two possible mapping solutions (electronic-optic): mono-class and multi-class.

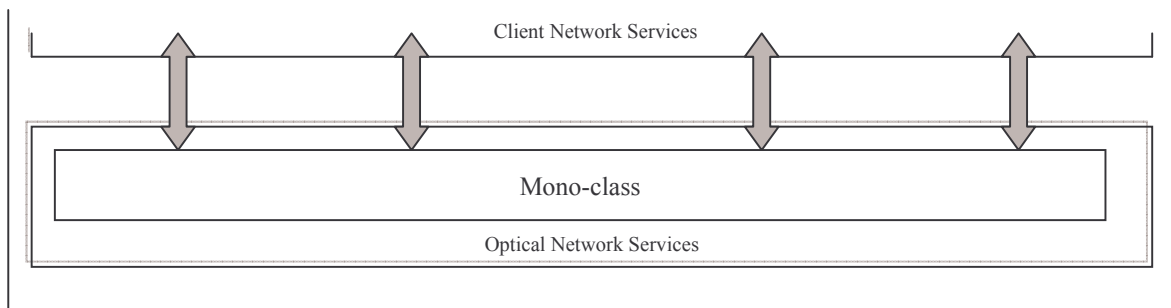


Figure 5-2: Mono-class case

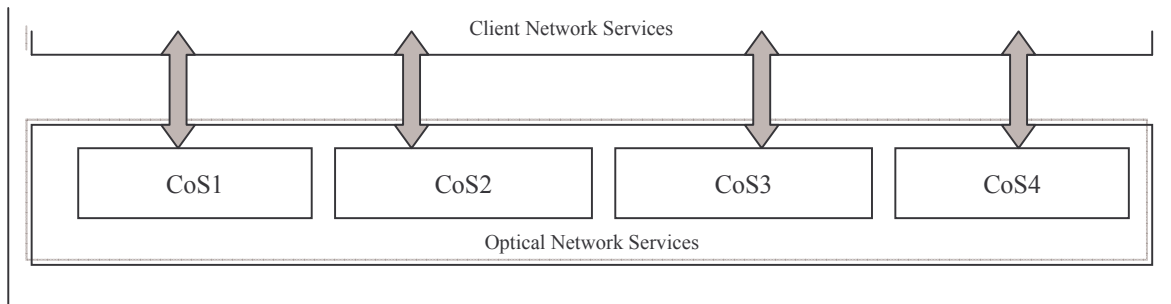


Figure 5-3: Multi-class case (supporting four class of service)

The problem of CoS mapping between electronic domain and optic domain remains a highly controversial issue. In fact, the mapping between end-user QoS requirements and services supported by the optical network has a large impact on the network performance. So, the network performance with different mapping solutions mentioned above will be investigated in the rest of this chapter.

5.2 Mono-Class Approach

This approach is similar to the basic timer-based mechanism. Client traffic is only classified by its destination (as shown in the following figure). One aggregation buffer is used for one destination. One timer is attached to each aggregation buffer. The approach treats all types of electronic packets in the same way.

Since mono-class does not allow the QoS-management at network level, so this approach has two following characteristics:

- Neutrality: there is no class of service associated with the optical packet. All optical packets are treated in the same way. Ring nodes observe only one type of the optical packet passing in the transit line.
- Reliability: there is no pre-emption packet. Each optical packet issued on the ring remains in transit until it reaches the destination(s). A mono-class packet can not be rejected in the intermediate station.

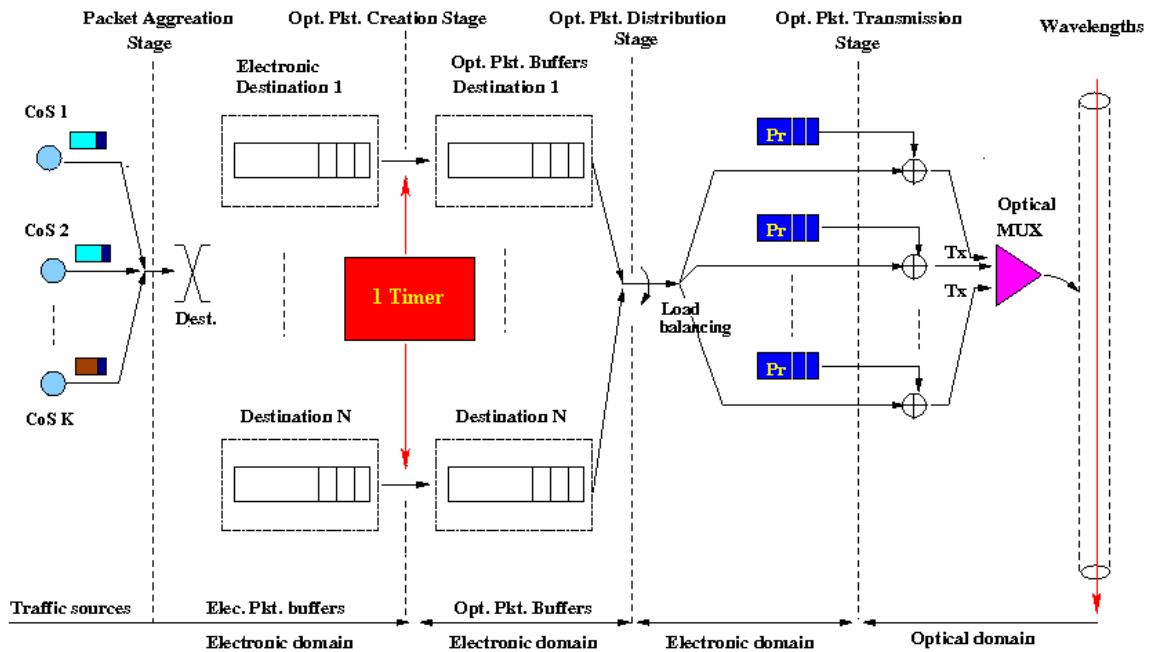


Figure 5-4: Mono-class optical packet creation process

5.3 Multi-Class Approach

In this approach, we typically create optical packets containing electronic packet with the same CoS. It classifies electronic packets, according to its CoS and destination. However, in order to obtain a maximum filling ratio of the optical packet, it is necessary to develop some advanced mechanisms. The detail of these mechanisms is presented in following sub-sections.

5.3.1 CoS-enabled Timer Mechanism (CTM)

Regarding electronic packets having the same destination, instead of using a timer for all class of service, CoS-enabled Timer mechanism uses the number of the aggregation buffer equal to CoS number. Each timer is attached to each aggregation buffer. The aggregation buffer independently fills and creates optical packets, depending only on its timer. The expiration time of timers, which are attached to aggregation buffers of different CoS, is different. In general, the expiration time of timers of higher priority queues is shorter than lower priority queues because the access delay of high priority packets should be limited. For this mechanism, we suppose that there are 8 CoS supported in the electronic domain. So, we have 8 aggregation buffers and 8 optical buffers inside a single node.

5.3.2 CoS-Upgrade Mechanism (CUM)

CTM given above can yield to more severe bandwidth loss in case of insufficient traffic rates. In fact, under a very low client traffic rate, the optical packet is sent with very low filling ratio after timer expiration. This causes the wasted bandwidth. For this reason, we propose a mechanism to exploit the CoS differentiation in order to optimize the optical packet filling and remedy this bandwidth loss. This packet filling mechanism is called “CoS-Upgrade mechanism”. This mechanism is based on the idea of filling the remaining empty space in the optical packet with electronic packets of lower priority. The details of this mechanism can be found in [FHT 05].

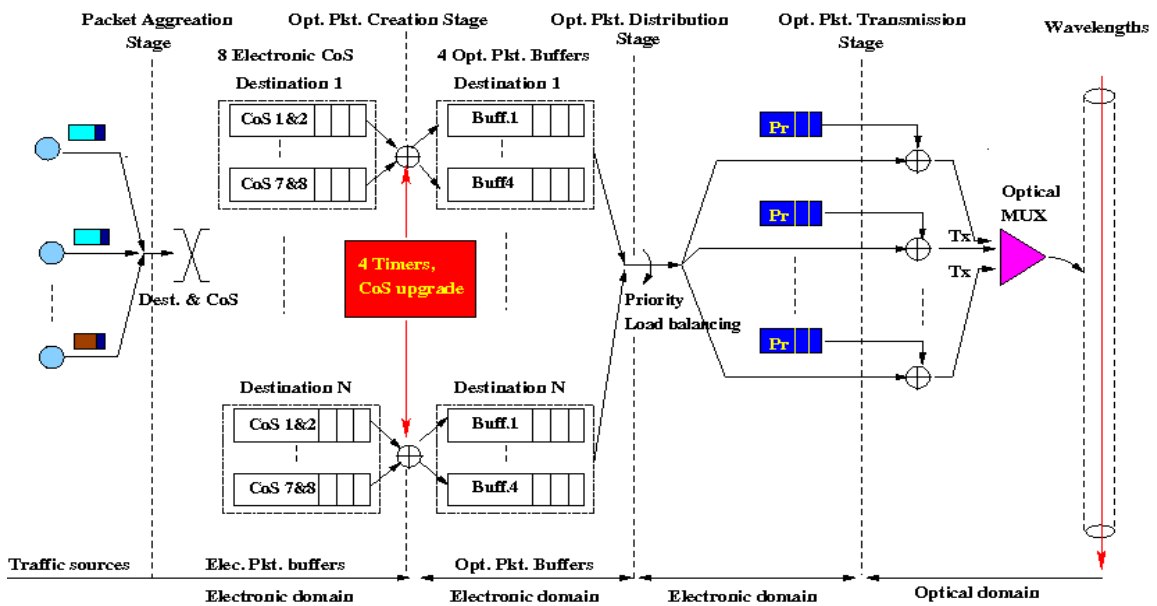


Figure 5-5: Multi-class optical packet creation process

Each node owns 4 aggregation and 4 optical buffers (corresponding to four different CoS: Premium, Silver, Bronze, and BE) to accommodate 8 electronic CoS (the detail will be presented in the next sub-section). Hence, 4 Timers are attached to 4 aggregation buffers (as shown in the following figure). The mechanism works like the following scheme:

1. Reset Timer
2. If filling buffer exceeds optical packet size, then we send the optical packet and go to step 1
3. If timer expires while the buffer filling level is still small:
 - Continue filling the current optical packet with electronic packets of the first lower CoS and same destination. We repeat this procedure successively by exploring lower CoS buffers until either the current optical packet becomes full or there are no electronic packets in the lower CoS buffers.
 - Send the packet
 - Go to step 1

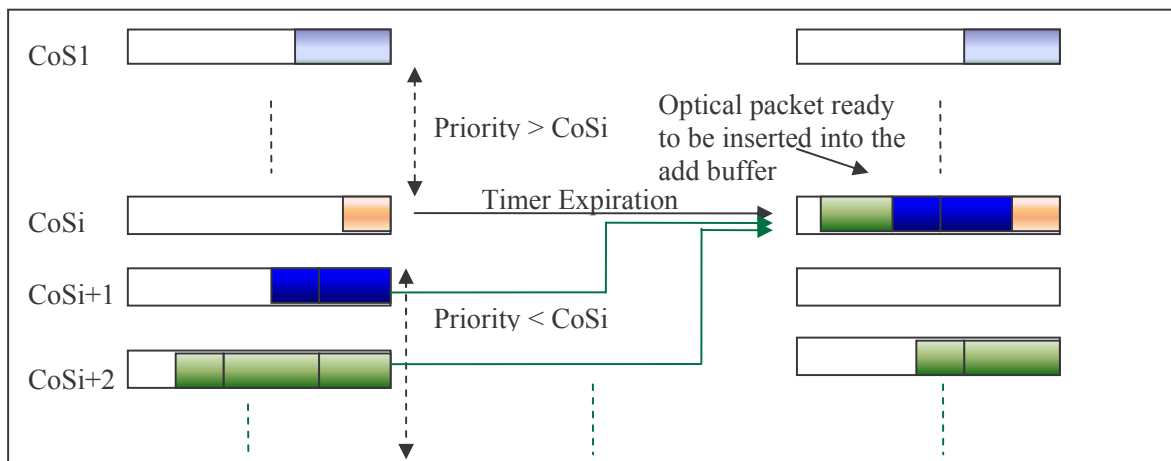


Figure 5-6: CoS-Upgrade mechanism function

By reducing the resource wastage, which occurs in the case of insufficient traffic rate, CoS-Upgrade mechanism contributes to improve the management of available bandwidth. However, when CoS-Upgrade mechanism is activated, an additional mechanism should be implemented in order to reclassify the electronic packets inside receiving nodes.

5.3.3 Dynamic CoS-Upgrade Mechanism (DCUM)

We now describe a novel mechanism which improves the filling ratio of the optical packet created by CoS-Upgrade Mechanism while limiting the access delay (in the aggregation buffer and in the optical buffer) in the safe-level. This mechanism is based on the idea of adjusting the timer value, according to the state of local transmission buffers and the transiting traffic, in order to obtain optical packets with high filling ratio. Based on this idea, we propose DCUM standing for Dynamic CoS-Upgrade Mechanism. Regarding the Timer-based Mechanism, since the timer is fixed in advance, the creation of optical packets might be triggered by the timer expiration, even if the optical packet is not well-filled. This leads to the situation where “a not well-filled optical packet” is created while some created optical packets are still being blocked in the optical buffer; thus the created optical packet must wait in the optical buffer until its transmission. In DCUM, a non well-filled optical packet is

created only in the case where both the current slot in the transit line and the local transmission buffer do not contain any optical packet. Therefore, an optical packet continues to be filled with electronic packets until it is either well-filled or resources on the network are available for its transmission (the transit line is free and there are no other optical packets waiting in transmission buffers of equal or higher priority). The “real” duration of the timer in DCUM depends on the “distributed state” of access nodes. Since DCUM offers high-filled optical packets, thus other ring nodes are able to allocate more usable bandwidth in the transit line.

However, a constructing optical packet can not wait to infinite time. So, it should be limited by a value which is specified in MEF. For each CoS, the mean access delay should be smaller than the maximum delay specified in MEF and it becomes a condition in DCUM. To understand DCUM, we show the first procedure of DCUM in Figure 5-7. This procedure is activated each time when an electronic packet arrives to the aggregation buffer. Let W^i be the current waiting time of the first packet in the buffer and W^i_{max} be the maximum value specified in MEF for electronic packets in the aggregation buffer CoS_i . Let F be the flag (whose values are ON and OFF) indicating the activation of the timer. If F is ON, the timer has been started and its size is equal to only one timeslot. Otherwise, the timer is stopped. Finally, let us denote α the current occupation ratio of the aggregation buffer and denote α_{max} the predefined threshold ($0 \leq \alpha \leq \alpha_{max} \leq 0$). As the CoS-Upgrade Mechanism, DCUM uses α_{max} to limit the probability of aggregation buffer overflow (the ratio α_{max} was presented in previous chapter).

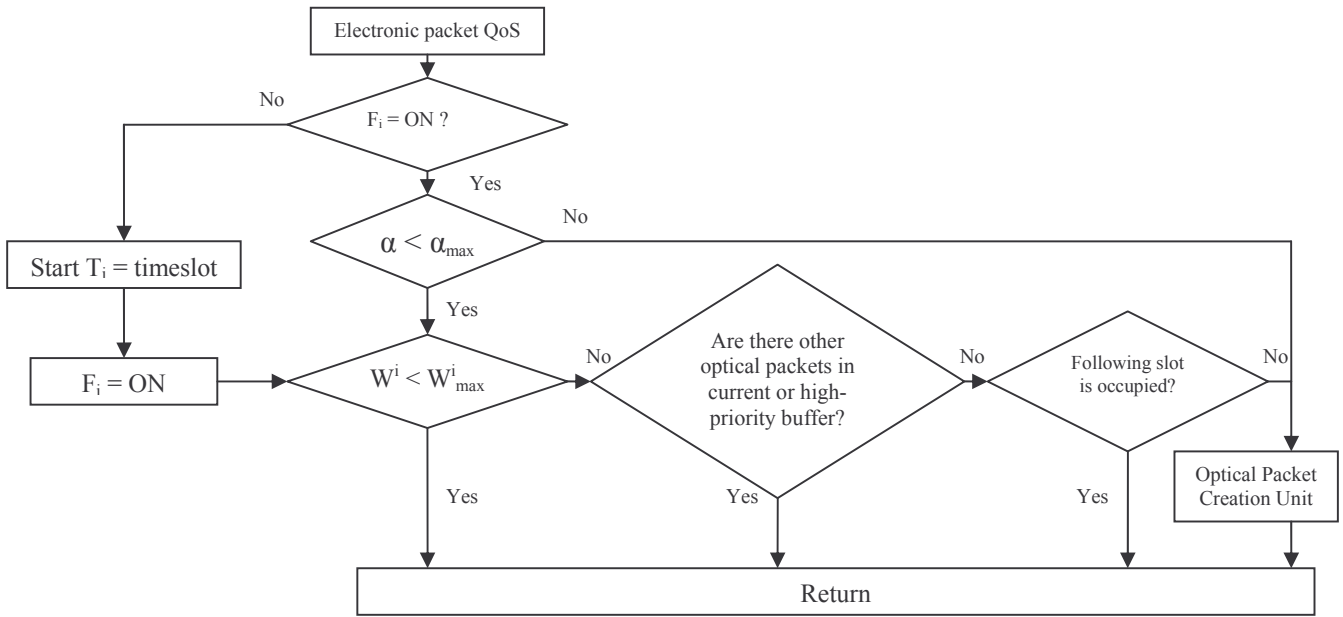


Figure 5-7: First procedure of DCUM

Each time when an electronic packet CoS_i arrives to the aggregation buffer, this procedure will be activated. It firstly switches the flag F (to the state ON if the flag is OFF) to allow the timer to be started. The timer is initially set equal to one timeslot. In the case where the flag is already turned on, the procedure must check the current filling ratio α (in relation to α_{max}) before enabling the Optical Packet Creation procedure. Otherwise, the Optical Packet Creation procedure will be triggered if all following conditions are satisfied:

- i. The waiting time W^i is higher than W^i_{max} .
- ii. There have not any optical packets in the corresponding optical buffer as well as in the optical buffer CoS_j with $0 < j < i$.
- iii. And current slot is occupied by other nodes but the following slot is free.

On the other hand, Optical Packet Creation procedure is not enabled. The second procedure is shown in Figure 5-8. This procedure is activated each time a timer (T_i) expires. Since the timer has been activated, this procedure does not require the flag examination. Similar to the first procedure, this procedure checks the current filling ratio α before checking three conditions (i,ii,iii). If one of these three conditions is not satisfied, the timer continues to be restarted. Otherwise, the Optical Packet Creation procedure will be triggered.

The last procedure in DCUM is the Optical Packet Creation process. Since we apply CoS-Upgrade Mechanism for DCUM, so Upgrade mechanism is called each time Optical Packet Creation is executed. It is based on the idea of filling the remaining space in the concerned optical packet by electronic packets from lower priority.

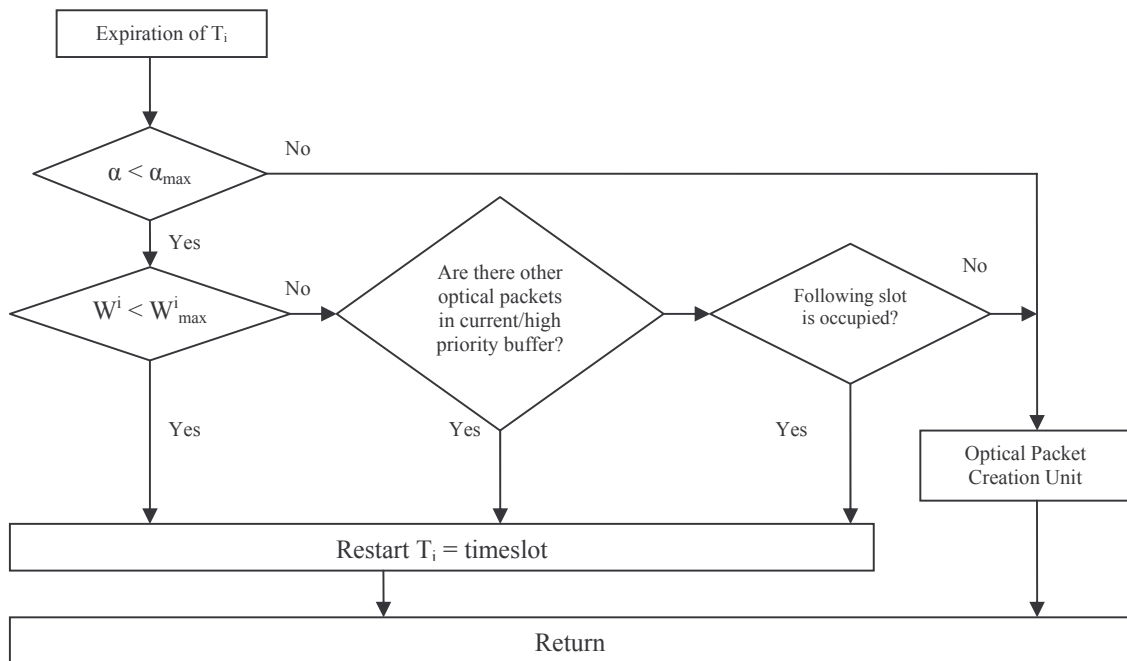


Figure 5-8: Second procedure of DCUM

When the Upgrade Process is finished, all “touched” aggregation buffers must update its state. For each aggregation buffer of CoS_j ($i+1 < j < N$, N is the maximum number of CoS), the timer T_j and the flag F_j must be stopped if the buffer becomes empty (we stop DCUM process attached to these empty aggregation buffers). Otherwise, the waiting time W^j must be recalculated according to the new first electronic packet in the buffer. Finally, the procedure stops the timer T_j and turns off the flag F_i in order to finish the DCUM algorithm which is attached to the aggregation buffer of i^{th} class.

In other words, DCUM algorithm begins if an electronic packet arrives and ends by the Optical Packet Creation process when conditions (i, ii, iii) at first two procedures are satisfied. Note that DCUM algorithm attached to other CoS’s buffers may still be continued.

Similar to CoS-Upgrade Mechanism, DCUM merges electronic packets of different CoS inside an optical packet; this is because it is necessary for an additional mechanism to reclassify electronic packets at destination nodes.

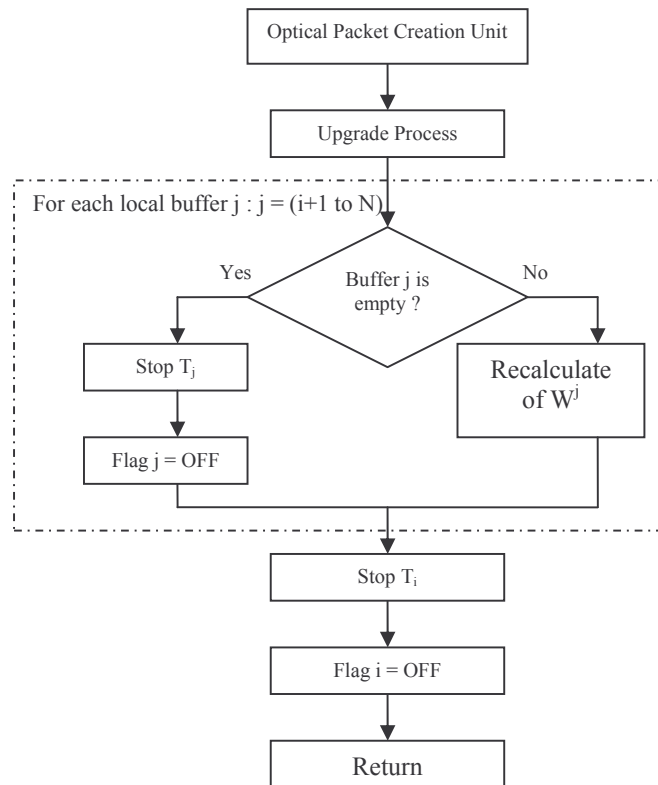


Figure 5-9: Optical Packet Creation process

5.3.4 Packet Erasing Mechanism (PEM)

When fixed-size format is activated, local buffering consists of two stages: aggregation buffers and optical buffers. The first stage is used for packets' aggregation, while the second contains optical packets (optical packets), which are ready to be inserted into the ring. As a general rule, transit traffic has the highest priority. This traffic can not be interrupted by the local traffic, except for the case of a packet erasing mechanism, defined as follows. The erasing mechanism prevents higher priority packets from being lost or having excessive access delay.

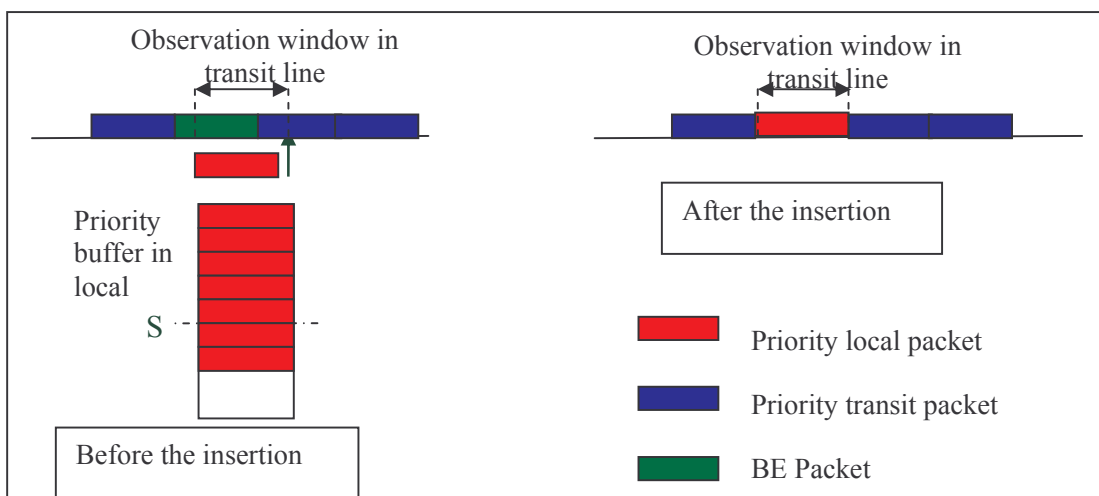


Figure 5-10: Packet Erasing Mechanism

When this mechanism is enabled, Best Effort packets at the transit line can be dropped in order to make available to insert higher priority packets, which are waiting in the Add buffer. The activation of the erasing mechanism is controlled by a threshold S , which represents a critical filling level of higher priority buffers (i.e. the erasing mechanism is enabled only when the filling level of higher priority buffer is superior or equal to S). We note that the term “erasing” used in this dissertation does not signify a photon absence. Figure 5-10 illustrates the erasing mechanism in the fixed-size model.

5.3.5 Extraction and Reemission Mechanism (ERM)

Some transit BE packets that are dropped by the PEM mechanism could have been rather stored locally for a very short delay, before being transmitted again on the ring. Moreover, it is more ingenious to avoid dropping packet which have already consumed network resources (from their source till the current node), especially when they become closer to their destination station. In order to remedy this problem, we have proposed the following mechanism:

- A buffer called “flash buffer” of a very limited capacity is added in order to store few optical BE packets which can be extracted from the transit line.
- When the current slot at the transit line is occupied by a BE packet, we observe the filling levels of high priority buffers (the ones with packets of high priority inside). If the filling level at one of them reaches a certain threshold “ θ ”, the service of the current BE packet (at the transit line) is interrupted and it is saved into the “flash buffer”. At the same time, one packet of the high priority overloaded buffer is transmitted instead in the same slot. Note here that θ can be different for each buffer.
- If the capacity of the “flash buffer” is saturated, the extracted transit BE packet is lost.
- Afterwards, packets waiting in the “flash buffer” will be retransmitted again, prior to other packets inside the same node, on the first next available timeslots on the ring.

In our work, we choose the threshold “ θ ” equal to 0.

5.4 Performance Evaluation

We use discrete event network simulation tool (ns 2.1b8 – [NWS 05]) to simulate the network with 10 ring nodes transmitting on some wavelengths of $10Gbit/s$ (the number of wavelength varies according to different scenarios). In these simulations, we use 8 CoS in electronic domain that has described in previous section. We assume that the propagation delay between adjacent nodes is $0.2ms$, which is equivalent to some $40 km$ (close to the real size of a metro network), and the optical header is composed of 16 bytes of preamble and 32 bytes of inter-packet gap. We firstly investigate the timer value and the erasing threshold when the multi-class approach is enabled. The comparison between mono-class and multi-class will be then approached.

5.4.1 Global parameters

In the simulation, optical packets which are transmitted on the ring are of fixed-size. This size is equal to $10\mu s$ at a wavelength transmission capacity of $10Gbits/s$, i.e. that the optical packet size is computed as:

$$\text{OpticalPkt Size In Bytes} = \frac{\text{PacketSizeInTime} * \text{WavelengthCapacity}}{8} = \frac{10e^{-6} * 10e^9}{8} = 12500\text{bytes}$$

Note that the optical packet size computed hereupon doesn't include the size of the optical header, which will be added to each optical packet.

The following table presents global parameters used in the multi-class case.

(**)	CoS1 – CoS2 Premium		CoS3 – CoS4 Silver		CoS5 - CoS6 Bronze		CoS7-CoS8 BE	
% CoS	10.4 %	10.4 %	13.2 %	13.2 %	13.2 %	13.2 %	13.2 %	13.2 %
Electronic Packet size (bytes)	810	810	50, 500, 1500	50, 500, 1500	50, 500, 1500	50, 500, 1500	50, 500, 1500	50, 500, 1500
Aggregation Buffer	≥ Optical Packet Size		≥ Optical Packet Size		≥ Optical Packet Size		≥ Optical Packet Size	
Optical (Add) Buffer (mono case)	2200 Kbytes							
Optical (Add) Buffer (multi case)	200 Kbytes		500 Kbytes		500 Kbytes		1.000 Kbytes	

Table 5-2: Traffic and electronic side hypothesis

For the premium traffic, we consider constant bit rate (CBR) sources, with the packet size of 810 bytes. This assumption comes from the fact that today's premium service such as voice, video are transported mainly over SONET/SDH networks, which are constant bit rate sources. The non premium traffic is modelled by an aggregation of IPP sources with different burstiness levels. Electronic packets generated by these sources are of variable length. According to the Internet packet length statistic, we consider three sizes of packets, 50 bytes, 500 bytes and 1500 bytes constituting respectively 10%, 40% and 50% of the traffic volume, for each non premium CoS (class ID 3 to 8). The size of the aggregation buffer is chosen so that its size is greater than an optical packet size (in bytes). Optical buffer in the multi-class approach are respectively equal to 200 Kbytes for premium traffic class, 500 Kbytes for silver and bronze traffic class and 1000 Kbytes for Best Effort traffic class while mono-class's optical buffer is equal to 2200 Kbytes. Only electronic CoS 1 to CoS 4 (corresponding to Premium and Silver class in the optical domain) can take benefit of the erasing mechanism. As shown above, we fix the Premium traffic equal to 10.4% total offered traffic at the workload of 80%, while other traffic is about 13%. Therefore, when we change the network load, traffic amount of CoS(s) will be changed except the Premium traffic.

Some assumptions case can be described as follows (showed in the Figure 5-5):

- In the multi-class case, client traffic is assembled into four optical class of service: Premium, Silver, Bronze and BE on the optical level. Limiting the number of services contribute to the packet filling optimization in the case of traffic starving. Client traffic is assembled only into one type of services for the mono-class case.
- In the multi-class case, with each destination, a node has four aggregation buffers and four optical buffers (one optical buffer for each optical CoS) while for the mono-class, it only owns one aggregation buffer and one optical buffer.

- In the multi-class case, erasing thresholds are expressed in terms of number of optical packets waiting in the optical buffer. From now on, only two thresholds are used to describe the function of the erasing mechanism. L1 (respectively L2) is the erasing threshold for the premium (respectively the silver) class of traffic. Moreover, as we have mentioned before, optical fixed-size packet creation time is bounded by a maximum value which corresponds to a Timer. In our study, timer values for optical CoS are given in the next summary table (k1, k2, k3, k4 is called timer factors while T is called basic Timer size, which equals Premium class’s Timer size. In the simulation, we use T as the reference timer by which we can compute other Timer sizes such as Silver, Bronze or BE class through timer factors) :

	CoS1 – CoS2 Premium	CoS3 – CoS4 Silver	CoS5 - CoS6 Bronze	CoS7-CoS8 BE
Timer (second)	$T1 = k1 * T$	$T2 = k2 * T$	$T3 = k3 * T$	$T4 = k4 * T$
Ecrasing threshold (#optical pkts)	L1	L2 (\geq L1)	None	None

Table 5-3: Optic side hypothesis

5.4.2 Investigation of the Timer duration in CUM

We may now analysis the performance of the described architecture through a set of simulation scenarios with two types of scenario: Bus and 1-N.

For both case, the offered network load is set to 0.75. In the Bus scenario, we focus on the results obtained with multi-nodes while we have limited the final study from the 1-N scenario to one single node.

A. Access Metro: Bus Scenario

For this experiment, the timer factors are 1:2:10:20. All nodes in the bus scenario send their traffic to the hub node and aggregation buffers are only classified by the optical CoS and not by the destination. Timer value for the premium traffic starts from $T = 50\mu s$ to infinity. We firstly show the filling ratio of optical packets for some different values of T, which are respectively $50\mu s$, $100\mu s$, $150\mu s$, $200\mu s$ and infinite value (the aggregation case). The filling ratio is presented in Figure 5-11.

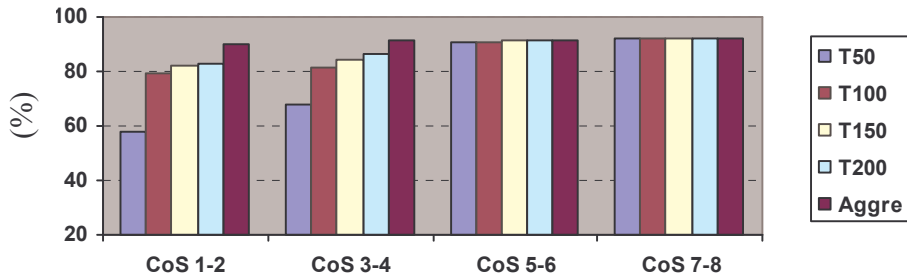


Figure 5-11: Filling ratio for values of Timer T: $50\mu s$, $100\mu s$, $150\mu s$, $200\mu s$ and infinite value

We observe that with the Timer $T = 50\mu s$, the filling ratio is the smallest (about 59% for Premium traffic) while this value comes to about 90% (Premium class) with the simple aggregation. The filling

ratio increases when the duration of Timer increases. The difference of the filling ratio due to the Timer's expiration time is high for the premium traffic but it becomes vaguer as the priority of traffic decreases. With a small Timer duration, more traffic priority increases, more bandwidth is wasted. This is due to the proportion of factors. We have used the factor equals 1 for the premium traffic's timer ($T_1 = T$) while the factors are respectively of 2, 10 and 20 for other class of service ($T_2 = 2*T$, $T_3 = 10*T$ and $T_4 = 20*T$).

Having a lower filling ratio, the optical packet of the premium class wastes more bandwidth than other CoS. Note that we can not choose a bigger factor for the premium class due to the explosion of the mean access delay that is not expected.

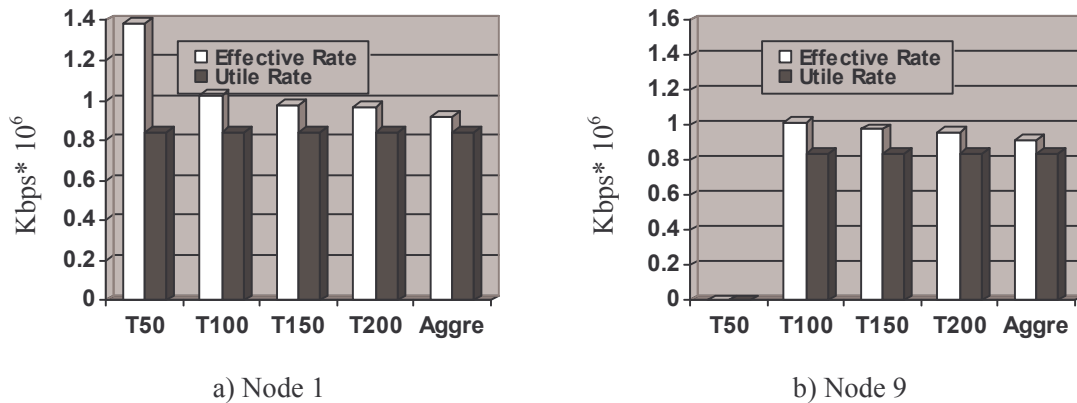
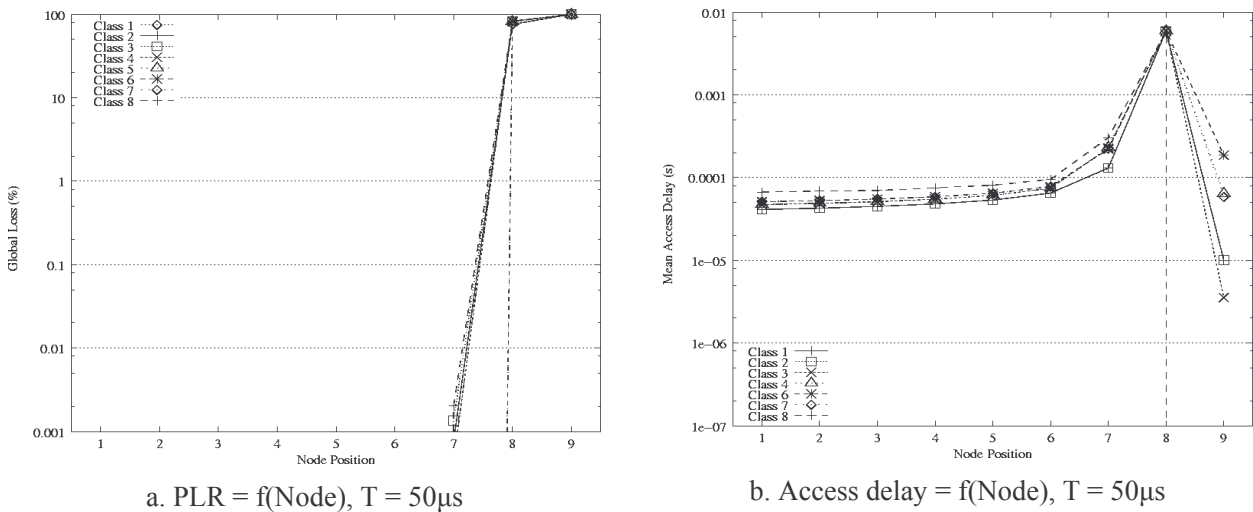
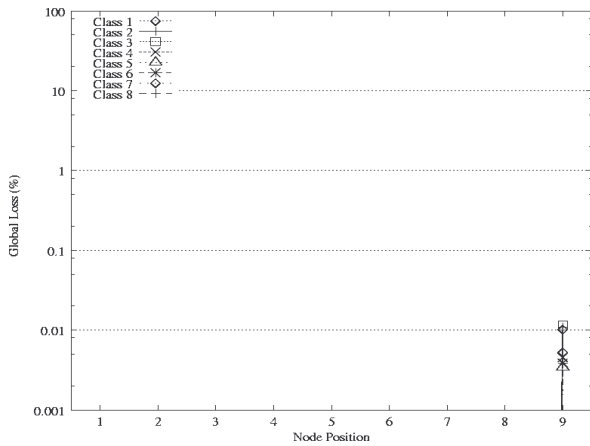


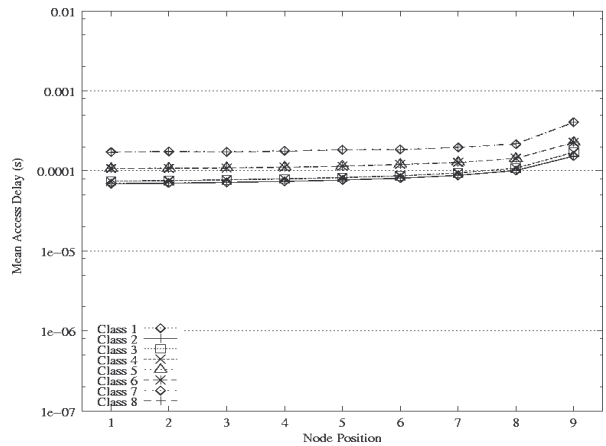
Figure 5-12: The utile / effective rates as the Timer T varies (Scenario Bus)

Figure 5-12 shows the utile / effective rates for node 1 and node 9 as the Timer T varies. The utile rate seems stable while the effective rate becomes lower while the Timer value increases. We explain this phenomenon as mentioned in the previous chapter that when the Timer duration is small, the number of created optical packets is greater than it is obtained with bigger Timer values, leading to more added optical header. The effective rate with small Timer values thus becomes more important, causing the loss of bandwidth. Due to the waste of bandwidth at first nodes on the bus, last nodes on the bus (for example: node 9) have not enough space for transmitting its data.

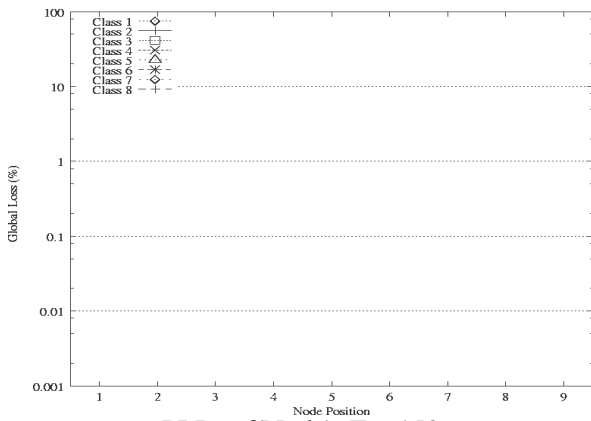




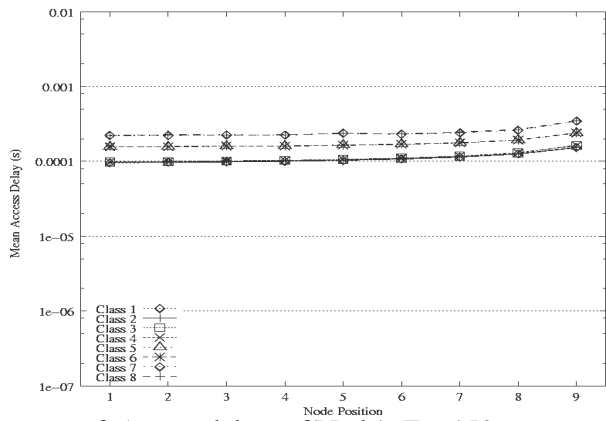
c. PLR = $f(\text{Node})$, $T = 100\mu\text{s}$



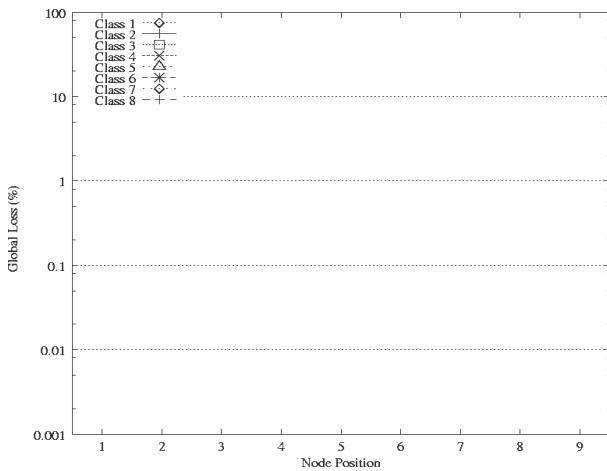
d. Access delay = $f(\text{Node})$, $T = 100\mu\text{s}$



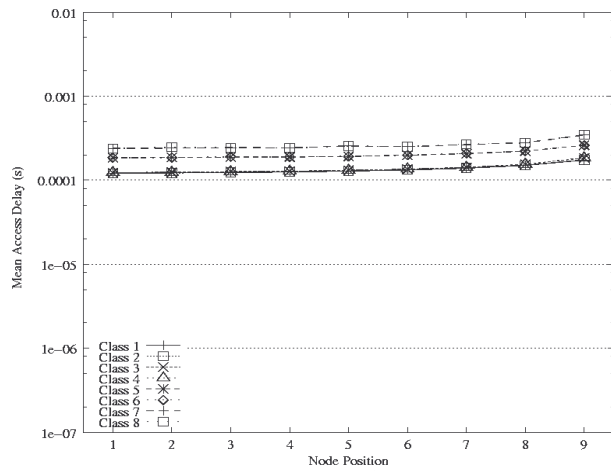
e. PLR = $f(\text{Node})$, $T = 150\mu\text{s}$



f. Access delay = $f(\text{Node})$, $T = 150\mu\text{s}$



g. PLR = $f(\text{Node})$, $T = 200\mu\text{s}$



h. Access delay = $f(\text{Node})$, $T = 200\mu\text{s}$

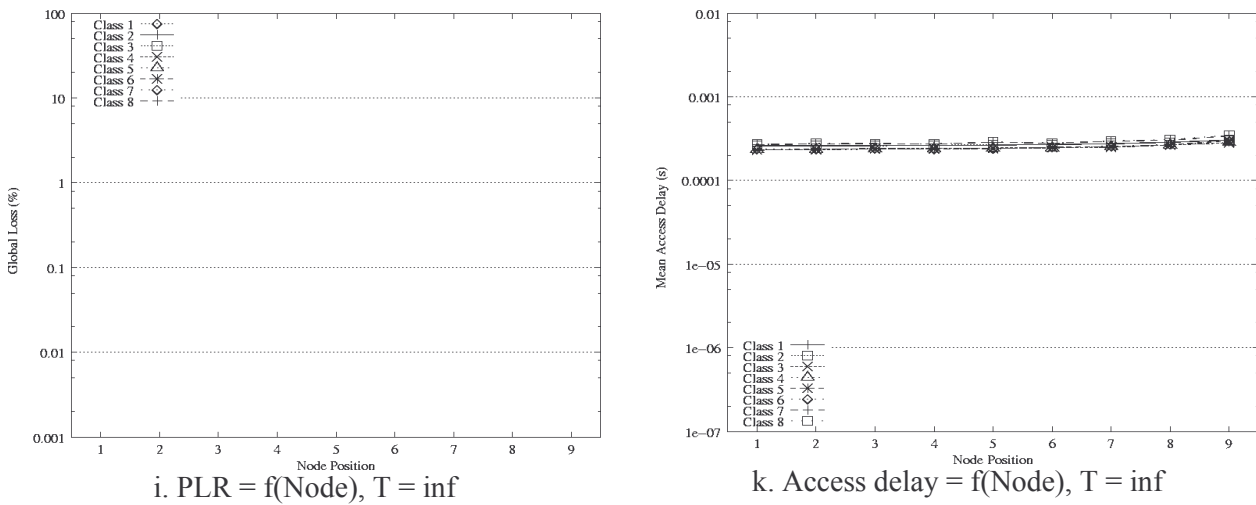


Figure 5-13: Timer value investigation with CUM

Figure 5-13 presents the access delay obtained with CUM. We observe that the network performance is degraded in terms of the access delay and PLR when the timer size is small (i.e. $50\mu s$). With a small Timer value, CUM may optimize the packet filling ratio of higher CoS, but not for the lower CoS. As the timer size increases, the network performance increases. We do not see PLR at last node (node 9) while the mean access delay measured at all nodes becomes more balanced.

Large Timer durations (i.e. $200\mu s$) optimize the filling ratio not only for high priority CoS but also for lower priority, and significantly improve the performance at last nodes by reducing the PLR and the access delay. With the simple aggregation, access delays of different CoS are nearly the same. This performance improvement comes from the global augmentation of the basic timer duration T.

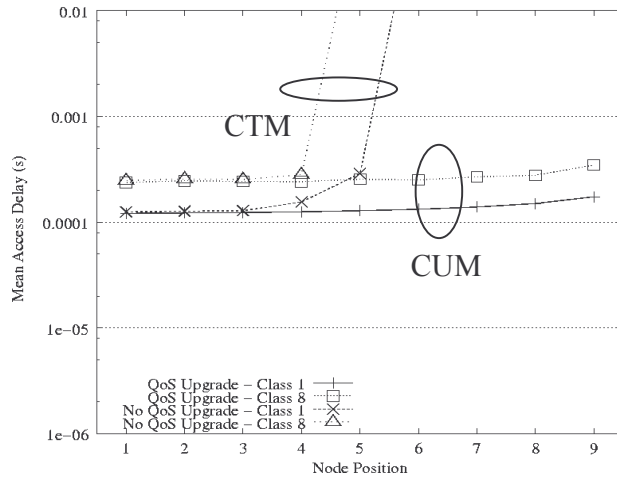


Figure 5-14: CTM and CUM comparison on the mean access delay

Let's us focus now on the performance improvement of the CUM as compared to CTM. We present here the access delay with the basic Timer value equal to $200\mu s$. Results are presented in Figure 5-14. For the sake of clearness, we illustrate performance results only for 2 CoS: Premium and BE. The figure shows that, with CTM, the mean access delay “explodes” from node 5. However, results at the same node, in the case of CUM, present a safe performance level. For instance, at the node 6, high mean

access delays (more than $0.01s$) are observed in the case with CTM, while these values are only about few hundreds μs ($0.0001s$ to $0.0005s$) when CUM is enabled. This is because CTM generates optical packets with low filling ratio, leading to a waste of bandwidth resources. Therefore, last nodes on the bus may not find enough space to transmit their data. On the contrary, CUM optimizes the filling ratio of high priority CoS by electronic packets of lower priority CoS and significantly improves the mean access delay as compared to CTM.

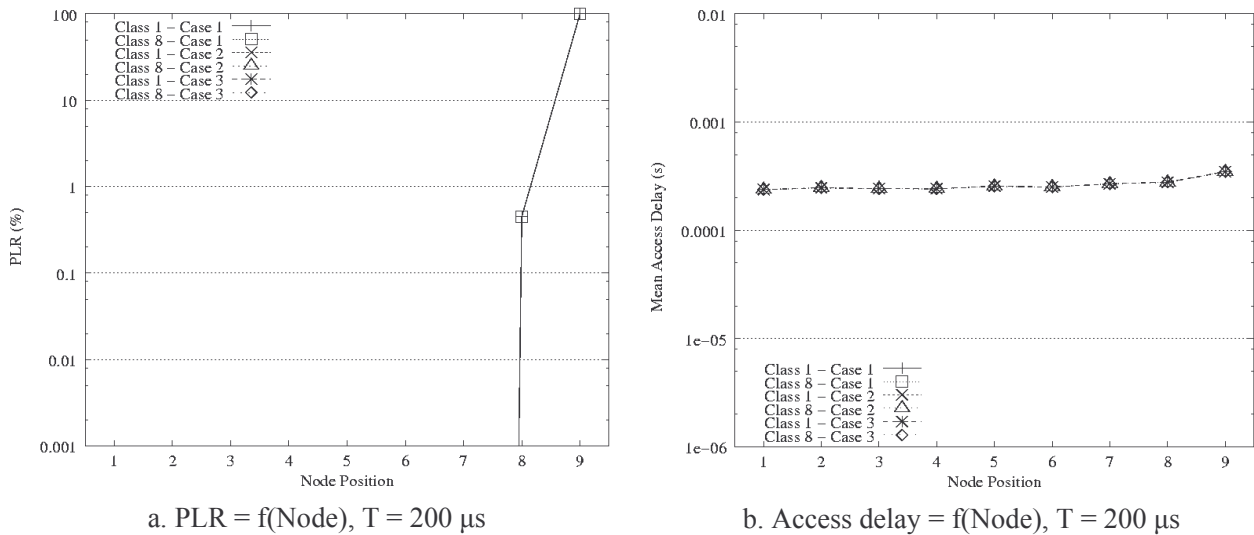


Figure 5-15: Investigation of the *factor k*

We may now investigate the impact of the *factor k* on the network performance. We start by “initial factor” where factor proportions are equal to 1:1:1:1 (case 1), this means that $T_1 = T_2 = T_3 = T_4$. By these factors, timer values of optic CoS are equal to the basic timer value T . We afterwards increase the factor ratio as 1:2:10:20 (case 2) and 1:2:50:100 (case 3). Note that the new factor of BE class in case 3 is one hundred times larger than the one of Premium Service. Figure 5-15 shows obtained results with the network load of 0.8. Note that we fix the basic timer T equal to $200\mu s$. The figure shows that case 1 does not offer good performance in terms of PLR. Indeed, the PLR observed at node 9 with case 1 is very high, while obtained results for cases 2 and 3 seem to be very small. So we should not choose factors of 1:1:1:1. Case 3 has the same result as case 2 while the simulation elapses very long.

Using the factors as in the case 2, we compare the fixed-size optical packet format (FS-OPF) to the variable size optical packet format (VS-OPF) with and without supporting “empty packets” [FOM 06]. This work may be considered as the comparison among POADM model; DBORN model (variable size without “empty packets”) and opto-electronic (variable size with “empty packets”) [FOM 06] model.

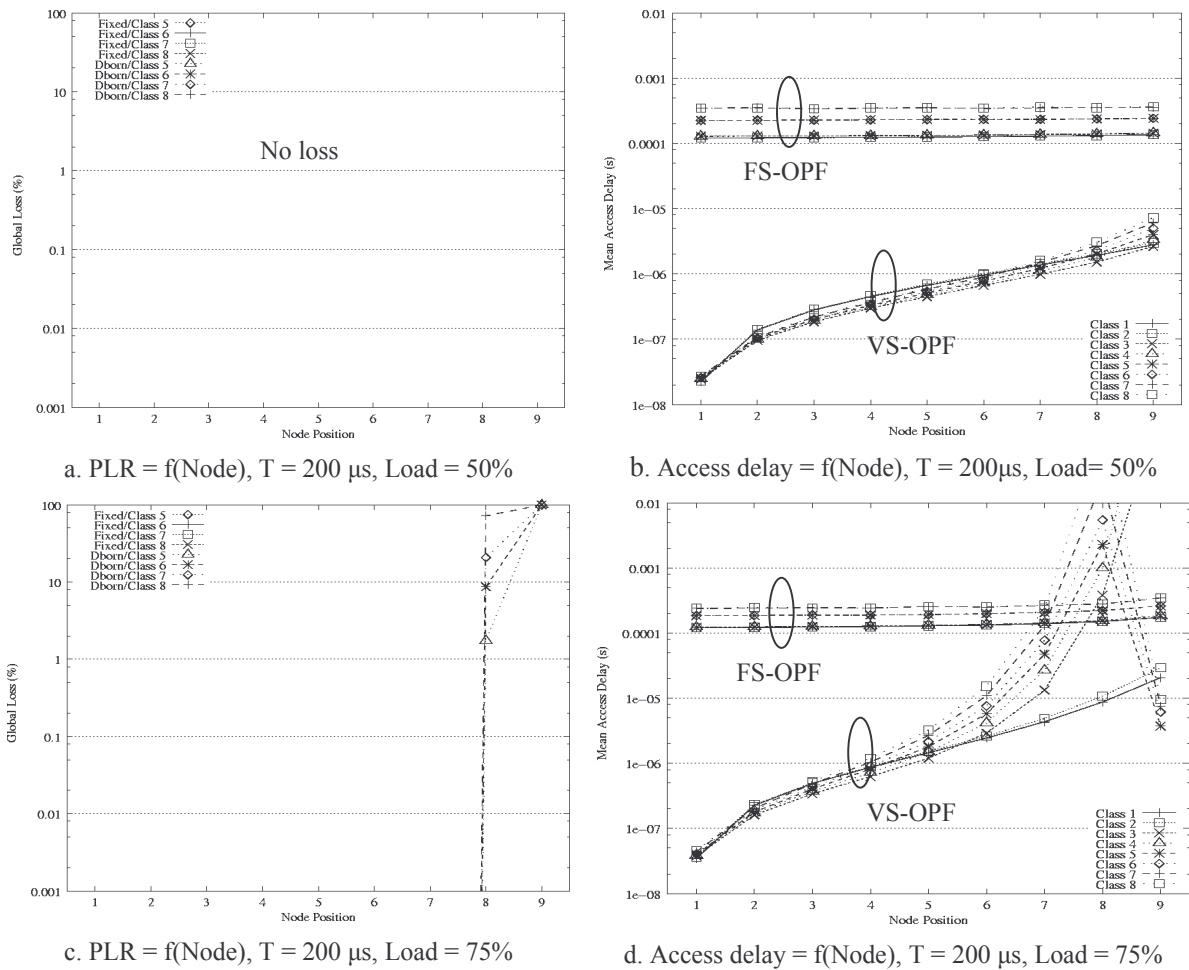


Figure 5-16: FS-OPF model and VS-OPF model without supporting *empty packets*

We focus on Figure 5-16 which firstly shows a comparison between FS-OPF and VS-OPF without supporting *empty packets*. Note that we use CUM for FS-OPF in this work. This performed comparison is considered under two different network offered loads: 50% and 75%. For FS-OPF, we have chosen the timer value equal to 200 μ s. With a small workload (50%), results show that the PLR is globally higher in FS-OPF, comparing to the case of VS-OPF as well as for the mean access delay. This is due to the fact that the creation of the optical fixed-size packet imposes an additional delay for higher priority CoS. In fact, if the bandwidth is free, an optical packet with high priority should wait until either it is filled or its timer expires before it can be inserted on the network. This additional delay isn't introduced in the case of VS-OPF, which provides much lower access delays when the bandwidth is available. On the other hand, when the network load increases to 75%, the access delay in VS-OPF model reaches a very high level at node 9 while the access delay obtained by FS-OPF seems to be unchanged. This is mainly caused by the bandwidth fragmentation and the position property problem. Regarding VS-OPF model in Figure 5-16d, the Premium class at first nodes (except node 1) abnormally has access delays higher than BE class. By using the electronic packet size distribution, we could explain this phenomenon. Since we use the electronic packet size of 810 bytes for the Premium class, Premium packets are normally waited a longer time than BE packets while looking for free voids.

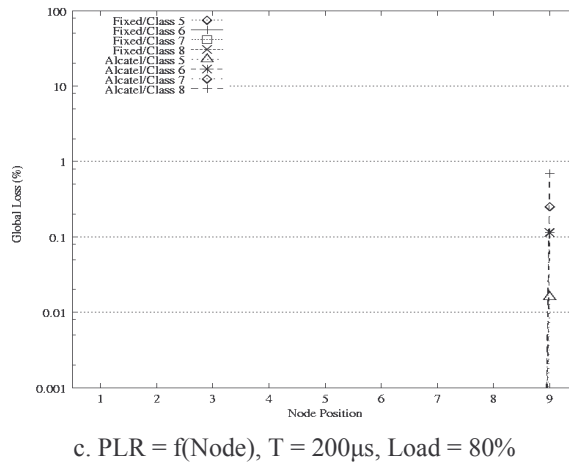
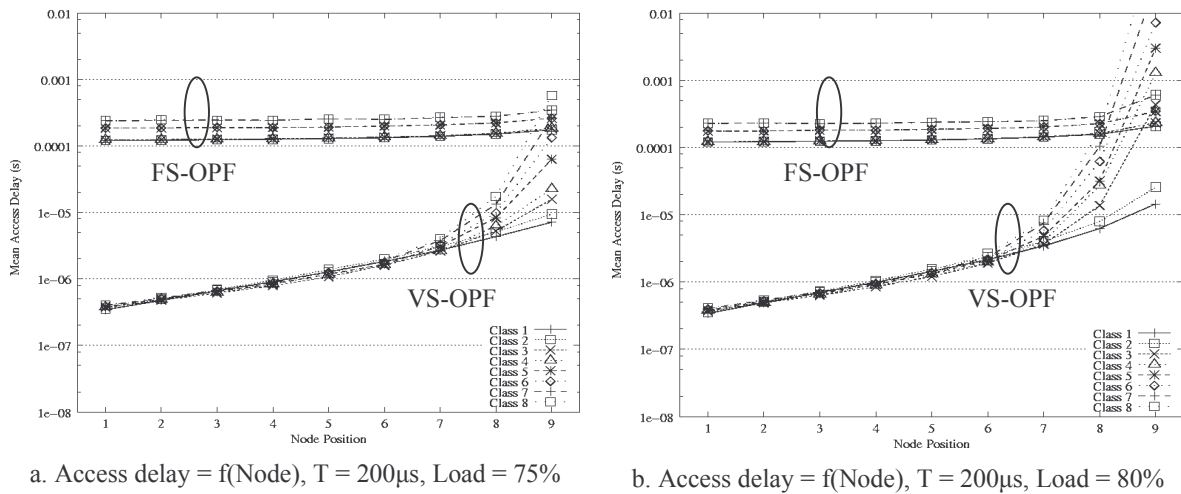


Figure 5-17: Performance comparison between FS-OPF model and VS-OPF model supporting *empty packets*.

Figure 5-17 shows a comparison between FS-OPF and VS-OPF supporting *empty packets*. Regarding PLR and access delay results, VS-OPF supporting *empty packets* also offers better performance with the workload of 75%, comparing to FS-OPF. However, when the network load increases to 80%, the access delay in the VS-OPF model becomes higher than that of FS-OPF at node 8 (notably for BE class) while the FS-OPF’s access delay seems to be unchanged. Additionally, observing Figure 5-16d and Figure 5-17b, results obtained by VS-OPF supporting *empty packets* seem to be more stable than that of VS-OPF without supporting *empty packets*. This is due to the fact that first nodes on the bus always transmit “*empty packets*”; it may limit the data transmission from first nodes while keeping more free voids for last nodes (last nodes could insert its data in the place of *empty packets*).

Overall, comparing to VL-OPF model, FL-OPF model provides more stable performance, notably under high offered network loads. With a good choice of the timer value (e.g., T is equal to or higher than $200\mu\text{s}$), FL-OPF model could provide fair and good access delay with a very low PLR for all services at all bus nodes. By contrast, VL-OPF model may offer small (but unfair) access delays when the network is not heavily loaded (60% of the workload with “*empty packets*” and 75% of the workload without “*empty packets*”), but excessive access delay and very high PLR at last nodes under heavy offered network loads (more 80%).

B. *Core Metro: 1-N Scenario*

In this section, we would like to study the network performance by analyzing the influence of the CUM’s timer value in the 1-N scenario. As mentioned, the arrival rate of electronic packets in this case is very small as compared to the bus scenario. Therefore, in order to fill up the optical packet, we should use larger timer values. From this assumption, we vary the timer value from 300µs to infinity.

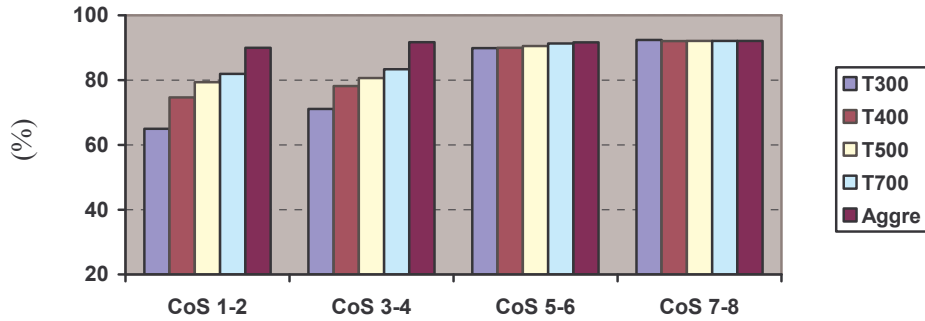


Figure 5-18: Filling ratio for values of Timer T: 300µs, 400µs, 500µs, 700µs and simple aggregation

Figure 5-18 shows the filling ratio as the Timer T varies. More the timer value increases, more the optical packet is filled. For Premium class, the filling ratio is about 64% with the Timer size equal to 300µs as compared to 90% of the simple aggregation. The filling ratio seems nearly the same as for BE class (about 92%). The resulting high filling level of optical packets optimizes the bandwidth utilization, leading to very good performance (as shown in Figure 5-19). For instance, the big value of timer (such as more than 700µs) has offered low access delays (less than 1ms) with no loss for all 8 CoS.

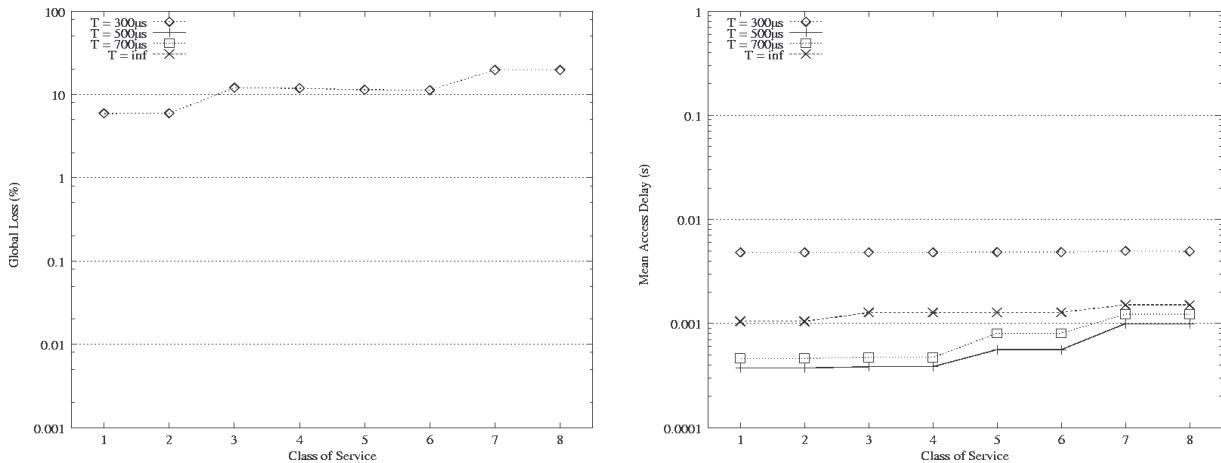


Figure 5-19: PLR and access delay obtained by CUM in 1-N scenario

Figure 5-20 shows the utile rate / effective rate as the Timer T varies (obtained in a node). As expected, the utile rate seems unchanged (except T = 300µs) while the effective rate becomes smaller as long as the Timer value increases. So, it is worth noting that the simple aggregation always offers the best performance in terms of utile / effective rates and it does not depend on the traffic matrix of the network.

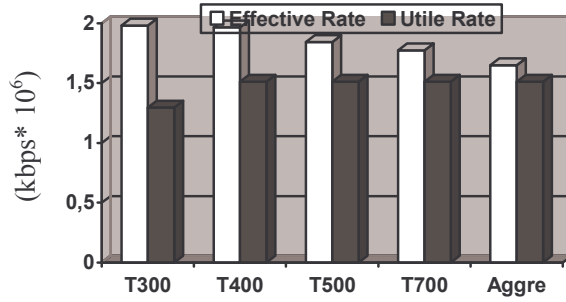


Figure 5-20: The utile rate and the effective rate as the basic Timer T varies (1-N scenario)

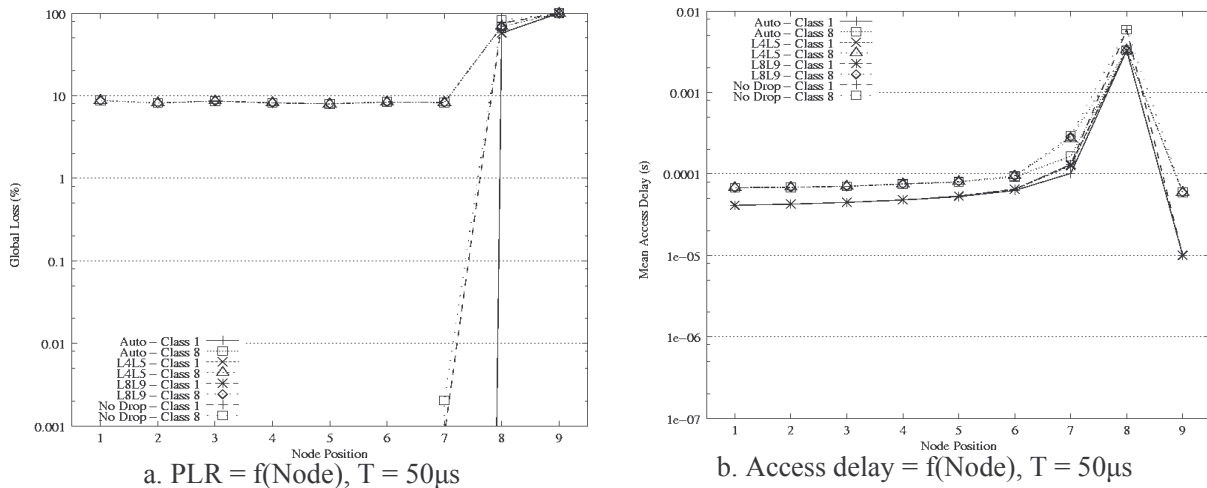
5.4.3 Investigation of the erasing threshold in PEM

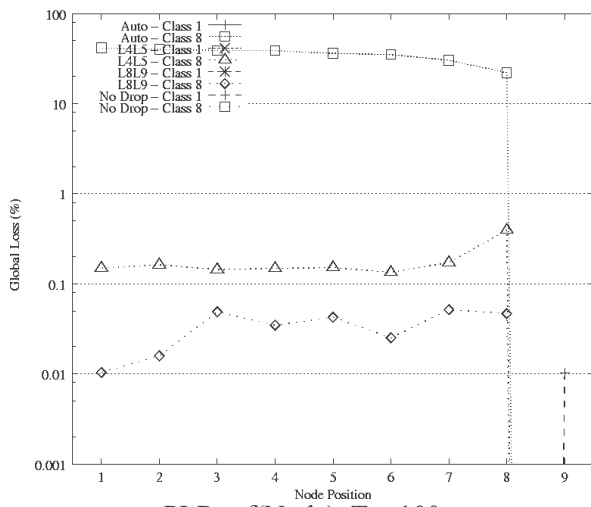
As for erasing thresholds, we study different cases:

- Automatic erasing: a transit BE packet is systematically destroyed for the insertion of the local traffic presenting in optical buffers of the premium and silver services.
- L1 = i, L1 = j: PEM is enabled with threshold values L1 = i and L2 = j (# optical packets).

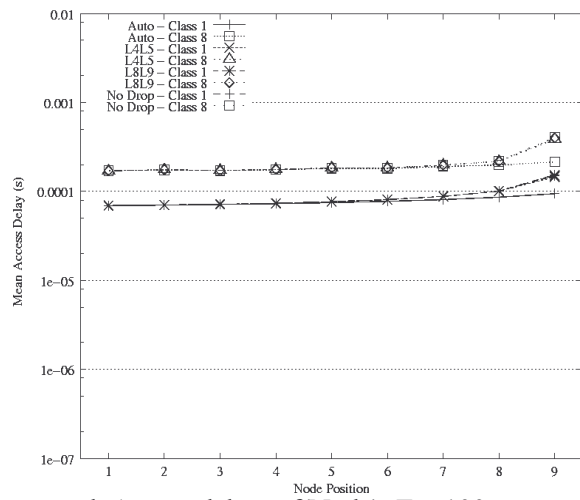
A. Access Metro: Bus Scenario

Figure 5-21 illustrates the access delay and PLR performance results in the case of the bus-based scenario with different erasing thresholds values.

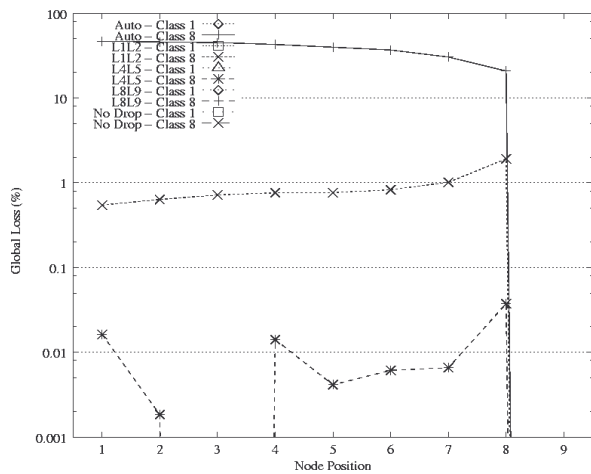




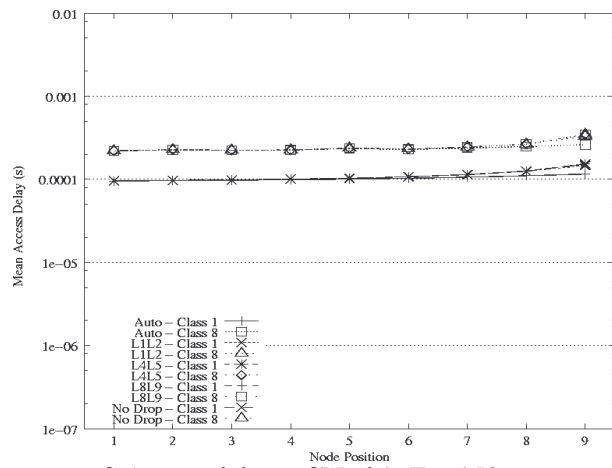
c. PLR = $f(\text{Node})$, $T = 100\mu\text{s}$



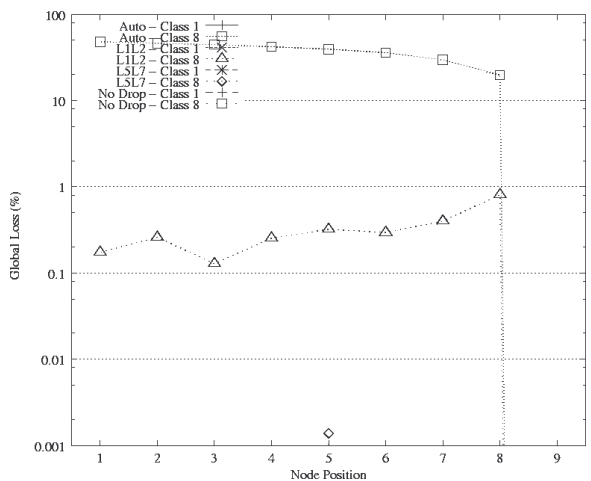
d. Access delay = $f(\text{Node})$, $T = 100\mu\text{s}$



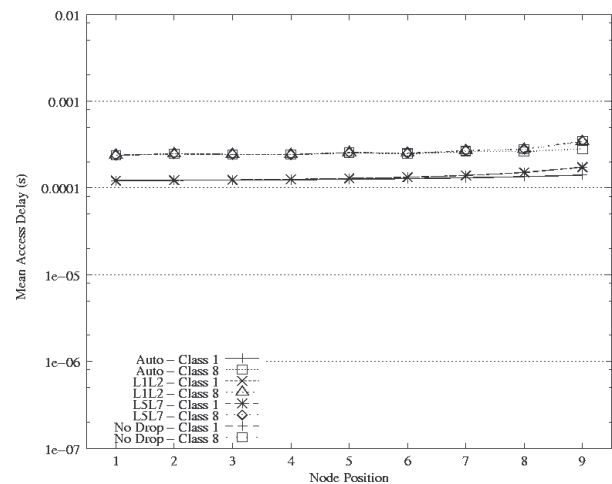
e. PLR = $f(\text{Node})$, $T = 150\mu\text{s}$



f. Access delay = $f(\text{Node})$, $T = 150\mu\text{s}$



g. PLR = $f(\text{Node})$, $T = 200\mu\text{s}$



h. Access delay = $f(\text{Node})$, $T = 200\mu\text{s}$

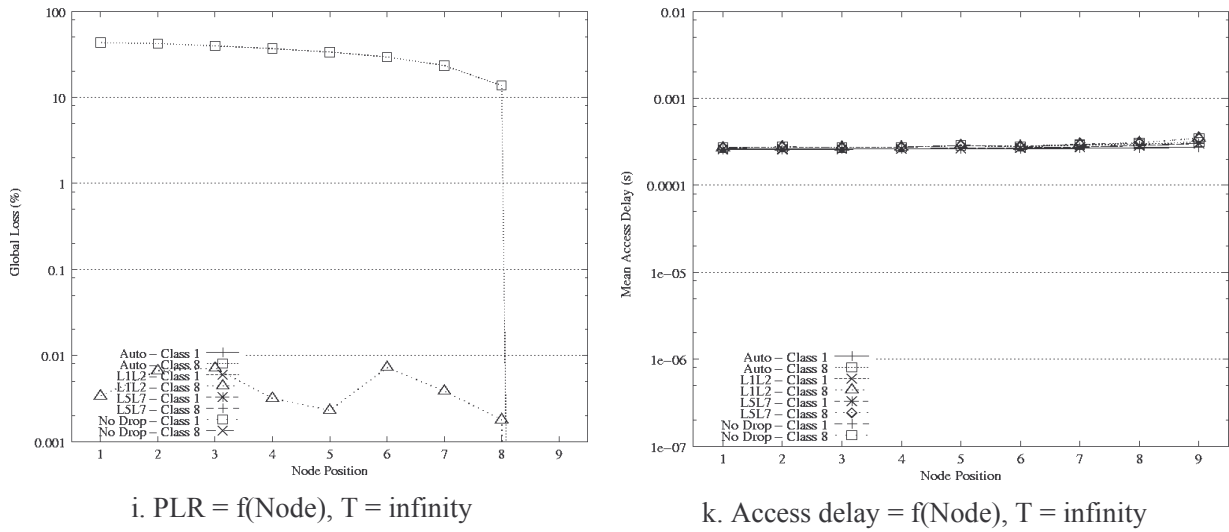


Figure 5-21: Erasing thresholds investigation in the fixed-size mode (Scenario Bus)

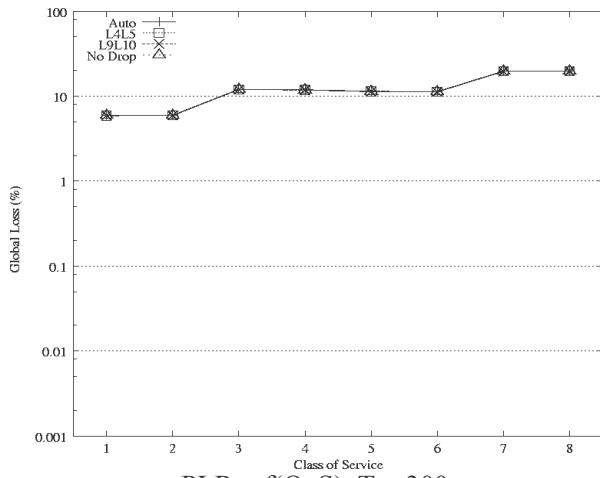
As shown in Figure 5-21, from nodes 1 to 9, we observe only packet loss for CoS 7 and 8, notably in the transit line (due to PEM). However, when the basic timer is fixed to $50\mu s$, node 9 suffers from highest packet loss in the aggregation buffer, even for the premium traffic. This is due to the fact that with a small Timer value, BE packets are created with a very low filling ratio, which increases the traffic load on the bus (by increasing the number of created BE packets), and thus decreases the bandwidth availability for the last node on the ring (node 9).

PEM with small threshold values causes a high loss ratio for class 7 and 8 while the access delay of higher priority traffic only benefits of a slight decrease. An appropriate choice of the Timer value offers reasonable access delay of high-priority traffic, while keeping the loss level of BE packets at safe levels. Therefore, the erasing mechanism in this case isn't recommended since it raises the PLR of BE traffic without offering a real improvement of the access delay of premium traffic.

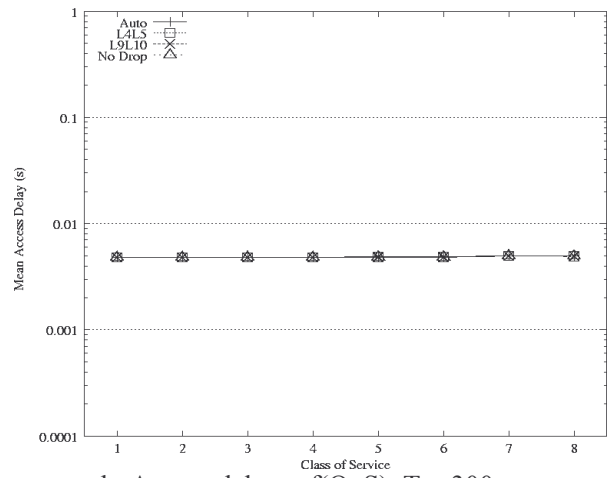
B. Core network: 1-N scenario

In this study, we investigate the node performance for five different values of basic timer T, which are $300\mu s$, $400\mu s$, $500\mu s$, $700\mu s$, and infinity. As for the erasing threshold, we study four different cases:

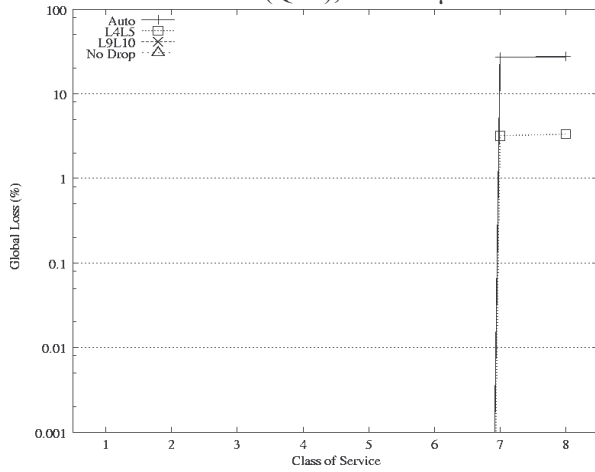
- Automatic erasing: a transit BE packet is systematically destroyed for the insertion of the local traffic presenting in the optical buffer of the premium and silver services.
- L1=4, L2=5: erasing mechanism is enabled with threshold values (in optical packets): L1 = 4 and L2 = 5.
- L1=9, L2=10: erasing mechanism is enabled with threshold values: L1 = 9 and L2 = 10.
- L1=20, L2=20: erasing mechanism is enabled with threshold values L1 = 20 and L2 = 20. Note here that in this case, the erasing mechanism is practically disabled since it is very unlikely that premium or silver optical buffers reach such filling levels.



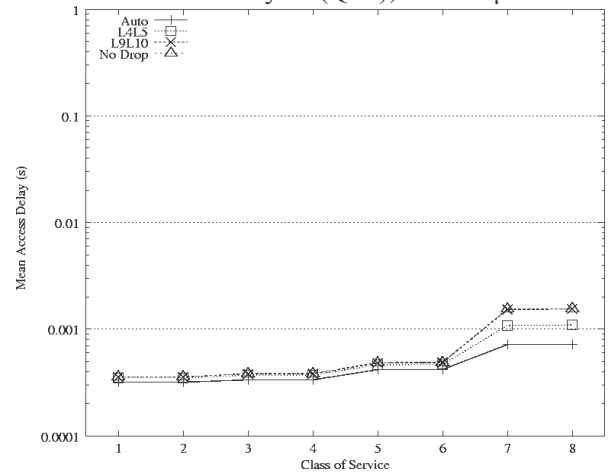
a. PLR = f(QoS), T = 300µs



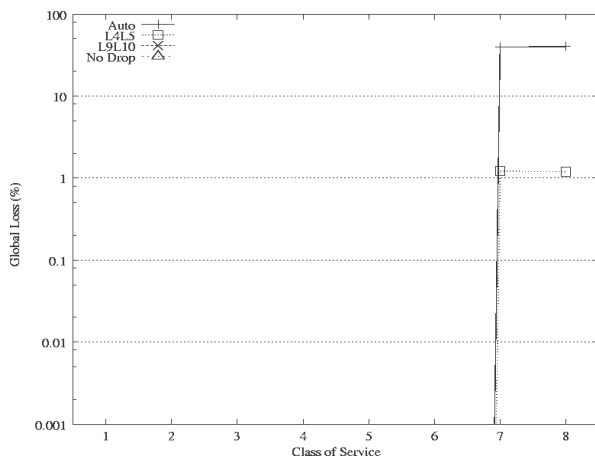
b. Access delay = f(QoS), T = 300µs



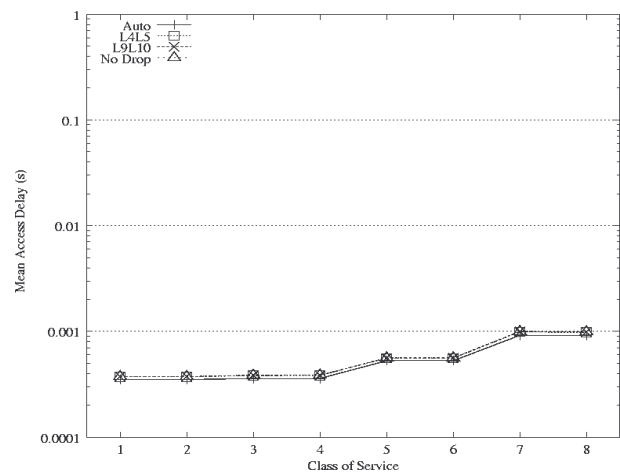
c. PLR = f(QoS), T = 400µs



d. Access delay = f(QoS), T = 400µs



e. PLR = f(QoS), T = 500µs



f. Access delay = f(QoS), T = 500µs

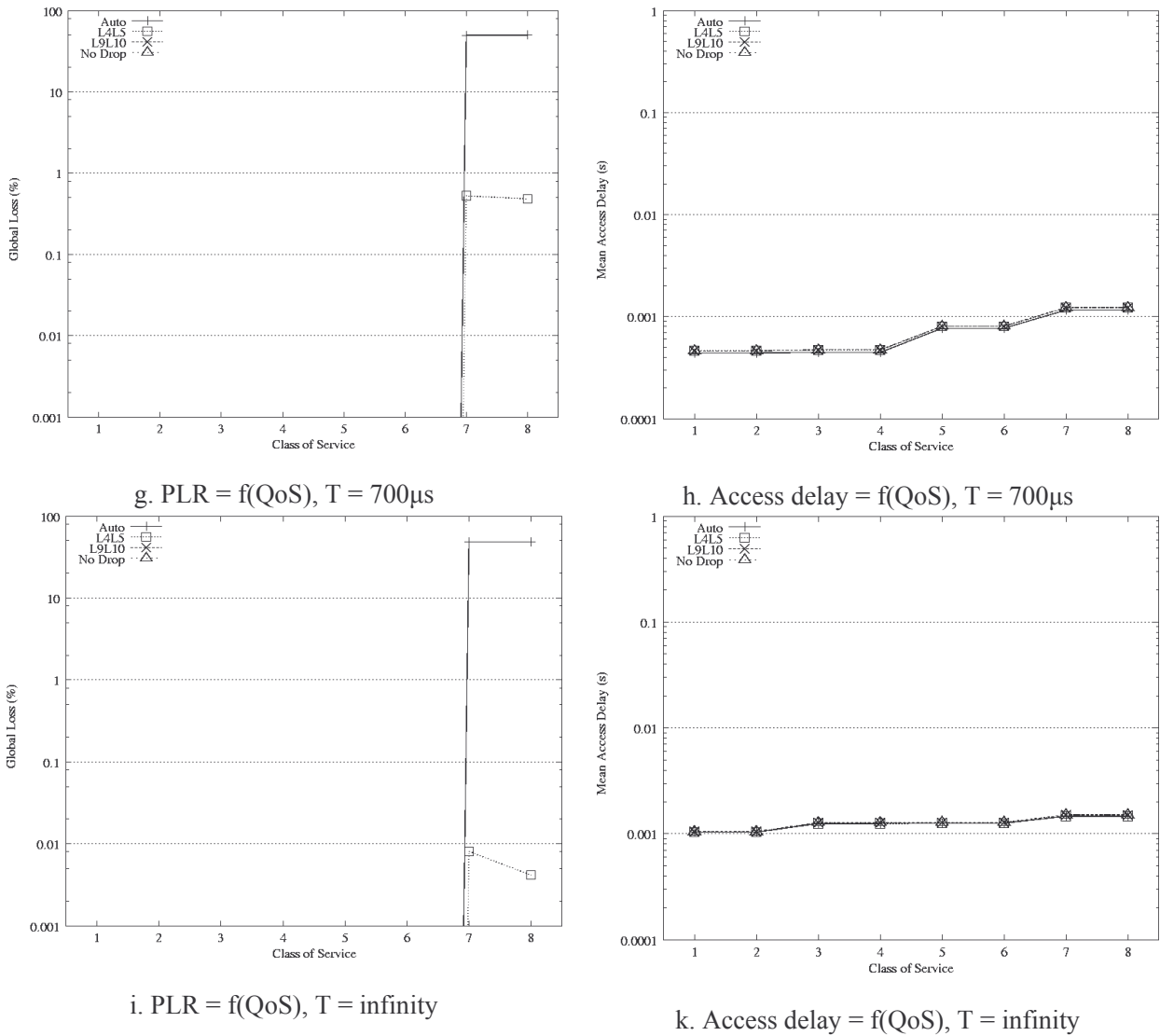


Figure 5-22: Timer values and erasing thresholds investigation with the fixed-size mode (Scenario 1-N)

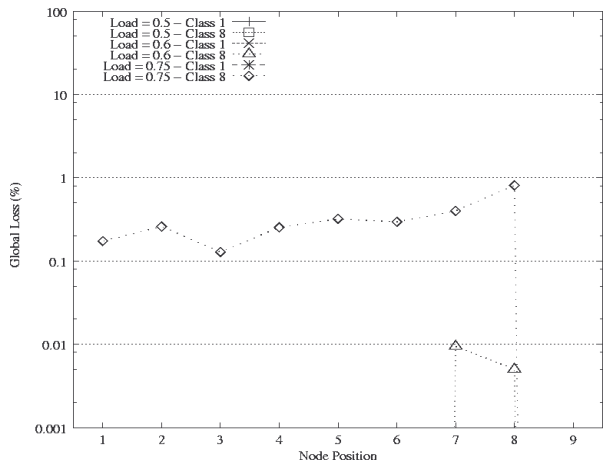
Figure 5-22 illustrates the node performance (in terms of access delay and PLR) with different Timer values and erasing thresholds. The access delay and the PLR are measured in a single ring node with each class of service.

When a small timer value is used ($T = 300\mu s$), the access delay is globally high for all class of service, even with Premium traffic in the ‘Auto Drop’ case. However, the access delay becomes more balanced with high timer values ($> 400\mu s$). Let’s have a look at PLR results. The packet loss is only observed with BE traffic (corresponding to the CoS7 and CoS8 in the electronic domain) in the transit line; thus, QoS for premium services is preserved. Simulation results show that a small erasing threshold (and also automatic erasing case) causes excessive PLR while a higher threshold provides a lower PLR in the transit line.

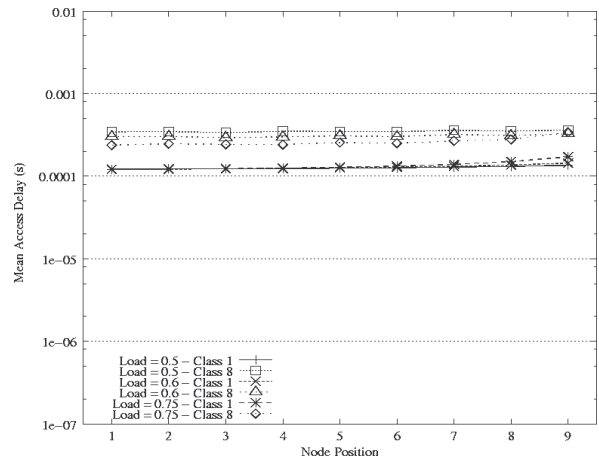
Additionally, the Premium traffic’s access delay doesn’t suffers from delay increasing when the PEM is limited by higher thresholds since it’s mainly caused by the waiting process inside the filling buffer. Thus, an appropriate choice of the timer value provides the performance guarantee for high priority class, without having to enable the PEM which negatively affects BE packet loss ratio.

C. Heavily loaded scenario

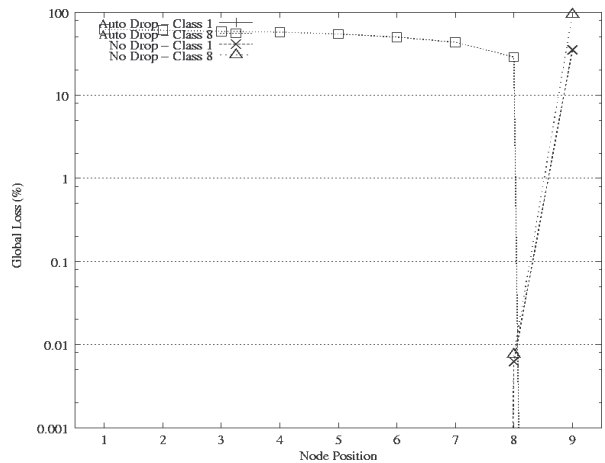
Regarding the bus-based scenario, we now focus on the heavily loaded network. Firstly, we present PLR and access delay results at medium load: 50%, 60% and 75% in Figure 5-23a and Figure 5-23b with the basic timer T of 200μs. We show only results for two classes: Premium class (best case) and BE class (worst case). Results of other class could be found in the middle of worse and best cases. We observe that as the network load increases, the PLR measured for BE packets in the transit line increases also at intermediate nodes. This is due to the fact that the BE traffic amount increases with the growth of the workload, leading to the more erased BE packet in the transit (i.e. more 75%). So, PEM is not useful in the case where the network is lightly loaded.



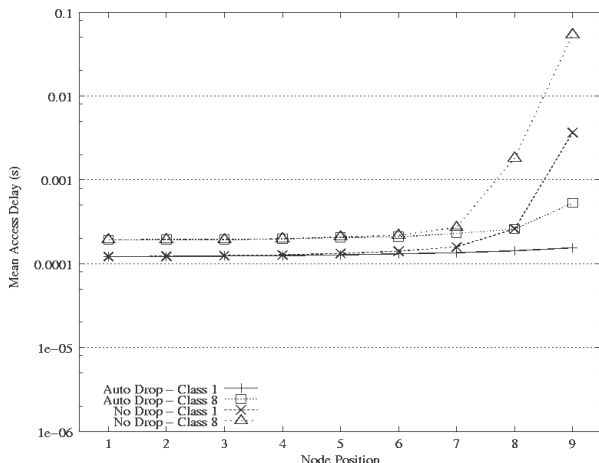
a. PLR = f(Node), T = 200 μs



b. Access delay = f(Node), T = 200μs



c. PLR = f(Node), T = 200μs w Load = 90%



d. Access delay = f(Node), T = 200μs w Load = 90%

Figure 5-23: Erasing thresholds investigation at medium and heavy network loads

Figure 5-23c and Figure 5-23d show the impact of PEM on the network performance when the network is very heavily loaded: 90%. On one hand, without PEM (or ‘No Drop’ curve), we do not observe the PLR from node 1 to node 7 but it occurs lightly at node 8. Particularly, PLR is observed very high at node 9. Indeed, we observe only 0.01% packet loss at node 8 but this value reaches about

15% for Premium class and 99% for BE at node 9. On the other hand, enabling PEM under a very high workload, there is a very high PLR in transit line for BE class (about 60%) but the PLR (both Premium and BE class) measured at last node such as node 8 and node 9 is negligible (less than 0.001%) while keeping the access delay (even BE class) in the safe mode. Therefore, we think that PEM could be useful when the network is heavily loaded in order to assuring QoS of high-priority class.

5.4.4 Investigation of the Timer duration in ERM

A. Access Network: Bus scenario

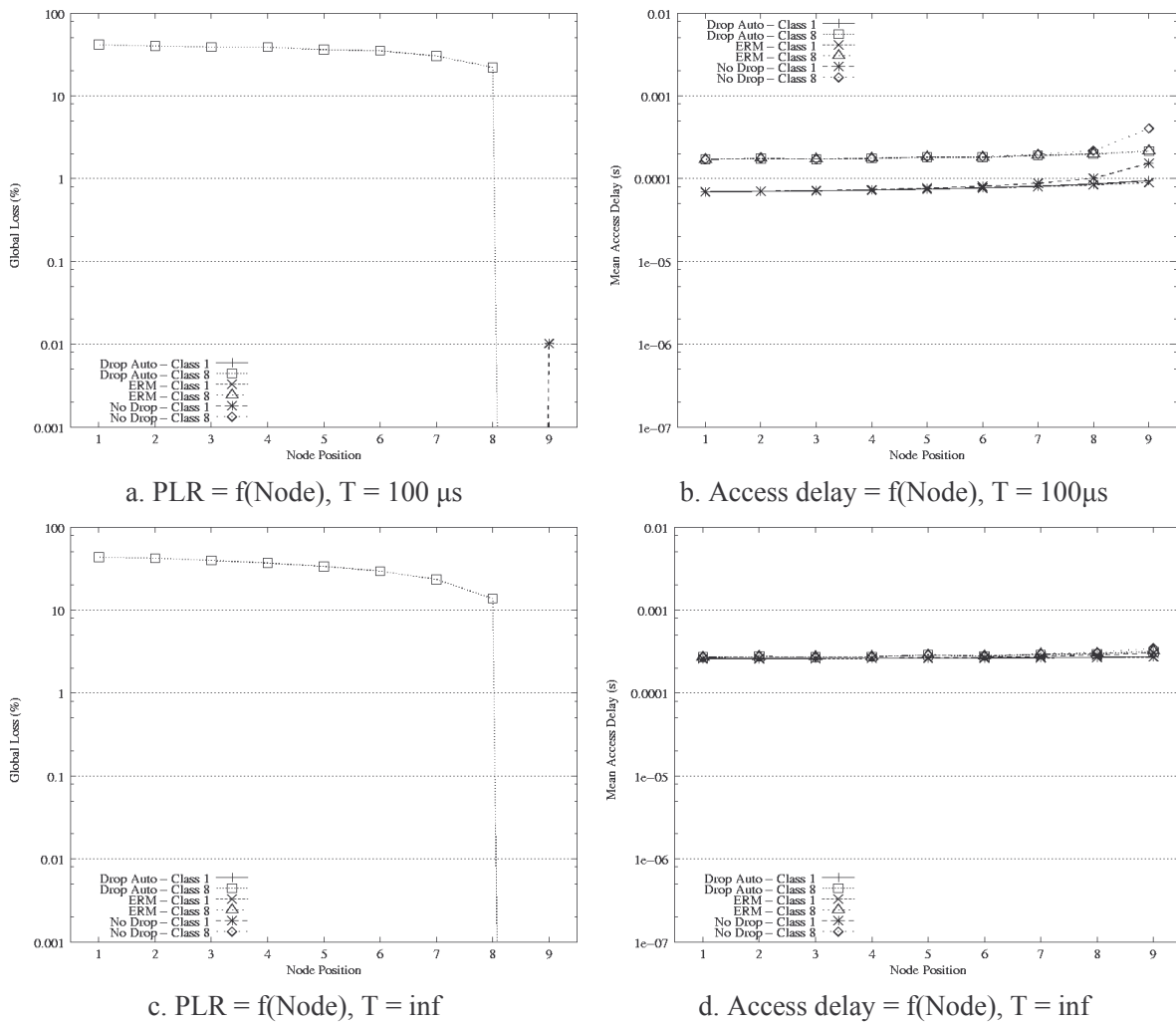


Figure 5-24: ERM’s timer value investigation in Bus scenario

Figure 5-24 show the packet loss and delay access obtained with ERM as compared to PEM (automatic drop and no drop). With big-enough timer value, we observe that ERM always offers the good performance. We haven’t seen the loss while the access delay is guaranteed. Even at last node, ERM could keep the access delay as small as that of PEM with ‘Automatic Drop’.

B. Core Network: 1-N scenario

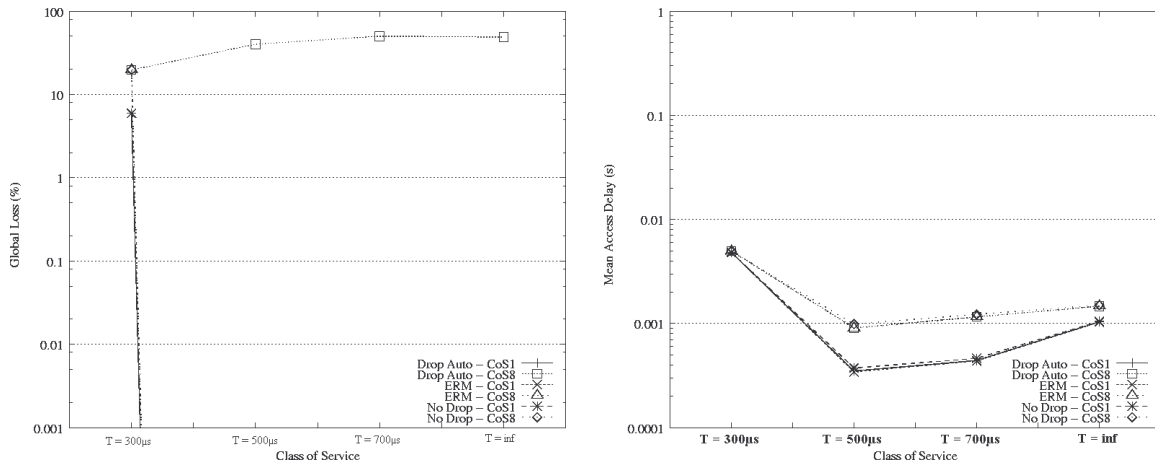


Figure 5-25: ERM’s timer value investigation in 1-N scenario

The same behaviour of ERM is observed in 1-N scenario (Figure 5-25) inside a single ring node. There is no loss with ERM when the timer value is more than 300µs while about 50% of the loss rate is viewed with *AutomaticDrop*-enabled PEM.

C. Heavily loaded scenario

ERM is also efficient when the network is heavily loaded. Figure 5-26 shows the performance results obtained in the bus-based network as the network load of 90%. Note that timer value of 200µs is used in this case. We see that there is no loss in the network with ERM. On the contrary, PEM shows a very high PLR. Indeed, in a one hand, PEM can not keep small PLR at the transit line with ‘Automatic Drop’. In the other hand, PEM can not guarantee Premium traffic without ‘Packet Erasing’. So, it is necessary to implement ERM instead of PEM when the network load reaches a very high level. Through these experiments, we have seen the advantage of ERM over PEM.

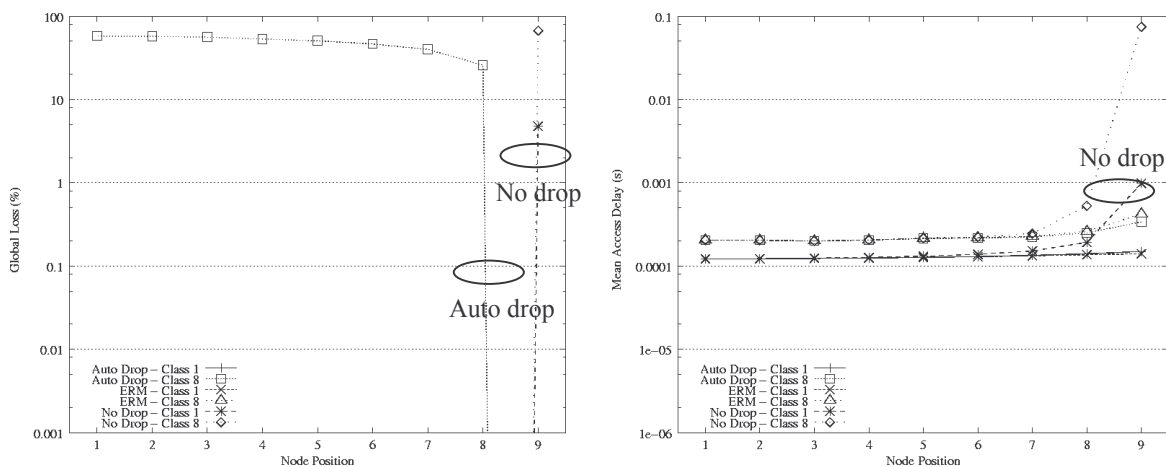


Figure 5-26: PLR and Access delay under heavy load

5.4.5 Mono-class Vs. Multi-class approaches

A. Access Network: Bus scenario

This section is dedicated to compare the network performance between two QoS mapping approaches of the optical packet creation: mono-class and multi-class. To understand the behaviour of each approach, we firstly consider the filling ratio obtained in Figure 5-27 where we set the network load to 80%. Note that CUM is enabled in the multi-class case. In the figure, we only present the filling ratio inside an access node.

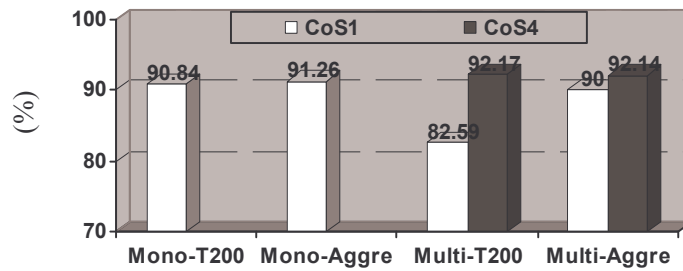


Figure 5-27: The filling ratio comparison between Mono-class and Multi-class

As shown in the figure, optical mono-class packets seem to be well filled, notably with the long timer size (about 90.84% when the timer size equals 200µs and more 91% with the simple aggregation). The filling ratio of optical mono-class packets is higher than that of multi-class packets except BE class. With the timer size equal to 200µs, the filling ratio in mono-class case is about 90.84%, comparing to only 82% of Premium class but it is less than BE class in multi-class case (about 92.17%). As the timer value tends to infinity, filling ratios obtained for both mono and multi class are more 90% (91,26% for mono-class; 90 and 92,14% respectively for Premium and BE).

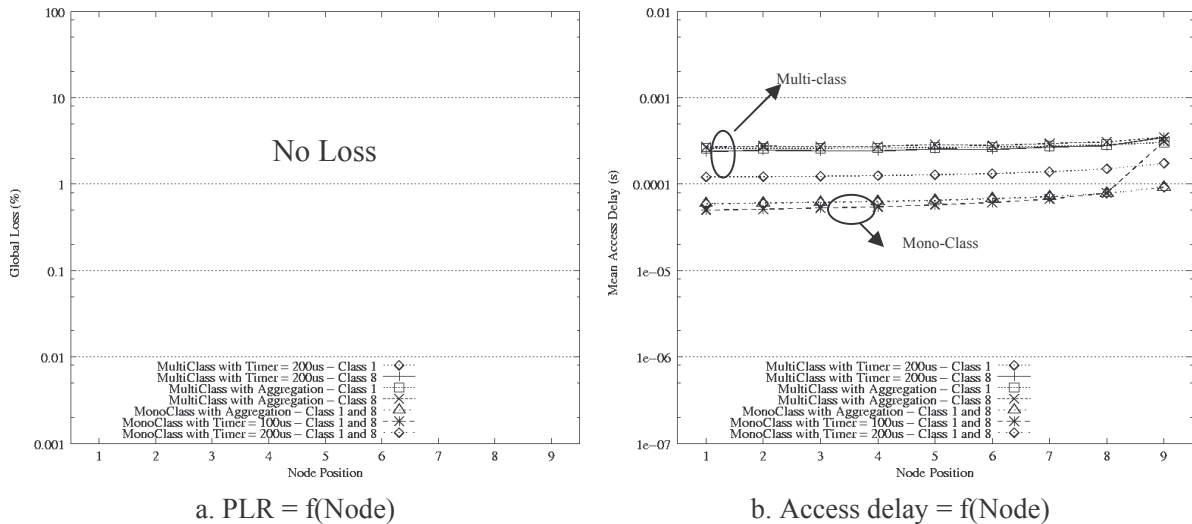


Figure 5-28: PLR and Access delay comparison between Mono-class and Multi-class approaches

In Figure 5-28a, both Mono-class and Multi-class cases do not perform the packet loss at local buffers (aggregation + optical buffers). So, we concentrate on Figure 5-28b which presents access

delay results. Since the process in the optical mono-class packet creation does not classify electronic packets according to its CoS, therefore the arrival rate of electronic packets to the aggregation buffer is high as compared to the multi-case. This leads to the situation that the waiting time of electronic packets in the aggregation buffer is smaller than that in the multi-class case and increases the number of optical packets contained in the optical buffer. Additionally, since ring bandwidth is well exploited, these packets may not be waited a long time. As a result, the total access delay (in aggregation and optical buffers) of electronic packets, which are encapsulated inside optical mono-class packets, is small. For instance, access delays measured with the timer size equal to or more than $200\mu s$ are about $0.001s$ in multi-class case while these values are less than $0.001s$ in the mono-class case, even when the timer size is set up $100\mu s$.

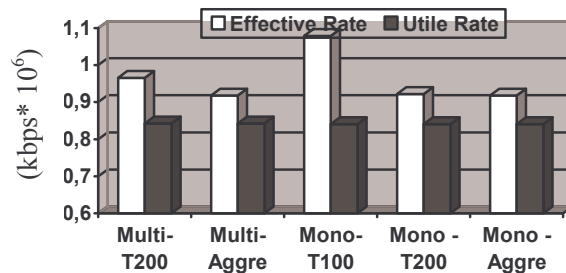


Figure 5-29: Utile and Effective Rates between Mono-class and Multi-class approaches

Figure 5-29 illustrates utile and effective rates of Mono-class and Multi-class at node 1 on the bus. When the timer size equals $100\mu s$, additional header amount observed in the Mono-class is very high. However, it rapidly decreases as the timer size increases. This value becomes as small as the one in Multi-class approach when the simple aggregation is enabled.

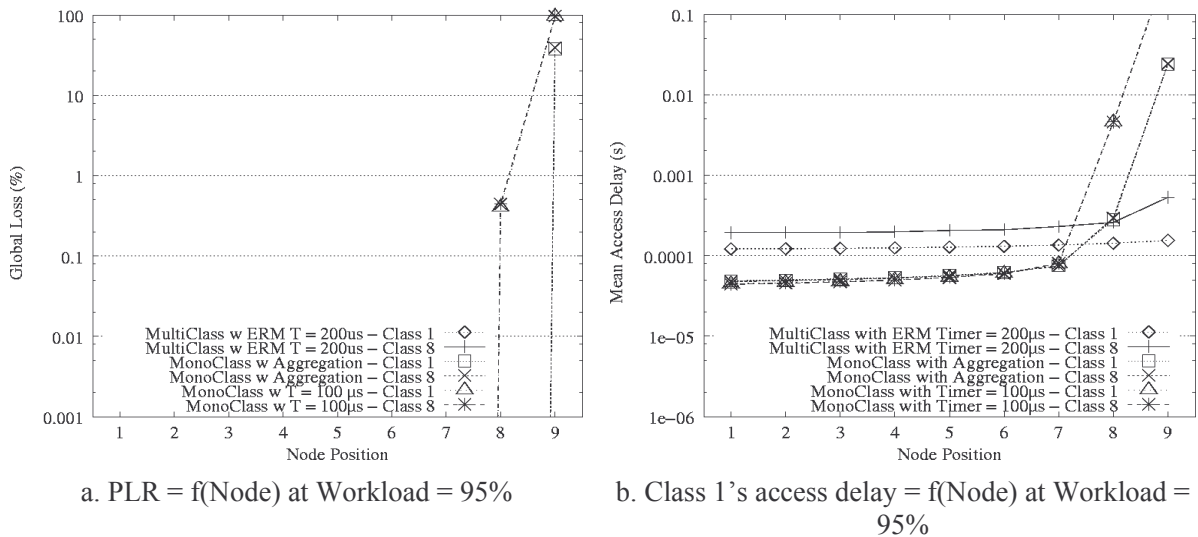


Figure 5-30: PLR and Access delay between Mono-class and Multi-class under heavy load

We now simulate the network under a very high workload (95%) with both approaches. Results obtained by the mono-class and the multi-class case with ERM ($T = 200\mu s$) are presented in Figure 5-30. Under a heavy load, the increase of offered and transit traffic raises up the delay and packet loss (even Premium packets) of optical packets at last access nodes for the mono-class. However, when ERM is enabled in Multi-class approach, the network performance is obviously improved (no loss is

observed with stable access delays). This example shows the advantage of multi-class case. Since the mono-class case does not allow any QoS-management at the network level, the ring node is not able to react actively to such an unexpected event.

B. Core Network: 1-N scenario

This subsection compares the performance of Mono-class with Multi-class approach in the core metro scenario. Figure 5-31 shows the filling ratio for both mono-class and multi-class cases with the network load of 75%. The result shows that the mono-class offers a lower filling ratio as compared to the multi-class with timer size of 500µs. This phenomenon is explained as follows. In the core metro the offered client traffic is divided into several sub-traffics, the amount of traffic coming to a node is not high. Therefore, Mono-class can not create lots of well-filled optical packets. By contrast, thanks to the simple aggregation, Mono-class may optimize its filling ratio from all packets.

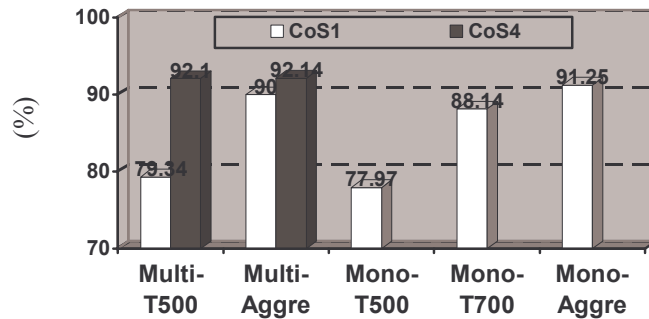


Figure 5-31: Filling ratios comparison between Mono and Multi class in the core metro

Similar to the bus-based scenario, the mono-class offers better performance (in terms of access delay) than the multi-class. This affirmation is observed in Figure 5-32. Indeed, observed access delays of the mono-class seem to be more balanced than that of the multi-class, notably for BE class.

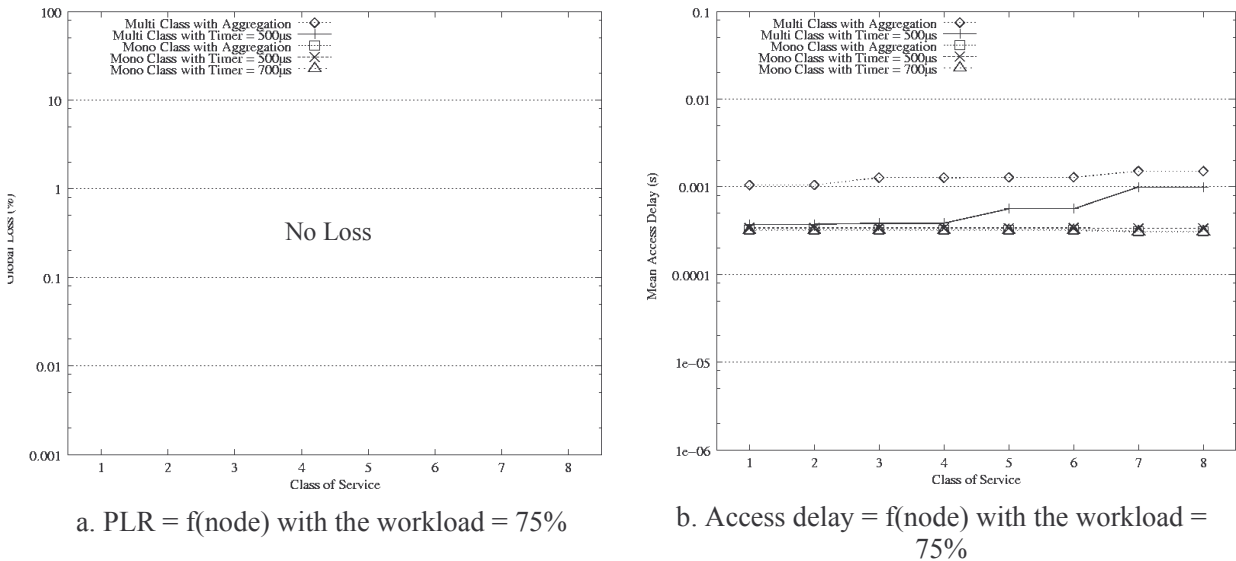


Figure 5-32: PLR and access delay of Mono-class and Multi-class for the core metro

5.4.6 Performance evaluation with DCUM

A. Access Network: Bus scenario

To show advantages of DCUM, we firstly compare obtained results from DCUM with those of CUM where the timer duration is set to $100\mu s$. The PLR and the mean access delay for Premium CoS are respectively shown in Figure 5-33a and Figure 5-33b. These values are measured according to the node position on the bus. Here, we vary the workload from 40% to 70%, 80%; and also vary the timeslot from $20\mu s$ down to $10\mu s$ and $5\mu s$ in order to having various traffic rates of electronic packets. For instance, with the small timeslot ($5\mu s$ – this value also equals the optical packet size) under a heavy workload (80%), the arrival rate of electronic packets is very high. In contrast, a big timeslot ($20\mu s$) under a lightly workload (40%) corresponds to the case where electronic packets arrive to the aggregation buffer very slowly.

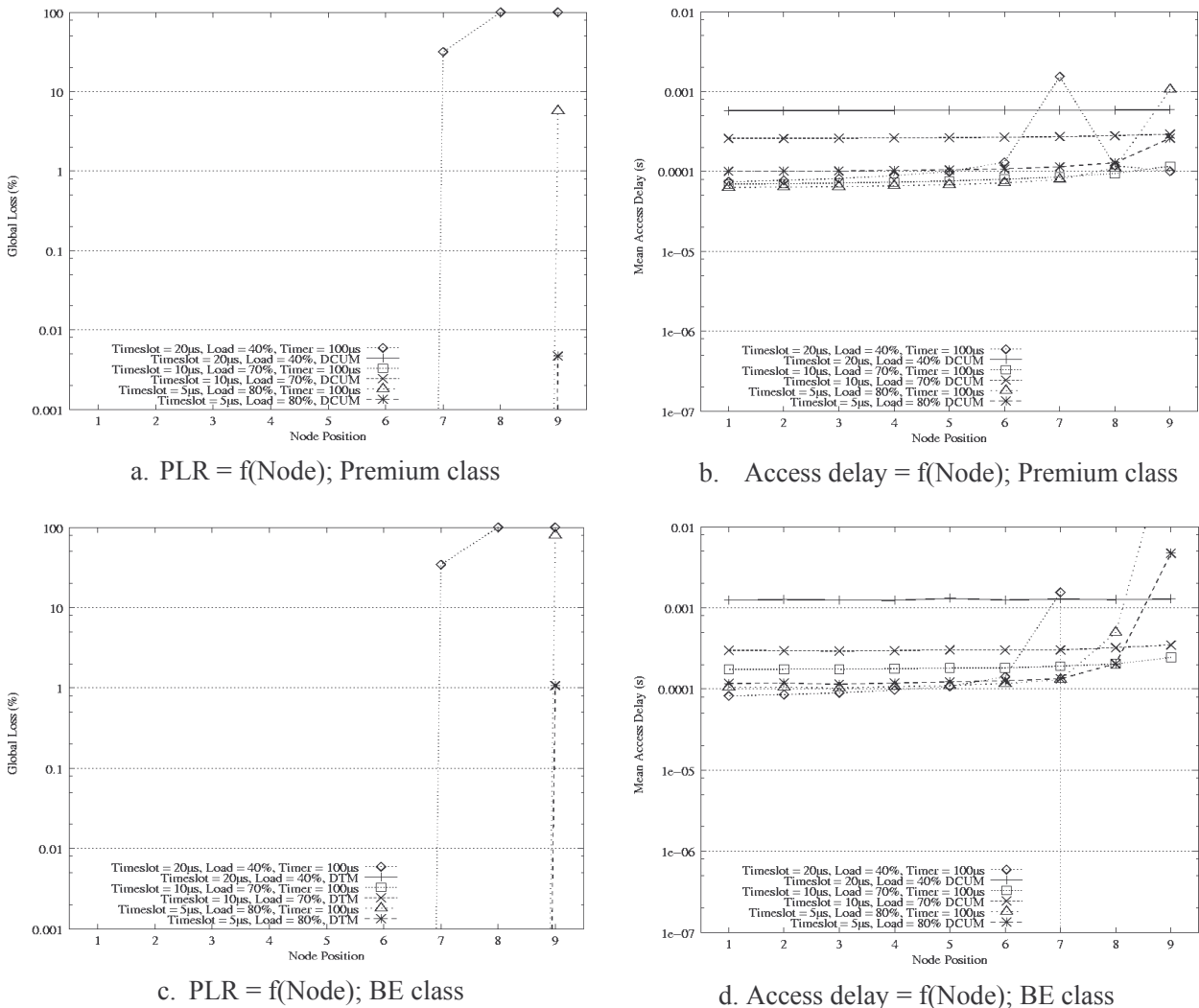


Figure 5-33: Performance comparison: DCUM vs. CUM with the timer size equal to $100\mu s$

Results show that when the arrival rate of electronic packets is very fast or very slow, CoS-Upgrade mechanism with the limited timer ($100\mu s$) cannot guarantee Premium class, notably at last nodes (from node 6). Under low arrival rate of electronic packets, we observe a very high packet loss ratio (about 30% at node 7 and nearly 100% at last node) while this value is measured about 7% under the high arrival rate. On the other hand, under the medium arrival rate (the workload of 70% and the timeslot of $10\mu s$) access delays obtained by this timer value are more balanced while it does not show any packet loss. Note that the small access delay, which is suddenly fallen (node 8 and node 9), is meaningless. They are caused by first successful insertions. Therefore, actual delay values for these nodes are infinite. In other words, CUM with the limited timer duration may only guarantee QoS of Premium class under the medium load.

Regarding DCUM, the packet loss occurs lightly under a very high arrival rate (about 0.001%) while the access delay always is kept in safe-mode (less than 0.001s) for all three cases. This is mainly due to the fact that under a very high arrival rate of electronic packets, the optical packet is filled rapidly with a very high number of generated optical packets in a small time unit, leading to the overflow of the optical buffer. Another reason comes from the ratio α_{max} . In this case, α_{max} is equal to 0.24 which usually corresponds to about 20% remaining space wasted in lots of created optical packets. But the PLR observed in DCUM is always smaller than that of CUM with limited timer. Regarding CUM, under very low and very high filling rates, CUM with the timer size equal to $100\mu s$ cannot provide a small PLR. In reality, last node shows the PLR very high; it reaches more 90% and becomes unacceptable for BE class.

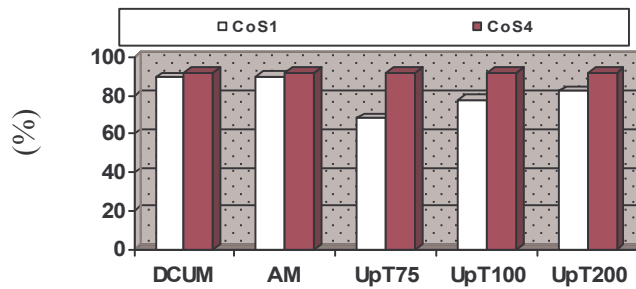


Figure 5-34: Filling Ratios (DCUM vs. CUM)

In order to understand how DCUM reduces the PLR, we continue to investigate the optical filling ratio. Figure 5-34 shows the average filling ratio (for both CoS1 and CoS4) with the timeslot of $10\mu s$ and the offered ring load of 70%. Note that the filling ratio for other class of service (Silver and Bronze) could be found between these two values.

Regarding Premium class, we observe that with the Timer $T = 75\mu s$, the filling ratio is the smallest (about 59%) while this value is higher than 90% in the case where the simple aggregation or DCUM mechanism is enabled. The filling ratio increases when the Timer duration increases (since we use the timer factor of 1:2:10:20). Similar to the aggregation case, DCUM offers a higher filling ratio for both Premium and BE class as compared to CUM with the limited timer duration. However, this value is not higher than the aggregation case.

Figure 5-35 shows Utile / Effective Rates with the timeslot equal to $10\mu s$ while the offered ring load is set to 70% (it corresponds to the medium arrival rate of electronic packets) at node 1. We observe that the utile rate keeps unchanged and equals to the offered rate in all cases (since no packet is lost). However, the effective rate with small timer values is very high as compared to bigger timer values. This is due to the fact that the number of the optical packet generated by small timer values is always higher than the one generated by bigger timer values. This leads to a very high number of optical headers added to the optical packet when small timer values are used, hence causing an excessive

effective rate. Similar to filling ratio results, DCUM and simple aggregation also offer the smallest effective rate.

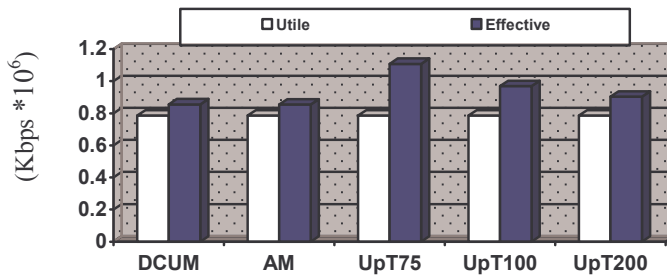


Figure 5-35: Utilite and Effective Rates with the timeslot equal to $10\mu s$ while the offered ring load set to 70% at node 1

Figure 5-36 shows the performance comparison (in terms of PLR and mean access delay) between the simple aggregation and DCUM with respectively Premium and BE class. Interestingly, values obtained with two mechanisms seem to be the same. Through various simulations, we could conclude that the simple aggregation and DCUM offers the best performance in the bus-based scenario.

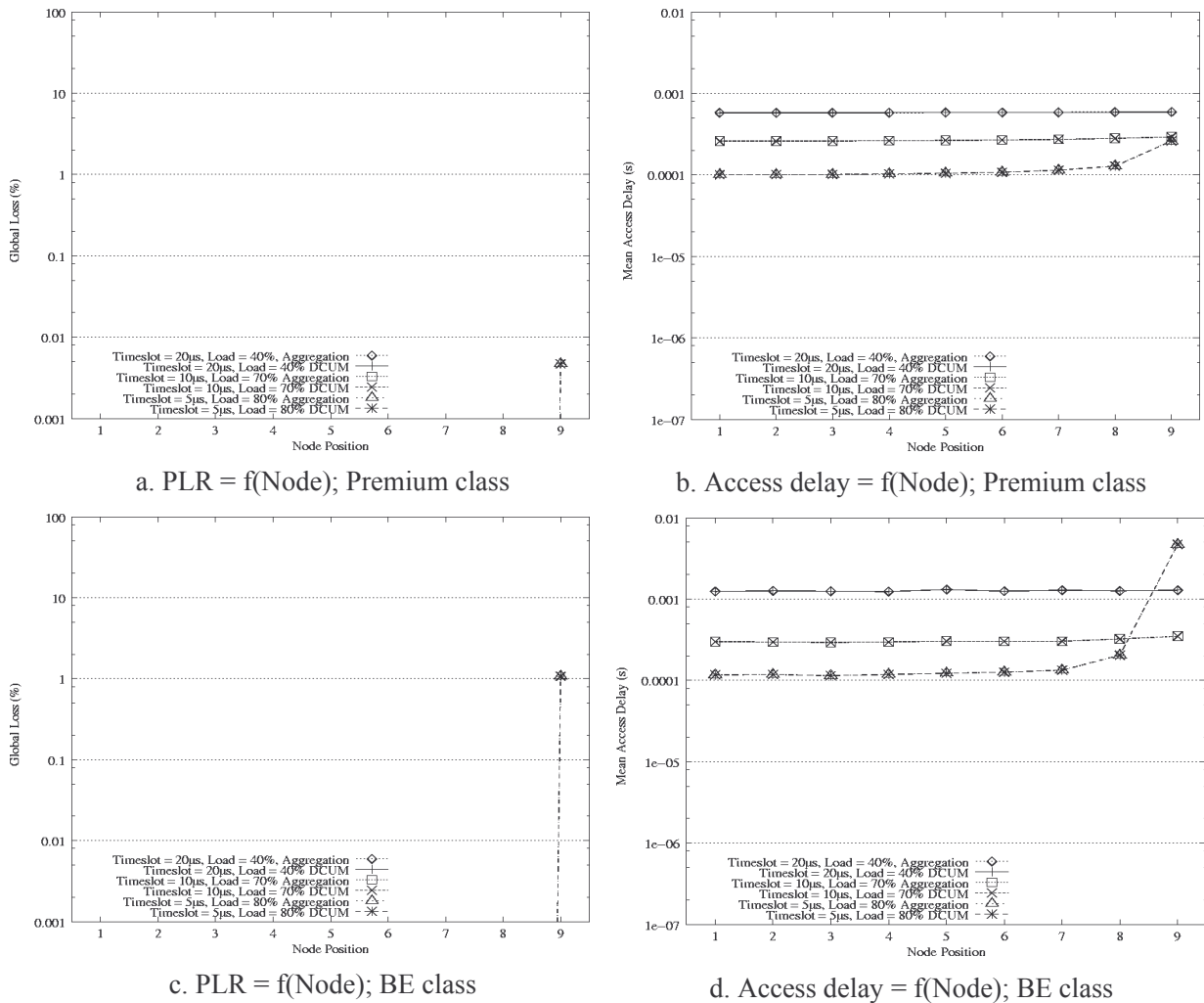


Figure 5-36: Performance comparison: DCUM vs. Aggregation case

Why DCUM is proposed while the simple aggregation may keep the network performance in the safe-level? In order to have the answer, we should investigate studied mechanisms in 1-N scenario.

B. Core Network: 1-N Scenario

In this scenario, we firstly compare results obtained by DCUM with the simple aggregation. The PLR and the mean access delay (observed in a single node) for all class of service are respectively shown in Figure 5-37. These values are also measured according to the workload from 40% to 70%, 80%; and the timeslot from 20μs down to 10μs and 5μs. These choices correspond to the slow, medium and high arrival rate of electronic packets.

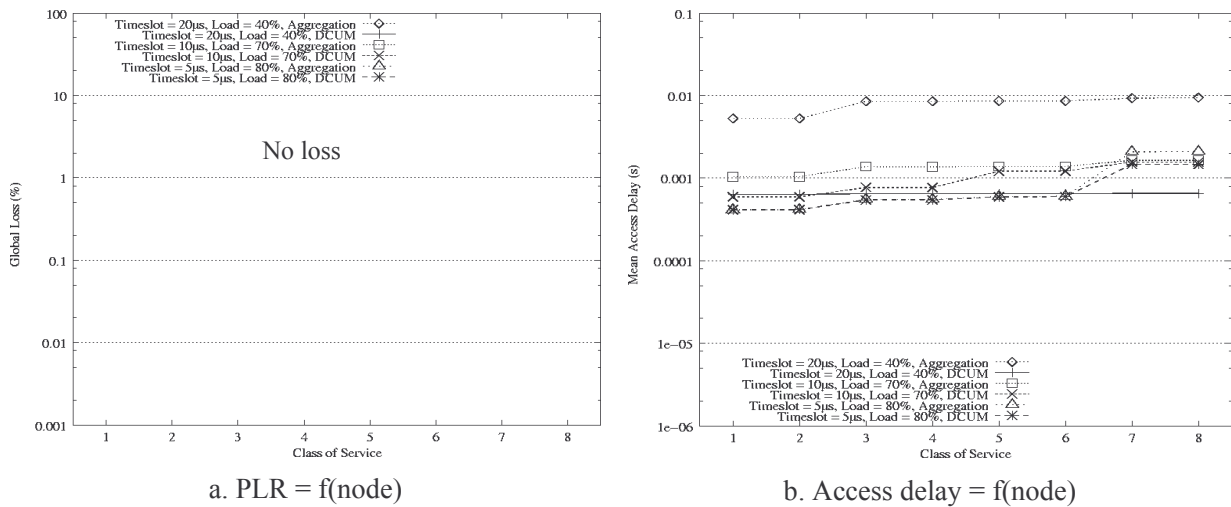


Figure 5-37: Performance comparison: DCUM vs. AM

These results show that when the arrival rate of electronic packets is very low, the aggregation mechanism cannot guarantee good network performance in terms of access delay. For instance, under a very low arrival rate of electronic packets, we observe that the access delay of the Premium class is higher than 5ms, hence exceeding MEF specifications. Regarding DCUM, under a low arrival rate the access delay is kept small for all CoS. This result shows the advantage of DCUM compared to the simple aggregation case.

Regarding Figure 5-38 and Figure 5-39, the aggregation mechanism always offers the best filling ratio and the smallest effective rate. Although that DCUM provides the filling ratio smaller than that obtained by the simple aggregation but it is still higher than that of CUM with limited timer value (i.e. T equals 300μs, 500μs or 700μs).

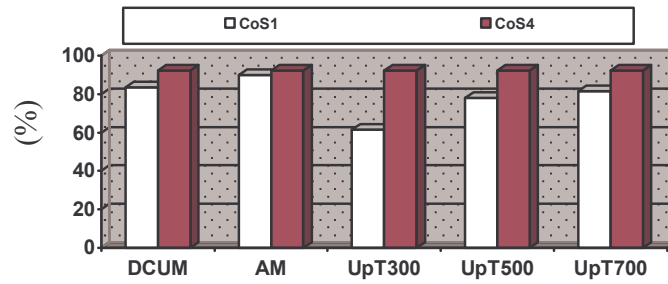


Figure 5-38: Filling ratio comparison between DCUM, CUM and Aggregation Mechanism.

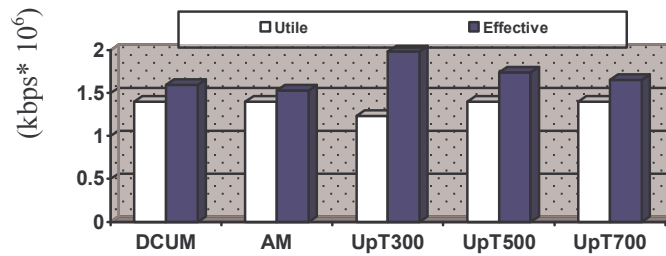


Figure 5-39: Utile and Effective rates between DCUM, CUM and Aggregation Mechanism

Figure 5-40 shows the performance comparison between DCUM and CUM with the timer value equal to $500\mu s$. Note that with CUM, this timer value is one of timer durations that offer the best performance to the network under the medium arrival rate of electronic packets. As shown in the figure, CUM using the timer size of $500\mu s$ cannot guarantee the performance (notably for PLR) in very high and slow arrival rates. It only offers a good performance to the network in the case of the medium arrival rate.

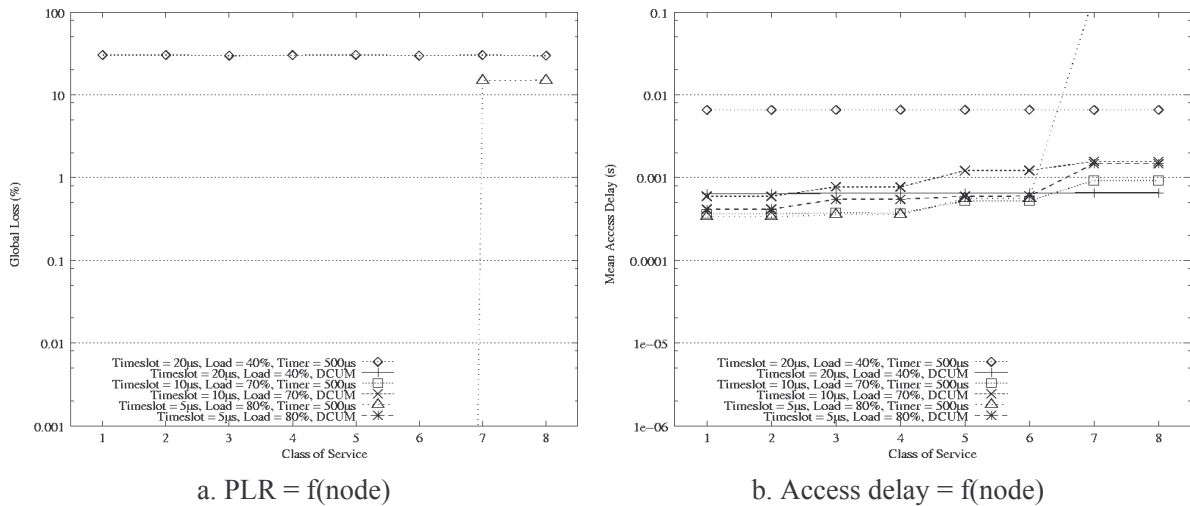


Figure 5-40: Performance comparison between DCUM and CUM with the timer size equal to $500\mu s$

On the other hand, DCUM does not show any packet loss while keeping the access delay in the safe mode for three cases of the arrival rate. We think that DCUM can improve significantly the performance of Metro Core Network as compared to CUM. So instead of using CUM in which we

must know reasonable values of the timer before installing the network (this work sometimes causes a very high maintenance cost), we just simply implement DCUM in each ring node.

5.5 Concluding remarks

This chapter has studied congestion management mechanisms: Packet Erasing Mechanism (PEM) and Extraction/Reemission Mechanism (ERM). PEM allows ring nodes to erase transit BE packets in case of congestion to insert high priority services on the ring. The result obtained with Fixed Length – Optical Packet Format (FL-OPF) model have shown that PEM seems to be not necessary if we choose reasonable timer values for the optical packet creation. Quite the reverse, with big enough values of timer, the complementary use of PEM may degrade network performances (e.g., high PLR for BE service due to packet erasing without significant improvement of access delay for Premium service).

As far as PEM is concerned, ERM seems to be also not necessary if we choose reasonable timer values for the optical packet creation. However ERM is very useful to guarantee QoS for high-priority services in case where the network becomes heavily loaded (more than 90%).

Model	Optical Packet Creation Process	Control processing	Performances		
			Low load: $\rho \leq 0.75$	High load: $0.75 < \rho \leq 0.8$	Very high load : $0.80 < \rho$
FL-OPF	- Complex. - How to determine Timer value?	- Simple, required only 1 control canal for all λ	- Good for all CoS - Fairness	- Good for all CoS - Fairness	- Maybe good for premium services
VL-OPF (empty packets)	- Simple	- Complex, required processing of control packets on all λ	- Good, better than Fixed model - No fairness	- Good for high priority CoS, bad for low priority CoS - No fairness	- Bad for others CoS

Table 5-4: Recapitulative comparison of FL-OPF vs. VL-OPF models

The following point that we would like to recall in this part is the comparison of two architectural approaches: Variable Length – Optical Packet Format (VL-OPF) model supporting empty packets versus FL-OPF model. Table 5-4 presents recapitulative performances comparison of both models. In a nutshell, FL-OPF model simplifies the control processing since a node has only one control wavelength to treat. And it also offers good and fair QoS for all CoS at all ring nodes under offered network load up to 0.80. However, this model requires not only a complex optical packet creation process but also the choice of timer value for a given packet length. VL-OPF model, in turn, does not require the optical packet creation process but more complex control processing since a node has to analyze optical headers on every wavelength. VL-OPF model provides better QoS for high priority CoS than FL-OPF model under low to medium offered loads (up to 0.75), but it cannot ensure fairness among ring nodes. Moreover it provides bad QoS for low priority CoS under high offered load (up to 0.80). Beyond an offered load of 0.80, both models seem not to be able to guarantee QoS for all CoS, only QoS of high priority CoS may be assured thanks to ERM.

With FS-OPF model we have proposed DCUM aiming to automatically adapt various arrival rates presenting the relative relation between the timeslot (optical packet size) and the network load. DCUM does not set a fixed value for timers. It increases each time the timer’s expiration value

according to the state of the optical buffer and the transit traffic. We have seen that under various arrival rates of electronic packets, our proposed mechanism always offers good performance (in terms of access delay and PLR) as compared with other mechanisms. DCUM presented stable results for all three cases: very high, medium and very low arrival rates. However, concerning DCUM, some open questions would be also interesting to be studied. The first one is the performance analysis of the impact of DCUM on network performance under non-uniform traffic repartition. The second question is how to find a scheme based on the state of all nodes in the network in order to develop a '*real*' dynamic timer. Such a scheme will be very helpful for network designers.

Now let us to discuss some perspectives for future work. The future work includes the study of a hybrid congestion control mechanism called the "3-T" model. Its principle is a combination of the threshold-based packet erasing mechanism, the load balancing using WDM dimension and a reactive feedback congestion control mechanism. To further improve the network performances and robustness, such a mechanism is interesting to be investigated.

Chapter 6

Access Network's Resource Allocation and Interconnection of Metro Ring Networks

This chapter firstly addresses a problem that is gaining much attention of researchers: the shared transmission media between end-users in Ethernet-based passive optical network (EPON). Since EPON merges inexpensive Ethernet equipments and the high-bandwidth optical fiber, it has been considered as an attractive solution for the next generation broadband access network. In this chapter, we propose an enhanced dynamical bandwidth allocation algorithm, which is based on an existent algorithm [AYD 03], to effectively and fairly allocate bandwidth between end-users. To address the idle period problem, the proposed algorithm calculates complementary granted bandwidth according to the arrival rate of electronic packets in a transmission cycle to facilitate the data transmission during the idle time. Then, we simulate the EPON-based multi-service network, in which the proposed algorithm is implemented with well-known algorithms. We will show that the proposed algorithm can significantly improve the network performance in terms of packet access delay and packet loss ratio as compared with existing algorithms. This chapter also covers how to guarantee the performance of high-priority traffic which is travelled inside a 'close' network, formed by interconnected POADM rings. Particularly, the behaviour of a node which interconnects two different types of the optical ring metro network will be investigated.

6.1 Resource Allocation in EPON

6.1.1 Passive optical network Overview

Recently, passive optical network has gained a great amount of interest both in industry and academia as a promising cost-effective solution to the 'last mile' problem in the broadband access network [KGB 02]. The increased demand for more bandwidth and bandwidth services in the access network has been growing rapidly and there have been great efforts to develop economical subscriber networks based on the optical technology. Actual technologies like digital-subscriber-line or cable-modem-based network have limitations, because they are based on the infrastructure that was built for carrying voice and analogue signals on the metallic fiber. Since EPON merges the inexpensive Ethernet equipments and the high-bandwidth optical fiber, it has been considered as an attractive solution and the best choice for the next generation broadband access network.

EPON system is a point-to-multipoint access network without active elements in the signal path from the source to the destination [ZMT 05]. In EPON system, a passive splitter connects several Optical Network Units (ONUs) with only one Optical Line Terminal (OLT) and all data transmitted in the network are encapsulated in Ethernet frames. ONUs reside on the subscriber to provide various services to end-users, while OLT connects the optical access network to the backbone. In the downstream direction (Figure 1a), Ethernet frames are broadcast by OLT to all ONUs and are selectively received at each ONU. In the upstream direction (Figure 1b), since all ONUs share the same transmission medium, EPON system must employ a medium access control (MAC) mechanism to arbitrate access to the shared medium. MAC mechanism prevents data of different ONUs transmitting simultaneously from the collision and efficiently shares the upstream transmission bandwidth among ONUs. In general, this goal is achieved by granting a number transmission window (or timeslot) to each ONU.

The scheme bandwidth allocation can be either static or dynamic. In static allocation, a fixed-size transmission window is allocated from OLT regardless of the instantaneous ONU's requirement to OLT. On the other hand, in the dynamic allocation, a variable-size transmission window is dynamically allocated from OLT to ONU based on its instantaneous requirement. Data frames should therefore be contained in the local ONU buffer until they are transmitted according to the assigned window. For support of the communication between OLT and ONUs, multipoint-control protocol (MPCP), should be implemented in the EPON network.

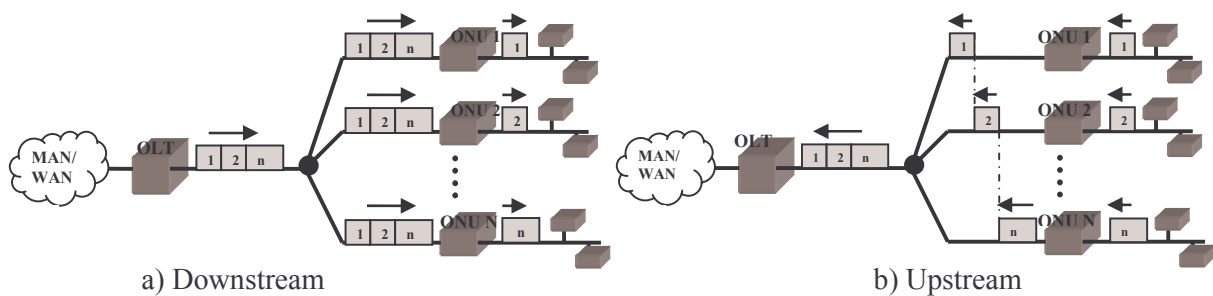


Figure 6-1 - EPON Architecture

MPCP is being developed by the IEEE 802.3 ah Task Force [ITF 04] to support the communication information between OLT and ONUs. MPCP is not concerned with any particular bandwidth allocation. It is used to facilitate the implementation of various dynamic allocation algorithms and to assign dynamically the upstream bandwidth from OLT to ONUs in EPON. MPCP has two operation modes: normal mode and auto-discovery mode [MMR 04]. In the normal mode, MPCP relies on two Ethernet control messages: GATE and REPORT. Each ONU has priority queues that hold Ethernet frames ready for upstream transmission to OLT. The REPORT message is used by an ONU to report its local state (may be the bandwidth requirement or the local buffer occupancy). Upon receiving a REPORT message, OLT take it as parameter for a DBA algorithm module, which is already implemented in OLT. This DBA algorithm calculates thus the transmission start time and the granted transmission window for ONUs such that channel collisions are avoided. After executing DBA algorithm, OLT transmits GATE messages to issue transmission grants to ONUs.

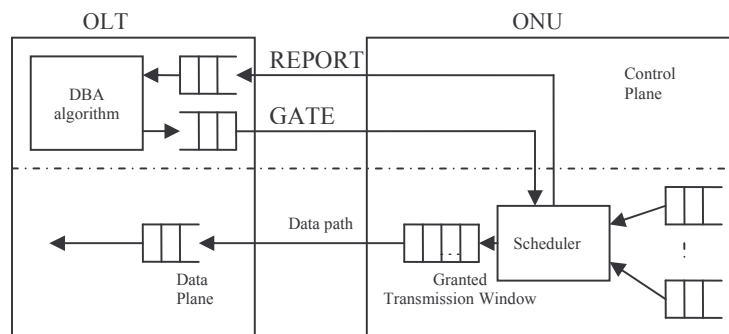


Figure 6-2 - MPCP Operation

ONU can update its local clock using the timestamp contained in each received transmission grant. Hence, each ONU is able to acquire and maintain the global synchronization. The transmission start time is expressed as an absolute timestamp according to this global synchronization. At the granted transmission start time, ONU will start its transmission for up to the granted transmission window size. The transmission may include multiple Ethernet frames depending on the transmission window size and the local buffer occupancy of ONU. No frame fragmentation is allowed during the transmission. If the next frame cannot be transmitted in the current transmission window, it will be deferred to the next transmission window.

In the auto-discovery mode, the protocol relies on three control messages, REGISTER, REGISTER_REQUEST, and REGISTER_ACK, which are used to discover and register a newly connected ONU, and to collect related information about that ONU, such as the round-trip time (RTT) and the MAC address.

Scheduling of different traffic class becomes now an inevitable role in supporting QoS of EPON-based multi-service network. Priority queuing is considered a useful and simple method for supporting multi-service [KMP 02]. The QoS management is performed in each ONU by maintaining several separate priority queues. Packets are classified and placed into their appropriate priority queues by the type-of-service field of each IP packet encapsulated in Ethernet frames. Priority scheduling mechanism schedules packets from the head of a given queue only if all higher priority queues are empty. If a higher priority packet arriving during waiting period of lower priority packet, it will be scheduled ahead of all the reported lower priority packets for the transmission time. This situation will penalize performance of lower priority traffic resulting in increasing, i.e. the access delay and the packet loss rate.

6.1.2 Dynamic bandwidth allocation (DBA) algorithms

In this section, we will approach existing DBA algorithms. DBA algorithms may be categorized into two types: with statistical multiplexing and with computation time.

A. Statistical multiplexing approach: Interleaved Polling with Adaptive Cycle Time (IPACT)

In IPACT, OLT polls ONUs individually and issues the granted transmission window to them in a round-robin cycle [KMP 02]. A polling message is scheduled in an interleaved way that reduces the

bandwidth overhead and thus increases the bandwidth utilisation rate of the upstream channel. On the other hand, the transmission cycle length is not static because it adapts to various cycle-based bandwidth requirements. By using a maximum transmission window (MTW), ONUs with high traffic volumes are prevented from monopolizing the upstream bandwidth.

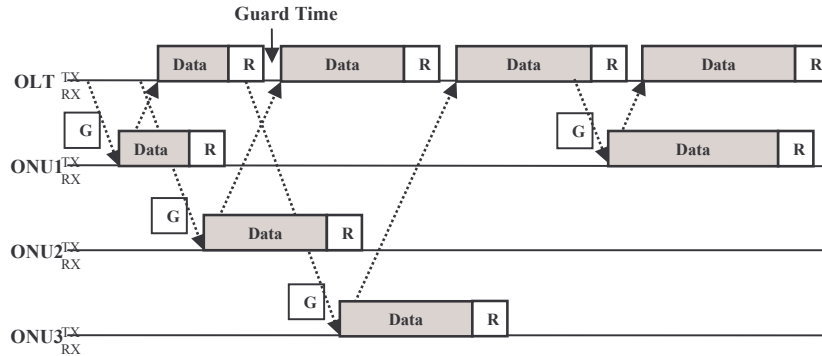


Figure 6-3 - IPACT scheme

Figure 6-3 presents an example of IPACT implemented in the EPON network with 1 OLT and 3 ONUs. Notice that the *guard time* exists between two consecutive data transmissions from different ONUs for purpose of the global synchronization.

The author studied various bandwidth allocation schemes as follows:

- Fixed service (FSA): This DBA scheme always allows the maximum transmission window (MTW) size to all ONUs regardless of the requested window size. As a result, the cycle length is always constant and equal to $N * MTW$ where N is the number of ONU in the network.
- Limited service (LSA): This DBA scheme grants the requested transmission bandwidth, but it is limited by the maximum transmission window (MTW). In this case, the cycle length adapts to ONU's instantaneous bandwidth requirements but it is limited by $N * MTW$ where N is the number of ONU in the access network.
- Credit service (CSA): This DBA scheme grants the requested window plus either a constant credit or a credit that is proportional to the requested window from ONUs.
- Elastic service (ESA): This DBA scheme attempts to overcome the limitation of assigning at most one fixed MTW to an ONU in a round.

B. Dynamic bandwidth allocation with computation time

The DBA algorithm with QoS support is detailed in [AYD 03]. In this allocation scheme, upon receiving the REPORT message from an ONU, OLT does not answer immediately to this ONU. It must wait until REPORT messages from all ONUs are successfully received. Then, OLT collects these messages as parameters for the DBA module to generate a table of granted transmission windows. It means that OLT needs a waiting time for the algorithm before retransmitting GATE messages. The data transmission is thus interrupted between two consecutive transmission cycles. As shown in Figure 6-4, this mechanism results in some idle time that the upstream channel of the access network is not utilized. The idle time is estimated by supposing that all ONUs have the same round-trip time (RTT) to OLT as follows: $T_{idle} = RTT + Computation\ Time$ (2.1)

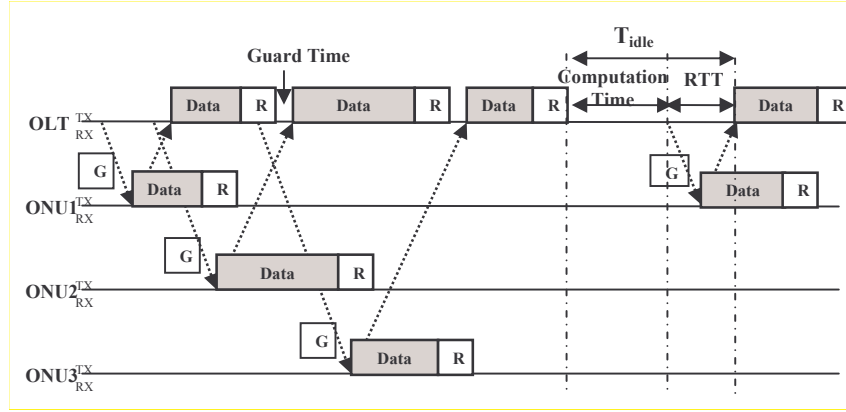


Figure 6-4 - Dynamic bandwidth allocation with QoS

For detail, authors consider an EPON access network with a transmission speed equal to R Mb/s (same for both upstream and downstream path). By denoting the granting cycle is T_{cycle} , the author first calculates the cycle-based minimum guaranteed bandwidth B_i^{MIN} (in bytes) for ONU like following equation:

$$B_i^{MIN} = \frac{(T_{cycle} - N \times T_g) \times R}{8} w_i \quad (2.2)$$

where T_g is the guard time and w_i is the weight assigned to each ONU based on its service agreement level (SLA) such that $\sum_{i=1}^N w_i = 1$.

By considering the case where all ONUs are not classified based on their SLA ($w_1 = w_2 = \dots = w_n$), they thus allocate the granted bandwidth B_i^g to ONU_{*i*} as follows:

$$B_i^g = \begin{cases} R_i & \text{if } R_i < B_i^{MIN} \\ B_i^{MIN} & \text{if } R_i \geq B_i^{MIN} \end{cases} \quad (2.3)$$

where R_i be the requested bandwidth of ONU_{*i*}. Finally, they fairly distribute the excessive bandwidth for all highly loaded ONUs as follows:

$$B_i^{excess} = \frac{B_{total}^{excess} \times R_i}{\sum_{k \in K} R_k} \quad (2.4)$$

$$B_i^g = B_i^{MIN} + B_i^{excess} \quad (2.5)$$

with B_i^{excess} is the excessive bandwidth allocated to ONU_{*i*} and K represents the set of heavy loaded ONUs.

Since this algorithm results in some idle time that the upstream channel of the network is not utilized, we thus propose an enhanced algorithm, by improving the bandwidth utilization rate. So we refer to this algorithm as older DBA (oDBA) algorithm and to our algorithm as enhanced DBA (eDBA) algorithm, for distinction in the rest of the chapter. The author does not provide a comparison over network performance between oDBA and LSA (the best choice among modified schemes of IPACT). Our later work also includes the answer for this open question.

6.1.3 Enhanced DBA algorithm

To improve the upstream channel utilization of oDBA, [ZEA 05] proposes a modified grant table generation algorithm based on oDBA in which OLT uses an early allocation mechanism. An ONU, who has requested bandwidth $R_i < B_i^{MIN}$, can be instantaneously scheduled without waiting oDBA algorithm results. At the same time, ONU, who has requested $R_i \geq B_i^{MIN}$, has to wait until the end of oDBA algorithm. Therefore, the new scheme benefits lightly loaded ONUs to compensate the idle time. This modified algorithm might increase the channel throughput and reduce the access delay in local buffer at ONUs. However, in the case where all ONUs are heavily loaded, this scheme does not seem to work well.

To further improve bandwidth utilisation under a high traffic load, we propose an enhanced mechanism to address the idle period problem. The enhanced DBA algorithm (eDBA) will be detailed in the following section.

Principle of eDBA

In this mechanism, we do not use the scheme that OLT employs an early allocation. We use the scheme that OLT calculates complementary granted bandwidth by using the arrival rate of client packets which is reported from ONU during the last transmission cycle. Upon receiving the complementary granted bandwidth from OLT, ONUs may continue its data transmission during the idle time T_{idle} .

For more details, let us present eDBA scheme as follows:

- i. For simplicity, we denote the parameter $r(n)$ as the cycle-based arrival rate of client packets for the cycle of rank n , which has been presented in [ZMC 06]. Each ONU is responsible for computing its cycle-based arrival rate (that expresses the requested bandwidth) and then transmit this information to OLT. To do this, each ONU must record the scan time during a cycle. A timer is set each time the ONU receives a GATE message from the OLT. When the next GATE message arrives to the ONU, it stops the current timer and gets the scan time Δt . At this moment, a new timer will be triggered. Upon receiving the GATE message, ONU starts to count the size of packets $S(n)$ (in bytes) arriving during Δt . The cycle-based arrival rate $r(n)$ hence is estimated for n^{th} cycle as follows: $r(n) = S(n) / \Delta t$ (3.1). This information is then included in REPORT message that will be sent to OLT in the next cycle.
- ii. Inside the OLT, eDBA algorithm is composed of two sub-modules: complementary allocation (CA) module and oDBA module. When OLT receives a REPORT message from an ONU, the included cycle-based arrival rate $r(n)$ will be entered into the CA module. Thanks to $r(n)$, CA module will calculate the ONUs's complementary transmission window which is authorized to be sent in T_{idle} . These values are calculated according to several conditions (in iii and iv). On the other hand, oDBA module must wait until REPORT messages from all ONUs are successfully received before performing oDBA algorithm as described in the previous section.

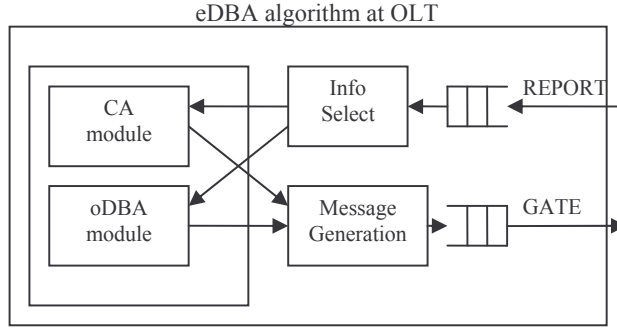


Figure 6-5: enhanced DBA algorithm

Figure 6-5 presents a logical relation between eDBA's modules. Necessary information from REPORT will be selected by 'Info Select' block before being passed to two modules. On the other hand, both CA and oDBA modules pass its results (such as transmission start time, granted transmission bandwidth, etc...) to 'Message Generation' block. Then, this block will determine and schedule appropriate GATE messages to ONUs.

iii. Using the cycle-based arrival rate in the n^{th} cycle, the amount of packets arrived during the $(n+1)$ cycle can be estimated for the ONU at the OLT as: $E(n+1) = \alpha \times r(n) \times T_e$ (3.2) where α is the estimation factor and T_e is the interval between two consecutive GATE messages from OLT to the same ONU. We denote R'_i is the complementary bandwidth request by ONU_i. Then, we have the complementary request for $(n+1)^{\text{th}}$ cycle as: $R'_i = E(n+1)$ (3.3). The factor α is used to represent the impact of the estimation to the complementary request.

iv. Now, we discuss how to allocate the complementary granted bandwidth. Notice that we can use all idle time for the complementary transmission but it is not recommended to do so because of limited processing capability at OLT. So, we denote by τ as authorized bandwidth utilisation rate during the idle time. If $\tau=1$, all idle time can be used for the complementary transmission. We denote by R the transmission capacity of the considered EPON access network (in Mbits/s). We compute at first the complementary minimum guaranteed bandwidth B_i^{MIN} (in bytes) for the idle

time as follows: $B_i^{\text{MIN}} = \frac{(\tau \times T_{\text{idle}} - N \times T_g) \times R}{8} w_i$ (in bytes) (3.4) where T_g is the guard time and

w_i is the weight assigned to each ONU based on its service agreement level (SLA) such that $\sum_{i=1}^N w_i = 1$. In the case where $w_1 = w_2 = \dots = w_n$, the previous formulae becomes:

$B_i^{\text{MIN}} = \frac{(\tau \times T_{\text{idle}} - N \times T_g) \times R}{8}$ (3.5). We allocate the complementary granted bandwidth B_i^{g} as:

$B_i^{\text{g}} = \begin{cases} R'_i & \text{if } R'_i < B_i^{\text{MIN}} \\ B_i^{\text{MIN}} & \text{if } R'_i \geq B_i^{\text{MIN}} \end{cases}$ (3.6). By using only R'_i as a parameter entry, CA module may

immediately calculate the complementary granted bandwidth B_i^{g} without receiving the REPORT messages.

v. The complementary granted bandwidth will be sent to ONUs via GATE messages. ONUs benefit the complementary transmission in the idle time while OLT runs oDBA algorithm.

vi. When oDBA module finishes its algorithm, the granted table will be classified in the ascending order by OLT. Then, OLT schedules the transmission start time of each ONU and answers to ONUs according to this order. The classification of the granted table assures that the more heavily loaded ONU will be more priority to access the upstream channel.

To better understand the concept of eDBA, we examine two examples shown in Figure 6-6(a,b). Figure 6-6a presents the case where there are only two ONUs which benefit the complementary transmission during the idle time. Figure 6-6b presents the case in which, three ONUs benefit the complementary transmission. Note that we have an utilisation rate τ calculated as follows: $\tau = T_c / T_{idle}$ (3.7) where T_c is the complementary transmission time.

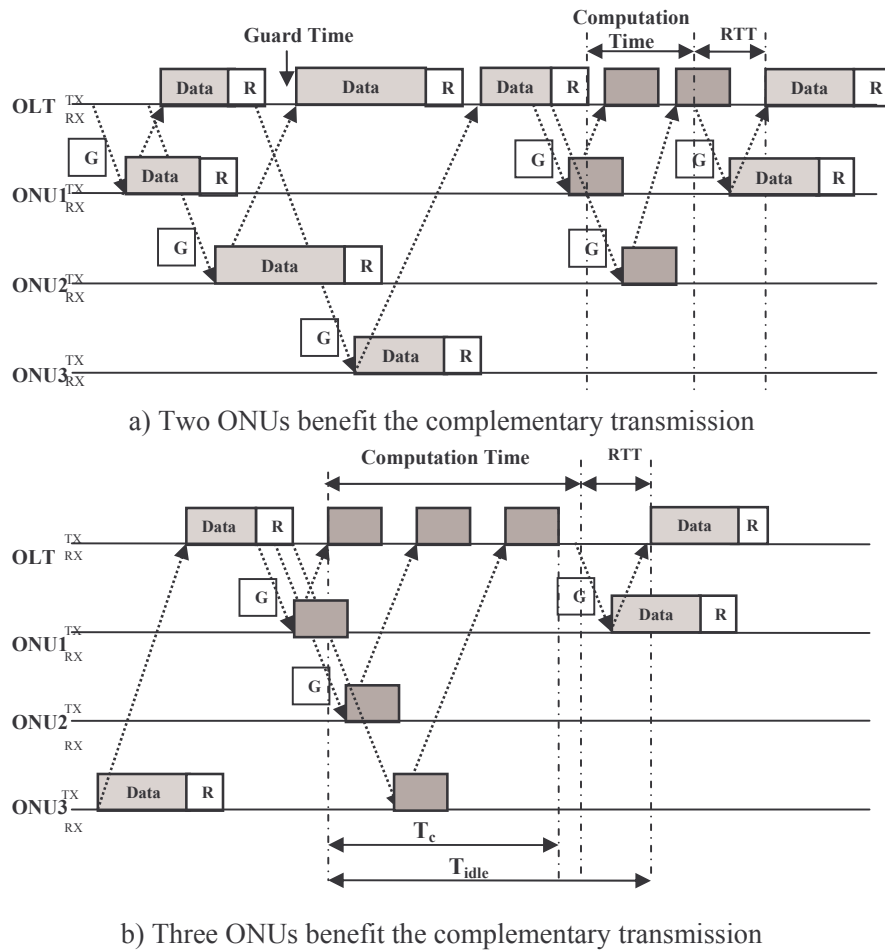


Figure 6-6: Example of eDBA algorithm

vii. For providing services to different traffic classes with different QoS requirements, ONU can request OLT to assign, within a granted window size, bandwidth for each class. This information is conveyed to the OLT, for bandwidth allocation, in the following message REPORT [KMP 02]:

$$R_i = \sum_{i=1}^n c_i \quad (3.8)$$

where R_i is the requested bandwidth and c_i is the requested bandwidth of i^{th} class

of service. Also, (if there is no intra-ONU scheduling) OLT can generate multiple grants, each for a specific traffic class, to be transmitted to ONU using a single GATE message: $B_i^g = \sum_{i=1}^n c_i^g$ (3.9)

where c_i^g is the bandwidth granted to the i^{th} traffic class.

6.1.4 Performance Evaluation

We consider an EPON access network consisting of 16 ONUs connected to one OLT through a passive coupler (Figure 1). To each ONU we assign a downstream propagation delay (from the OLT to the ONU) and an upstream propagation delay (from the ONU to the OLT). We assume that the distance between the coupler and the OLT is about 10 km (about 0.05 ms) while the distances between ONUs and the coupler are about 15 km (about 0.075 ms). For the sake of simplicity, we suppose that the distance between ONUs and the coupler are equal. In our study, we consider two cases:

Case 1 - the rate of the upstream link from an ONU to the OLT is of 1Gbps and the maximum cycle time is set at 2ms (maximum window of 15 Kbytes in the LSA scheme).

Case 2 - the rate of upstream link from an ONU to the OLT is 2.5Gbps and the maximum cycle time is set at 3ms (maximum window of 50 Kbytes in the LSA scheme).

The guard time separating two consecutive transmission windows is set to 5 μ s. The computation time used in DBA is set at 10 μ s in case 1 and 20 μ s in case 2.

We use discrete event network simulation tool (ns 2.1b8) to simulate the network. Each ONU supports four classes of traffic described as follows:

	CoS1 Premium	CoS2 Silver	CoS3 Bronze	CoS4 BE
%CoS	10 %	10 %	30 %	50 %
Packet size (in bytes)	70	70	50, 500 & 1500	50, 500 & 1500
Source and Burstiness	CBR	CBR	PPBP / $\mu=1.4$	PPBP / $\mu=1.4$
Burst Length (Number of Packets)	CBR	CBR	10	20
Local Buffer Size (in Kbytes)	100	250	250	500

Table 6-1: EPON simulation's traffic hypothesis

To generate self-similar traffic of Ethernet LAN, we use the method described in [ZMC 06], where the resulting traffic is an aggregation of multiple sources of Poisson Pareto Burst Process (PPBP) (so called Pareto-distributed ON-OFF). The shape parameter μ is fixed at 1.4. The choice of μ was prompted by measurements on actual Ethernet traffic performed in [RSM 03]. Note that Hurst parameter can be calculated from the shape parameter: $H = (3-\mu)/2$ [ZMC 06]. Then, we have Hurst parameter of the data source equal to 0.8.

In this simulation, we use LSA scheme supporting multi-service and oDBA to compare with our proposed algorithm. By default, we fix the utilisation rate τ equal to 80 %. We may now consider the network performance by analyzing obtained results when three algorithms LSA, oDBA, eDBA are implemented. Figure 6-7 presents the mean access delay of Ethernet frames in the local buffer of an

ONU node. As different services may require different quality levels, it would be useful to investigate the behavior of algorithms towards different network loads.

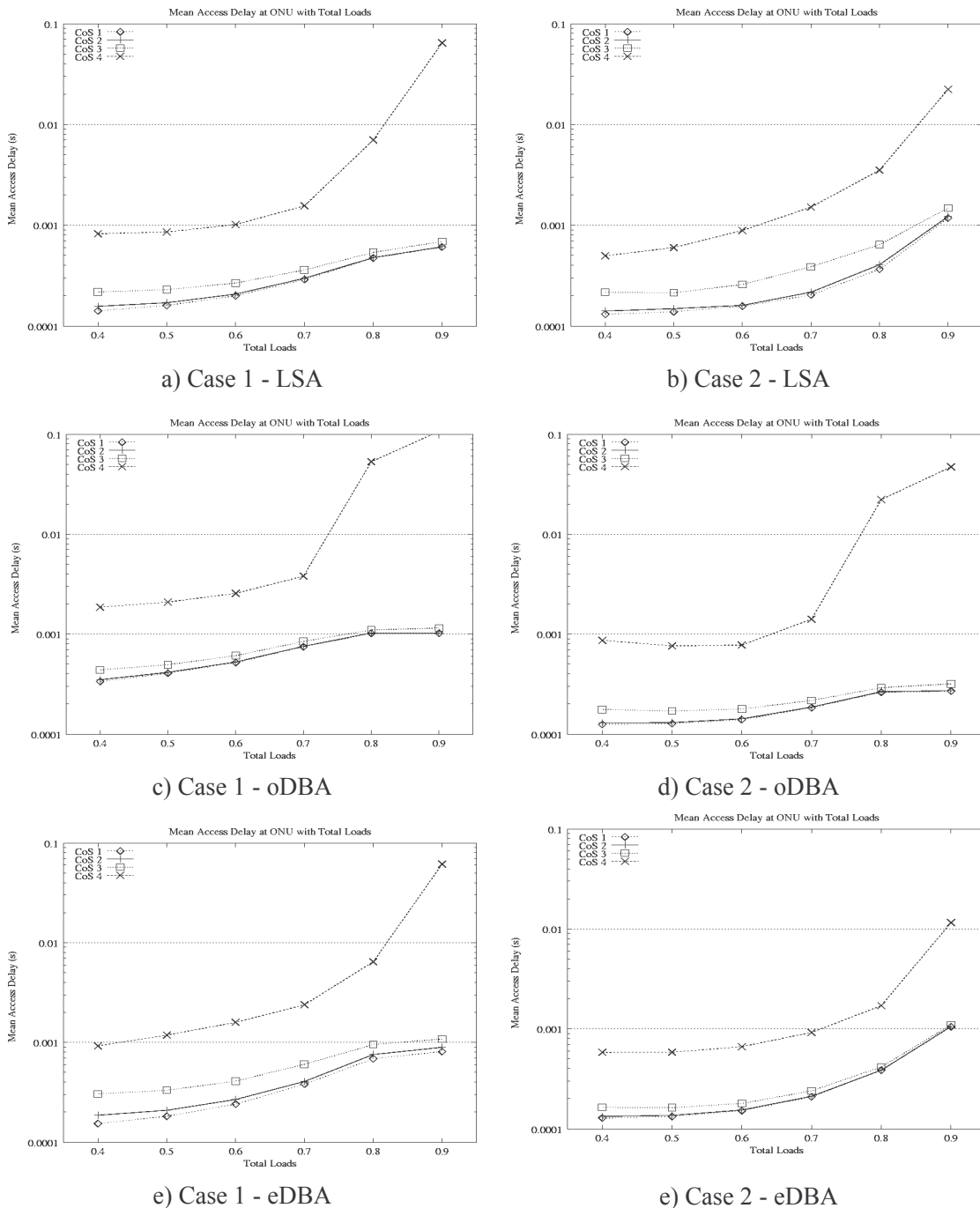


Figure 6-7: Mean access delay at the ONU according to the network load

For this experiment, we first observe that all three algorithms capture the expected behavior of the access delay: the mean access delay increases as the network load value increases. Moreover, the mean access delay also increases rapidly as the priority of CoS decreases, particularly with the 4th CoS. Besides, the mean access delay of eDBA and LSA seems to be small while the delay measured

for oDBA is very high (higher than 0.1s with 4th CoS), notably at heavy loads. This is due to the fact that eDBA and LSA exploit upstream bandwidth better than oDBA where the bandwidth is wasted during the idle time.

Now, we consider the packet loss ratio (PLR) of Ethernet frames in the local buffer at a single ONU for each class. Figure 6-8 presents these values for both study cases. We observe that packet loss occurs only in the local buffer corresponding to Best Effort traffic. The algorithms eDBA and LSA offer similar PLR results (with small values), while oDBA provides the highest PLR. Under a heavy traffic load (90%), oDBA provides a very high PLR (about 11%), followed by LSA (0.6%) and eDBA (0.2%) (Figure 6b). The performance improvement offered by eDBA comes from the increase of the cycle time. A longer cycle time corresponds to a larger complementary transmission window granted to ONUs. Thanks to a larger granted window size, eDBA is able to send more data during a cycle than in the first case. Moreover, eDBA has smaller PLR with regard to LSA (but lightly) because it forecasts the number of client packets which arrive in the next cycle.

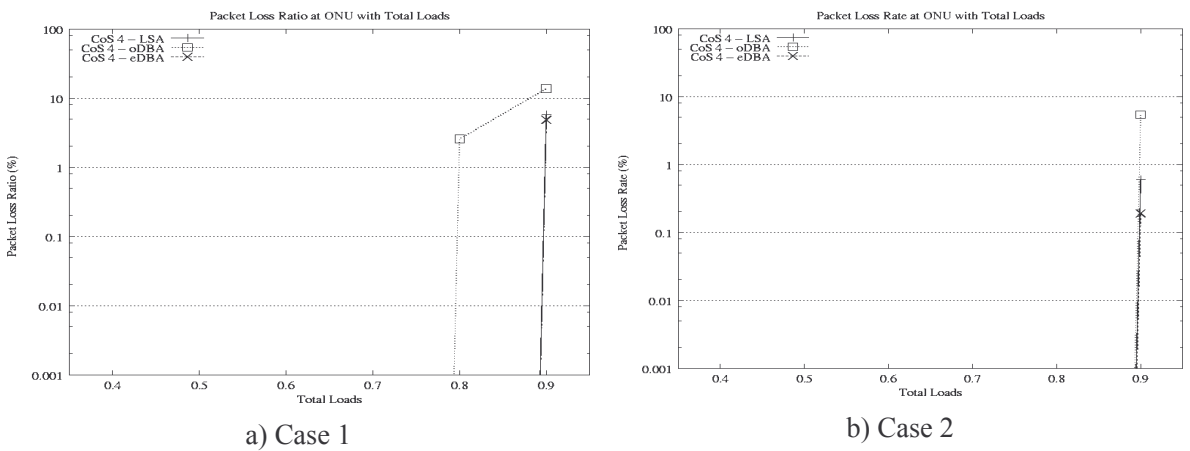


Figure 6-8: PLR at the ONU's local buffer according to the network load

The last result (shown in Figure 6-9) displays the bandwidth utilization rate measured in the passive coupler. The figure shows that eDBA algorithm utilizes more bandwidth than LSA and oDBA as the network load increases. Thanks to the active period, eDBA might send more data than other existing mechanisms. For instances, as the network load sets to 90%, eDBA is able to exploit about 87% bandwidth while LSA and oDBA respectively occupy 84% and 80% bandwidth capacity.

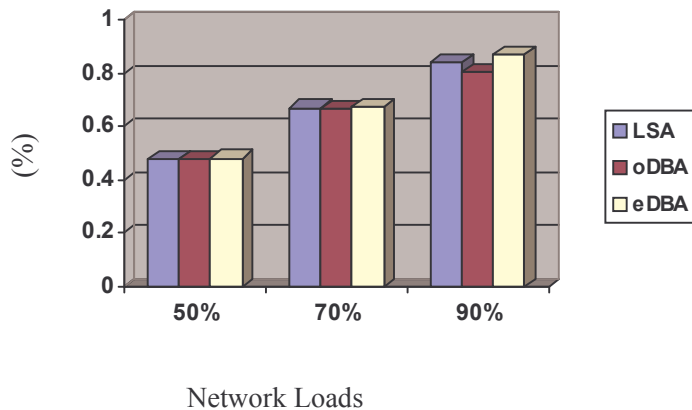


Figure 6-9: Bandwidth utilization rates (%)

6.2 Performance Evaluation of Interconnected Metro Ring Networks

In this sub-section, we evaluate the performance of interconnected metro ring networks. The considered multi-ring architecture consisting of two slotted MAN rings: a synchronous metro access connected with a synchronous metro core. These rings are transparently interconnected through a single access node (so-called Hub node). The major problem in this architecture is how to resolve the synchronization shift between metro rings in order to form core-based optical packets while assuring the traffic routed efficiently through Hub node.

6.2.1 End-to-End Network Architecture

Long haul networks (also called backbone networks) carry huge loads of information between countries, through mountains to keep the signal clear and the loss minimal. Long-haul networks provide connectivity between points of presence (POPs), consist of multiple edge and core routers. Each serves one or multiple MAN. Unlike long-haul networks, which transport point-to-point traffic, metro networks are ring-based in multiples of the wavelength granularity.

Metro rings (core/region networks) interconnect the high-speed backbone networks and the high-speed access networks. The metro rings can be interconnected transparently through single access node (Hub node) or multiple access nodes. Current metro networks are typically SONET/synchronous digital hierarchy (SDH)-over-WDM rings which carry the huge amount of bursty data traffic. The metro core and regional networks are normally both 2-fiber rings. A fiber failure in a metro access ring does not affect the traffic in the core and other access rings. The network thus becomes more reliability.

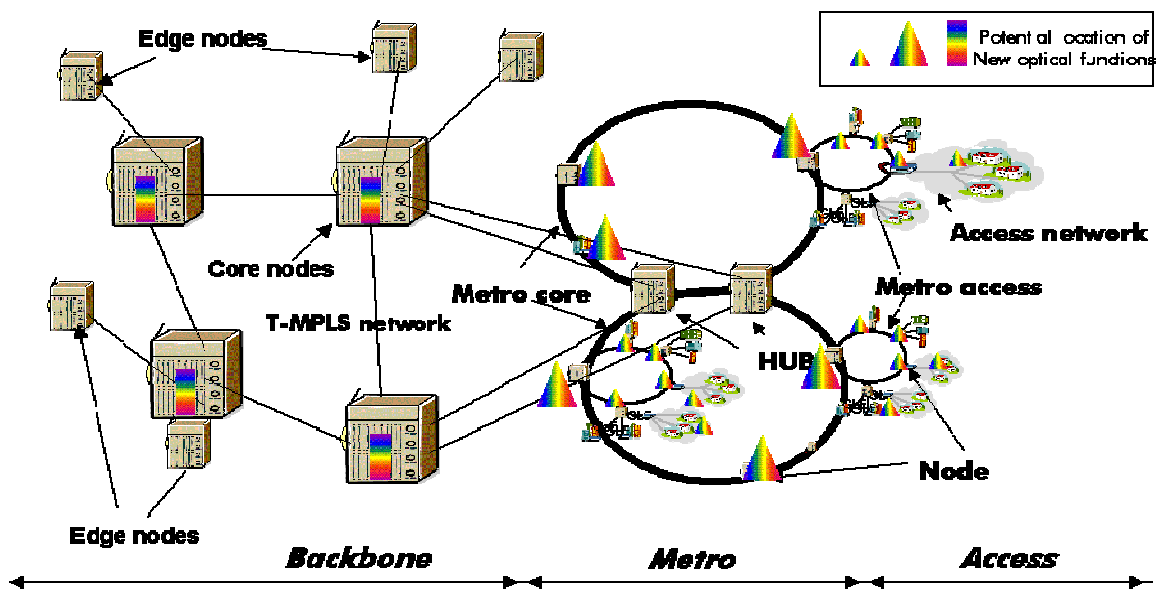


Figure 6-10: Access, Core and Backbone Metro Networks [ECO 08]

The technology evolution for an end-to-end architecture can be: ADSL towards PON in the access network and SONET/SDH/WDM towards all-optical packet switching/DWDM in the metro network.

Besides, upstream traffic flux from OLTs to the metro access is statistically multiplexed through a DSCU (Distant Subscriber Connection Unit). A DSCU can be connected with several OLTs while an access node of the metro access can be connected with several DSCUs. As a result, a metro access (about 10 ring nodes) can support some thousands of PONs. An example of an end-to-end network is shown as in Figure 6-11.

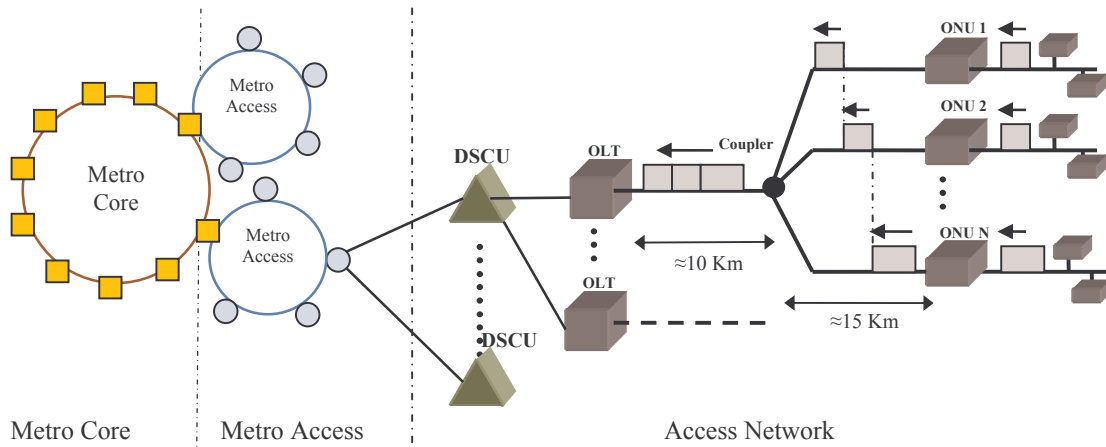


Figure 6-11: End-to-End Metro Network Architecture

In this example, we consider 2 million subscribers. They are connected to the metro core (primary ring with 10 core stations) through access networks and metro networks. Each core station is connected with a secondary ring composing of 4 access stations (access nodes). So we have a total of 40 stations which are accessible. Each access station connects with 25 DSCUs which manages approximately 2000 subscribers across 60 PONs. We suppose that the amount of traffic from each network PON is approximately equal to 32Mbits/s, which requires a metro access with a capacity exceeding 200Gbit/s (40 wavelengths of 10Gbit/s responsible for 50%). Note that optical frames are transmitted from ONUs to OLT and from OLTs to DSCU under point-to-point connections.

6.2.2 Multi-Ring Network Simulation

We may now describe the proposed simulation. For the sake of simplify, we use 2 metro rings in which one ring-based metro access connected to one ring-based metro core through a Hub node as shown in xxx. Regarding the upstream path of the metro access, all access nodes send its local traffic to a destination node residing on the metro core network. The traffic is firstly transported to Hub node before being routed to the core metro network. Inside the Hub, since electronic packets coming from different sources have the same destination (the destination node is the node which stands behind Hub node in the metro core), they may be aggregated into a core-based optical packet in order to be transmitted in the core network.

From assumptions, the traffic matrix in the core network consists of two following traffic:

- A symmetric traffic matrix: node i send its local traffic to node $(i+2)$ (Hub node is not taken into account).
- ‘Single’ traffic: from Hub node (the traffic is emitted from access nodes) to the destination node.

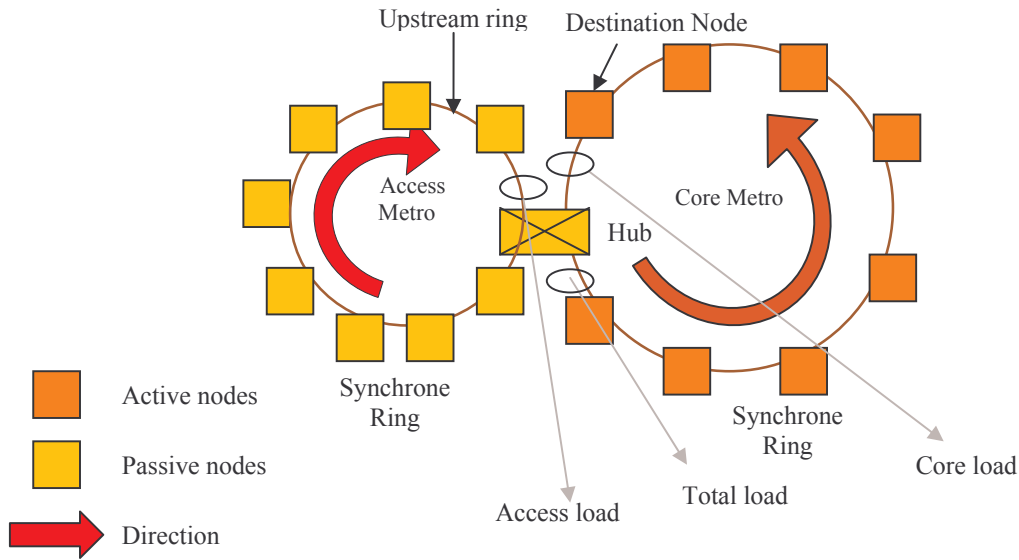


Figure 6-12: Multi-Ring Network Simulation

The travel of electronic packets is described as follows. From an access node residing in the metro access, electronic packets are firstly encapsulated into optical packets and then transported to the Hub. Depending on the access control mechanism used in Hub node, the optical packets may be directly put on optical buffers (to be ready for being routed to the core network) or be separated again into electronic packets which will be then contained in electronic buffers. The second one leads to the situation that incoming electronic packets (from different access nodes) may be together combined (*mutual combination*) or be combined with local electronic packets (*local combination*) of Hub node (Hub node can be a point of presence) or both (*total combination*) in order to create a new optical packet with high filling ratio. This behaviour is very similar to GPFO mechanism [ENA 08] (which is developed in order to increase the filling ratio of the optical packets by entering electronic packets in intermediary nodes), so-called *GPFO behaviour*. In order to limit the complexity of the simulation, we consider only *GPFO behaviour* supported by *mutual combination* while resuming that Hub node does not function as a POP.

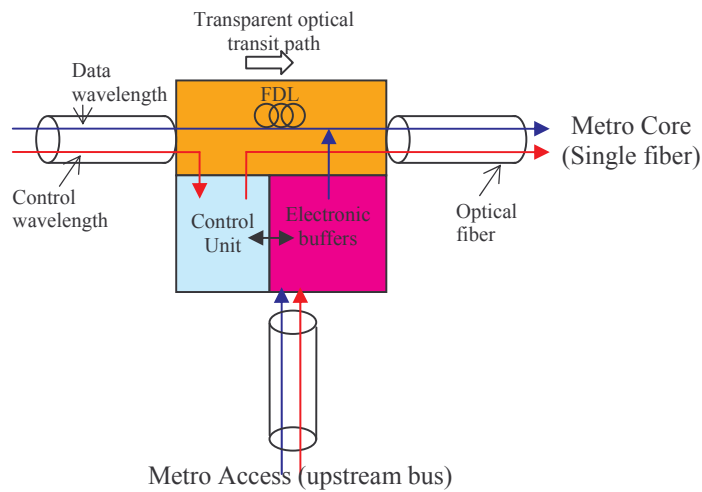


Figure 6-13: Hub node's traffic

There are two key challenges to simulate a Hub node. The first one is the synchronization between interconnected rings. Transmitting transparently optical packets through Hub node needs to consider this synchronization shift (called Δt). The other challenge to simulate Hub node is the optical packet size supported by different rings. This is referred as “granularity” problem. In the second one, optical packets must be disassembled and re-aggregated but in different sizes before being switched.

For simplicity, we suppose that two simulated rings support the same optical packet size. In general, a control packet will be dropped when corresponding data packets are received in Hub node. Inside Hub node, an optical control packet needs to be created and when a new optical data packet is created. Obviously, these created packets must accord characteristics of the core network. The insertion of data packets must satisfy the discipline of the traffic priority at Hub node (Figure 6-13): the traffic in the core network has the priority higher than that in Hub node.

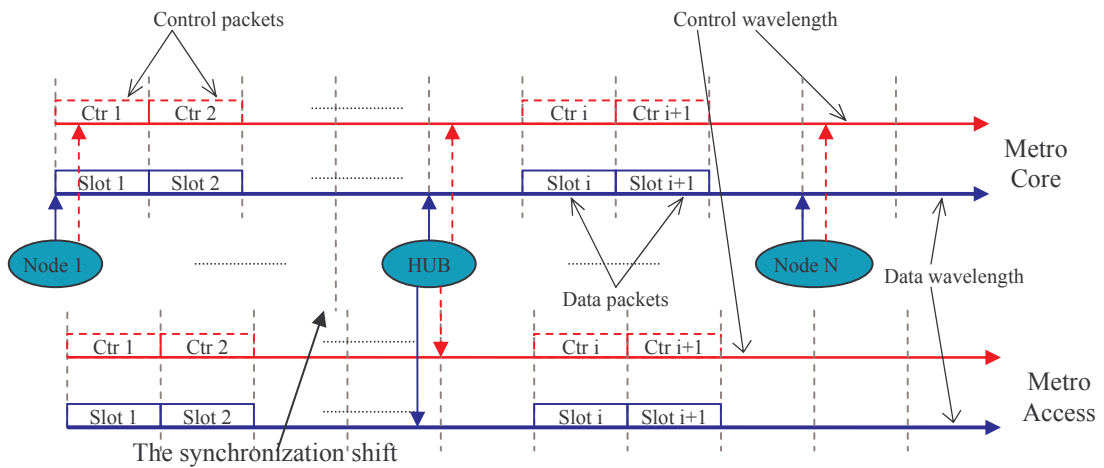


Figure 6-14: The synchronization shift between metro rings

6.2.3 Access Mechanisms

In this sub-section, we describe two proposed mechanisms that will be implemented in Hub node. As mentioned, Hub node must interconnect two or more metropolitan rings. Therefore, the amount of traffic, which passes through Hub node for both directions: upstream and downstream paths, is normally very high. In order to be able to switch such high amount of traffic, Hub node should implement advanced mechanisms that take into account the optical packet creation process, the conversion O/E/O and the synchronization shift. Note that we should not apply directly existing mechanisms such as QoS-Upgrade, DCUM... because of their complexity which may lead to the situation where Hub node is loaded. For this reason, we propose two mechanisms: Opportunist and Common Timer.

Opportunist Mechanism (OM)

The creation of the optical fixed-size packet is only triggered when Hub node detects a free slot in the core network. Hub node firstly creates an optical packet from electronic packets of different CoS and then transmits the optical packet on the detected free. The creation of optical packets is similar to the CUM's process: high-priority electronic packets are firstly taken; otherwise low-priority electronic packets are taken.

COmmon Timer Mechanism (COTM)

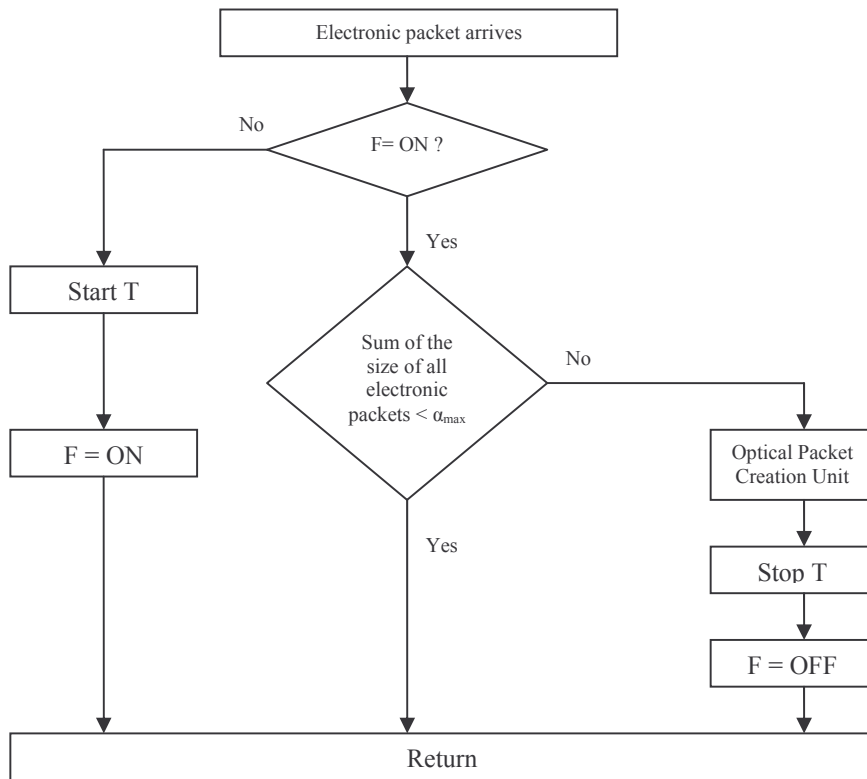


Figure 6-15: First procedure of COTM

In well-known timer-based mechanisms (CUM, Simple Aggregation), several timers are used. Each timer is attached to an aggregation buffer. Therefore, the number of timers increases as the number of optical CoS increases. This may cause the processing problem and they are not suitable methods which should be implemented inside Hub node. The main idea of COTM (COmmon Timer Mechanism) aims at minimizing the number of used timers. A good solution is to use only one timer for all CoS. In this context, all aggregation buffers are attached by a common timer. The details of this mechanism are shown like two following procedures: Figure 6-15 and Figure 6-16.

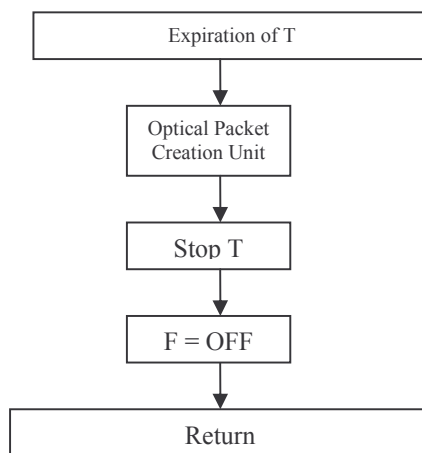


Figure 6-16: Last procedure of COTM

Each time when the first electronic packet of any CoS arrives to any aggregation buffers, the mechanism is activated: It firstly examines the flag F (to the state ON if the flag is OFF) to verify the timer. In the case where the flag is already turned on, the procedure must check the sum of the size of all electronic packets in all aggregation buffers before enabling the Optical Packet Creation. If this sum is superior to α_{max} , the Optical Packet Creation hence will be triggered. On the other hand, the Optical Packet Creation is automatically triggered when the timer expires. At this moment, the Flag will be re-turned to OFF.

The creation of optical packets is similar to Opportunist Mechanism: high-priority electronic packets are firstly taken; otherwise low-priority electronic packets are taken.

6.2.4 Simulation Parameters

Generally, many performance requirements must be met in order to transport specified data from the access network to the core network. Based on parameter requirements for the metropolitan Ethernet network defined in MEF, we use parameters in this scenario as follows: end-to-end Packet Loss Ratio (EPLR), end-to-end Accumulated Packet Delay (EAPD) and Electronic Packet Jitter (EPJ). EPJ is one of the most important parameters for real-time data transfer.

	Metro Access	Core Metro	
Capacity	10Gbps	40Gbps	
TimeSlot	10 μ s	5 μ s	
Packet Size	12500 B	25000B	
Fixed-Size Packet Creation	Aggregation	DCUM	
Access Load	60%@10Gbps (6Gbps) cors. 15%@40Gbps(6Gbps)		
Core Load		70%@40Gbps (28Gbps)	
Total Load			85%@40Gbps (34Gbps)

Table 6-2: Multi-Rings Simulation Parameters

In reality, the capacity of the core metro network is higher than the access network. So, we set the capacity of the access network to 10Gbps as compared with 40Gbps of the core metro network. We suppose that the access network supports the optical fixed-size packet of 12500 bytes corresponding to the duration of 10 μ s @10Gbps. Since the capacity of the core metro network is very high, so we keep a small duration of the timeslot: 5 μ s, which corresponds to 25 KBytes @40Gbps

The multi-class approach is used for both network types. As the previous chapter, we assume 8 CoS for client packets in the electronic domain. The premium traffic is generated from CBR sources with the packet size of 810 bytes. The non-premium traffic is modelled by an aggregation of IPP sources with different burstiness levels. Generated packets are of variable lengths according to the Internet packet length statistic (see chapter 5) for each non premium CoS (ID from 3 to 8). The optical buffer size is equal to 200 Kbytes for the premium traffic class, 500 Kbytes for silver and bronze traffic classes, 1000 Kbytes for the BE traffic class. Note that PEM and ERM are disabled in this work.

We simulate the network with different configurations as shown in Table 6-2. Other simulation parameters are kept identical as in the preceding chapter. We suppose that Hub node does not function as a POP in this scenario, so the GPFO-behaviour is deactivated. Simple Aggregation/DCUM mechanisms are implemented in the metro access/core networks.

6.2.5 Numerical Results

Now, we may focus on Hub node. We investigate OM and COTM as Δt is fixed to $1\mu s$. In order to have significant results, we load the metro access network up to 60%@10Gbps (about 6Gbps). As shown in Figure 6-12, the core load is set up to 70% (corresponding to 28 Gbps), so the total load can be up to 34 Gbps (corresponding to about 85% of core network capacity). We see that there is no packet loss not only at source nodes but also in Hub node. For this reason, only the waiting time is presented. Figure 6-17 presents the waiting time of electronic packets at Hub node as a function of different source nodes in the metro access. The figure shows results obtained with both OM and OCTM. As mentioned above, source nodes enable the process for the fixed-size packet creation with the aggregation mechanism; so optical packets coming to Hub node encapsulate many electronic packets of different CoS. We observe that electronic packets of different sources have nearly the same waiting time. This is due to the fact that Hub node treats electronic packets according to CoS and not to the source node. In other words, these mechanisms offer good performance in terms of waiting time ($< 0.1ms$ even with CoS8) and packet loss rate.

We also observe that COTM show high access delays as compared with OM in Hub node. This phenomenon is explained as follows. With OM, Hub node immediately sends optical packets if it finds a free slot in the core network. By contrast, COTM uses a timer to fill optical packets well and thus increases the waiting time of electronic packets.

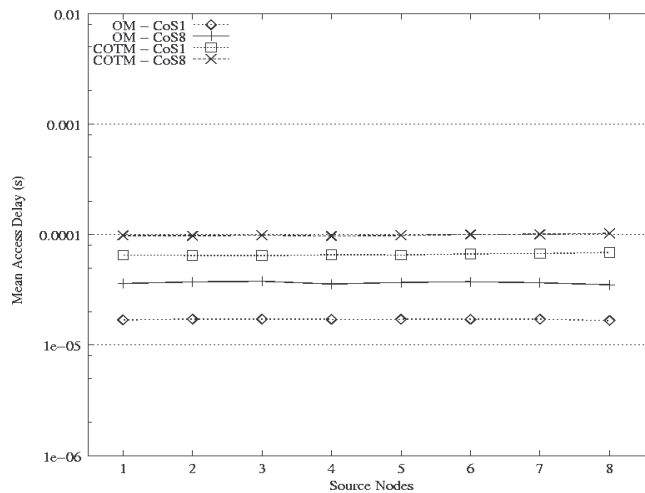


Figure 6-17: Waiting time of electronic packets elapsed in Hub node

Let's look at the average filling ratio of optical packets in Hub node. Interestingly, the filling ratio of Premium packets is higher than that of BE class for both mechanisms. Similar to the CUM described in previous chapter, OM and COTM treat electronic packets of different CoS according to the priority discipline: high priority first. Since no timers is used in OM (or only one timer is used in COTM), BE packets are normally created when all high-priority electronic packets are taken for high-priority optical packets. In this moment, there are no much electronic packets in Hub node (even low-priority electronic packets) and this causes the small filling ratio for BE packets.

We observe also that the filling ratio obtained by COTM is higher than OM, particularly with Premium class. A common timer used in COTM may retard electronic packets while maximizing the filling ratio. With small additional amount of the optical header, COTM offers effective rate smaller than OM. For instance, about 2,3 Gb of additional amount are obtained with COTM as compared to 3,9 Gb (38,06 – 34,25 Gbps) with OM. It is worth to mention that if the total load reaches 90%@40Gbps (about 36 Gbps of utile rate), the effective rate may exceed the core network capacity (100% filled). As a result, a very high packet loss may be observed with OM.

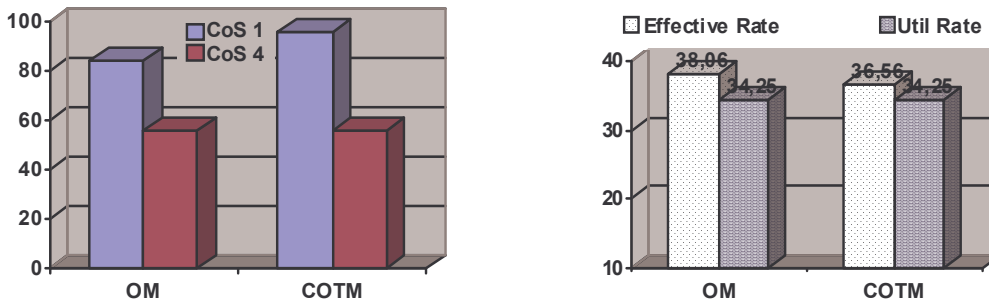


Figure 6-18: Filling ratio and Util/Effective Rates obtained with OM and COTM

Figure 6-19a plots the accumulated end-to-end delay observed at the destination node in function of access nodes. We observe that low priority classes provide slightly higher delay as compared to high priority classes. However, the delay of electronic packets having the same CoS from different source nodes is nearly the same. Note that the access delay obtained in the last node (node 8) is always higher than the access delay obtained in the first node (node 1) due to ‘priority problem’ [NGA 05]. Since this value is very small as compared to several FDL lengths, so it can not affect to the total end-to-end delay that an electronic packet needs to travel from the source node to the destination node.

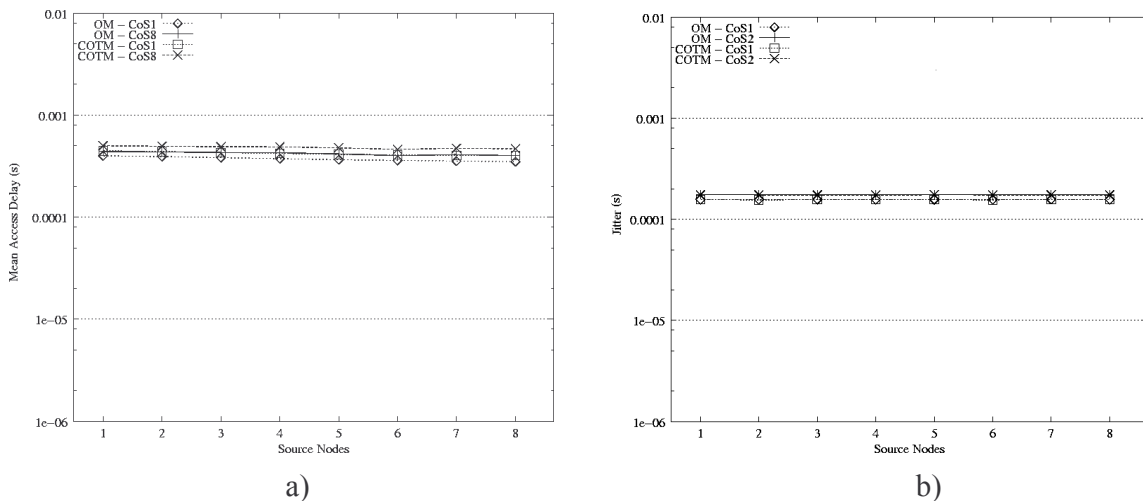


Figure 6-19 - Average accumulated delays and standard of electronic packet jitter at each node for different cases with the access load of 15%

Regarding the electronic packet jitter shown in Figure 6-19b, we see that both mechanisms provide nearly identical average electronic packet jitter for all source nodes. Additionally, the electronic packet jitter obtained with different CoS seems to be the same. This is due to the fact that electronic packets, which are encapsulated in an optical packet, will be received in the same time when the optical packet finishes its travel at the destination node. In general, there are about from ten to

hundred electronic packets encapsulated inside an optical container; this leads to low inter-arrival time measured at the destination node. Obtained packet jitters are smaller than values specified by MEF. This could be considered as satisfaction in terms of QoS, even for strictly delay-sensitive voice traffic.

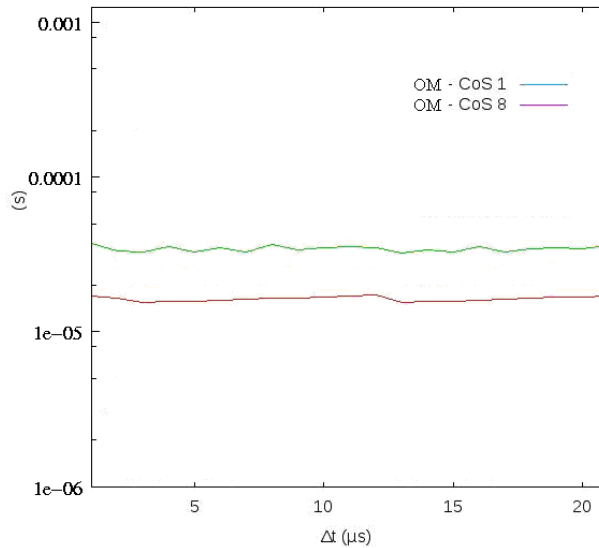


Figure 6-20: Waiting time of electronic packets in Hub node in function of Δt

Figure 6-20 shows the impact of the synchronisation shift over the performance of Hub node. Note that in this case, we use the timer size equal to $100\mu s$ for sources nodes (the aggregation mechanism is not used). The figure presents the average time of electronic packets passing across Hub node in function of Δt . Only electronic packets, which come from a source node, are viewed. As an interesting result, the obtained waiting time is nearly the same. It seems that the waiting time does not depend on the Δt . In other words, the synchronisation shift has not much impact over the waiting time of electronic packets passing across Hub node. An explanation for this phenomenon is described as follows. Small Δt does not affect the electronic packets. However, as the Δt becomes larger, the waiting time increases at the beginning of the simulation but it decreases due to the stability of the simulation. Therefore, the average waiting time of all electronic packets is not changed much.

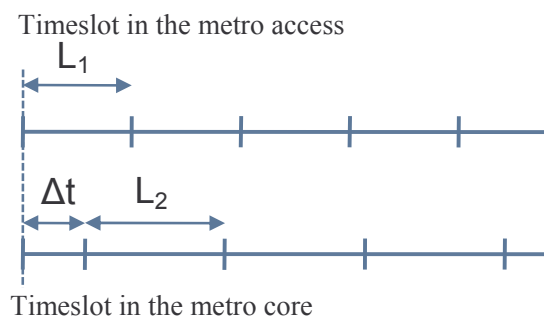


Figure 6-21: An example of Synchronization shift

6.3 Concluding Remarks and Future Works

We have proposed an enhanced algorithm for dynamic bandwidth allocation in the downstream path of EPON. We have addressed the problem of bandwidth utilization rate by improving the data transmission during the idle time between two transmission cycles. This idle time is due to the non-

active computation period used in some existing bandwidth allocation algorithms such as DBA. Also, we have used network simulator to validate the performance of the proposed algorithm with several classes of traffic and under different network load conditions. We have shown that our algorithm, under considered network traffic parameters, provides better performance than other existing dynamic bandwidth allocation algorithms (namely LSA of IPAC and DBA). This performance improvement is measured in terms of mean access delay and packet loss rate as well as the bandwidth utilization rate of the access network. In our future research, we will evaluate the network performance in the case of a synchronous EPON-based multi-service network, in which all ONUs and OLT are synchronized. In this network, the guard time is not necessary between data transmissions from different ONUs.

We have evaluated the performance of interconnected multi-ring networks. The network consists of two metro rings in which a synchronous metro access (i.e. DBORN) connected to a synchronous metro core (i.e. POADM). The capacity of the metro core is larger than the metro access. By implementing proposed mechanisms, we have seen that the performance of Hub node is guaranteed (in terms of access delay and packet loss) regardless of the synchronization shift. Additionally, the end-to-end performance does not depend on the source nodes. In the future, we will take into account the “granularity” problem in which each network supports different sizes of the optical packet.

In order to simulate an end-to-end network (access network/ metro access/ metro core), we need to know the traffic coming from passive coupler to OLT. Because there are many EPON networks connected to the metro network, we cannot hence simulate directly all of them in order to obtain a quite simulation. Indeed, given a high number of EPONs (i.e. 60), with the volume of traffic and different mechanisms to implement, we are rapidly reaching a complexity level that is difficult and impossible to integrate directly into the network simulation. So, one of open questions is how to generate these traffic from a well-known source without implementing a quite EPON network. We proceed to one of following alternatives:

- Generate trace files of coming traffic at the entrance of OLT by running simulations of an EPON network (in which ONUs are interacted with OLT).
- The generated traffic pattern will be ‘considered’ with a well-known traffic model.
- From the well-known traffic model, we may get a similar traffic without simulating a quite EPON network.

The study over generated traffic characterization is very important in the future work. This may help us to find a traffic source which is the most similar to the generated traffic at OLT. Classical sources such as CBR (Constant Bit Rate) or Poisson [SMR 83] and their superposition are candidate traffic for comparing. However, in many real-world cases, it has been found that for some environments, the traffic pattern is rather self-similar than Poisson [PSW 94].

6.4 Appendix

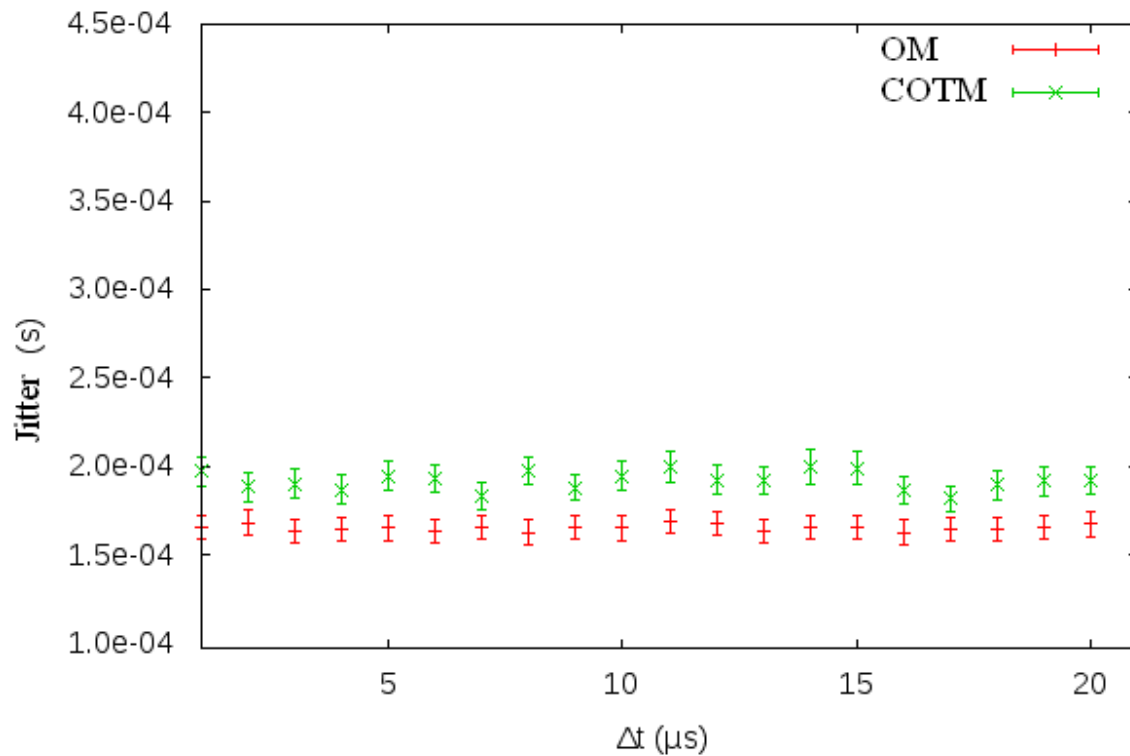


Figure 6-22: Average Jitter and Confidence Interval of 95% with 10s simulation

Chapter 7

General conclusion

7.1 General Concluding Remarks

Optical technologies are growing at an unprecedented rate to accommodate the explosion in data traffic. New devices (e.g. routers, storage devices) more reliable at higher speeds are appeared in order to adapt to more bandwidth requirements. Wavelength division multiplexing (WDM) is an emerging technology to meet increasing demands for bandwidth capacity, which is accelerated by the proliferation of mobile and fixed network-attached devices, such as smartphones, e-readers, PCs... Sometimes the term dense wavelength division multiplexing (DWDM) is used to distinguish the technology from the broadband WDM systems. The cost reduction of WDM devices and the constant increase of the data traffic have motivated network operators to invest in the deployment of the optical metro network.

Due to widespread services and tremendous user population on Internet, the traffic of IP packets has dominated data networks. By sharing transmission channel among IP packets, optical packet-switching (OPS), which support bursty data traffic better than optical circuit switching (OCS), are beginning to be deployed in metro networks. Combining with WDM technology, IP packets are now transferred, switched, and manipulated through complex protocol stacks such as IP/ATM/SONET/WDM, IP/HDLC/SONET/WDM, and so on.

This dissertation started with a global view of the optical network and its advantages as compared with the copper-based network. The second chapter describes fundamentals of fiber, high-speed equipments and major transmission techniques for the optical network. The limit of conventional circuit switching technology (i.e. SONET/SDH) for supporting new traffic pattern have particularly pointed out. To overcome inflexible and non-scalable properties of the circuit switching technology, OPS - which offers significant benefits in terms of both network efficiency and control scalability - now is becoming the base of the MAN infrastructure.

In the scope of the dissertation, we have provided an analytical solution to evaluate the performance of a synchronous bus-based metropolitan network. Our analytical model based on Embedded Discrete Time Markov Chains (EDTMCs). The whole network has modeled as a multiple priority M/G/1 queuing system with Non-Preemptive-Repeat-Identical service discipline. To estimate the queue length distribution and the mean waiting time, we model the steady-state queue-length in each node by an EDTMC thanks to the probability that the access node “sees” the free slot in the transit line. To solve the model, we have used a recurrent level-by-level (node-by-node) analysis technique. We obtained the stationary probabilities for the steady-state of the local buffer and proposed a formula to

approximately calculate the mean waiting time of client packets at each access node. Obtained results represent the correlation between the local transmission at the downstream node and the transit traffic flowing from upstream nodes. Results have shown that our models (both mono-service and multi-service) are very close to the simulation model under low or medium loads. Additionally, the measured mean waiting time depends not only on the timeslot duration but also on the network load and its position on the bus. Particularly, the difference of obtained results between analytical and simulation models is small with first nodes but it becomes very high at last nodes. The main reason explaining this phenomenon comes from the distribution of the free slot in the transit line. For the Markov chain solution, we used the “constant” free probability which corresponds to the uniform distribution of the free slot but in reality, the distribution of the free slot “viewed” by a bus node is not uniform.

For the synchronous network architecture, when the fixed-size packet format is enabled, a fixed-size packet creation must be implemented inside the access node in order to accommodate electronic packets of variable-size into a large optical packet. Well-known mechanisms, which efficiently fill optical packets while limiting the access delay experienced by electronic packets, include the simple aggregation and the timer-based mechanisms. In our work, we have investigated the impact of the timer duration on the network performance and provided the comparison between these mechanisms in a ring-based MAN: metro access and metro core networks. Our main objective was to identify and address some problems that characterize different architectural choices such as the network topology, the provision of connectivity (connection-oriented Vs datagram architectures), the transmission mode (synchronous Vs asynchronous) and the optical packet format (fixed-size Vs variable-size). We have shown that the simple aggregation always offers good performance regardless of the network topology, notably under the medium and high workloads. Through various simulations, we found that the reasonable timeslot duration, which should be chosen, is about $10\mu\text{s}$ in order to having stable network performance.

The bandwidth fragmentation and the unfairness property are the main problems in the asynchronous bus-based network using OU-CSMA/CA protocol where the bandwidth is wastefully used by access nodes. To overcome these problems, we have proposed a novel concept called “Virtual SynChronization” (VSC) which significantly improves the bandwidth utilization rate. The new scheme is based on the optical fixed-size packet creation. However, the use of synchronizing packets in VSC reduces the amount of accessible bandwidth for transmission.

Supporting multiple classes of service in order to serve different types of applications (voice, video, data, best effort, etc.) is a major challenge in the optical MAN. This QoS-based differentiation requires advanced mechanisms such as priority-based service schemes, preemptive access, class-based resource reservation, load balancing, failsoft operation schemes, admission control, packet scheduling. A problem that rises-up in QoS-enabled ring architectures with transparent transit mode is the lack of flexibility in the scheduling between the local traffic waiting for transmission and the transit traffic that bypasses the considered ring node. Therefore, the transmission of high priority traffic, at a given node, may be blocked by lower-priority traffic sent by other ring nodes. PEM (Packet Erasing Mechanism) and ERM (Extraction/Reemission Mechanism) are the answer to this problem. These mechanisms use preemptive methods in order to prevent such blocking situation from happening. By erasing BE optical packets (PEM) or delaying BE optical packets (ERM) in the transit line, the mechanisms may facilitate high-priority optical packets, which are waiting in optical buffers, to be more rapidly transmitted. Contrary to promising results obtained by ERM, PEM may cause serious degradation of the BE traffic performance. However, when the network is heavily loaded (more than 90%), PEM is still useful in order to guarantee Premium CoS.

An important point that we studied is the comparison of two architectural approaches: VL-OPF model versus FL-OPF model. FL-OPF model simplifies the control processing since a node has only one control wavelength. And it also offers good and fair QoS for all CoS at all ring nodes even under a very high network load (thanks to ERM or PEM). However this model requires a complex optical packet creation process at the access interface and an optimum choice of the timer value. By contrast,

VL-OPF model does not need such process but it requires more complex control processing since a node has to analyze optical headers on every wavelength. VL-OPF model provides good QoS for high priority CoS under low and medium offered loads but it cannot ensure fairness among ring nodes at high offered load.

Regarding levels of the differentiation of service, two QoS mapping approaches are considered when forming the fixed-size optical packet: mono-class and multi-class. Mono-class approach is neutral. No service differentiation is associated with packets transported on the optical ring. Unlike the mono-class, multi-class approach allows to control and manage packets according to their CoS. This control allows installing advanced mechanisms to manage traffic of different CoS. Simulation works were carried out for the validation of both proposed approaches. Obtained results have shown that the mono-class approach provides better improvement of the network performance with comparison to the multi-class approach. However, the multi-class approach, combined with ERM, should be used in order to guarantee high-priority traffic when the network is heavily loaded.

A novel mechanism (called Dynamic CoS-Upgrade Mechanism - DCUM), which targets to the creation of the optical container, was proposed and was carefully investigated. The idea of this mechanism is based on the dynamic timer duration which does not depend on the arrival rate of electronic packets. At the beginning of the mechanism, the duration of timers is not fixed. It increases dynamically according to the state of local transmission buffers and the transit traffic on the optical ring. We shown that under various arrival rates of electronic packets (high, medium and low rates), the proposed mechanism always offers stable performance results as compared with other mechanisms (Simple Aggregation, CUM, CTM).

Based on a well-known dynamic bandwidth mechanism DBA [AYD 03], we have proposed an enhanced algorithm -eDBA- for fair bandwidth allocation in the downstream path of EPON. The proposed algorithm allows the node to transmit complementary data during the idle time which is normally non-active period. An access network is then simulated to validate the performance of the proposed algorithm with several classes of traffic and under different network load conditions. We have seen that under some proposed traffic parameters, the algorithm provides better performance (in terms of mean access delay and packet loss rate) than other existing dynamic bandwidth allocation algorithms (e.g. IPACT [KMP 02] and DBA). Results also show the improvement of the bandwidth utilization rate in the EPON's downstream path.

Metropolitan ring networks are usually used to connect the high speed backbone networks with the high speed access networks. In the last chapter, we have focused on the end-to-end performance of a multi-ring architecture in which a metropolitan access network is interconnected with a metropolitan core network. These rings are synchronized and can be interconnected transparently through single access nodes (Hub node). Multi-ring architecture with a pair of Aggregation/DCUM implemented in each network is simulated. The major problem in this architecture is how to resolve the synchronization shift between rings while assuring the traffic routed efficiently from the metro access to the metro core network. To ensure this efficiency, we propose two optical packet filling mechanisms in Hub node: CoMmon Timer Mechanism (CoTM) and OpporTunist Mechanism (OM). Through various simulations, we presented some performance results in terms of jitter and average end-to-end delay which show that both OM and CoTM offer good performance in Hub node, even the core network is loaded until 85% of the network capacity.

7.2 Perspectives for future works

The analytical model proposed in this dissertation has provided an approximately analysis of the performance of a slotted bus-based network. The difference between two models becomes larger at the lowest node priority due to the variation of the free slot distribution in the transit line. To simplify

the complexity of the model, we have used the uniform distribution of the free slot. This consideration is not absolutely correct and the free probability needs to be more ‘instantly’ estimated. To do this, variables representing the variation of the free probability should be added to the EDTMCs, from first nodes to the last nodes.

We have analyzed the performance of a bus-based network. As well, our solution can be used for the performance analysis of a metro core network. In proposed analytical model, we have also assumed that arriving packets come from Poisson sources with fixed-size while each node has an unlimited buffer size. A possible extension of the model will accommodate different packet arrival patterns with finite buffer sizes. The future work may also include an analytical study which considers different packet assembly mechanisms such as the simple aggregation mechanism.

The future work of VSC must answer a question: VSC works well with other topologies (e.g. mesh, tree...). Originally, VSC algorithm was developed for OPS-based ring network, where ring nodes use burst mode transceivers for transmission and reception, thus its principle can be used in the mesh network whose nodes employing burst mode transceivers as well. However, the problem is how to configure VSC while avoiding packet-switched collisions in such network. In this context, empty packets can be used not only for purpose of signaling but also for the bandwidth reservation.

As for DCUM, our future research will concern with the development of a filling container mechanism with ‘real’ adaptive timer (advanced-DCUM) in which a ring node can exchange information with other nodes. Advanced-DCUM implemented in an access node may consider not only its local state but also the state of other nodes. So the duration of the timer which is associated to each optical CoS may be dynamically changed according to the current load offered to the network and the ready-state queue of its adjacent nodes. This mechanism may solve the decisive problem of choosing adequate values for the timer. It may optimize considerably the global performance of the network while providing more efficient bandwidth utilization.

In chapter 5, we have specifically compared the impact of Mono-class and Multi-class on the network performance with FL-OPF, for both metro access and metro core scenarios. Although each one provides good performance from different aspects of the network, an interesting question is still pending: is it necessary to compare the impact of Mono-class and Multi-class on the network performance in the case where the traffic distribution is not uniform between ring nodes? Particularly, could a combination of Mono and Multi approaches be used in a ring network? And is this work able to increase the network performance or improve the protection of priority traffic?

Future works of the resource allocation in EPON will concern with the synchronous transmission mode and will take into account different distances from ONUs to OLT. A new version of enhanced DBA to take advantages of spectrum resource allocation will also be investigated. As for a complete simulation of the end-to-end metro network, we plan to generate file traces from different simulations of a PON and the superposition of these traces will be subsequently used as input data in the simulation. This work may take into account the “granularity” property. And the ‘end-to-end’ performance will be evaluated with the case in which an asynchronous ring (i.e DBORN) connected to a synchronous ring.

Bibliography

- [ACC 06] P. Chanclou and S. Gosselin, J.F. Palacios and V.L.Alvarez, “Overview of the Optical Broadband Access Evolution: A Joint Article by Operators in the IST Network of excellence e-Photon/ONe”, IEEE Communications Magazine, August 2006
- [AFQ 89] A. Demers, S. Keshav, and S. Shenker, “Analysis and simulation of a fair queuing algorithm,” Proceedings of ACM SIGCOMM’89, pp. 1-12, 1989.
- [AGG 05] M. Chaitou, G. Hebuterne, H. Castel, “On aggregation in almost all optical networks”, Wireless and Optical Communications Networks, 2005. WOCN 2005. Second IFIP International Conference on 6-8 March 2005 Page(s):210 – 216, Digital Object Identifier 10.1109/WOCN.2005.1436021
- [AYD 03] Chadi M. Assi, Yinghua Ye, Sudhir Dixit, and Mohamed A.Ali, "Dynamic Bandwidth Allocation for Quality-of-Service Over Ethernet PONs", IEEE Journal on Selected Areas in Communications, Vol. 21, No. 9, Nov. 2003, pp. 1467-1476.
- [BBH 00] B. Baynat, “Théorie de files d’attends”, HERMES Science Europe, 2000.
- [BDC 04] N. Bouabdallah, E. Dotaro, L. Ciavaglia, et al., Resolving the fairness issue in bus-based optical access networks, IEEE Communications Magazine, Volume 42, Issue 11, Page(s):S12 - S18, Nov. 2004.
- [BMS 06] Thaere Eido, Daniel Popa, Tülin Atmaca, “Burst Mode Study and Packet Scheduling Algorithm in Optical Packet-Switched Networks”, IEEE AICT conference, February 2006.
- [BST 00] C. Qiao and M. Yoo, “Choices, Features and Issues in Optical Burst Switching,” Optical Net., vol. 1, no. 2, Apr. 2000, pp. 36–44.
- [BSQ 00] M. Yoo, C. Qiao, and S. Dixit, “QoS Performance of Optical Burst Switching in IP-Over-WDM Networks,” IEEE JSAC, vol. 18, no. 10, Oct. 2000, pp. 2062–71.
- [CAD 99] <http://www.caida.org/analysis/AIX> (still accessible)
- [CCH 05] H. Castel, M. Chaitou, and G. Hébuterne, Preemptive Priority Queues for the Performance Evaluation of an Optical MAN Ring, Proceedings of Performance Modeling and Evaluation of Heterogeneous Networks (Het-Net’05), 2005.
- [CON 05] Harry G. Perros, “Connection-oriented networks – SONET/SDH, ATM, MPLS and Optical Networks”, WILEY Edition 2005
- [CSM 00] “Carrier sense multiple access with collision avoidance”, American National Standard T1.523-2001, Telecom Glossary 2000.
<http://www.atis.org/glossary/definition.aspx?id=6101>
- [CSM 97] Pablo Brenner, “A Technical Tutorial on the IEEE 802.11 Protocol – The basic Access Method: CSMA/CA”, Copyrights © BreezeCOM 1997
- [CTL 04] G. Bernstein, B. Rajagopalan, D. Saha, “Optical Network Control – Architecture, Protocols and Standards”, Copyrights © 2004 by Pearson Education, Inc.
- [DBO 02] N. Le Sauze, E. Dotaro, A. Dupas and al., “DBORN: A Shared WDM Ethernet Bus Architecture for Optical Packet Metropolitan Network”, Photonic in Switching, July 2002.
- [DBO 04] N. Le Sauze, E. Dotaro, L. Ciavaglia, “DBORN (Dual Bus Optical Ring Network), An Optical Metropolitan Ethernet Solution”, Research Report – Alcatel, 2004.
- [DPA 05] D.Popa, T.Atmaca, “Glue MAC: A Modified CSMA/CA Scheme for a Dual-Bus Optical Ring Network (DBORN)”,??
- [DQB 91] DQDB Standard, IEEE standard for local and metropolitan area net-works: Distributed Queue Dual Bus (DQDB) of metropolitan area network (MAN)”, IEEE STD 802.6-1990, July 1991.

- [EAS 04] N. Banerjee and S. Sharan, "Evolutionary Algorithm for Solving the Single Objective Static Routing and Wavelength Assignment Problem in WDM Networks", IEEE ICISIP 2004.
- [ECO 08] Thaere EIDO, Tuan Dung NGUYEN, Tülin Atmaca, P. Gravey, A. Gravey, M. Morvan, J. Roberts, S. Oueslati, T. Ronald, D. Barth, D. Chiaroni, "Définition du Plan de Transport (MAC, Protocoles)", Livrable D2.1. French ANR Project / ECOFRAME (Eléments de convergence pour les futurs réseaux d'accès et métropolitains à haut débit), Conventions n° 2006 TCOM 002 -01 à -08. Project Report, January 2008.
- [ENA 08] Thaere EIDO, Dung Tuan NGUYEN, Tülin ATMACA, "Packet Filling Optimization in Multiservice Slotted Optical Packet Switching MAN Networks", paper accepted for the Advanced International Conference on Telecommunications, AICT'08, Athens June 2008.
- [ENC 08] Tulin Atmaca, Thierry Eido, Tuan Dung Nguyen, Dominique Chiaroni, Gema Buform, "Aggregation issues in Time Slotted packet ring networks", International Conference on Photonics in Switching (PS) 2009, September 15-19, 2009 – Pisa, Italy
- [EOS 04] E. ALANQAR, A. JUKAN, "Extending End-to-End Optical Service Provisioning and Restoration in Carrier Networks: Opportunities, Issues, and Challenges", IEEE Communications Magazine, January 2004.
- [FDI 86] FDDI Token Ring – Media Access Control, American National Standard, ANSI X3. 139-1987, November 5, 1986.
- [FDI 89] F. E. Ross, "Overview of FDDI: The Fiber Distributed Data Interface," IEEE JSAC, vol. 7, no. 7, Sept. 1989.
- [FHT 05] F. Haciomeroglu, T. Atmaca, "Impact of packet filling in an optical packet switching architecture", AICT, Lisbon, Portugal, 2005.
- [FOM 06] Thaere EIDO, Tuan Dung Nguyen, Viêt Hung Nguyen & Tülin Atmaca, "Report N° 1", Collaboration 2006 Alcatel-Lucent / GET-INT; Performance Analysis of DATA Oriented Metro Area Networks (PERFOMAN), 2006.
- [FOM 07] Thaere EIDO, Tuan Dung Nguyen, Viêt Hung Nguyen & Tülin Atmaca, "Report N° 2 on Comparative Study between Fix Packet Format & Variable Packet Format in an Optical Ring Network", Collaboration 2006 Alcatel-Lucent / GET-INT; Performance Analysis of DATA Oriented Metro Area Networks (PERFOMAN), 2007.
- [GRG 98] P. Gambini, M. Renaud, C. Guillemot, F. Callegati, I. Andonovic, B. Bostica, D. Chiaroni, G. Corazza, S.L. Danielsen, P. Gravey, P.B. Hansen, M. Henry, C. Janz, A. Kloch, R. Krähenbühl, C. Raffaelli, M. Schilling, A. Talneau and L. Zucchelli, Transparent Optical Packet Switching: Network Architecture and Demonstrators in the KEOPS Project, IEEE Journal on Selected Areas in Communications, Vol. 16, No. 7, September 1998.
- [GRM 01] E. Modiano, "Traffic Grooming in WDM Networks," IEEE Commun. Mag., July 2001, pp. 124–29
- [GUE 91] R. Guerin et al., "Equivalent Capacity and Its Application to Bandwidth Allocation in High-Speed Networks", IEEE Journal on select communications, Vol. 9, N° 7, Sept. 1991.
- [HGJ 05] G. Hu, C.M. Gauger, and S. Junghans, Performance Analysis of the CSMA/CA MAC Protocol in the DBORN Optical MAN Network Architecture, Proceedings of the 19th International Teletraffic Congress (ITC 19), 2005.
- [ICT 03] M. Mattiello and C. Bungarzeanu, "Static Wavelength Assignment in WDM Networks with Optical Crossconnects", 7th International Conference on Telecommunications – ConTel June 2003.
- [INF 03] P. Saengudomlert, E.H. Modiano and R.G. Gallager, "On-Line Routing and Wavelength Assignment for Dynamic Traffic in WDM Ring and Torus Networks", IEEE INFOCOM 2003.
- [ITF 04] IEEE 802.3ah task force home page [Online]. Available: <http://www.ieee802.org/3/efm>
- [JAI 66] Jaiswal. Priority Queues. New York: Academic 1966.

- [KGB 02] Kramer, G., and Pesavento, G.: “Ethernet passive optical network (EPON): building a next-generation optical access network”, *IEEE Commun. Mag.*, 2002, 40, (2), pp. 66–73.
- [KMP 02] Krammer, G., Mukherjee, B., and Pesavento, G.: ‘IPACT: a dynamic protocol for an Ethernet PON (EPON)’, *IEEE Commun. Mag.*, 2002, 40, (2), pp. 74–80.
- [KNI 08] Stamatios V. Kartalopoulos, *Next Generation Intelligent Optical Networks*, Springer Science+Business Media, 2008.
- [MCD 87] M.H. McDougall, *Simulating Computer Systems: Techniques and Tools*, The MIT, Press, 1987.
- [MEF 03] Ralph Santitoro, “Metro Ethernet Services – A Technical Overview” © 2003. http://www.metroethernetforum.org/PPT_Documents/Overview_of_MEF_6_and_10.ppt
- [MGH 01] Regis J. “Bud” Bates, *Optical Switching and Networking Handbook*, McGraw-Hill 2001.
- [MMR 04] Michael P. McGarry, Martin Maier, and Martin Reisslein, ‘Ethernet PONs: A Survey of Dynamic Bandwidth Allocation (DBA) Algorithms’, *IEEE Communications Magazine*, Vol. 42, No. 8, pages S8-S15, August 2004.
- [NAC 08] Thierry Eido, Tuan Dung Nguyen, Tülin Atmaca, Dominique Chiaroni, “Performance of Optical Ring Architectures with Variable-Size Packets: In-line buffers Vs Semi-Synchronous and Asynchronous Transparent MAC Protocols”, *International Workshop on Traffic Management and Traffic Engineering for the Future Internet, IEEE FITraMEN’2008*, Porto, Portugal, December 10-14, 2008.
- [NEA 08] Tuan Dung Nguyen, Thierry Eido, Viet Hung Nguyen, Tülin Atmaca, “Impact of Fixed-Size Packet Creation Timer and Packet Format on the Performance of Slotted and Unslotted Bus-Based Optical Man”, *International Conference on Digital Telecommunications IEEE ICDT’08*, Bucharest, Romania, June 29 - July 5, 2008.
- [NEA 09] Tuan-Dung NGUYEN, Thierry EIDO, Tülin ATMACA, “DCUM: Dynamic Creation of Fixed-Size Containers in Multiservice Synchronous OPS Ring Networks”, *International Workshop on the Evaluation of Quality of Service through Simulation in the Future Internet, IEEE QoS’09*, Roma, Italy, March 6th, 2009.
- [NEE 09] Tuan Dung Nguyen, Thierry Eido, Tülin Atmaca, “An Enhanced QoS-enabled Dynamic Bandwidth Allocation Mechanism for Ethernet PON”, *The Fifth European Conference on Universal Multiservice Networks, ECUMN’09*, October 11-16, 2009 - Sliema, Malta
- [NEV 09] Tuan Dung NGUYEN, Thierry EIDO, Tülin ATMACA, “Performance of a Virtual Synchronization Mechanism in an Asynchronous Optical Network”, *Advanced International Conference on Telecommunications, IEEE AICT’09*, Venice/Mestre, Italy, May 24-28, 2009.
- [NGA 05] V.H. Nguyen, T. Atmaca, “Performance analysis of the Modified Packet Bursting mechanism applied to a metropolitan WDM ring architecture”, *IFIP Open Conference on Metropolitan Area Networks: Architecture, protocols, control and management, Technical proceeding*, pp.199-215, HCMC Viet Nam, 11-13 April 2005.
- [NGA 06] V.H. Nguyen and T. Atmaca, *Dynamic Intelligent MAC Protocol for Metropolitan Optical Packet Switching Ring Networks*, *IEEE International Conference on Communications – ICC 2006*, Istanbul, Turkey, 11-15 June, 2006.
- [NGI 08] Thaere EIDO, Tuan Dung NGUYEN, Tülin ATMACA, Gérard HEBUTERNE, Viêt Hùng NGUYEN, “EURO-FGI: Report on activities in WP.JRA.1.2” and “EURO-FGI: Report on activities in WP.JRA.5.5”, *European Network of Excellence Euro-FGI Project Reports*, Partner: GET/INT Institut National des Télécommunications, Evry, France, SAMOVAR CNRS Laboratory: ARMOR Team, March 2008.
- [NNA 07] T.D. Nguyen, V.H. Nguyen and T. Atmaca, “Delay analysis and queue-length distribution estimation of a slotted bus-based metro network using embedded discrete time Markov chain”, *The Second Beijing-Hong Kong International Doctoral Forum 2007*, Hongkong, China, 3-6 July 2007.
- [NWS 05] *Network Simulator*. Available at HTTP: <http://www.isi.edu/nsnam/ns/>.

- [OPF 05] D. Popa and T. Atmaca, "On Optical Packet Format and Traffic Characteristics". In proceedings of IEEE/EuroNGI SAINT'05 Workshop on Modelling and Performance Evaluation for Quality of Service in Next Generation Internet, 31 Jan. – 4 Feb. 2005, Trento, Italy.
- [OPN 02] Regis J. "Bud" Bates, "Optical Network", McGraw-Hill 2002.
- [ORW 00] C. Law, "Online Routing and Wavelength Assignment in Single-Hub WDM Rings", IEEE Journal on Selected Areas in Communications, Vol. 18, NO. 10, October 2000.
- [OWN 06] Springer, "Optical WDM Networks", January, 2006.
- [PSW 94] V. Paxson and S. Floyd. "*Wide-area traffic: the failure of poisson modeling*", ACM SIGCOM, pp: 257-268, Aug. 1994
- [R2A 05] Thaere EIDO, V.Hung NGUYEN and Tülin ATMACA, "Dynamic Resource Allocation Algorithm for Metropolitan Optical Packet-Switched Ring Networks", IEEE AICT conference, Lisbon, July 2005. This paper is the winner of the Best Paper Award in this conference.
- [ROM 02] ROM-EO -- Réseau Optique Multi-Service Exploitant des Techniques Electrooptiques et Opto-electroniques, RNRT Project, Available at : http://www.telecom.gouv.fr/rnrt/rnrt/projets/res_02_52.htm, 2002.
- [RPR 03] IEEE 802.17 Resilient Packet Ring Tutorial Fredrik Davik, Mete Yilmaz, Stein Gjessing, Necdet Uzun.
- [RSM 03] Ralph Santitoro, "Metro Ethernet Services – A Technical Overview", <http://www.metroethernetforum.org/metro-ethernetservices.pdf>, 2003.
- [SMR 83] S. M. Ross, "*Stochastic Simulation*", John Wiley & Sons, 1983.
- [SRT 05] Springer, "Optical Burst Switched Networks", 2005.
- [SSO 03] A. Stavdas, S. Sygletos, M. O'Mahoney, H.L. Lee, C. Matrakidis and A. Dupas, IST-DAVID: Concept Presentation and Physical Layer Modeling of the Metropolitan Area Network, Journal of Lightwave Technology, Vol. 21, No. 2, February 2003.
- [TAK 91] H. Takagi, Queuing Analysis, Vol.1, pp. 365-373. North-Holland, 1991.
- [TDP 05] D.Popa, "Performance Issues in Metropolitan Optical Network: Packet Format, MAC Protocol and QoS", Dissertation of Philosophy Doctor, Evry 06-2005.
- [TEQ 01] L. Xu, H.G. Perros, and G. Rouskas, "Techniques for Optical Packet Switching and Optical Burst Switching", IEEE Communications Magazine, January 2001.
- [TNH 06] V.H Nguyen, "Performance Evaluation and QoS Management in Multiservice Optical Packet Switched Networks", Dissertation of Philosophy Doctor, Evry 06-2006.
- [TOP 02] A. Gumaste, D. Bihon, E. Kooperstock and S. Kinoshita, "Comparison of WDM network topologies", In Proceedings of the 15th international Conference on Computer Communication (Mumbai, Maharashtra, India, August 12 - 14, 2002)
- [TTE 08] T.Eido, "Performance Evaluation, Resource Allocation and QoS in Multiservice Optical Packet Switched Networks", Dissertation of Philosophy Doctor, Paris 07-2008.
- [WAD 98] X. Zhang and C. Qiao, "Wavelength Assignment for Dynamic Traffic in Multi-fiber WDM Networks", IEEE 1998
- [WSH 95] W. Willinger et al., "Self-Similarity through High-Variability: Statistical Analysis of Ethernet LAN Traffic at the Source Level," Proc. ACM SIGCOMM '95, pp. 100–13.
- [ZEA 05] J. Zheng, University of Ottawa, "Efficient bandwidth allocation algorithm for Ethernet passive optical networks" IEEE Proceedings online no. 20050358, 10th November 2005
- [ZMC 06] Yongqing Zhu, Maode Ma and Tee Hiang Cheng, Nanyang Technological University, Singapore, "IPACT with Grant Estimation for EPON", Proc-IEEE Tenth International Conference on Communication Systems (ICCS'06), Singapore, November, 2006.
- [ZMT 05] Zheng, J., and Mouftah, H.T.: 'Media access control for Ethernet passive optical network', IEEE Commun. Mag., 2005, 43, (2), pp. 145–150.